UNIVERSITÀ DEGLI STUDI DI MESSINA

Dipartimento CHIBIOFARAM

TESI DI DOTTORATO DI RICERCA IN SCIENZE CHIMICHE

Curriculum: progettazione, sintesi, analisi e proprietà di sistemi molecolari funzionali

XXXII CICLO

2016-2019

Synthetic Strategies, Photophysical and First Biological Applications of New Glycoamino OPEs

Aurora Mancuso

Supervisor

Prof.ssa Anna Barattucci

Index

Abstract

Oligo(phenyleneethynylenes) (OPEs) and the corresponding polymers, Poly(phenyleneethynylenes) (PPEs), are organic molecules with π-conjugated backbone, which could be designed to display high electrical conductivity, outstanding photophysical properties, and excellent biocompatibility. While they have been extensively explored for a wide range of applications, from electronics and optoelectronic devices, to energy harvesting and nanotechnology, they attracted attention in the biomedical field only in the past decades. Specifically, they have found innovative applications in a variety of biotechnologies, as biosensors, probes for cell imaging, biocides and many others.

In the last years, my research group has widely studied the photophysical and biological properties of a new class of end-only glucose functionalized oligo(phenyleneethynylenes): thanks to the modulation of substituents and length of the central conjugated chain, some of the obtained OPEs have demonstrated to be promising dyes in bioimaging and superficial Photodynamic Therapy (PDT) (**Figure A1**).

On the basis of these assumptions, my PhD work consisted in the synthesis of differently modified glycosilated OPEs with the aim to better modulate their photophysical features and biological behaviour, studying new possible applications in the biomedical field.

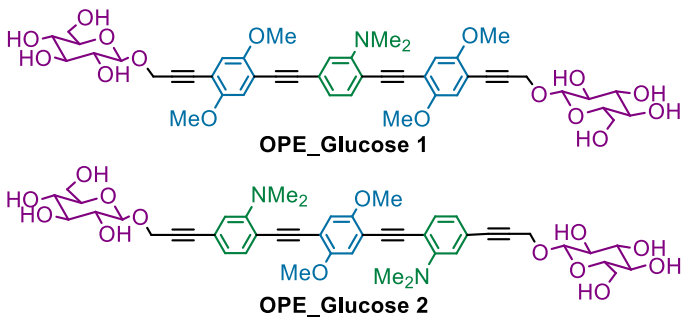

Figure A1

In particular, **Chapter 1** consists in a literature survey and gives an overview on general principles and previous works upon which this research draws. In paragraph **1.1**, carbohydrates conjugation, as an efficient strategy for delivering and targeting drugs, is discussed. Paragraph **1.2** deals with the main applications of luminescent dyes in the biomedical field: at first, in **1.2.A**, a general view on the principles of bioimaging and the design of suitable fluorescent probes is reported; in **1.2.B**, the mechanisms that are the basis of photodynamic therapy (PDT) and a brief literature overview on different classes of dyes and nanoparticles, which have found application as photosensitizers in this type of treatments, are described; **1.2.C** deals with drugs interactions with nucleic acids, with particular attention to the principal binding modes and to the possible uses of luminescent dyes for DNA labelling; finally, in **1.2.D**, applications of specific kinds of fluorescent dyes, whose luminescence is pH dependent, as intracellular pH indicators are reported. To conclude, paragraph **1.3** provides an overall picture of Oligo(phenyleneethynylenes) (OPEs) features and biomedical applications, mainly focusing on the previous works of my research group.

Chapter 2 deals with the discussion of the synthetic pathways used for the obtainment of the new glycosylated OPE systems and the structural modifications introduced during the PhD work. In fact, in paragraph **2.1** the synthetic approach and the optimization of yields and methods for the obtainment of the already reported **OPE_Glucose 1** and **OPE_Glucose 2** (**Figure A1**), which had shown the best results in terms of cell internalization and applications as photosensitizers in PDT, are described. In paragraph **2.2**, the synthetic routes which led to the elongation of the OPE chain are reported: the extension of the π-conjugated system is meant to further study the influence of chain length on the photophysical behaviour. The synthesis of three new amino-OPE systems, bearing different sugar terminations (monosaccharide galactose and mannose, and disaccharide maltose) are described in paragraph **2.3**: the presence of different carbohydrate residues could, in fact, influence the biological behaviour of the new compounds,

with respect to the glucosylated systems. Furthermore, the synthesis of several tetralkylammonium OPEs is the subject of paragraph **2.4**: the disappearance of the lone pair on the amino nitrogen and the formation of a positive charge on the OPE chain could, in fact, strongly influence the photophysical OPE features but also the water solubility, opening the way to other biological applications. Finally, the last modifications reported in paragraph **2.5** are focused on the desymmetrization of the OPE chain. In part **2.5A** the introduction of electron withdrawing fluorinated aromatic groups as chain termination is discussed: the new moiety, which is able to interact with the methoxy and amino electron donating groups already present as substituents on the OPE conjugated chain, could influence the photophysical features, leading to the obtainment of new push-pull systems. In part **2.5B** the synthesis of OPEs, bearing suitable termination for the functionalization of upconverting nanoparticles (UCNPs), is described. These nanoparticles, after excitation with NIR light (980 nm), emit in a region of UV that matches the absorption of our OPEs (~380 nm): an energy transfer process from the NPs to our conjugated system could extend their applications in NIR-PDT.

Chapter 3 deals with the preliminary photophysical and biological studies performed on some selected compounds. In particular, in paragraph **3.1** the effects of the different modification on our OPE systems (chain elongation, nitrogen quaternarization and desymmetrization) on the spectroscopic features are discussed, in comparison with the already reported **OPE_Glucose 1** and **OPE_Glucose 2**. In fact, it has been demonstrated that each structural change in the OPE chain causes different variations in the photophysical properties; moreover, preliminary studies on the fluorinated compounds show that the emission of one of these derivatives is pH-sensitive. On the other hand, the first biological tests, carried out on some of the synthesized compounds, are described in paragraph **3.2**. It has been found that the two positive charged tetralkylammonium OPEs, analogues of **OPE_Glucose 1** and **OPE_Glucose 2,**

strongly bind the double helix of DNA: this interaction is also responsible for their absorption and emission switching-off and reduction of cancer cells proliferation. Moreover, the first internalization and PDT tests on healthy and cancer cells performed with the synthesized compound bearing two maltosidic residues are also reported.

Finally, in **Chapter 4** experimental synthetic methods, spectral and analytical characterizations of the obtained compounds, equipment, materials and methods for the photophysical and biological experiments are reported.

CHAPTER 1

Introduction

1.1 CARBOHYDRATES IN DRUG DELIVERY

Carbohydrates represent one of the most abundant and pervasive class of biomolecules. Besides being important for survival of living organisms as an important dietary component, their role in many biological processes is fundamental for life. Their role is polyvalent: a) they can serve as immediate source of energy in the form of table sugar, starch, and fibres; b) they are part of the structural building blocks of genetic materials (DNA and RNA) and c) play a key role in cell recognition events, acting as extracellular and intracellular components in molecular recognition. Thanks to advancements in carbohydrate research and to the fact that carbohydrates are now recognized as important players in numerous processes such as cell recognition (facilitated by cell surface saccharides), cell migration, and immune defence, the use of carbohydrates as direct drug delivery systems has been a fundamental subject in the last decades.[1]

The process of their absorption is cell-selective and sometimes limited to few saccharides. For example, among the large number of theoretically existing simple carbohydrates, glucose remains the principal food or 'fuel' for most cells; in fact, other carbohydrates are routinely transformed to glucose before their storage as glycogen in the liver.

[1] Mishra, S.; Upadhay, K.; Mishra, K. B.; Shukla, A. K.; Tripathi, R. P.; Tiwari, V. K. *Studies in Natural Products Chemistry*, **2016**, *49*, 307.

Due to its polar nature and size, glucose molecules cannot traverse the lipid membrane of the cell by simple diffusion; the regulation of glucose transport in humans is complex and involves two classes of membrane proteins:

1) Na^+-dependent glucose transporters, which are involved in the active transport of glucose from the lumen of the small intestine and from the proximal kidney tubule in the process of reabsorption;

2) the facilitative glucose transporters, which are still not fully characterized proteins but present on all the cells.

These transporters possess distinct physiological and biochemical properties, which endow them with specific functions in the tissues in which they are expressed. For these reasons, glucose-selective proteins and other proteins, which exhibit selectivity for a variety of simple carbohydrates are the preferred choice for an emerging new form of cell-specific drug delivery system.[2]

Carbohydrates with structural and functional diversity have enabled chemists to synthesize novel carbohydrate-based therapeutic agents or to make cardinal modifications to improve the activity and selectivity of existing drugs. In fact, many natural and semisynthetic glycoconjugates are clinically used as antimicrobials and anticancer agents. Carbohydrates can guarantee water solubility, minimized toxicity and can enhance pharmacokinetics to conjugated drugs with respect to their aglycones.[3] In addition to this, carbohydrates also establish stereochemically defined scaffolds to project pharmacophores, that can give rise to a number of carbohydrate-based compound libraries.

Carbohydrates are also extremely important for processes involved in cell transformation and tumour genesis. Almost a century ago, the scientist Otto Warburg discovered that cancerous tissues consume larger amounts of glucose compared to healthy tissues. Glucose transporters (GLUTs), which are located on

[2] Palomino, E. *Advanced Drug Delivery Reviews*, **1994**, *13*, 311.
[3] Mishra, S.; Upadhay, K.; Mishra, K. B.; Shukla, A. K.; Tripathi, R. P.; Tiwari, V. K. *Studies in Natural Products Chemistry*, **2016**, *49*, 307.

membranes of endothelial cells and facilitate the entry and the diffusion of glucose and other carbohydrates into cells, are widely overexpressed in human cancers.[4]

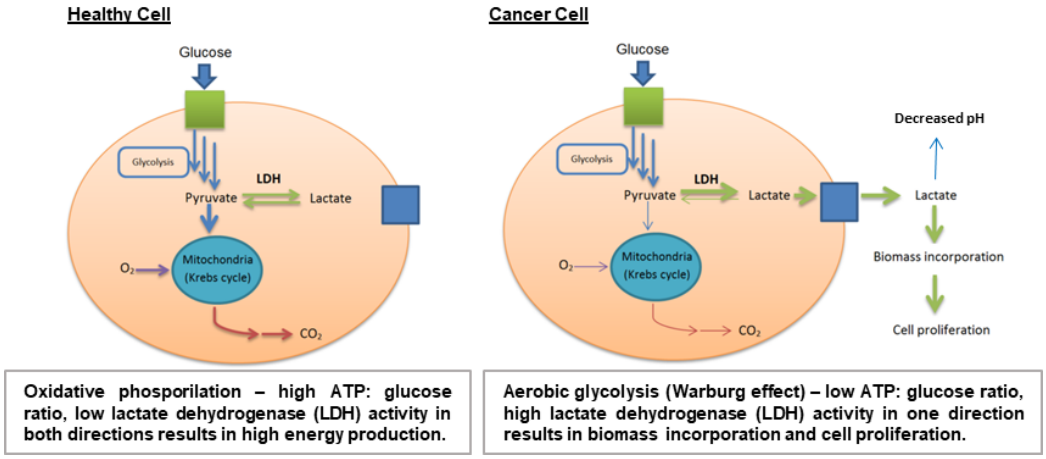

Figure 1.1. Metabolism in healthy and cancer cells.

In order to sustain the uncontrolled growth rate, cancer cells have adopted a different unconventional mechanism to produce energy. Usually, healthy cells do not stop glucose metabolism to lactate when oxygen is available, but they undergo oxidative phosphorylation, producing high ATP level: they exploit anaerobic glycolysis (metabolism of glucose to lactic acid) only when the oxygen is absent or limited. In contrast, cancer cells metabolize glucose to lactate even in the presence of oxygen (aerobic glycolysis), producing low levels of ATP; because of the great quantity of produced lactate, it is ejected outside the cell membrane, also causing a decreasing of the pH in the external microenviroment.[5] (**Figure 1.1**) Thus, altered cancer cell metabolism can modulate the tumor microenvironment, which plays important roles in cancer cell somatic evolution, metastasis, and therapeutic response.[6] Today this phenomenon is known as the "Warburg effect" and is recognized as one of the hallmarks of cancer and gives

[4] Warburg, O.; Wind, F.; Negelein, E. *J. Gen. Physiol*., **1927**, 8, 519–530; Warburg, O. *Science*, **1956**, 123, 309.
[5] Koppenol, W. H.; Bounds, P. L.; Dang, C. V. *Nat. Rev. Cancer* **2011**, *11*, 325.
[6] Justus, C.; Sanderlin, E. J.; Yang, L. V. *Int. J. Mol. Sci.* **2015**, *16*, 11055.

us the information that cancer cells consume huge amounts of glucose for their proliferation. Increased understanding of this dysfunctional metabolism has led to an interest in targeting it for cancer therapy. For this reason, one promising strategy for drug design is glycoconjugation: the linking of a drug to glucose or other mono- and disaccharides. Monosaccharide-conjugated analogues of diverse agents, designed to improve the water solubility, serum stability, and targeting of their aglycones, have been reported in the chemical literature since the early 1990s.

One of the first clinically used carbohydrates-based drug is 2-deoxy-2-(^{18}F)fluoro-D-glucose (^{18}F-FDG; **Figure 1.2**), a radiolabelled glucose analogue. ^{18}F-FDG is used to visualize tumours and their metastases due to the tendency of these cancerous tissues to uptake glucose at a higher rate than most normal tissues. Moreover, positron emission tomography (PET) with ^{18}F-FDG has been used to assess alterations in glucose metabolism in brain, cancer, cardiovascular diseases, Alzheimer's disease and other central nervous system disorders, infectious, autoimmune and inflammatory diseases.

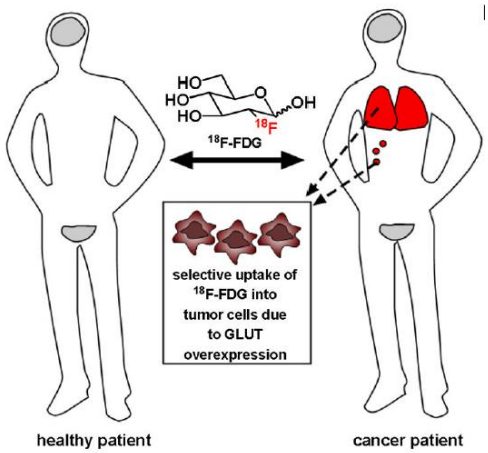

Figure 1.2. Localization of ^{18}F-FDG in healthy (grey) and cancer (red) patient.

In healthy patients, ^{18}F-FDG is taken up only by tissues that constitutively consume glucose, such as the brain and bladder (grey in figure). In a sick patient, tumour cells preferentially uptake ^{18}F-FDG, allowing clinicians to identify sites

of tumours and metastases (red in figure), as well as stage cancer and monitor response to treatment. Currently, lung, breast, colorectal, and endometrial carcinomas, as well as bone and soft tissue sarcomas and Hodgkin's and non-Hodgkin's lymphomas, are commonly staged based on their ability to preferentially uptake this radiolabelled glucose analogue compared to noncancerous tissues.

Since then, this field has grown exponentially and in the last decades several cytotoxic agents, e.g., glufosfamide,[7] chlorambucil,[8] busulfan,[9] paclitaxel,[10] have been glycoconjugated and found to be cancer selective and less toxic to normal cells than the parent aglycons.[11] Furthermore, other sugars such as galactose, mannose, fucose, etc., have been used as powerful scaffolds, installed on drug molecules, for targeting specific tissues.[12] In fact, it is known that other non-glucosidic monosaccharides can be substrates for GLUT transporters, and thus can be considered candidates for a GLUT-targeting approach. Specifically, using light diffraction measurement in human erythrocytes that express GLUT-1 as their sole glucose transporter, 2-deoxy-D-glucose, D-galactose, D-mannose, D-xylose, 2-deoxy-D-galactose, L-arabinose, D-ribose, D-fucose, and D-lyxose, in order of decreasing affinity, were all found to be transported into cells in a transporter mediated mechanism. In contrast, D-arabinose, L-fucose, and L-rhamnose were poor substrates, and the enantiomers of several GLUT substrates, L-glucose and L-xylose, were not GLUT substrates.[13] Thus, it seems that many sugars can be conjugated to anticancer agents to take advantage of GLUT-mediated cellular uptake; the choice of which sugar to utilize may depend on the desired cleavage mechanism of the compound. For instance, D-galactose, the C4

[7] Pohl, J.; Bertram, B.; Hilgard, P.; Nowrousian, M. R.; Stuben, J.; Wiessler, M. *Cancer Chemother Pharmacol.* **1995**, *35*,364.
[8] Halmos, T.; Santarromana, M.; Antonakis, K.; Scherman, D. *Eur J Pharmacol.* **1996**, *18*, 477.
[9] Halmos, T.; Santarromana, M.; Antonakis, K.; Scherman, D. *Carbohydr. Res.* **1997**, *299*, 15.
[10] Lin, Y. S.; Tungpradit, R.; Sinchaikul, S.; An, F. M.; Liu, D. Z.; Phutrakul, S.; Chen, S. T. *J. Med. Chem.* **2008**, *51*, 7428.
[11] Calvaresi, E. C.; Hergenrother, P. J. *Chem. Sci.* **2013**, *4*, 2319.
[12] Yuan, S. S.; Li, M. L.; Chen, J. S.; Zhou, L.; Zhou, W. *ChemMedChem.*, **2018**, 13, 764.
[13] LeFevre, P.G. *Pharmacol Rev.* **1961**, *13*, 39.

epimer of glucose, has been reported to possess an equivalent affinity and uptake rate by GLUT-1 compared to glucose.[14] Galactose-conjugated drugs may be used to selectively target certain types of cancers known to highly express galactosidase enzymes, such as breast and colon cancers.[15] In the absence of substantial tumour galactosidase expression, galactose-conjugated prodrugs can be used in conjunction with tumour-selective monoclonal antibodies linked to galactosidases, which ideally cleave the inactive conjugate to its active form in tumour tissue. Thus, glycocojugation generally offers selective targeting to cancer cells, if the glycoside of choice is a GLUT substrate. For instance, in 2001, Mikuni, Mandai, and coworkers[16] reported the synthesis and cancer cell potency of several glycoconjugates of docetaxel, including conjugates with glucose, galactose, mannose, and xylose. These compounds were shown to have a 3- to 18-fold improvement in activity compared to the aglycone against B16 murine melanoma cells and it was particularly highlighted the *in vivo* potency of galactose-conjugated docetaxel, compared to the aglycone.

Moreover, with the great development of carbohydrate synthesis technology, carbohydrate chain analysis methods and nanotechnology, research on the biological effects associated with carbohydrate has become a hot topic in recent years. Nanomaterials as the carriers of carbohydrates have been gradually developed since the first synthesis of carbohydrate functionalized gold nanoparticles in 2001[17] and related reports have gradually increased. They have shown great potential for applications in biomedical imaging, diagnosis, and treatment.[18] Compared with the use of other molecules as carriers, nanoparticles can regulate the density of ligands on the surface by adjusting their size and shape.

---

[14] Melisi, D.; Curcio, A.; Luongo, E.; Morelli, E.; Rimoli, M. G. *Curr. Top. Med. Chem.* **2011**, *11*, 2288.
[15] Devalapally, H.; Rajan, K. S.; Akkinepally, R. R.; Devarakonda. R. K. *Drug Dev Ind Pharm.* **2008**, *34*, 789.
[16] Mandai, T.; Okumoto, H.; Oshitari, T.; Nakanishi, K.; Mikuni, K.; Hara, K.; Iwatani, W.; Amano, T.; Nakamura, K.; Tsuchiya, Y. *Heterocycles* **2001**; *54*, 561.
[17] de la Fuente, J.M.; Barrientos, A. G.; Rojas, T. C.; Rojo, J.; Cañada, J.; Fernández, A.; Penadés S. *Angew. Chem. Int. Ed.* **2001**, *40*, 2257.
[18] García, I.; Marradi, M.; Penadés, S. *Nanomedicine (Lond)* **2010**, *5*, 777.

In addition, nanoparticles have unique optical, electrical, magnetic, mechanical, and chemical activities. These properties make glyconanoparticles not only useful for studying sugar-related biological effects but also for cell imaging and tumour cell-targeted drug delivery.[19]

Among the large number of nanomaterials, gold, an extremely inert and biocompatible material, is one of the main exploited scaffolds for producing glyconanoparticles.[20] At nanosize, gold nanoparticles (AuNPs) are characterized by unique optical features, which result extremely useful in many diagnosis and affinity studies or protocols. Moreover, gold can be easily and covalently decorated on its surface by exploiting the strong soft–soft interaction between an Au atom and sulphur.[21] Therefore, glyco-gold nanoparticles (GAuNPs) represent a smart, multimodal and versatile nanoplatform to develop carbohydrate-based nanotechnology and nanomedicine systems.[22]

Also glycoside lanthanide ion-doped upconversion nanoparticles (UCNPs) (paragraph **1.2.B**), which can convert low-energy infrared photons into high-energy visible and ultraviolet photons, have recently found several applications in advanced biomedical and biophotonics fields.[23] For instance, in 2010, Bogdan *et al*.[24] reported the synthesis of mannose-coated lanthanide-doped upconverting nanoparticles (**Figure 1.3**) for the selective detection of proteins based on selective carbohydrate-protein complementary recognition, succeeding in interacting and detecting bacteria or virus infections.

[19] Jafari Malek, S.; Khoshchehreh, R.; Goodarzi, N.; Khoshayand, M. R.; Amini, M.; Atyabi, F.; Esfandyari-Manesh, M.; Tehrani, S.; Mohammad Jafari, R.; Maghazei, M. S.; Alvandifar, F.; Ebrahimi, M.; Dinarvand, R. *Colloids Surf. B: Biointerfaces* **2014**, *122*, 350 .
[20] Compostella, F.; Pitirollo, O.; Silvestri, A.; Polito, L. *Beilstein J. Org. Chem.* **2017**, *13*, 1008.
[21] Saha, K.; Agasti, S. S.; Kim, C.; Li, X.; Rotello, V. M. *Chem. Rev.* **2012**, *112*, 2739.
[22] Chaudhary, P. M.; Sangabathuni, S.; Murthy, R. V.; Paul, A.; Thulasiram, H. V.; Kikkeri, R. *Chem. Commun.* **2015**, *51*, 15669; Sangabathuni, S.; Vasudeva Murthy, R.; Chaudhary, P. M.; Surve, M.; Banerjee, A.; Kikkeri, R. *Nanoscale* **2016**, *8*, 12729.
[23] Gee, A.; Xu, X. *Surfaces* **2018**, *1*, 96.
[24] Bogdan, N.; Vetrone, F.; Roy, R.; Capobianco, J. A. *J. Mater. Chem.* **2010**, *20*, 7543.

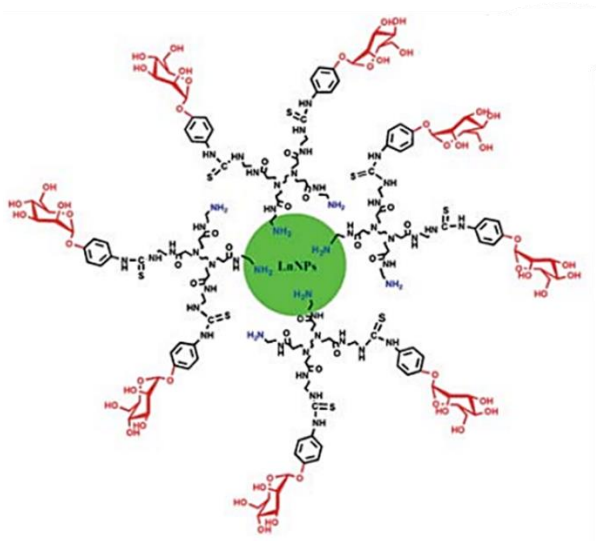

Figure 1.3. Mannose-coated UCNPs

1.2 LUMINESCENT DYES FOR BIOMEDICAL APPLICATIONS

1.2.A Bioimaging. Methods to "see into the body" or "see into cells" are essential for the diagnosis and treatment of disease, as well as for research into the basic processes of life. It is desirable that the used methods should not be invasive, i.e., should not involve cutting into the body or isolating cellular constituents. Therefore, techniques to visualize physiological or pathophysiological changes in the body and cells have become increasingly important in biomedical sciences.[25] Compared to other technologies such as radioisotope labelling, magnetic resonance imaging (MRI), electron spin resonance (ESR) spectroscopy, and electrochemical detection, fluorescence bioimaging is the most versatile and widely used visualization method to study the structure and function of biological systems and the molecular process in living organisms without perturbing them. This technique offers many advantages for this purpose, because it is characterized by high sensitivity, high resolution,

[25] Nagano, T. *Proc. Jpn. Acad. Ser. B. Phys. Biol. Sci.* **2010**, *86*, 837.

less-invasive and safe detection using readily available instruments. Today, fluorescent probes based on small organic molecules have become indispensable tools in modern biology because they provide dynamic information concerning the localization and quantity of the molecules of interest, without the need for genetic engineering of the sample.

The design of new fluorophores for biological applications is essential, but often suffers from intrinsic problems: keeping high structural homology with natural molecules is generally useful to provide biocompatibility but often prevents the achievement of remarkable results in term of fluorescence properties (e.g. fluorescence quantum yield, bathochromic emission); on the other hand, more elaborate modifications of the molecular skeleton could induce perturbation of normal cellular activity or, in the worst case, be lethal for living systems.

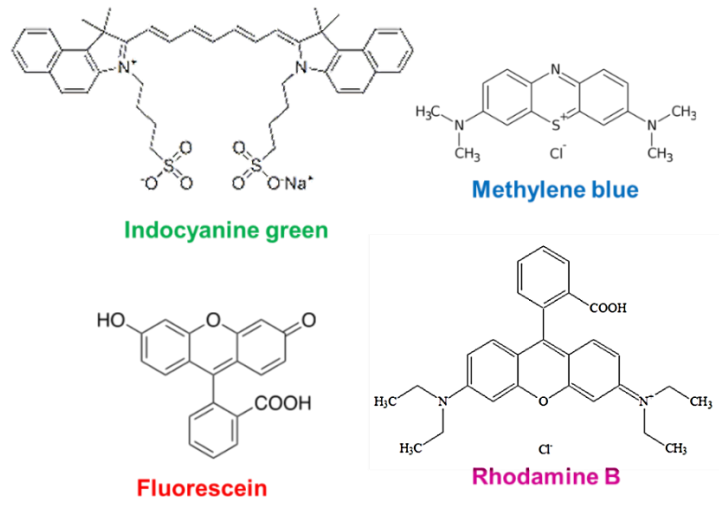

Figure 1.4

For this reason, only few fluorophores are currently approved by the U.S. Food and Drug Administration (FDA) for medical use such as indocyanine green

(ICG),[26] methylene blue[27] and fluorescein (**Figure 1.4**).[28] Another fluororophore, rhodamine B, approved for use in 1966, was subsequently banned in 1987 after being linked to cancer in mice and rats.[29]

A successful optical molecular probe for medical imaging has to possess specific features, including wavelength, brightness, bio- and photostability, and pharmacokinetics including nonspecific tissue accumulation.[30] First of all, fluorophores require excitation light to give emission: excitation in the UV range can cause direct tissue damage, whereas excitation in the IR can lead to tissue heating; blue and/or green excitation light is compatible with surface imaging applications because it has poor tissue penetration. On the other hand, yellow or red light (at around 600 nm) leads to excessive autofluorescence, because of naturally occurring endogenous fluorophores (mostly haemoglobin and related), also excited in this range. The optimal excitation wavelength of a fluorophore is in the deep red or near-infrared range because of the combined virtues of good tissue penetration and low autofluorescence.[31] However, for surface applications, such as detecting tumours on a mucosal or epithelial surface, lower wavelength (e.g., blue, green, yellow) emitters with high quantum efficiency may produce as good or better results compared to NIR probes.

The sensitivity and resolution for bioimaging depend also by the difference between excitation and emission wavelengths of the probe, known as the Stokes shift: in fact a small Stokes shift may result in self-quenching and back scattering from biological samples.[32] Other important considerations in choosing a

[26] Yoshida, M.; Kubota, K.; Kuroda, J.; Ohta, K.; Nakamura, T.; Saito, J.; Kobayashi, M.; Sato, T.; Beck, Y.; Kitagawa, Y.; Kitajima, M. *J. Gastroenterol. Hepatol.* **2012**, *3*, 29.
[27] Verbeek, F. P.; van der Vorst, J. R.; Schaafsma, B. E.; Swijnenburg, R. J.; Gaarenstroom, K. N.; Elzevier, H. W.; van de Velde, C. J.; Frangioni, J. V.; Vahrmeijer. A. L. *J. Urol.* **2013**, *190*, 574.
[28] McGinty, J. J. Jr.; Hogle, N.; Fowler, D. L. *D. Surg Endosc.* **2003**, *17*, 1140.
[29] European Food Safety Authority. Review of the toxicology of a number of dyes illegally present in food in the EU. *EFSA J.* **2005**, *263*, 1.
[30] Kobayashi, H.; Ogawa, M.; Alford, R.; Choyke, P. L.; Urano, Y. *Chem. Rev.* **2010**, *110*, 2620.
[31] Ntziachristos, V.; Bremer, C.; Weissleder, *R. Eur. Radiol.* **2003**, *13*, 195.
[32] Li, J.-B.; Liu, H.-W.; Fu, T.; Wang, R.; Zhang, X.-B.; Tan, W. *Trends Chem.* **2019**, *1*, 224.

fluorophore are the emission quantum yield, which needs to be high enough to guarantee low excitation light to obtain fluorescence, and the stability *in vivo*, which can be extremely different from the one *in vitro*, leading for instance to a loss of fluorescence or degradation after internalization.[33]

An array of low molecular weight synthetic fluorophores with various core structures including fluorescein, BODIPY, rhodamine, and cyanine derivatives, ranging from 300 to 2000 Da, are available from commercial providers and span the emission spectrum from blue to NIR. Furthermore, low molecular weight fluorophores can be designed to be sensitive to enzymatic catalysis so that they activate in specific environments.[34]

Other conditions such as pH range variation and production of singlet oxygen or other reactive oxygen species can influence the performance of small molecule fluorophores.[35] Furthermore, due to the developing field in material science and nanotechnology, in the last years the synthesis of nanocrystals, such as quantum dots [36] and upconverting nanoparticles, [37] gained particular attention too.

1.2.B Photodynamic Therapy.

General principles. Photodynamic therapy (PDT) is a relatively new, non-invasive therapeutic method used for the destruction of various cells and tissues consisting in the administration of a photosensitizing drug followed by irradiation of light and generation of reactive oxygen species (ROS) which lead to cell

---

[33] Longmire, M. R.; Ogawa, M.; Hama, Y.; Kosaka, N.; Regino, C. A.; Choyke, P. L.; Kobayashi, H. *Bioconjugate Chem.* **2008**, *19*, 1735.
[34] Pham, W.; Weissleder, R.; Tung, C.-H. *Angew. Chem., Int. Ed.* **2002**, *41*, 3659.
[35] Koide, Y.; Urano, Y.; Kenmoku, S.; Kojima, H.; Nagano, T. *J. Am. Chem. Soc.* **2007**, *129*, 10324.
[36] Burda, C.; Chen, X.; Narayanan, R.; El-Sayed, M. A. *Chem. Rev.* **2005**, *105*, 1025; Giepmans, B. N. G.; Deerinck, T. J.; Smarr, B. L.; Jones, Y. Z.; Ellisman, M. H. *Nat. Methods* **2005**, *2*, 743; Giepmans, B. N. G.; Deerinck, T. J.; Smarr, B. L.; Jones, Y. Z.; Ellisman, M. H. *Nat. Methods* **2005**, *2*, 743.
[37] Wang, X.; Yu, W. W.; Zhang, J.; Aldana, J.; Peng, X.; Xiao, M. *Phys. Rev. B* **2003**, *68*, 125318; Ortgies, D. H.; Tan, M.; Ximendes, E. C.; del Rosal, B.; Hu, J.; Xu, L.; Wang, X.; Rodríguez, E. M.; Jacinto, C.; Fernandez, N.; Chen, G. Jaque, D. *ACS Nano* **2018**, *12*, 4362.

death.[38] It has been employed in several medical fields including dermatology, urology, ophthalmology, pneumology, cardiology, dentistry and immunology. Moreover, antimicrobial and antiviral PDT have been found useful for the treatment of various infectious diseases, water sterilization and inactivation of pathogens in blood products.[39]

PDT requires the simultaneous presence of three components: a photosensitizer (PS), a light source and the presence of oxygen.[40] The PS preferentially accumulates in tumour cells and in macrophages; when it is exposed to light of specific wavelength it becomes activated to the short-live (nanoseconds) excited singlet state (S_1). This state can decay to the ground state or undergo intersystem crossing to the long-live (microseconds) triplet state (T_1).

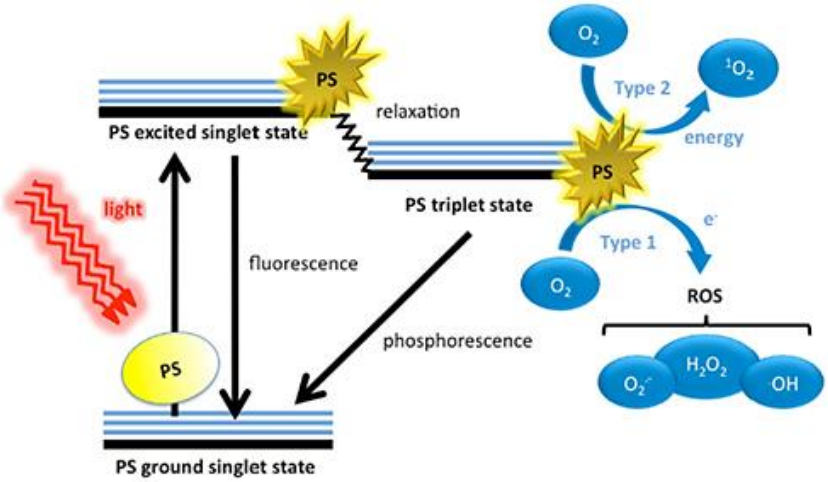

Figure 1.5

The PS in the triplet state interacts with the surrounding molecules through two types of reactions (**Figure 1.5**). For type I pathway, electron transfer and/or hydrogen abstraction occur between PSs and substrates, generating free radicals.

[38] Tampa, M.; Sarbu, M.-I.; Matei, C.; Mitran, C.-I.; Mitran, M.-I.; Caruntu, C.; Constantin, C.; Neagu, M.; Georgescu, S.-R. *Oncol. Lett.* **2019**, *17*, 4085.
[39] Benov, L. *Med. Princ. Pract.* **2015**, *24*, 14.
[40] Matei, C.; Tampa, M.; Poteca, T.; Panea-Paunica, G.; Georgescu, S.-R.; Ion, R. M.; Popescu, S. M.; Giurcaneanu, C. *J. Med. Life.* **2013**, *6*, 50.

These radicals have very short lifetime (about 1 ns) and instantaneously react with molecules such as water and oxygen, producing hydrogen peroxide (H_2O_2), superoxide anion ($O_2^{\bullet-}$) and hydroxyl radical ($^{\bullet}OH$);[41] ideal PSs for type I process possess good electron donating ability, i.e. low oxidation potential. As for type II process, energy transfer occurs from PSs at T_1 to triplet oxygen ($^3O_2$), producing cytotoxic singlet oxygen ($^1O_2$). Type I and type II processes generally occur in parallel in PDT. Their ratio depends on PSs concentrations, properties of PSs and substrates, and is closely related to environment.

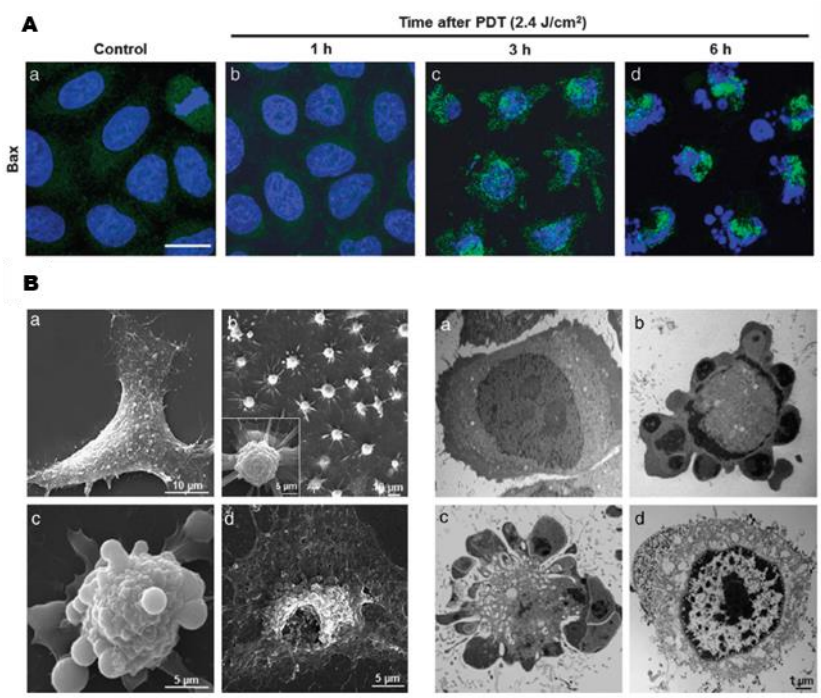

Figure 1.6. (A) Apoptosis induction after 1 h treatment with Ps followed by irradiation in HeLa cells. (B) Cell morphological changes of HeLa cells incubated 1 h with PS and subjected to light irradiation, visualized by scanning electron microscopy (SEM).

In general, appropriate concentration of ROS supports normal cellular proliferation and homeostasis.[42] They could modify protein structures and protect

[41] Wang, Y.-Y.; Liu, Y.-C.; Sun, H.; Guo, D.-S. *Coord. Chem. Rev.* **2019**, *395*, 46.
[42] Zhou, Z.; Song, J.; Nie, L.; Chen, X. *Chem. Soc. Rev.* **2016**, *45*, 6597.

cells from invading organisms. In order to regulate the concentration of ROS at a moderate level, an antioxidant system is involved in cells, including enzymes such as superoxide dismutase and non enzymatic chemicals such as glutathione and vitamin C. However, once the balance between ROS generation and detoxification is disturbed, cellular constituents would be damaged by oxidation, which is the core idea of PDT. PDT-mediated oxidative cytotoxicity induces tumour tissue destruction via cell apoptosis or necrosis, vascular damage, and inflammation-mediated immune response (**Figure 1.6**).[43]

Photosensitizers. A PS should ideally be a single pure compound with low manufacturing costs and good stability in storage. It should have a strong absorption peak in the red to near-infrared spectral region (between 650 and 800 nm) and should possess a substantial triplet quantum yield leading to good production of ROS upon irradiation. It should have no dark toxicity and relatively rapid clearance from normal tissues, thereby minimizing the side effects of phototoxicity.[44]

In the past few years, many molecules have been reported for PDT, especially porphyrins, phtalocyanines, etc (**Figure 1.7**). Tetrapyrrole backbones occur naturally in several important biomolecules such as haemoglobine, chlorophyll and bacteriochlorophyll. As the double-bonds are successively reduced when moving from backbones that are porphyrins to chlorins to bacteriochlorins the emission band is substantially red-shifted and the height of the band also increases. Phthalocyanines also have a large band in the 670 nm region.[45] Several compounds belonging to this first generation of PSs, such as the hematoporphyrin derivative HpD (Photofrin), are already in clinical use or in clinical trials to treat cancer patients and are approved by the Food and Drug

[43] Dolmans, D. E.; Fukumura, D.; Jain, R. K. *Nat. Rev. Cancer* **2003**, *3*, 380; Acedo, P.; Stockert, J. C.; Cañete, M.; Villanueva, A. *Cell Death Dis.* **2014**, *5*, 1122.
[44] Allison, R. R.; Sibata, C. H. *Photodiagn. Photodyn.* **2010**, *7*, 61.
[45] Abrahamse, H.; Hamblin, M. R. *Biochem J.* **2016**, *473*, 347.

Administration for the palliative treatment of obstructive lung and esophageal cancers.[46]

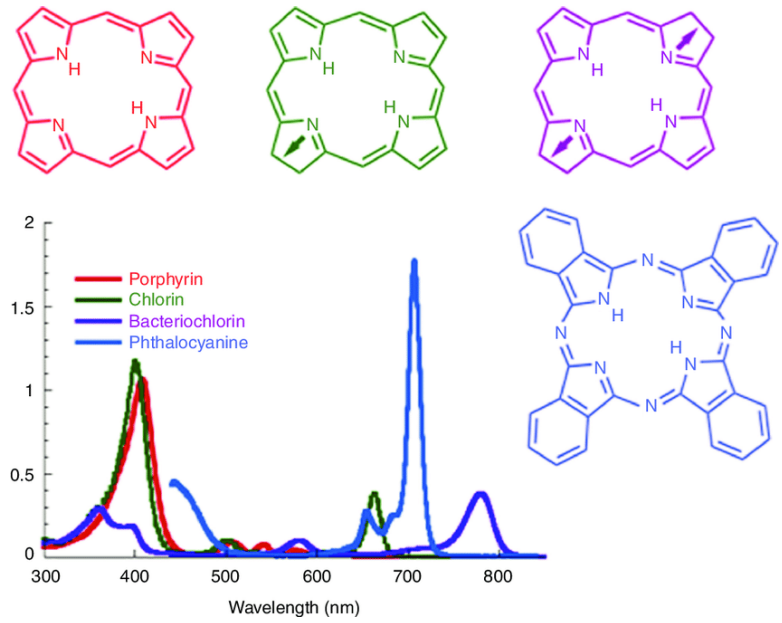

Figure 1.7. Absorption spectra of porphyrins, chlorins, bacteriochlorins, and phthalocyanines.

Moreover, porphyrins possess the characteristic of producing singlet molecular oxygen with high quantum yields after photoexcitation. Nowadays, numerous porphyrin-derivatives have been prepared for PDT, based on substitution pattern of the chromophore and inner heavy atom. Furthermore, several other natural products, such as, riboflavin[47] (vitamin B2, λ_{abs}=360 nm and 440 nm) and hypericin[48] (a long-known medicinal plant, λ_{abs}=600 nm) have been extensively explored as PSs. Moreover, in recent years, PDT has been improved by the synthesis of many other synthetic dyes (**Figure 1.8**), including methylene blue

[46] Agostinis, P.; Berg, K.; Cengel, K. A.; Foster, T. H.; Girotti, A. W.; Gollnick, S. O.; Hahn, S. M.; Hamblin, M. R.; Juzeniene, A.; Kessel, D.; Korbelik, M.; Moan, J.; Mroz, P.; Nowis, D.; Piette, J.; Wilson, B. C.; Golab, J. *Cancer. J. Clin.* **2011**, *61*, 250.

[47] Makdoumi, K.; Backman, A.; Mortensen, J.; Crafoord, S. *Graefes Arch. Clin. Exp. Ophthalmol.* **2010**, *248*, 207; Ettinger, A.; Miklauz, M. M.; Bihm, D. J.; Maldonado-Codina, G.; Goodrich, R. P. *Transfus Apher Sci.* **2012**, *46*, 153.

[48] Theodossiou, T. A.; Hothersall, J. S.; De Witte, P. A.; Pantos, A.; Agostinis, P. *Mol Pharm.* **2009**, *6*, 1775.

(phenothiazinium salt, **Figure 1.4**), rose Bengal and eosine Y (water soluble xanthene dyes), neutral red and acridine orange (phenazine dyes), crystal violet (triarylmethane), BODIPY dyes and transitions metal coordination complexes.[49]

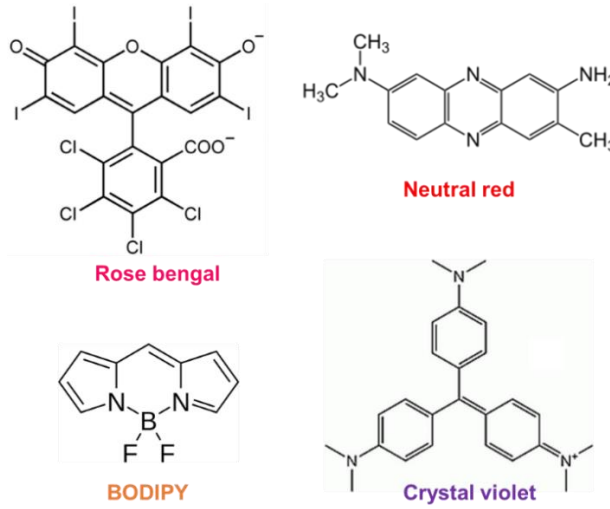

Figure 1.8

Recently, there also have been a large number of targeting studies in which PSs are covalently attached to various molecules that have some affinity for neoplasia or to receptors expressed on specific tumours.[50] The intention is to rely on the ability of the targeting vehicle to control localization so that the PS can be chosen based on its photochemical properties rather than on its tumour targeting properties, which are often unimpressive. These targeting vehicles include monoclonal antibodies,[51] peptides and proteins,[52] various carbohydrates,[53] folic acid[54] and many others.

[49] Ghorbani, J.; Rahban,D.; Aghamiri, S.; Teymouri, A.; Bahador, A. *Laser Ther.* **2018**, *27*, 293.
[50] Sibani, S. A.; McCarron, P. A.; Woolfson, A. D.; Donnelly, R. F. *Expert Opin. Drug. Deliv.* **2008**, *5*, 1241.
[51] Sato, K.; Nagaya, T.; Choyke, P. L.; Kobayashi, H. *Theranostics*. **2015**, *5*, 698.
[52] You, H.; Yoon, H. E.; Jeong, P. H.; Ko, H.; Yoon, J. H.; Kim, Y. C. *Bioorg Med Chem.* **2015**, *23*, 1453.
[53] Park, S. Y.; Baik, H. J.; Oh, Y. T.; Oh, K. T.; Youn, Y. S.; Lee, E. S. *Angew. Chem. Int. Ed. Engl.* **2011**, *50*, 1644.
[54] Li, D.; Li, P.; Lin, H.; Jiang, Z.; Guo, L.; Li, B. *J. Photochem. Photobiol. B.* **2013**, *127*, 28.

The first applications of glyco-OPEs in PDT are described in paragraph **1.3**.[55]

Up-converting nanoparticles and PDT. Many nanostructures such as plasmonic gold nanoparticles, mesoporous silica nanoparticles, carbon nanotubes, graphene, upconversion nanoparticles, fullerenes and quantum dots have found uses in PDT.[56]

In particular, upconverting nanoparticles (UCNPs) are a class of luminescent nanomaterials that can emit light with shorter wavelength than the excitation light.[57] This photophysical phenomenon is based on an anti-Stokes process and referred to as photon upconversion; that is, sequential absorption of two or more low-energy photons to populate real, intermediate excited electronic states followed by emission of a single high-energy photon (**Figure 1.9**).

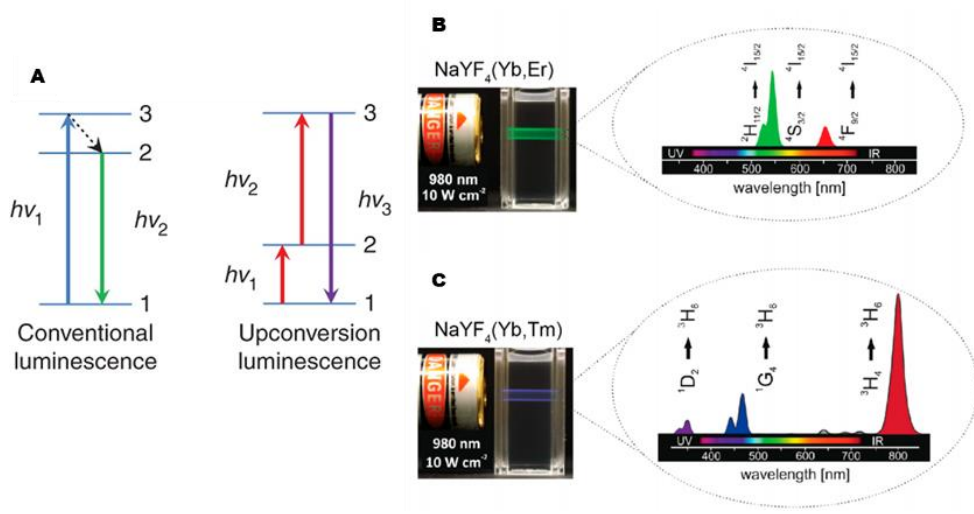

Figure 1.9. (A) Schematic representation of the conventional luminescence and upconversion luminescence processes. (B and C) Emission spectra of typical UCNPs upon Near-Infrared (NIR) excitation.

[55] Deni, E.; Zamarrón, A.; Bonaccorsi, P.; Carreño, M. C.; Juarranz, A.; Puntoriero, F.; Sciortino, M. T.; Ribagorda, M.; Barattucci A. *Eur. J. Med. Chem.* **2016**, *111*, 58.
[56] Huang, Y. Y.; Sharma, S. K.; Dai, T.; Chung, H.; Yaroslavsky, A; Garcia-Diaz, M.; Chang, J.; Chiang, L. Y.; Hamblin, M. R. *Nanotechnol. Rev.* **2012**, *1*, 111.
[57] Wilhelm, S. *ACS Nano* **2017**, *11*, 10644.

In conventional luminescence (**Figure 1.9.A**), the absorption of a high-energy photon (hv_1) by a system in the ground state can lead to promotion of the system to the excited state. The system can then undergo non-radiative decay to a lower-excited state, followed by relaxation to the ground state accompanied by the emission of a lower-energy photon (hv_2). In the upconversion process, the system in the ground state is initially promoted into the first excited state by an excitation photon and then is further excited into a higher-energy level by receiving energy from another excitation photon. Radiative transition of the excited state into the ground state leads to emission of a photon with higher energy than the individual excitation photon.[58]

In recent years, lanthanide-doped upconversion nanoparticles (Ln-UCNPs) have been developed as a new class of luminescent optical labels that have become promising for applications in biological assays and medical imaging. Generally, Ln-UCNPs are composed of a crystalline inorganic host and lanthanide dopants added to the host lattice in low concentrations [$NaMF_4$:$Ln3^+$, Yb^{3+} (M = Y or Gd) is the general structure], leading to the preparation of nanomaterials with well defined optical properties. These systems offer the possibility to irradiate with Near-Infrared (NIR) light (which deeper penetrates tissues), low autofluorescence background, large anti-Stokes shifts, sharp emission bands and high resistance to photobleaching. These optical properties make Ln-UCNPs attractive candidates for a variety of broad applications, including sensing, imaging, diagnosis, and therapy, as well as photovoltaic, security, and display technology.[59]

However, in comparison to conventional PSs, quantum yields of lanthanide-doped UCNPs are generally lower. Moreover, knowing that most effective PSs tend to be insoluble and hydrophobic, with a high propensity to aggregate, their conjugation and encapsulation in nano-drug carriers, could be useful to overcome

[58] Liu, Q.; Feng, W.; Yang, T.; Yi, T.; Li, F. *Nat. Protoc.* **2013**, *8*, 2033.
[59] Wilhelm, S. *ACS Nano* **2017**, *11*, 10644.

their complementary limitations. For this reason, UCNP-based PS delivery systems have recently been developed.[60] UCNPs are easy to synthesize, can support high loading volumes of therapeutic drugs (due to there are-to-volume ratios), have a small size (so easily accumulate in cells) and their surface chemistry allows further functionalization (e.g. with biomolecules for selective targeting of cancer tissues). In a UCNP drug delivery-based approach, a PS is either encapsulated or immobilised on the NPs surface using covalent or non-covalent interactions to form a nano-photosensitizer (NPPS).[61] Then, the surface functionalization of PS nano-drug with biomolecules, polymers, lipids, protein, polysaccharides or targeting receptors moieties, overexpressed in tumour cells, guarantees high selectivity, allowing active uptake only in cancer cells and minimizing damage and toxicity to normal tissues.

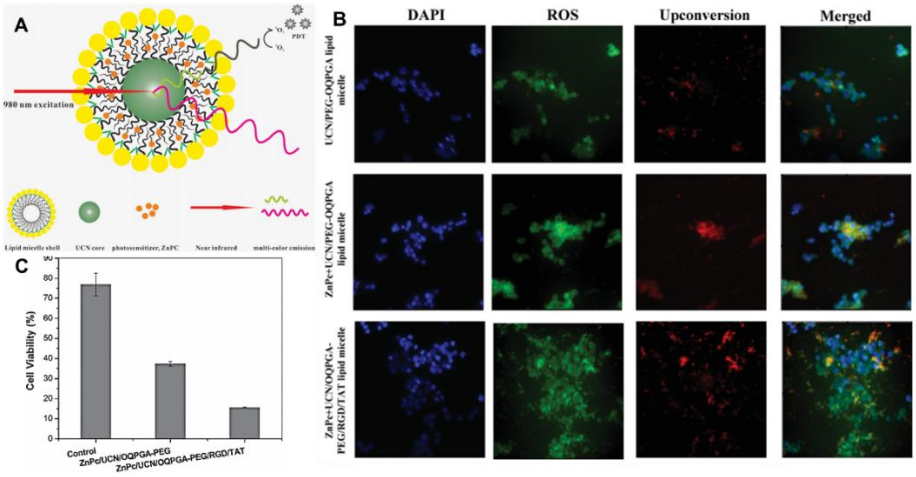

Figure 1.10. (A) Schematic picture of the lipid micelles encapsulating both the photosensitizer ZnPc and UCNs for simultaneous PDT and fluorescence imaging. (B) ROS production in cells PDT treated with various lipid micelle nanoparticles. Cells were labelled with carboxy-H_2DCFDA that fluoresces when oxidized in the presence of reduced oxygen species (green). Nuclei were counterstained with DAPI (blue), and the nanoparticles are shown by their red fluorescence colour. (C) Efficacy of PDT treatment assessed by measuring cell viability.

[60] Kruger, C. A.; Abrahamse, H. *Molecules* **2018**, *23*, 2628.
[61] Calixto, G. M.; Bernegossi, J.; de Freitas, L. M.; Fontana, C. R.; Chorilli, M. *Molecules* **2016**, *21*, 342.

For instance, in 2014 Wang *et al*.[62] reported the encapsulation of UCNPs, functionalized with the photosensitizer zinc phthalocyanine (ZnPc) into lipid micelles (**Figure 1.10**). It was demonstrated that by increasing the amount of ZnPc loaded in the nanoparticles, their red fluorescence is significantly quenched because of the energy transfer from the UCNs to the Ps ZnPc, while the lipid shell is essential to help the system to cross the cell membrane.

1.2.C DNA-targeted drugs and sensors. Deoxyribonucleic acid (DNA) is a natural product of an enormous importance for understanding the mechanism of genetic processes such as growth, differentiation and aging of the cell. Binding of small organic and inorganic molecules to DNA can influence numerous biological processes in which DNA participate, like transcription and replication. These processes begin when DNA receives the signal from regulatory protein, which binds to its particular part. If, instead of the regulatory protein, some other small molecule binds to DNA, its function is artificially changed – inhibited or activated.[63] Such interference can retard or even prevent the cell growth, or, on the other hand, it can lead to excessive production of some protein and uncontrolled cell growth. Extensive chemical and biochemical studies have characterised a variety of DNA interacting molecules which are classified as antibiotic, antitumor, antiviral or antiprotozoal agents.

Drugs interact with DNA helix both covalently and non-covalently. Covalent binding in DNA is irreversible and undoubtedly leads to complete inhibition of DNA functions and subsequent cell death. A major advantage of covalent binders is the high binding strength. Moreover, covalent bulky adducts can cause DNA backbone distortion, which in turn can affect both transcription and replication, by disrupting protein complex recruitment.[64] The most famous

[62] Wang, H. J.; Shrestha, R.; Zhang, Y. *Part. Part. Syst. Charact.* **2014**, *31*, 228.
[63] Aleksić, M. M.; Kapetanović, V. *Acta Chim. Slov.* **2014**, *61*, 555.
[64] Liu, H. K.; Sadler, P. J. *Acc. Chem. Res.* **2011**, *44*, 349.

covalent binder is cisplatin, [65] which is used as an anticancer drug since it is able to induce apoptosis and necrosis of the cancer cell. On the other hand, non-covalent binding of drugs to DNA is reversible, and considering drug metabolism and potential toxic effects, it is more desirable comparing to covalent. However, non-covalent DNA interacting agents can change DNA conformation, DNA torsional tension, interrupt protein–DNA interaction, and potentially lead to DNA strand breaks. One of the main principles of DNA chemistry is molecular recognition, the process when molecules (small or large) selectively recognize each other. This is manifested through a couple of interaction modes: electrostatic, hydrogen bonds, and van der Waals (dipole–dipole) interaction. The stability of the formed complex DNA–drug depends on the intensity of the mentioned interactions.

Drugs that react non-covalently with DNA are classified in the following categories (**Figure 1.11**):[66]

1. Intercalating agents
2. Minor groove binders
3. Major groove binders
4. Electrostatic binders

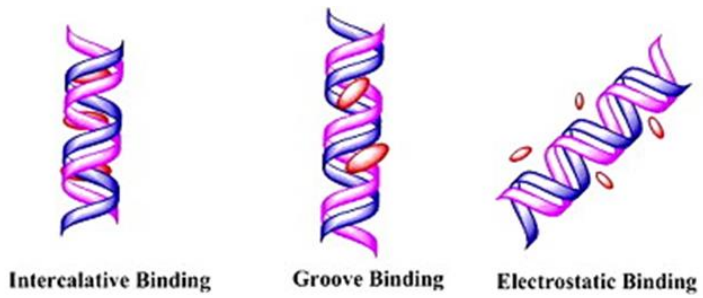

Figure 1.11

[65] Jakupec, M. A.; Galanski, M.; Keppler, B. K. *Rev. Physiol. Biochem. Pharmacol.* **2003**, *146*, 1.
[66] Ni, Y.; Lin, D.; Kokot, S. *Anal. Biochem.* **2006**, *352*, 231.

Intercalators are molecules that stack perpendicular to the DNA backbone without forming covalent bonds and without breaking up the hydrogen bonds between the DNA bases. The only known forces that sustain the stability of the DNA–intercalator complex, even more than DNA alone, are van der Waals, hydrogen bonding, hydrophobic, and/or charge transfer forces. Intercalation stabilizes, lengthens, stiffens, and unwinds the DNA double helix.[67] Intercalators contain planar heterocyclic groups, which stack between adjacent DNA base pairs, forming complex which is stabilized by π–π stacking interactions between the drug and DNA. The phenomenon of intercalation involves the aromatic part of a drug molecule positioning itself between base pairs. These agents introduce strong structural perturbations in DNA molecule by increasing the distance between the adjacent base pairs. In order for an intercalator to fit between base pairs, the DNA must dynamically open a space between its base pairs. Stacking interactions between the bases and the intercalating molecule are the major stabilising factors for the complex formed.

The most famous groove binding drugs usually have shape which is complementary to the shape of the groove,[68] and facilitates binding by promoting van der Waals interactions. These drugs typically have several aromatic rings, such as pyrrole, furan or benzene connected by bonds possessing torsional freedom. Additionally, these drugs can form hydrogen bonds to bases, typically to adenine/thymine rich sequences. In all complexes, the drug fits closely into the minor groove and displaces the hydration layer. The loss of water-mediated hydrogen bonding, which acts as a major complex stabilising force in DNA, leads to serious perturbations of the DNA helix from the normal geometry and induces changes in the conformation of the groove.

Finally, some ligands are capable of forming non-specific, external electrostatic interactions with the DNA phosphate backbone. This mode usually

[67] Bauer, W.; Vinograd, J. *J. Mol. Biol.* **1970**, *54*, 281.
[68] Moravek, Z.; Neidle, S.; Schneider, B. *Nucleic Acids Res.* **2002**, *30*, 1182.

occurs when the ligand self-associates to form higher-order aggregates, which may stack on the anionic DNA backbone in order to reduce charge–charge repulsion between ligand molecules. Some metal complexes interact with DNA through external binding. This association mode was proposed for $[Ru(bpy)_3]^{2+}$ as the luminescence enhancement of this complex upon binding to DNA is strongly dependent on the ionic strength.[69]

DNA is highly polymorphic and can adopt different motifs such as the A-form, left-handed Z-form, triplexes, G-quadruplexes, i-motif and unpaired DNA structures.[70] These unique DNA conformations make DNA a critical binding target for small molecules and allow for regulation of DNA function. As a consequence, enormous interest exists in developing small molecules that can bind and react with DNA. Over the past few decades, small molecules that bind to DNA have shown significant promise as diagnostic probes, reactive agents and therapeutics.[71]

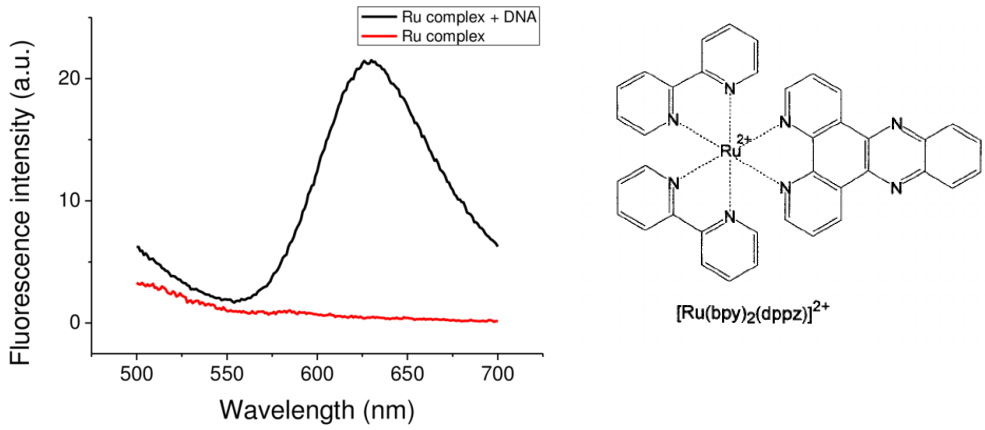

Figure 1.12. Fluorescence emission spectra of 10 μM $Ru(bpy)_2(dppz)^{2+}$ in the absence (red line) and presence (black line) of 10 μM DNA.

In particular, in 1990, Barton *et al*. first reported that $[Ru(bpy)_2dppz]^{2+}$ (bpy = 2,2′-bipyridine, dppz = dipyrido[3,2-a:2′,3′-c]phenazine) could serve as a non-

[69] Kelly, J. M.; Tossi, A. B.; McConnell, D. J.; OhUigin, C. *Nucl. Acids Res.* **1985**, *13*, 6017.
[70] Gueron M.; Leroy, J. L. *Curr. Opin. Struct. Biol.* **2000**, *10*, 326.
[71] Li, G.; Sun, L.; Ji, L.; Chao, H. *Dalton Trans.* **2016**, *45*, 13261.

radioactive luminescent DNA probe.[72] This complex shows no photoluminescence in aqueous solution at ambient temperature but displays intense photoluminescence in the presence of double-helix DNA, with an enhancement factor of >104 (**Figure 1.12**). This phenomenon, which is known as the DNA "light-switch" effect, has attracted much attention and has been used extensively to study the interaction of small molecules and metal complexes with DNA.

1.2.D pH fluorescent indicators. Intracellular pH (pH_i) plays many critical roles in cell, enzyme, and tissue activities, including proliferation and apoptosis, ion transport, endocytosis, and muscle contraction.[73] Monitoring pH changes inside living cells is also important for studying cellular internalization pathways, such as phagocytosis, endocytosis, and receptor ligand internalization. Cells and their components usually have different pH values, such as cytoplasm (pH 6.8−7.6), nucleus (around pH 7.6), lysosomes and endosomes (pH 4.5−6.0), mitochondria (pH 7.8–7.9), and Golgi (pH 6.4–6.8).[74] Intracellular pH (pH_i) regulates a number of cell metabolism processes: for instance, low intracompartmental pH values can serve to denature proteins or to activate enzyme and protein functions that would be too slow around pH 7.0. Cellular dysfunction is often associated with abnormal pH values in cells and organelles: for example, changes of pH_i effect the nervous system, by influencing synaptic transmission, neuronal excitability and signal cascades. Moreover, abnormal pH_i values are associated with inappropriate cell function, growth, and division and are observed in some common disease types such as cancer and Alzheimer's. In fact, acidic extracellular pH is a major feature of tumour tissue; extracellular acidification is primarily considered to be due to lactate secretion from anaerobic

[72] Friedman, A. E.; Chambron, J. C.; Sauvage, J.-P.; Turro, N. J.; Barton, J. K. *J. Am. Chem. Soc.* **1990**, *112*, 4960.
[73] Han, J.; Burgess, K. *Chem. Rev.* **2010**, *110*, 2709.
[74] Cody, S. H.; Dubbin, P. N.; Beischer, A. D.; Duncan, N. D.; Hill, J. S.; Kaye, A. H.; Williams, D. A. *Micron* **1993**, *24*, 573.

glycolysis (paragraph **1.1**) and it is thought to increases the expression of some genes involved with pro-metastatic factors.[75] Thus, intimate connections between the cell functions with intracellular pH means that precise measurement of intracellular pH can provide critical information for studying physiological and pathological processes down to cells and organelles.

As seen in paragraph **1.2.A**, fluorescence techniques have high sensitivities, tend to be operationally simple, and are, in most cases, non-destructive to cells. Compared to other methods such as microelectrodes, NMR, and absorption spectroscopy for sensing pH_i, fluorescence spectroscopy has several advantages: (1) high spatial-temporal resolution, which can monitor the dynamic change of pH_i; (2) non-invasive feature in most cases, which would not disturb the normal pH_i; (3) simplicity.[76] These advantages make fluorescence spectroscopy a widely used method for sensing pH_i, and thus excellent fluorescent pH probes attract the extensive and frequent attention. Qualitative measurements of pH_i can be achieved using fluorescent indicators that switch (ON/OFF or OFF/ON) or shift their emission at sharply defined pH values. To achieve high sensitivity and accuracy, the designed pH probe should have a pKa value that matches the pH of the specific cell organelle. Moreover, in addition to sensitivity and selectivity, some special properties of fluorescent probes are highly desired for sensing pH_i, such as wavelength, brightness, permeability, and so on.[77] The excitation and emission wavelengths are the key parameters of fluorophores: light with short wavelength often causes significant photobleaching, severe biological autofluorescence and damage; on the contrary, fluorophores with long wavelength can effectively avoid these problems. In addition, large difference between excitation and emission wavelength (Stokes shift) is favourable for decreasing autofluorescence as well. Therefore, various fluorescent pH probes

[75] Kato, Y.; Ozawa, S.; Miyamoto, C.; Maehata, Y.; Suzuki, A.; Maeda, T.; Baba, Y. *Cancer Cell Int.* **2013**, *13*, 89.
[76] Wencel, D.; Abel, T.; McDonagh, C. *Anal. Chem.* **2014**, *86*, 15.
[77] Shi, W.; Li, X.; Ma, H. *Methods Appl. Fluoresc.* **2014**, *2*, 042001.

with near infrared (NIR) and/or large Stokes shift features have aroused great interest in this area. As regards brightness (Bs) (Bs = ε × Φ; ε=molar absorptivity and Φ=quantum yield), brighter fluorophores show higher signal-to-noise ratios and require less dosage and weaker excitation light, diminishing cell damages.

Typically, three types of response mechanisms for fluorescent probes can be used: fluorescence quenching (ON/OFF), fluorescence enhancement (OFF/ON) and ratiometry, which exploits dyes that can absorb or emit light at two different wavelengths.[78] The fluorescence ON/OFF probes show less practicability because of their high background and poor selectivity. Fluorescence OFF/ON probes, as compared to ON/OFF or ratiometric probes, have the advantage of the ease detection of low-concentration contrast relative to a near dark background, which is very desired for qualitative analysis due to the high sensitivity.

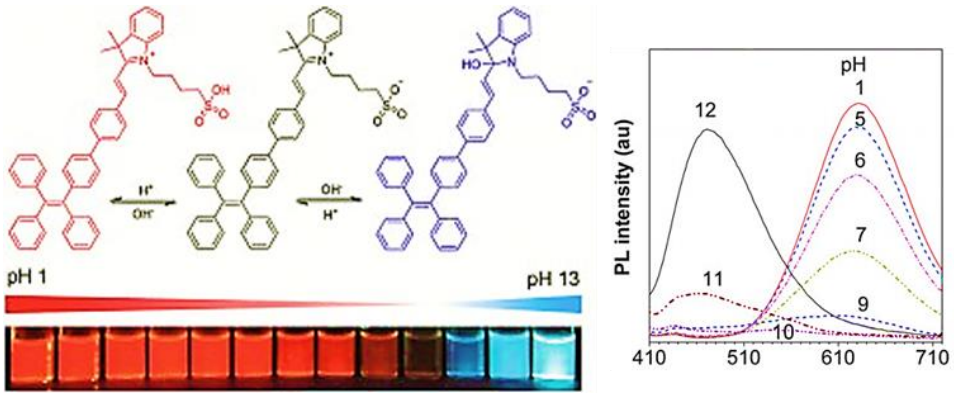

Figure 1.13. Emission spectra of a cyanine-based dye in aqueous solutions at different pH values.

However, for imaging studies in cells, the intensity-based fluorescence probes suffer easily from the influence of many variants, such as probe concentration, instrumental efficiency, and environmental conditions. To address these issues, ratiometric fluorescent probes are preferred. They exhibit different

[78] Shi, W.; Li, X.; Ma, H. *Methods Appl. Fluoresc.* **2014**, *2*, 042001.

responses to an analyte (e.g. pH) at two different excitation/emission wavelengths. The simultaneous recording the fluorescence intensities at the two wavelengths and the calculation of their ratio can provide more accurate measurement than that at only one wavelength (**Figure 1.13**).[79]

Moreover, to obtain the intact information about pH_i, fluorescent probes would better non-destructively enter cells and have less leakage from the cells. A typical strategy to achieve this is to mask the charged groups (e.g. carboxyl) with neutral acetoxymethyl esters. The resulting probes can diffuse into cells and then are hydrolysed by intracellular esterases to afford the free, charged probes, on which the charges facilitate the probe stay in cells.[80] Another strategy for delivering a probe is to take advantage of the ligand-receptor interactions, especially for nanoprobes. The receptors in cellular membrane can bind with specific ligands and then transport the ligands into cytoplasm. In this way, if the nanoprobes are modified with these kinds of ligands, they can be easily internalized into cells through the ligand-receptor interactions.

Finally, the pK_a values of probes are strongly dependent on the microenvironment of media, such as ionic strength, viscosity, and coexisting substances.[81] For instance, many pH probes can bind with proteins, causing a change in their pK_a values and thus a large error in pH measurements. To decrease the microenvironmental influence, the interference from coexisting substances (e.g. metal ions, proteins, etc) should be studied carefully, and the pH calibration curve in cells (cytosol) instead of in plain buffer solution should be established for the calculation of pH_i values.

[79] Li, X. H.; Gao, X. H.; Shi, W. Ma, H. M. *Chem. Rev.* **2014**, *114*, 590; Chen, S.; Liu, J.; Liu, Y.; Su, H.; Hong, Y.; Jim, C. K. W.; Kwok, R. T. K.; Zhao, N.; Qin, W.; Lam, J. W. Y.; Sing Wong, K.; Zhong Tang, B. *Chem. Sci.* **2012**, *3*, 1804.
[80] Tsien, R. Y. *Nature* **1981**, *290*, 527.
[81] Miao, F.; Song, G. F.; Sun, Y. M.; Liu, Y.; Guo, F. Q.; Zhang, W. J.; Tian, M. G.; Yu, X. *Biosens. Bioelectron.* **2013**, *50*, 42.

Fluorescein[82], cyanines[83] and their derivatives are the most widely used pH probes. However, many other organic molecular pH probes have been recently, developed, such as naphthalimide derivatives,[84] lanthanide complexes,[85] BODIPY dyes, carbazoles,[86] quinolines[87] and other fluorophores. Most of them exhibit ratiometric response to pH and have been used to sensing the change of pH_i under different conditions. However, it should be pointed out that pH probes with a wide linear response range are still rare. To increase the response range of pH, a useful strategy is to design a probe with multiple H^+ binding sites by assembling several electronegative atoms (e.g. N and/or O) in the different positions of a conjugated molecule.[88]

Moreover, Horiuchi *et al*.[89] recently applied the properties of different pH-sensitive aniline moieties to the synthesis of porphyrin derivatives that could be used as photosensitizers in PDT. In fact, in this kind of therapy, the tumour specificity is very important to minimize photo-induced side effects. One of the major strategies to improve the tumour specificity is to develop activatable photosensitizers.[90] The fluorescence and $^1O_2$ sensitization efficiencies of activatable photosensitizers are inefficient in normal tissues. However, a certain trigger in the tumour tissue can modify the photosensitizer's chemical properties, increasing the fluorescence and $^1O_2$ sensitization efficiencies. As triggers for the tumour selectivity, activation in low-pH cancer cells condition has been proposed.

---

[82] Venn, A. A.; Tambutté, E.; Lotto, S.; Zoccola, D.; Allemand, D.; Tambutté, S. *Proc. Natl Acad. Sci. USA* **2009**, *106*, 16574.
[83] Li, P.; Xiao, H. B.; Cheng, Y. F.; Zhang, W.; Huang, F.; Zhang, W.; Wang, H.; Tang, B. *Chem. Commun.* **2014**, *50*, 7184.
[84] Hu, J. L.; Wu, F.; Feng, S.; Xu, J. H.; Xu, Z. H.; Chen, Y. Q.; Tang, T.; Weng, X. C.; Zhou, X. *Sensor. Actuat. B-Chem.* **2014**, *196*, 194.
[85] Fan, L.; Liu, Q. L.; Lu, D. T.; Shi, H. P.; Yang, Y. F.; Li, Y. F.; Dong, C.; Shuang, S. M. *J. Mater. Chem. B* **2013**, *1*, 4281.
[86] Miao, F.; Song, G. F.; Sun, Y. M.; Liu, Y.; Guo, F. Q.; Zhang, W. J.; Tian, M. G.; Yu, X. Q. *Biosens. Bioelectron.* **2013**, *50*, 42.
[87] Huang, W. M.; Lin, W. Y.; Guan, X. Y. *Tetrahedron Lett.* **2014**, *55*, 116.
[88] Su, M. H.; Liu, Y.; Ma, H. M.; Ma, Q. L.; Wang, Z. H.; Yang, J. L.; Wang, M. X. *Chem. Commun.* **2001**, *11*, 960.
[89] Horiuchi, H.; Hirabara, A.; Okutsu, T. *J. Photoch. Photobio. A.* **2018**, *365*, 60.
[90] Lovell, J. F.; Liu, T. W. B.; Chen, J.; Zheng, G. *Chem. Rev.* 2010, *110*, 2839.

These activatable photosensitizers can minimize erroneous diagnoses and photo-induced side effects.

1.3 OLIGO(PHENILENE ETYNYLENE)s

Oligo(phenylene-ethynylenes) (OPEs) and the corresponding polymers, Poly(phenyleneethynylenes) (PPEs), represent a peculiar class of luminescent dyes with stable π-conjugated rigid rod-like skeletons.[91] In particular, their structure is a succession of aromatic rings linked by carbon-carbon triple bonds (**Figure 1.14**). This feature guarantees a high electronic conjugation and, consequently, their photochemical properties evidence high quantum yields and luminescence features. The synthetic approaches leading to the construction of these oligomers allow easy functional group manipulation and make modulable their functional features. Their tunable properties depend not only on their molecular structure, but also on the supramolecular interactions and on the aggregation of the chains both in solution and in the solid state.[92] OPEs and PPEs have attracted for the above mentioned reasons significant attention in the scientific community and, in the last decades, have been widely applied in organic electroluminescent light emitting devices, molecular electronic switches, nonlinear optical materials, biological sensors.

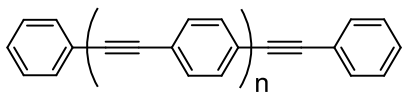

Figure 1.14

The photophysical properties of OPEs are directly connected to their extensive conjugation. Modulation of these properties depends on their structure

[91] Bunz, U. H. F. *Chem. Rev.* **2000**, *100*, 1605.
[92] Waters, M. L. *Curr. Opin. Chem. Biol.* **2002**, *6*, 736.

and on substitution on the aromatic conjugated skeleton. In 2011, Dehaen e*t al*.[93] reported that, on increasing the number of phenyl acetylene units, varying from 1 to 7, the absorption and emission maxima of OPEs are increasingly redshifted; this effect becomes smaller with each addition of a repeating unit. Moreover, it was demonstrated that the introduction on the chain of moieties bearing a lone pair could influence the photophysical properties of phenylenethynylene-based systems.

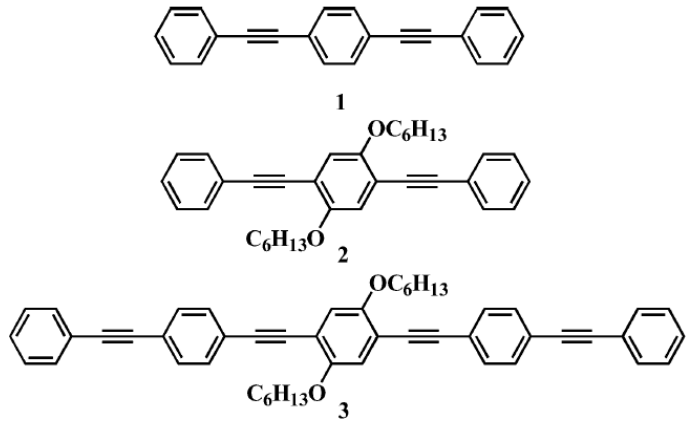

Figure 1.15

In fact, the synthesis of 2,5-dialkoxy-substituted derivatives of OPEs[94] leads to lower-wavelength absorbing and emitting systems, with respect to unsubstituted compounds (**Figure 1.15**), and to the increase of the molar extinction coefficient and emission quantum yields; for this reason, these molecular systems are now widely used as building blocks for various functional molecular materials.

Furthermore, in 2005 Yamaguchi *et al*.[95] reported a study about spectroscopic features of OPEs (absorption and emission wavelengths, quantum yield Φ_f, lifetime τ) and their behaviour when the π-conjugated molecular rods

[93] Yin, S.; Leen, V.; Jackers, C.; Beljonne , D.; Van Averbeke, B.; Van der Auweraer, M.; Boens, N.; Dehaen, W. *Chem. Eur. J.* **2011**, *17*, 13247.
[94] James, P. V.; Sudeep, P. K.; Suresh, C. H.; George Thomas, K. *J. Phys. Chem. A* **2006,** *110,* 4329.
[95] Yamaguchi, Y.; Tanaka, T.; Kobayashi, S.; Wakamiya, T.; Matsubara, Y.; Yoshida, Z.-i. *J. Am. Chem. Soc.* **2005**, *127*, 9332.

consisting of *p*-(phenylene)ethynylene units were modified by donor (OMe) and/or acceptor (CN) groups situated at the aromatic rings. They reported three different cases: (1) side-donor modification systems (SD systems), (2) side-acceptor modification systems (SA systems), and (3) systems consisting of donor blocks and acceptor blocks (BL systems, **Figure 1.16**).

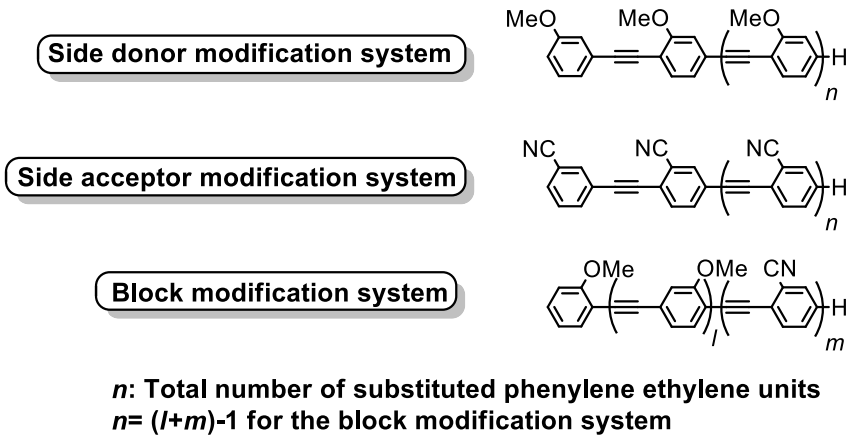

Figure 1.16

The best values in terms of Φ_f, were obtained for the block modification systems (BL,Φ_f>0.95). This result evidenced that the building of a push-pull system (paragraph **2.5B**) by combination of electron donating and electron withdrawing groups in the same skeleton strongly influences the photophysical properties of the OPEs. On the other side, the values of quantum yields obtained for the systems functionalized with –OMe in the side donor moiety (SD) or with –CN in the side acceptor fragment, (SA) were higher (Φ_f>0.90). Moreover, the study of the trend of bathochromic shift of emission (λ_{em}), compared to the elongation of aromatic chain and the introduction of the electron withdrawing groups, showed the shift of λ_{em} toward higher wavelengths for the largest OPEs systems and for the ones containing the acceptor moieties.

Another appealing property of OPEs corresponds to their possibility to generate singlet oxygen ($^1O_2$) (**Figure 1.17**). The study by Monnereau and

Andraud,[96] reported in 2012, highlighted this characteristic of the OPEs systems through the synthesis of a series of compounds containing two amino groups as chain terminations.

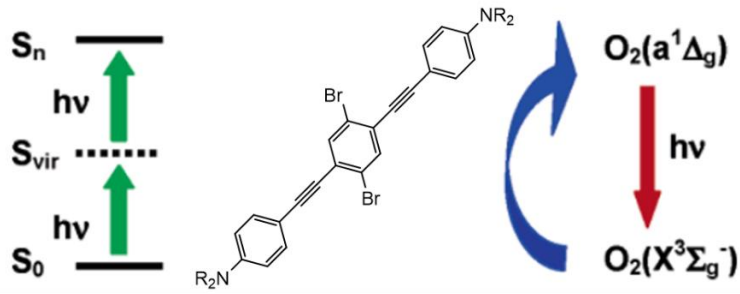

Figure 1.17

It was demonstrated, by the detection of the characteristic $\Delta^1O_2 \rightarrow \Sigma^3O_2$ phosphorescence at 1270 nm, that all the compounds generated singlet oxygen and that the presence of the "heavy-atom" bromine on the aromatic rings has an advantageous effect on the singlet oxygen production yield. Moreover, fluorescence quantum yields and lifetimes evolved opposite to the $^1O_2$ generation quantum yield. This result gave the possibility to use OPEs as photosensitizers in Photodynamic Therapy (paragraph **1.2.B**), and showed that these are molecules possessing an accessible triplet excited state able to generate singlet oxygen by an energy transfer to ground state oxygen, ultimately leading to cell death.

Biological applications of OPEs. While in the last decades OPEs showed a rapid development in optoelectronic devices, their use for biomedical applications has more recently gained increasing attention.[97]Specifically, they have found innovative applications in a variety of biotechnologies, ranging from biosensing,[98]

[96]Lanoë, P. H.; Gallavardin,T.; Dupin,A.; Maury, O.; Baldeck, P. L.; Lindgren, M.; Monnereau C.; Andraud, C. *Org. Biomol. Chem*. **2012**, 10, 6275.
[97] Liu, B. *Conjugated Polymers for Biological and Biomedical Applications* **2018**, Wiley-VCH.
[98] Feng, X.; Liu, L.; Wang, S.; Zhu, D. *Chem. Soc. Rev.* **2010**, *39*, 2411.

cell imaging sensing,[99] DNA detection,[100] enzyme activity assays,[101] biocides[102] and as stains for amyloid.[103]

For instance, in 2012 Whitten *et al.*[104] reported the use of cationic end-only functionalized OPEs for preventing and eliminating Escherichia coli (E. coli) biofilms (**Figure 1.18**). This water soluble family of conjugated oligomers had affinity for bacterial cell membranes and exhibited light-activated biocidal activity, causing membrane disruption, agglomeration, and bacterial death.

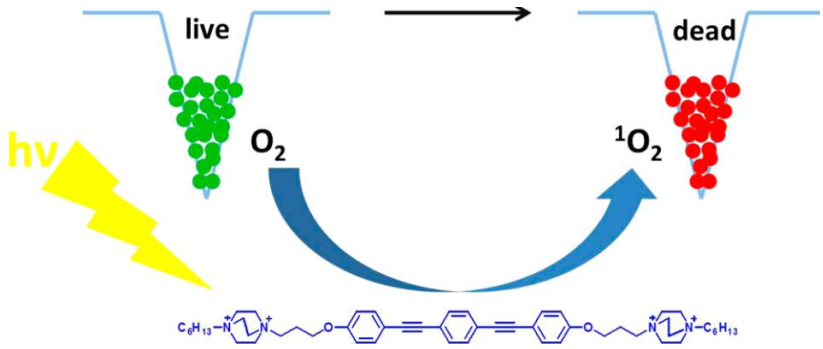

Figure 1.18

In a previous study, Whitten also reported a new protocol to detect sequence-specific DNA based on a related self-assembly between OPEs and DNA.[105] The OPE complexation with DNA causes red-shifted absorption and emission spectra, with an increased emission intensity with respect to the one of the considered OPE

[99] Ho Moon, J.; McDaniel, W.; MacLean, P.; Hancock, L. F. *Angew. Chem. Int. Ed.* **2007**, *46*, 822.
[100] Tang, Y.; Achyuthan, K. E.; Whitten, D. G. *Langmuir* **2010**, *26*, 6832.
[101] Hill, E. H.; Zhang, Y.; Evans, D. G.; Whitten, D. G. ACS *Appl. Mater. Interfaces* **2015**, *7*, 5550.
[102] Wang, Y.; Jett, S. D.; Crum, J.; Schanze, K. S.; Chi, E. Y.; Whitten, D. G. *Langmuir* **2013**, *29*, 781.
[103] Donabedian, P. L.; Pham, T. K.; Whitten, D. G.; Chi, E. Y. *ACS Chem. Neurosci.* **2015**, *6*, 1526; Fanni, A. M.; Monge, F. A.; Lin, C.-Y.; Thapa, A.; Bhaskar, K.; Whitten, D. G.; Chi, E. Y. *ACS Chem. Neurosci.* **2019**, *10*, 1813.
[104] Dascier, D.; Ji, E.; Parthasarathy, A.; Schanze, K. S.; Whitten, D. G. *Langmuir* **2012**, *28*, 11286.
[105] Tang, Y.; Achyuthan, K. E.; Whitten, D. G. *Langmuir* **2010**, *26*, 6832.

alone. Moreover, the different induced CD signals have been used to monitor sequence-specific DNA and single nucleotide mismatches in a real time assay.

Furthermore, the fluorescent sensing of two novel oligomeric *p*-phenylene ethynylenes for detecting prefibrillar and fibrillar aggregates of Alzheimer's disease (AD) associated amyloid-β and Parkinson's disease (PD) -associated α-synuclein proteins has been recently reported by the same group.[106] AD and PD are complex and multifactorial diseases, the misfolding and aggregation of largely intrinsically disordered proteins into highly ordered fibrillar amyloid aggregates is still recognized as a central pathogenic event. Compounds that bind specifically to amyloids tend to share a common "rigid conjugated rod" motif, where the linear shape and aromaticity favours binding to hydrophobic sites on the amyloid fibril. Thus, the synthesized OPEs have been shown to selectively bind to β-sheet enriched fibrillar aggregates made of the model amyloid protein hen egg white lysozyme (HEWL) and, OPEs exhibited fluorescence turn-on and red-shifted spectra. Furthermore, the performance of OPEs was evaluated and compared to thioflavin T (ThT), the most widely used fibril dye (**Figure 1.19**) and OPEs resulted to exhibit higher selectivity, higher binding affinity, and comparable limits of detection for Aβ40 fibrils compared to ThT.

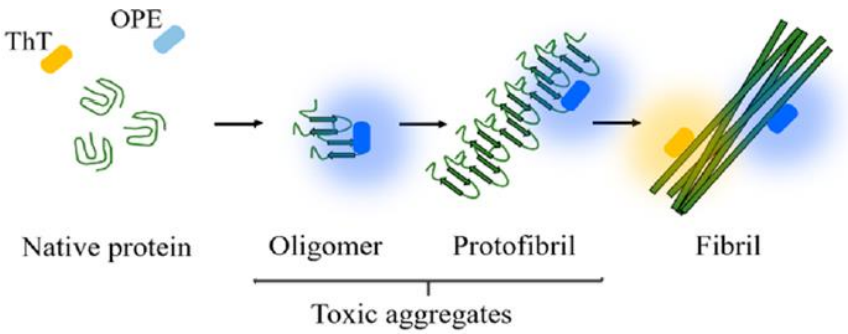

Figure 1.19

[106] Fanni, A. M.; Monge, F. A.; Lin, C.-Y.; Thapa, A.; Bhaskar, K.; Whitten, D. G.; Chi, E. Y. *ACS Chem. Neurosci.* **2019**, *10*, 1813.

Another very recent example is the one reported by Moon *et al.*[107], who studied water soluble phenyleneethynylene trimer-based rigid-flexible [2+2] macrocycles for nucleic acid labelling in live cells. As seen in paragraph **1.2.C**, fluorescent labelling of nucleic acids is an essential way of studying the function of live cells; moreover, selective labelling of nucleoli is important for studying cellular functions and processes since the number, morphology, and size of nucleoli are closely associated with the cell growth and metabolism. Thanks to their high quantum yields, the introduction of appropriate functional groups, which are responsible for the high water solubility, and their low molecular weight, these new macrocycles entered cells by fast diffusion through the cell membranes. In this case, the presence of mono alkyl ammonium side chains resulted essential for the penetration of the OPE macrocycle in the nuclear membrane. Furthermore, the fluorescence intensity profile in the confocal images (**Figure 1.20**) indicates high localization of the species in the nucleoli, which are the site for ribosomal RNA transcription and processing. Because structurally similar DNA is abundant in the nucleus, the bright nucleoli spots found inside the nucleus imply that the OPE macrocycle has better selectivity to RNA over DNA.

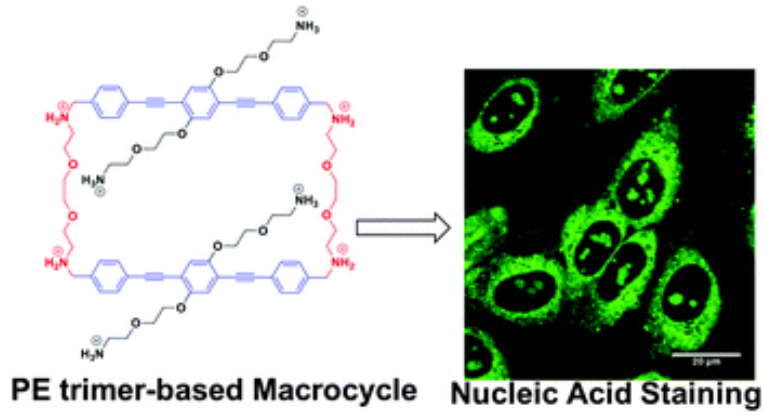

Figure 1.20

[107] Moon, J. H.; Manandhar, P.; Torabi, H.; Rohman, M. R.; Mathivathanan, L.; Lee, K. H.; Irle, S. *Chem. Commun.* **2019**, *55*, 5930.

As already seen in paragraph **1.1**, the conjugation with carbohydrates is one efficient strategy to increase the solubility and the biocompatibility of biologically active compounds and to specifically target them. With the aim to extend their biological applications, in 2013, the synthesis of a new class of sugar functionalized OPEs was described by Bernardi *et al*.[108] The copper(I)-catalyzed alkyne-azide cycloaddition (CuAAC) "click" cycloaddiction of ethynyl terminated OPE spacers, of variable length, with glycosil azides (**Figure 1.21**) led to the formation of the sugar terminated OPEs. The activity of the synthesized oligomers on bacterial adhesion inhibition has been demonstrated, choosing as the target, the bacterial lectin LecA, a virulence factor of the problematic pathogen Pseudomonas aeruginosa.

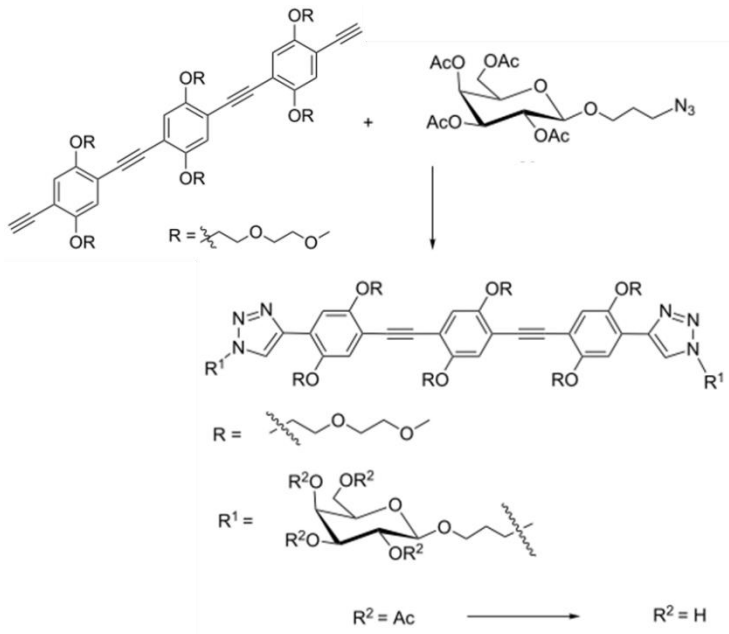

Figure 1.21

In the last years, my research group focused on the synthesis of differently substituted Oligo(phenylene ethynylene) (OPE) systems incorporating two

[108] Pertici, F.; Varga, N.; van Duijn, A.; Rey-Carrizo, M.; Bernardi, A.; Pieters, R. J. *Beilstein J. Org. Chem.* **2013**, *9*, 215.

glycosides at the external units (**Figure 1.19**).[109] It was chosen to synthesize differently elongated OPE chains in order to study the influence of the hydrophilic/hydrophobic balance, between the aromatic part and the glucosidic terminations, in the photophysical and biological behaviour of the different species. Moreover, with the aim to study the influence of a different aromatic substitution on the properties of these systems, the introduction of a basic NMe_2 group appeared to be really promising (**OPE_Glucose 1** in **Figure 1.22**).

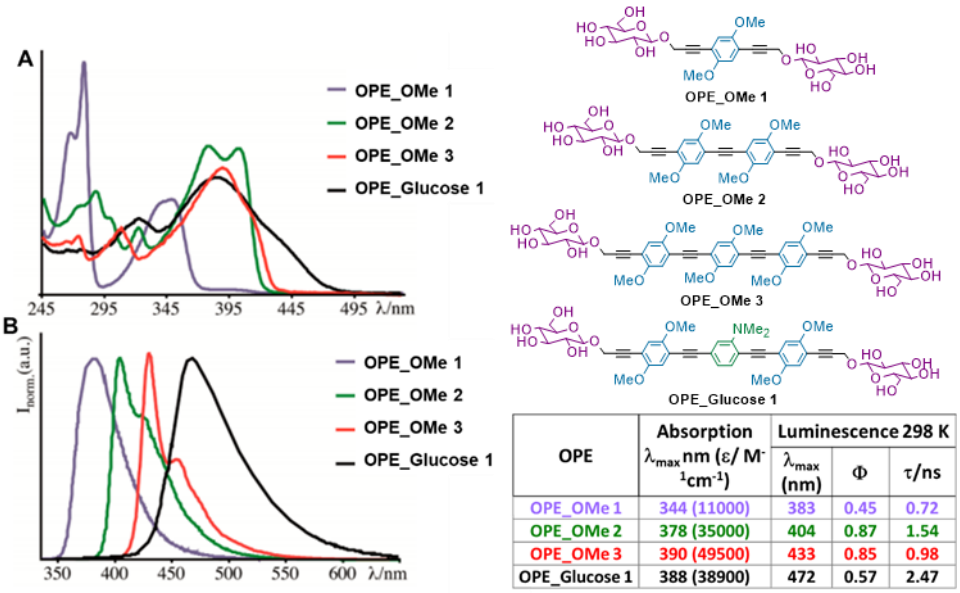

OPE	Absorption λ_{max} nm (ε/ $M^{-1}cm^{-1}$)	Luminescence 298 K λ_{max} (nm)	Φ	τ/ns
OPE_OMe 1	344 (11000)	383	0.45	0.72
OPE_OMe 2	378 (35000)	404	0.87	1.54
OPE_OMe 3	390 (49500)	433	0.85	0.98
OPE_Glucose 1	388 (38900)	472	0.57	2.47

Figure 1.22. (A) Absorption and (B) emission spectra of the reported glucoOPEs.

All the compounds are characterized by an intense absorption in the UV region, due to spin-allowed $\pi \rightarrow \pi^*$ transitions of the aromatic moieties.[110] A batochromic effect is observed by increasing the number of ethynylene aromatic moieties, as a consequence of the increased conjugation. The same effect is observed in the emission spectra: by increasing the chain length, the emission

[109] Barattucci, A.; Deni, E.; Bonaccorsi, P.; Ceraolo, M. G.; Papalia, T.; Santoro, A.; Sciortino, M. T.; Puntoriero F. *J. Org. Chem.* **2014**, *79*, 5113.
[110] Lanoë, P.-H.; Gallavardin, T.; Dupin, A.; Maury, O.; Baldeck, P. L.; Lindgren, M.; Monnereau, C.; Andraud, C. *Org. Biomol. Chem.* **2012**, *10*, 6275.

energy decreases whereas the emission quantum yield doubles. The insertion of one electron-donating group (NMe_2) on the central subunit of the oligomer **OPE_Glucose 1** shifts the luminescence to the red, while the quantum yield decreases.

The cell internalization experiments for the OPE compounds on HEp-2 cells (cells from epidermoid carcinoma larynx tissue) showed that **OPE_Glucose 1** is massively uptaken, showing the main localization in vesicles within the cytoplasmic compartment (**Figure 1.23**).The observations and experimental results allowed to conclude that the massive internalization of **OPE_Glucose 1** is due to the synergic effect of several contributions: 1) elongation of the hydrophobic chain; 2) substitution of the aromatic central ring with a dimethylamino group instead of a bis-methoxy moiety; 3) presence of the sugar moieties, improving the hydrophilicity.

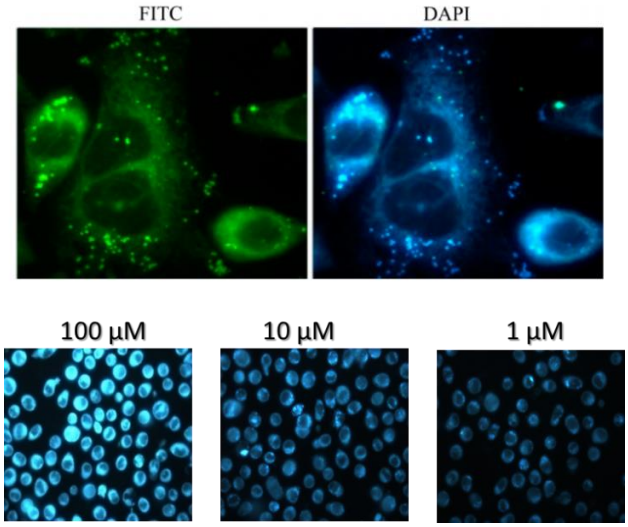

Figure 1.23. Fluorescence microscopy images of Hep-2 cells incubated with **OPE_Glucose 1** and analyzed using a FITC (green emission) or DAPI (blue emission) filter.

Moreover, the reduced quantum yield and the increased lifetime of **OPE_Glucose 1** (Φ=0.57, τ/ns=2.47) with respect to compound **OPE_OMe 3** (Φ =0.85, τ/ns=0.98), in which the dimethylamino group is not present, suggested a

partial non radiative decay of the excited singlet state (S_1), in **OPE_Glucose 1**, to a long-lived triplet excited state (T_1) via intersystem crossing.

Thus, in a second work,[111] my research group reported the application of **OPE_Glucose 1** and **OPE_Glucose 2** (**Figure 1.24**), analogue of **OPE_Glucose 1** containing two dimethylamino groups as substituents, as photosensitizers in Photodynamic Therapy (paragraph **1.2.B**). The production of singlet oxygen of the two species was evaluated, in comparison with the model compound **OPE_OMe 3**, and the results are in line with the photophysical features, confirming that the reduced luminescence quantum yield for **OPE_Glucose 1** could be ascribed to a more efficient sensitization of the triplet excited state of these species.

OPE	Absorption λ_{max} nm (ε/ $M^{-1}cm^{-1}$)	Luminescence 298 K			
		λ_{max}, nm	Φ	τ/ns	Φ_{1O2}
OPE_Glucose 1	388 (38900)	472	0.57	2.47	0.15
OPE_Glucose 2	392 (40000)	474	0.74	3.54	0.09
OPE_OMe 3	390 (49500)	433	0.85	0.98	-

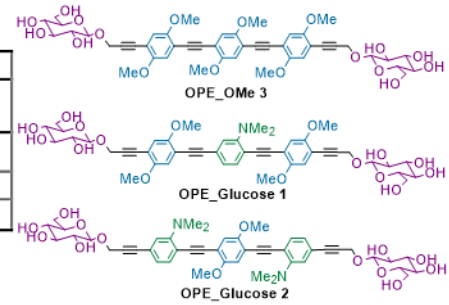

Figure 1.24. Spectroscopic data and $^1O_2$ evaluation of **OPE-Glucose 1** and **OPE_Glucose 2** in comparison with **OPE_OMe 3**.

Finally, the effectiveness, of both **OPE_Glucose 1** and **OPE_Glucose 2**, in combination with UVA light, on two tumour cell lines (HEp-2 and HeLa cells, derived from a larynx carcinoma and a cervical carcinoma, respectively) was checked. The cell internalization and subcellular localization showed their uptake in all the cell lines and their localization in Golgi apparatus and endoplasmic reticulum. Then, the toxicity evaluations showed that in the absence of light both compounds did not induce any relevant toxic effect, until concentrations of $3.5 \cdot 10^{-6}$ M, while the photodynamic treatments induced cytotoxic effects in

[111] Deni, E.; Zamarrón, A.; Bonaccorsi, P.; Carreño, M. C.; Juarranz, A.; Puntoriero, F.; Sciortino, M. T.; Ribagorda, M.; Barattucci A. *Eur. J. Med. Chem.* **2016**, *111*, 58.

HaCaT, HeLa and HEp-2, depending on the OPE concentration and the UVA dose. Both the species reached a good photodynamic effect when combined with UVA light, but, unfortunately, selectivity for tumour HeLa and HEp-2 cells, compared to non-tumour HaCaT cell line, was not observed. However deeper studies suggested that photodynamic treatment could be triggering a mitotic blockage in tumour cell lines, while in HaCaT mainly induce apoptotic processes (**Figure 1.25**).

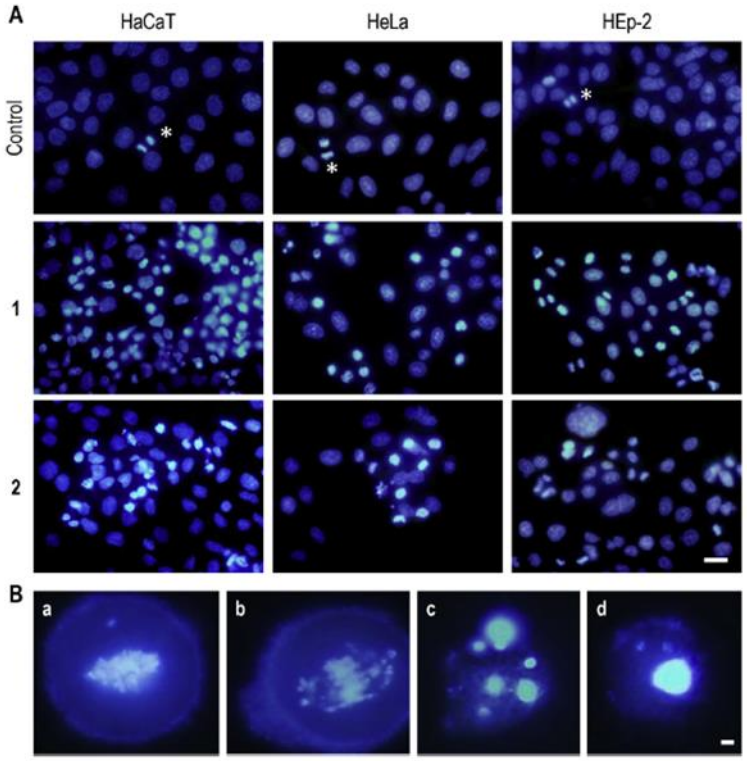

Figure 1.25. (A) The controls (untreated cells) display well defined interphasic and mitotic nuclei; PDT treatment with **OPE_Glucose 1** (1) or **OPE_Glucose 2** (2) causes an increment of apoptotic and necrotic nuclei and increase of mitotic cells in HeLa and HEp-2 cells. (B) Details of normal (a) and altered (b) mitotic figures, as well as apoptotic (c) and necrotic (d) cells.

CHAPTER 2

Results and Discussion

SYNOPSIS

As already shown in Chapter **1** (paragraph **1.3**), Oligo(phenylene ethynylene)s (OPEs) are an interesting class of materials, due to their applications in the electronic[112] and photonic[113] fields, but also in the biomedical one, including uses as bio-imaging sensors,[114] light-activated biocides,[115] biomolecules detectors.[116] Thanks to their rigid backbone, they exhibit high fluorescence quantum yields, combined with large molar extinction coefficients and a high photostability.[117] Moreover, the synthetic versatility of OPEs offers a wide selection of possible functionalized side chains, allowing a fine-tuning of their properties. Photophysical properties can be modulated by acting on the electronics of the conjugated molecular skeleton. Modulation of the hydrophobic chain length and insertion of different substituents at the same chain influences the bioaffinity too.

---

[112] Hong, W.; Li, H.; Liu, S.-X.; Fu, Y.; Li, J.; Kaliginedi, V.; Decurtins, S.; Wandlowski, T. *J. Am. Chem. Soc.* **2012**, *134*, 19425.
[113] Tsamouras, D.; Nierengarten, J.-F.; Gu, T.; Krasnikov, V.; Hadziioannou, G. *Mat. Res. Soc. Symp. Proc.* **2001**, *708*, 1036.
[114] Cardone, A.; Lopez, F.; Affortunato, F.; Busco, G.; Hofer, A. M.; Mallamaci, R.; artinelli, C.; Colella, M.; Farinola, G. M. *Biochim Biophys Acta*. **2012**, *1818*, 2808.
[115] Dascier, D.; Ji, E.; Parthasarathy, A.; Schanze, K. S.; Whitten, D. G. *Langmuir* **2012**, *28*, 11286.
[116] Fanni, A. M.; Monge, F. A.; Lin, C.-Y.; Thapa, A.; Bhaskar, K.; Whitten, D. G.; Chi, E. Y. *ACS Chem. Neurosci.* **2019**, *10*, 1813.
[117] Bunz, U. H. F. *Chem. Rev*. **2000**, *100*, 1605.

In the last years my research group, through the introduction of one or two NMe_2 groups on the aromatic OPE residue and two glucose terminations, afforded the synthesis of highly efficient biocompatible fluorescent probes that can be taken up in cells cytoplasmic vesicles.[118] Moreover, the presence of a lone electron pair on the nitrogen atom of the NMe_2 group was the key topic to make these OPEs to form singlet oxygen ($^1O_2$) and consequently to be in principle utilized in superficial PDT.[119]

On the basis of these results, my PhD work consisted in the synthesis of differently modified glycosilated amino-OPEs with the aim to better modulate their photophysical features and behaviour, and trying to find new applications in the biological and nanomedical fields.

The synthetic approach and the optimization of yields and methods for the obtainment of the already reported **OPE_Glucose 1** and **OPE_Glucose 2** (**Figure 1.24**), are described in paragraph **2.1**.

With the aim to further study the influence on the photophysical behaviour (paragraph **1.3**) of the extension of the π-conjugated system, in paragraph **2.2** the synthetic routes which led to the elongation to a five-aromatic rings OPE chain are reported. The study on the effect of the elongation of the chain on absorption and emission is reported in paragraph **3.1B**.

As seen in paragraph **1.1**, the mechanisms through which the different carbohydrates are recognized by cellular receptors can influence many biological pathways with respect to glucose. The synthesis of three new species, analogue to **OPE_Glucose 1** and bearing different sugar terminations (monosaccharide galactose and mannose, and disaccharide maltose) are described in paragraph **2.3**

[118] Barattucci, A.; Deni, E.; Bonaccorsi, P.; Ceraolo, M. G.; Papalia, T.; Santoro, A.; Sciortino, M. T.; Puntoriero F. *J. Org. Chem.* **2014**, *79*, 5113.
[119] Deni, E.; Zamarrón, A.; Bonaccorsi, P.; Carreño, M. C.; Juarranz, A.; Puntoriero, F.; Sciortino, M. T.; Ribagorda, M.; Barattucci A. *Eur. J. Med. Chem.* **2016**, *111*, 58.

and the first internalization and PDT tests on healthy and cancer cells are reported in paragraph **3.2B**.

Furthermore, the quaternarization of the aromatic dimethylamino groups is the subject of paragraph **2.4**. In fact, the disappearance of the nitrogen lone pair and the formation of a positive charge on the OPE chain can strongly influence the OPE features, from the photophysical ones to the water solubility, opening the way to other biological applications (paragraph **1.2**). It has been demonstrated and recently by us reported[120] that the synthesized tetralkylammonium OPEs interact with the negative charged double helix of DNA: the photophysical and DNA interaction studies are reported in paragraphs **3.1A** and **3.2A**, respectively.

Finally, the last modifications reported in paragraph **2.5** are focused on the desymmetrization of the OPE chain. In particular:

In part **2.5A** the functionalization with electron withdrawing fluorinated aromatic groups as chain termination will be discussed. The introduction of this new moiety, able to interact with the -OMe and -NMe_2 electron donating groups, was intended to create a push-pull effect (paragraph **1.3**, **Figure 1.16**). The influence of this new group on the photophysical features of our original OPE is described in paragraph **3.1C**. In particular it has been preliminary found that the emission of one of these derivatives is pH-sensitive (paragraph **1.2**).

In part **2.5B** the projected synthetic routes described are directed towards the introduction of a suitable termination for the functionalization of upconverting nanoparticles (NPs) (paragraph **1.2**). The chosen NPs are characterized by a strong absorption in the NIR region (980 nm) and by a UV emission band, matching the absorption of our OPEs (~380 nm): an energy transfer process from the NPs to our conjugated system could open the way to their use in NIR-PDT.

[120] Mancuso, A.; Barattucci, A.; Bonaccorsi, P.; Giannetto, A.; La Ganga, G.; Musarra-Pizzo, M.; Salerno, T. M. G.; Santoro, A.; Sciortino, M. T.; Puntoriero, F.; Di Pietro M. L. *Chem. Eur. J.* **2018**, *24*, 16972.

2.1 OPE_GLUCOSE 1 AND 2 SYNTHESIS

The synthesis of both **OPE_Glucose 1** and **OPE_Glucose 2** (**Figure 2.1a**), reported by my research group[121] and that I at first repeated, is based on a convergent approach (**Figure 2.1b**) involving the coupling of an opportunely substituted aromatic "*core*" with two equivalents of an "*arm*", also bearing the glucose termination. The same approach is used for many of the new synthesized OPEs too.

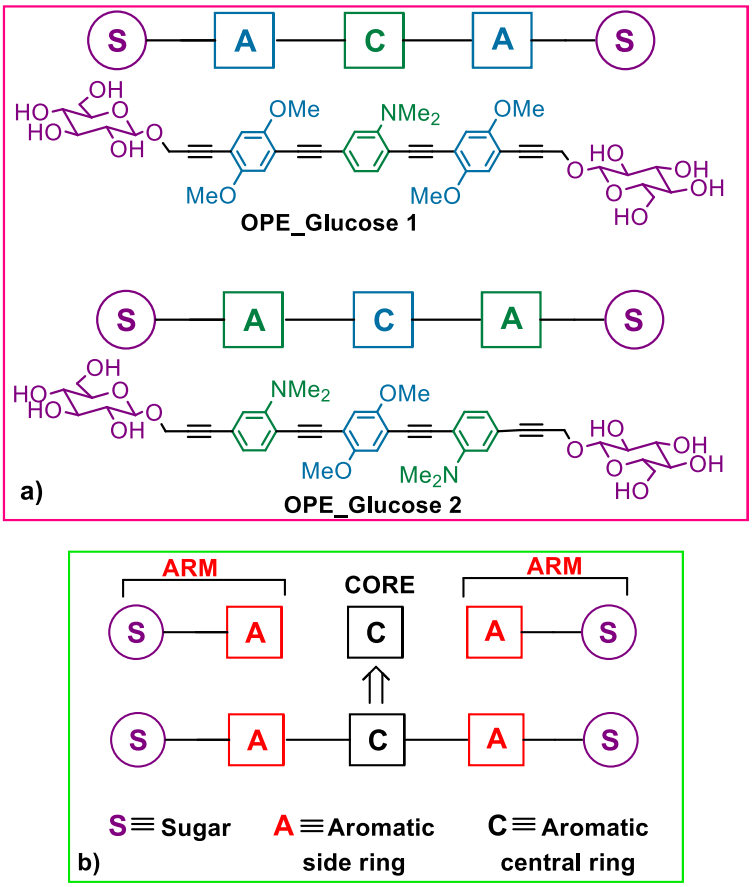

Figure 2.1

[121] Barattucci, A.; Deni, E.; Bonaccorsi, P.; Ceraolo, M. G.; Papalia, T.; Santoro, A.; Sciortino, M. T.; Puntoriero F. *J. Org. Chem.* **2014**, *79*, 5113; Deni, E.; Zamarrón, A.; Bonaccorsi, P.; Carreño, M. C.; Juarranz, A.; Puntoriero, F.; Sciortino, M. T.; Ribagorda, M.; Barattucci A. *Eur. J. Med. Chem.* **2016**, *111*, 58.

The skeleton of all the conjugated oligomers here reported was synthesized exploiting the cross-coupling Sonogashira reactions,[122] in particular:

A) The copper-free approach, in presence of $Pd(PPh_3)_4$, has been generally adopted since it helps to reduce the generation of homocoupling products of the terminal alkyne.

B) The $Pd(PPh_3)_2Cl_2$ mediated coupling, co-catalysed by CuI, has been chosen in the presence of less reactive substrates or commercially available alkynes (e.g. ethynyltrimethylsilane).

C) A modification of the $Pd(PPh_3)_4$ cross-coupling, mediated by Ag_2O,[123] has been used for the *in situ* generation of free ethynyl reactive groups, starting from ethynyltrimethylsilyl substrates; even if this method acts in harsher conditions, leading to lower yields in comparison with A and B, in some cases it has been the only one possible way

OPE_Glucose 1, containing a central aromatic moiety bearing an electron-donating NMe_2 group, was efficiently prepared, starting from commercially available 2,5-dibromoaniline **1** (**Scheme 2.1**).

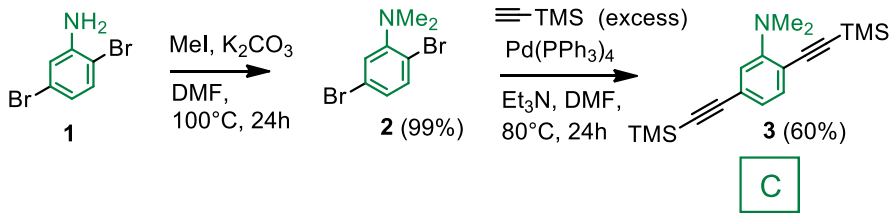

Scheme 2.1

The methylation[124] of the aromatic nitrogen of 2,5-dibromoaniline with a large excess of CH_3I and in presence of K_2CO_3, gave dimethylamino derivative **2** in quantitative yields. Compound **2** was then reacted,[125] in a copper-free

[122] Chinchilla R.; Nájera C. *Chem. Rev.* **2007**, *107*, 874.
[123] Babudri, F.; Colangiuli, D.; Di Lorenzo, P. A.; Farinola, G. M.; Hassan, O.; Naso, F. *Chem. Commun.* **2003**, 130.
[124] Moroni, M.; Le Moigne, J.; Pham, T. A.; Bigot, J.-Y. *Macromolecules* **1997**, *30*, 1964.
[125] Shunichi, O.; Seok, R.C., Heinz, C.; Kung, H. F. *J. Med. Chem*. **2002**, *45*, 4716.

Sonogashira coupling, with a large excess of ethynyltrimethylsilane furnishing **3** (**C**, **Figure 2.1a**) in good quantities.

The second step was the synthesis of the glucoconjugated arm **8** (**S**–**A**, **Figure 2.1a**), still containing a reactive iodoaryl moiety, available for a further cross-coupling reaction. (**Scheme 2.2**). Compound **8** was obtained through the coupling of 2-propynyl-O-β-glucopyranoside-2,3,4,6-tetraacetate **5** and 2,5-dimethoxy benzene **7**. Although **5** was commercially available, it was synthesized in the laboratory following a known procedure.[126] Thus, reaction between β-glucopyranoside-1,2,3,4,6-pentaacetate **4** and propargyl alcohol in the presence of trimethylsilyl trifluoromethanesulfonate (TMSOTf), acting as a Lewis acid, led to **5** in good yields. The control of the reaction is essential for its full success: in fact, a longer time causes considerable decrease in the yield, because of the decomposition, in the reaction conditions, of the just formed glucoderived alkyne **5**.

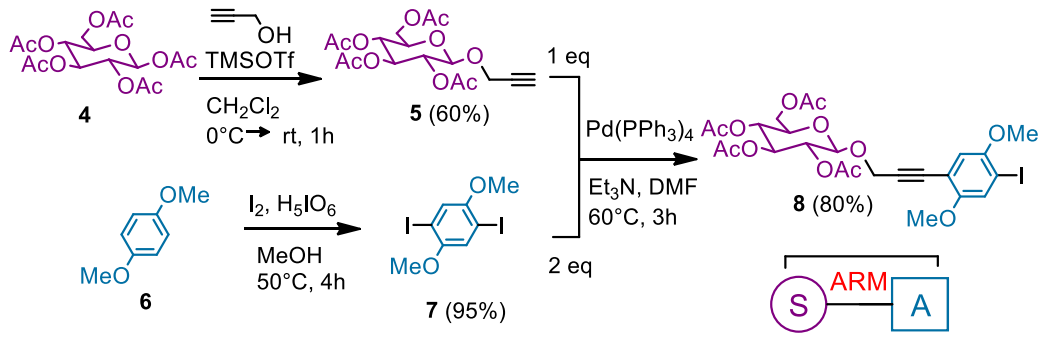

Scheme 2.2

The second precursor, 1,4-diiodo-2,5-dimethoxy benzene **7**, was synthesized from commercially available 2,5-dimethoxy benzene **6** by treatment with H_5IO_6 and I_2 in quantitative yield.[127] Compound **7** was purified through a simple precipitation of the product by the crude in methanol. **7**, in fact, is insoluble in this solvent and can be recovered as a pure white solid by filtration, leaving in

[126] Giovenzana, G. B.; Lay, L.; Monti, D.; Palmisano, G.; Panza, L. *Tetrahedron* **1999**, *55*, 14123.
[127] Yi, C.; Blum, C.; Lehamann, M.; Keller, S.; Liu, S. X.; Frei, G.; Neels, A.; Hauser, J.; Schürch, S.; Decurtins, S. *J. Org. Chem.* **2010**, *75*, 3350.

solution the eventual small amount of unreacted **6**. Afterwards, compound **8** was formed, starting from **5** and **7** in a 1:2 ratio, under the same coupling conditions as above for **3**. The use of two equivalents of **7** is essential to achieve the formation of the mono-substituted derivative as the major product, leading only to a small amount of the bis-sugar coupled product which can anyway be separated by chromatography. Furthermore, since it was known that **7** is not soluble in methanol, a previous precipitation of the unreacted compound from this solvent was performed. The resulting mother liquor, containing our desired product **8** and a small amount of **7**, was finally purified through a very rapid and easy column chromatography.

A modified cross-coupling reaction, adopting Ag_2O to generate *in situ* the free ethynyl reactive group, was employed to obtain OPE **9** (**Scheme 2.3**) from **3** reacted and two equivalents of the glucoconjugated arm **8**. The reaction resulted in the formation, after column chromatography, of the highly luminescent compound **9** as a yellow solid.

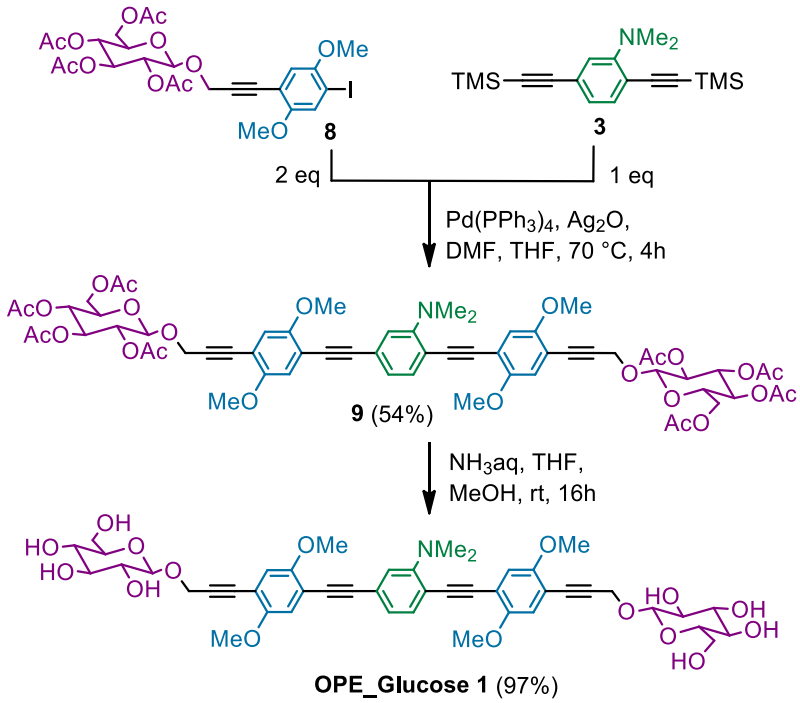

Scheme 2.3

The choice to work with the acetylated compounds until the end of our synthetic routes is due to the better solubility of glyco-OPEs in most of the common organic solvents, facilitating their handling in the different steps. On the other hand, the final deprotection of the hydroxyl groups is essential for an efficient use of the species in the biological field (see paragraph **1.3**). Thus, OPE **9** was finally subjected to deacetylation, in the presence of aqueous ammonia. After one night stirring in THF/MeOH at room temperature, the free carbohydrate derivative **OPE_Glucose 1** was obtained. After evaporation of the solvents under *vacuo*, further washings of the obtained solid with Et_2O, in order to remove the acetamide formed as side product, led to a glossy yellow crystalline powder in quantitative yield.

For the construction of **OPE_Glucose 2** chain (**Scheme 2.4**) it was projected to build the new mono-functionalized building block **10** (**S-A**, **Figure 2.1.a**), analogous to **8** but containing a dimethylamino aromatic ring adjacent to the sugar moiety.

Compound **10** was prepared using a Pd(0) cross-coupling reaction from propargyl glucoside **5** and two equivalents of 2,5-dibromo dimethyl aniline **2**. Under these conditions, compound **10**, with only one derivatized arm, was formed in good yields. The reaction was completely regioselective and proceeded with the formation of only one product bearing the triple bond in *meta* position with respect to the bulky dimethylamino group. This result is due to the different steric hindrance of the two bromine atoms on compound **2**, which leads to a different reactivity of the two and prevents the mono-substitution in *ortho* position. The regiochemistry of compound **10** could be unequivocally demonstrated by the NMR bidimensional experiment HMBC (Heteronuclear Multiple Bond Correlation).[128]

[128] Deni, E.; Zamarrón, A.; Bonaccorsi, P.; Carreño, M. C.; Juarranz, A.; Puntoriero, F.; Sciortino, M. T.; Ribagorda, M.; Barattucci A. *Eur. J. Med. Chem.* **2016**, *111*, 58.

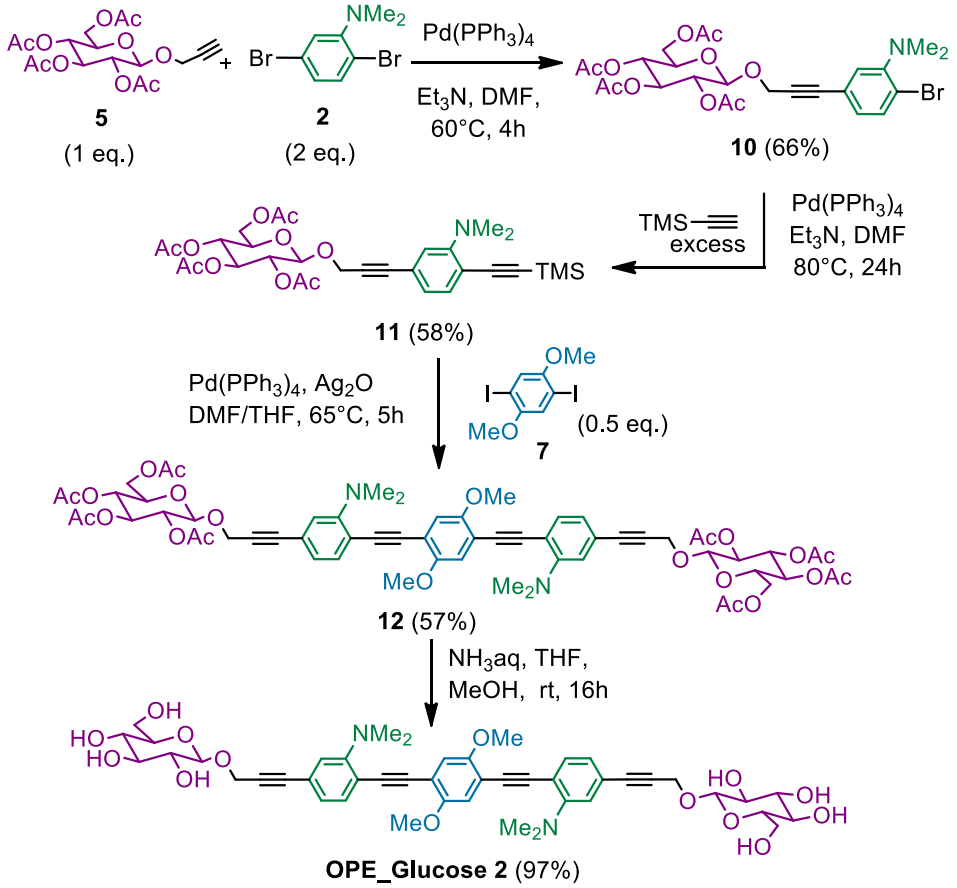

Scheme 2.4

The cross-coupling reaction of **10** with an excess of commercially available ethynyltrimethylsilane gave rise to the key intermediate **11** in good yields. The reaction was carried out at higher temperature on respect to **10** (60°C *vs.* 80°C), in order to improve the reactivity of the most sterically hindred bromo substituent. The final Ag_2O-modified coupling of 1,4-diiodo-2,5-dimethoxy benzene **7** (**C**) with two equivalents of **11** gave rise to the second glycosilated amino OPE **12**. Quantitative deacetylation of **12** in the presence of an excess of aqueous ammonia gave the **OPE_Glucose 2** as a brilliant yellow solid, easily separated from residual acetamide by subsequent washings with Et_2O, in almost quantitative yields.

2.2 CHAIN ELONGATION

Going on with the intention of modulating the properties of our oligomers, we thought to study the effect of the chain length on the spectroscopic features. According to literature (paragraph **1.3**),[129] on increasing the number of phenyl acetylene units the maximum absorption and emission peaks of OPEs are expected to show an increasingly redshift. For this reason, the first objective of my work has been the synthesis of the longer pentameric analogues **13** and **14** (**Figure2.2**).

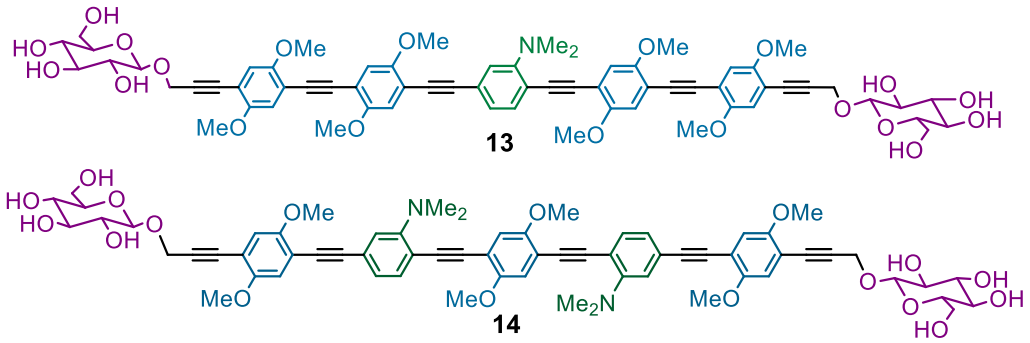

Figure 2.2

OPE_Glucose 1 and **OPE_Glucose 2** are characterized by a strong absorption in UV-Vis region (λ_{abs}=388 nm and λ_{abs}=392, respectively). However, it is known that this region of wavelengths, needed for our OPEs excitation and exploitation in the biological field, is slightly absorbed by tissues (**Figure 2.3**). Moreover, prolonged exposure to short-wavelength light can seriously harm cells by inducing photochemical reactions.[130] For this reason, shifting the absorption

[129] Yin, S.; Leen, V.; Jackers, C.; Beljonne , D.; Van Averbeke, B.; Van der Auweraer, M.; Boens, N.; Dehaen, W. *Chem. Eur. J.* **2011**, *17*, 13247.
[130] Ruggiero, E.; Alonso-de Castro, S.; Habtemariamb, A.; Salassa L. *Dalton Trans.* **2016**, *45*, 13012.

of our OPEs at lower energy, through the extension of the π-conjugated system, could be useful for their use as photosensitizers in Photodynamic Therapy (PDT).

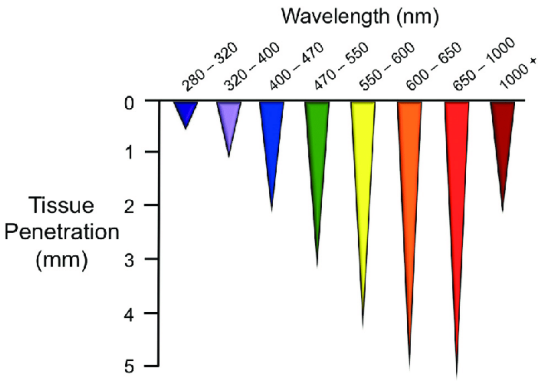

Figure 2.3

The structures of the two new species are similar to the ones of O**PE_Glucose 1** and **OPE_Glucose 2**, in order to retain the most important features. The dimethylamino groups contribute to the internalization in cancer cells and to enhance the formation of the highly-reactive singlet oxygen species ($^1O_2$). The methoxy groups helps the high emission quantum yields and photostability (paragraph **1.3**).[131] Finally, the glucose terminations have an essential role for biological purposes: they help in the solubility in aqueous medium and allow the permeation of the cytoplasmic membrane (see paragraph **1.1**).

The synthetic strategies for the obtainment of **13** and **14** are based on the same convergent approach (**Figure 2.1**) used for the synthesis of O**PE_Glucose 1** and **OPE_Glucose 2**. All the synthetic pathways require Sonogashira cross-couplings and modifications as key steps for the chain assembling.

The synthesis of the first pentameric analogue **13** is reported in **Scheme 2.5**. It has been thought that the simplest way for the building of the elongated chain

[131] Ochi, T.; Yamaguchi, Y.; Wakamiya, T.; Matsubara, Y.; Yoshida Z-i. *Org. Biomol. Chem.* **2008**, *6*, 1222.

could be the synthesis of the new longer aromatic *core* **16**, characterized by three phenylene ethynylene units: the central one bearing the dimethylamino group, the side ones containing either the methoxy substituents or two iodo terminations, useful for further modifications through palladium-mediated cross-couplings. **16** was obtained through the Ag_2O-mediated coupling between the bis-trimethylsilylacetylene derivative **3** with six equivalents of 1,4-diiodo-2,5-dimethoxy benzene **7**. Despite this latter is used in great excess, it is very difficult to avoid the polymerization of the starting materials and the intermediate products formed, since they are all very reactive in the reaction conditions.

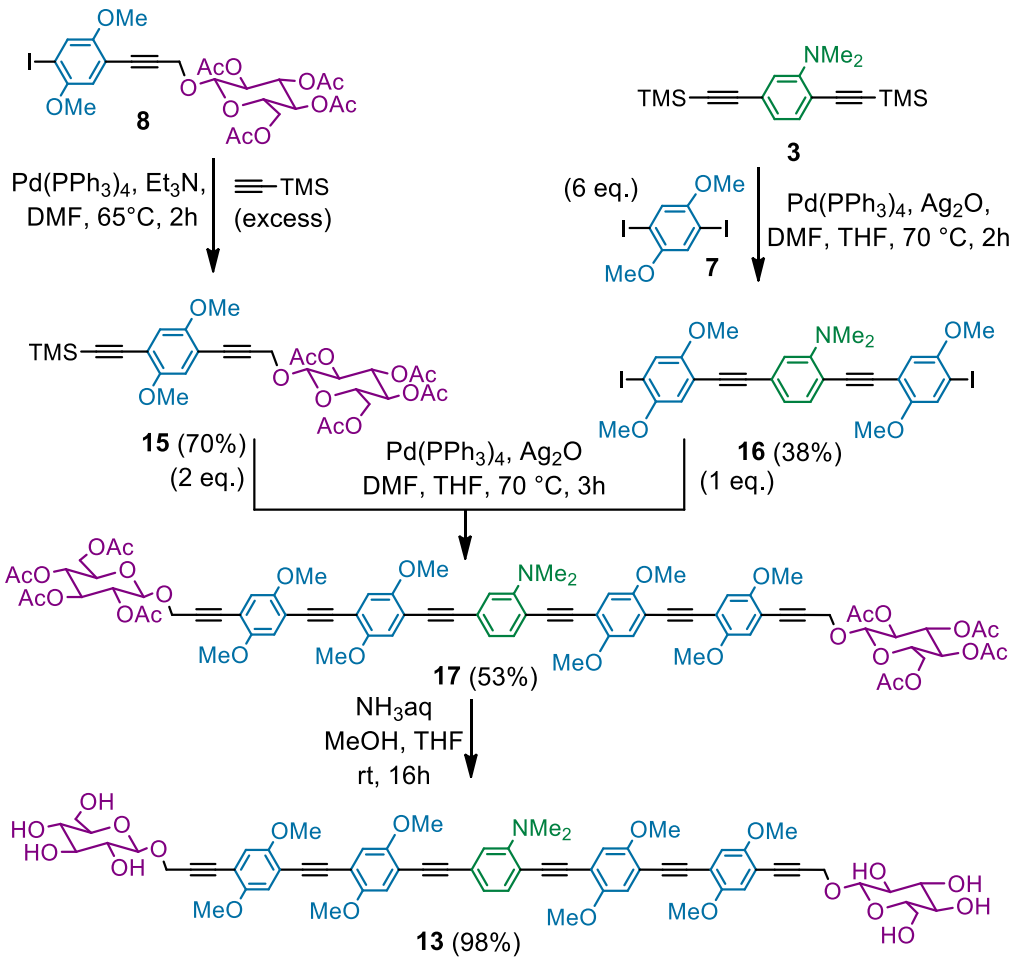

Scheme 2.5

However, even though the yield is low (38%), it was thought this way to be the easiest to achieve the desired result. **15**, obtained by the functionalization of the free iodo substituent present in **8** with an excess of ethynyltrimethylsilane, was chosen as the reactive *side-arm*. Thus, **16** reacted with two equivalents of **15** in presence of $Pd(PPh_3)_4$ and Ag_2O to give the acetylated pentamer **17**. The product was purified by chromatography and isolated as a bright yellow solid. The usual treatment with aqueous ammonia, followed by the solvents evaporation and the solid washings with Et_2O was finally employed to get the pure first elongated OPE **13** in quantitative yields.

As regards the synthesis of the second pentamer **14**, bearing two dimethylamino groups as substituents on the aromatic chain, we considered two different alternative approaches. The first way could involve the synthesis of a second elongated *core*, such as **18** (**Scheme 2.6**), with the same strategy as seen before for **16** (**Scheme 2.5**).

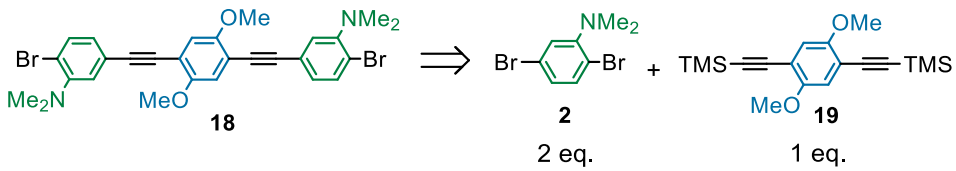

Scheme 2.6

Nevertheless, taking into account the low yield achieved in the synthesis of **16** and, above of all, the lower reactivity of bromine with respect to iodine in Sonogashira cross-couplings, the synthesis of **18** was excluded in advance.

It was then evaluated the second alternative path: the exploitation of the same convergent approach used for **OPE_Glucose 1** and **OPE_Glucose 2**, but through the synthesis of an elongated *side-arm*. The new species should bear two aromatic rings, opportunely substituted, containing a glucose termination and a halogenated or acetylenic group suitable for the coupling with a one-ring aromatic

core. Therefore it was projected to add to the 2,5-dimethoxy-iodoaryl glucoside **8** (**Scheme 2.2**) a further ethynylaromatic unit containing a dimethylamino group.

For this purpose, **20** characterized by the presence of two reactive function as one bromine atom and a trimethylsilyl acetylenic group was synthesized from **2**, whose regioselective substitution at one bromine was already demonstrated (**Scheme 2.4**): the best reaction conditions for its obtainment are reported in **Scheme 2.7**. In fact, if the reaction is carried out at high temperature and in presence of a large excess of ethynyltrimethylsilane the major product is the bis-substituted **3**; on the contrary, in conditions of lower temperature and a slight excess of ethynyltrimethylsilane, a low boiling reactive (52-53°C), the mono-substituted compound **20** is favoured. The best results in terms of yield of **20** were obtained in the presence of $Pd(PPh_3)_2Cl_2$, while the use of a mixture of $PPh_3/Pd(PPh_3)_2Cl_2$ [132] resulted the best way to obtain **3**.

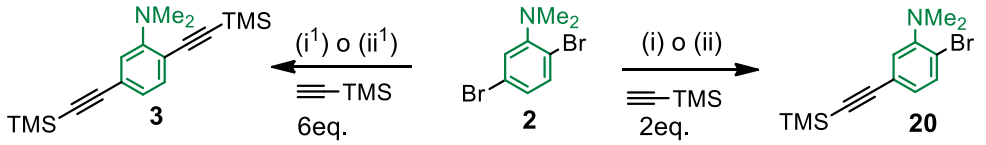

(i^1) $Pd(PPh_3)_4$, DMF, Et_3N, 80°C, 24h (60%) (ii^1) 1) $Pd(PPh_3)_2Cl_2$, PPh_3, Et_3N, 80°C, 1h 2) DMF, CuI, 80°C, 16h (65%)	(i) $Pd(PPh_3)_4$, DMF, Et_3N, 40°C, 16h (68%) (ii) 1) $Pd(PPh_3)_2Cl_2$, Et_3N, 40°C, 1h 2) DMF, CuI, 40°C, 4h (78%)

Scheme 2.7

In order to avoid subsequent low-yield Ag_2O-mediated coupling, **20** was first desilylated. The treatment of **20** with tetra-*n*-butylammonium fluoride (TBAF),[133] a common reactive for this scope led to the almost exclusive formation of **22**, derived from a process of homocoupling of the free ethynylenic species

[132] Amatore, C.;Carré, E.; Jutand, A.; M'Barki M. A. *Organometallics* **1995**, *14*, 1818.
[133] Dawood, K. M.; Hassaneen, H. M.; Abdelhadi, H. A.; Ahmed M. S. M.; Mohamed, M. A.-M. *J. Braz. Chem. Soc.* 2014, *25*, 1688.

(**Scheme 2.8**). Alternatively, the treatment with an excess of K_2CO_3,[134] in a mixture 1:1 of CH_2Cl_2 and MeOH at room temperature led to **21** in quantitative yield.

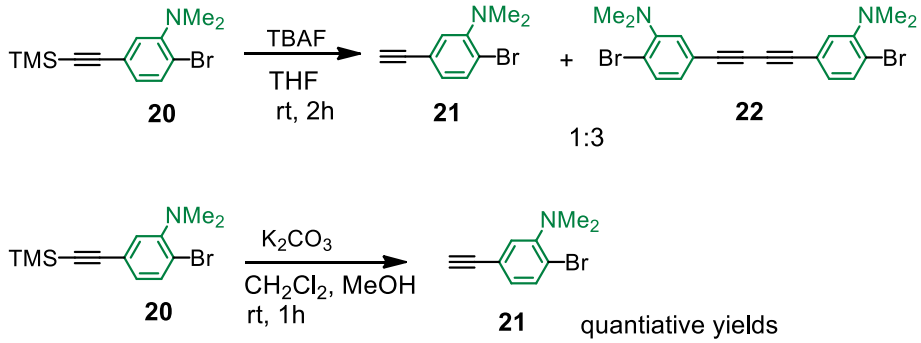

Scheme 2.8

Coupling of **21** with an equimolar amount of **8** led to the exclusive formation of **23** (**Scheme 2.9**), then transformed into **24** by a successive coupling with an excess of ethynyltrimethylsilane. It has to be noted that the higher reactivity of iodine with respect to bromine avoids the polimerization of **21**.

The treatment of **24** with K_2CO_3, useful for a previous desilylation of the triple bond, led also to the undesired glucose deacetilation (**26**). Indeed, the ^{1}H-NMR analysis of the crude showed how this collateral reaction was even faster than the cleavage of the C-Si bond. Since the reduced solubility of **26** in organic solvents should have made its use harder, the best solution for the convergent synthesis of **25** has chosen to be the Ag_2O co-catalysed coupling [$Pd(PPh_3)_4$, Ag_2O, DMF, THF, 70 ºC] of **24** with one equivalent of **7**. Compound **25** was obtained as a brilliant yellow solid after the purification of the crude by chromatography. Finally, it was deacetylated with aqueous ammonia to give **14** as a yellow solid.

[134] Zhao, Y.; Liu, L.; Zhang, W.; Sue, C.; Li, Q.; Miljanić, O. Š.; Yaghi, O. M.; Stoddart, J. F. *Chem. Eur. J.* **2009**, *15*, 13356.

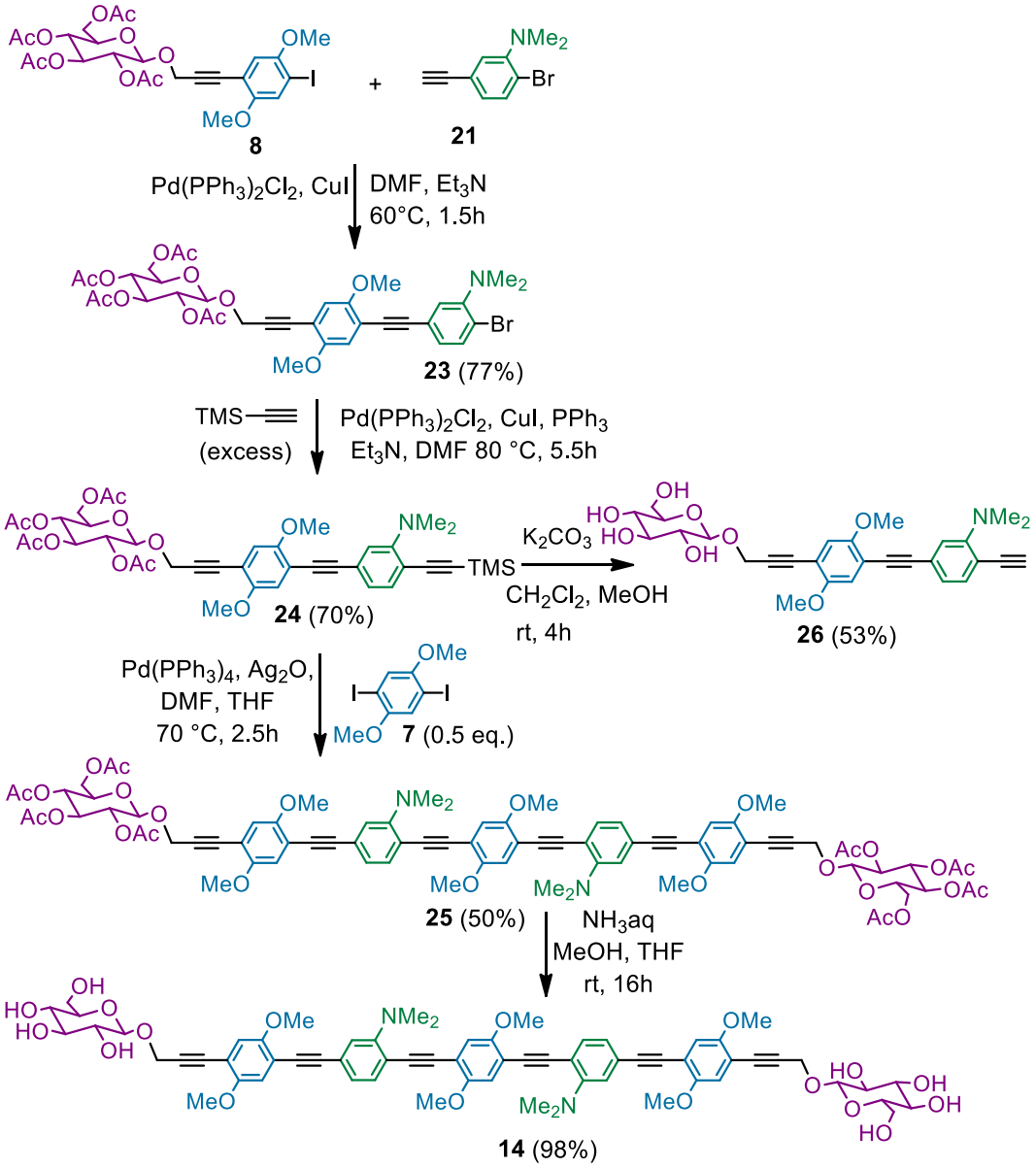

Scheme 2.9

All the new synthesized compounds were also investigated by NMR spectroscopy. The ^{1}H_NMR and ^{13}C_NMR characterization is reported in Chapter 4. Some details of the ^{1}H_NMR spectra, in $CDCl_3$, of the two acetylated pentamers **17** and **25** are reported in **Figure 2.4**.

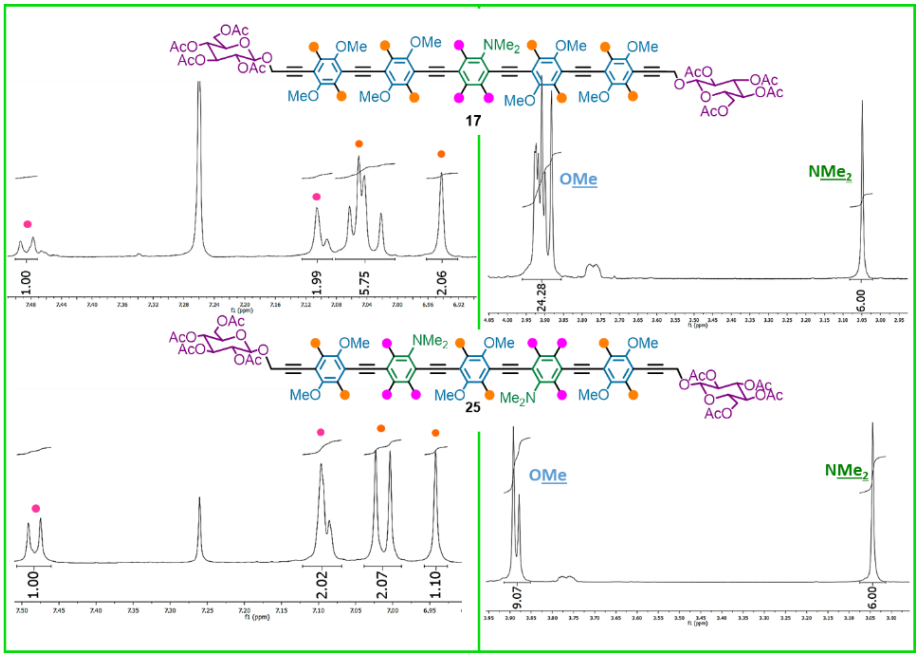

Figure 2.4

In particular, in the region between 6.90 and 7.50 ppm (on the left) it can be seen that the pattern of the three protons, related to the dimethylamino aryl moiety (pink circles), is very similar for both the species. On the contrary, the signal related to the aryldimethoxy moieties (orange circles) show a more subdivided pattern in **17**. In fact, in this latter compound, the presence of only one dimethylamino group desimetrize the ethynylaromatic chain, causing different chemical shift for all the aromatic and methoxy protons. On the other hand, the presence of two dymethilamino groups, with a well-defined regiochemistry, provides a higher symmetry in compound **25**, which is reflected in a simpler spectrum.

The absorption and the emission spectra of the two new pentamers, also in comparison with their shorter analogues, are reported and discussed in paragraph **3.1B**.

2.3 SUGAR CHANGE

As already seen in paragraph **1.1**, it is now well established that tumours undergo changes in cellular metabolism and many tumours exhibit enhanced glucose uptake; therefore, there are several antitumor agents, which contain glycosidic moieties embedded in their structure for their easy absorption. Moreover, it is known that other sugars besides D-glucose, like D-galactose, [135] can be substrates for GLUT transporters, and thus can be considered candidates for a GLUT-targeting approach.[136]

Considering the role of carbohydrates in biological systems and the chance to exploit them in projecting new drugs and delivery systems, the second part of this work dealt with the insertion of different sugars as terminations of the OPE chains. Looking at the results in the use of **OPE_Glucose 1** and **OPE_Glucose 2** in bioimaging and Photodynamic Therapy (paragraph **1.3**),[137] it was thought that changing the sugar residues could cause different behaviour of our glyco-OPEs in the biological field. For this reason, we worked on the synthesis of three different derivatives, characterised by the same chain of **OPE_Glucose 1**, which had given the best results in terms of $^1O_2$ production, but introducing respectively galactosid, mannosidic and maltosidic terminations (**Figure 2.5**), exploiting the same convergent logic shown in **Scheme 2.1**, but adding some little synthetic modifications.

[135] Melisi, D.; Curcio, A.; Luongo, E.; Morelli, E.; Rimoli, M. G. *Curr. Top. Med. Chem.* **2011**, *11*, 2288.
[136] LeFevre, P.G. *Pharmacol Rev.* **1961**, *13*, 39.
[137] Barattucci, A.; Deni, E.; Bonaccorsi, P.; Ceraolo, M. G.; Papalia, T.; Santoro, A.; Sciortino, M. T.; Puntoriero F. *J. Org. Chem.* **2014**, *79*, 5113; Deni, E.; Zamarrón, A.; Bonaccorsi, P.; Carreño, M. C.; Juarranz, A.; Puntoriero, F.; Sciortino, M. T.; Ribagorda, M.; Barattucci A. Eur. J. Med. Chem. 2016, 111, 58.

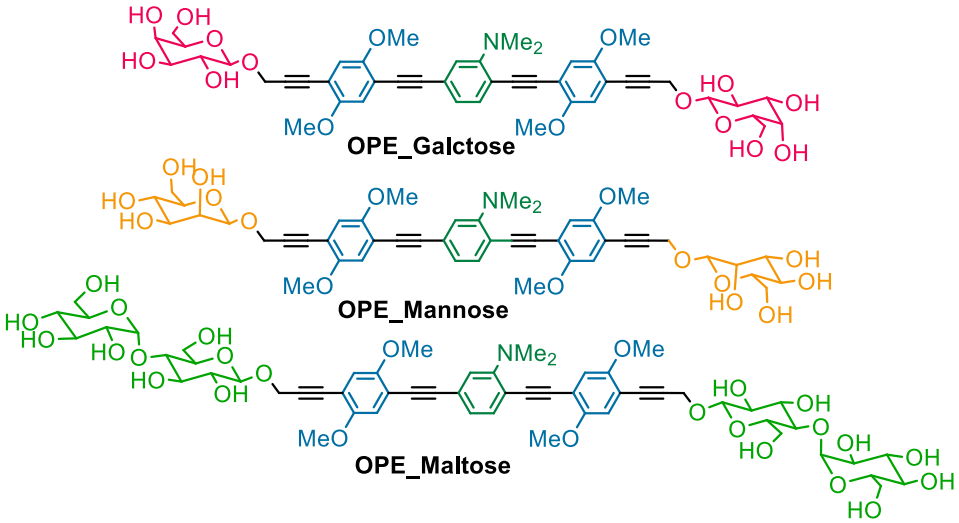

Figure 2.5

As for the glucose terminations, in order to facilitate the handling of the intermediate products, the sugars derivatives have been used in the acetylated form until the end of our synthetic routes. While both β-D-Galactose pentaacetate and α-D-Mannose pentaacetate were already available in our laboratory, we had to synthesize D-maltose octaacetate **27** from D-(+)-Maltose monohydrate. Thus, the quantitative acetylation of this latter in presence of acetic anhydride and a catalytic amount of 4-dimethylaminopyridine is reported in **Scheme 2.10**.[138]

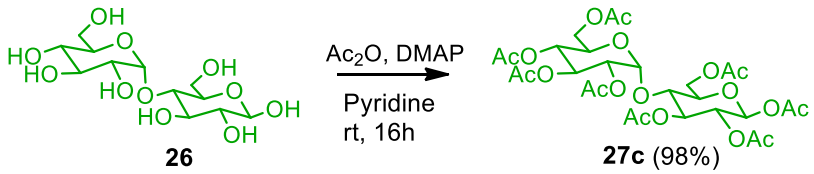

Scheme 2.10

After the obtainment of the acetylated maltosidic residue **27c** too, the following step was the synthesis of the glycoconjugated *side-arms*, analogue to **8**, containing a iodoaryl termination. Thus, **27a-c** were treated with propargyl

[138] Ye, H.; Xiao, C.; Zhou, Q.-Q.; Wang, P. G.; Xiao, W.-J. *J. Org. Chem.* **2018**, *83*, 13325.

alcohol in the presence of TMSOTf as a Lewis acid (**Scheme 2.11**).[139] Propargyl derivatives **29a-c** were isolated by column chromatography and reacted with two equivalents of **7** in a Pd(0) mediated cross-coupling conditions. The unreacted excess of **7**, added in order to minimize the formation of the bis-adduct, was removed by precipitation with MeOH, where **7** is not soluble (**2.1**). The resulting crudes were purified by chromathography and the three *side-arms*, respectively **30a**, **30b** and **30c** (**S**–**A**), isolated in good yields.

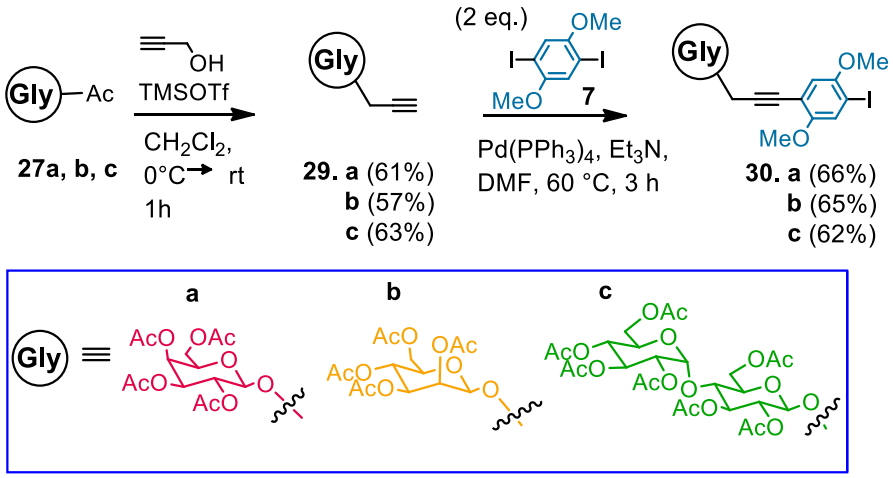

Scheme 2.11

The *core* **31**, coming from the K_2CO_3-mediated (**2.2**) quantitative desilylation of **3** (**Scheme 2.12**), was chosen as synthetic counterpart of **30a-c** in the synthesis of the final glycosidic OPEs, so excluding the low-yield Ag_2O-mediated step, as it happened for the synthesis of **OPE_Glucose 1**.

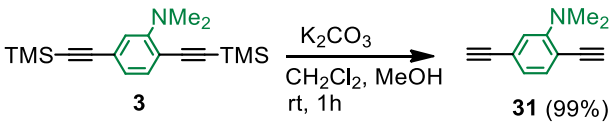

Scheme 2.12

[139] Giovenzana, G. B.; Lay, L.; Monti, D.; Palmisano, G.; Panza, L. *Tetrahedron* **1999**, *55*, 14123.

The Pd(0) mediated cross-coupling of one equivalent of **31** with two equivalents of **30a-c** (**Scheme 2.13**), led to **32a-c**. Following this new route, the three new products were obtained, after the crudes purification by chromatography, in higher yields than the Ag_2O-mediated synthesis of glucosidic OPE **9** (**Scheme 2.3**). The conclusive deacetylation of **32a**, **32b** and **32c**, gave respectively **OPE_Galactose**, **OPE_Mannose** and **OPE_Maltose** as bright yellow solids in quantitative yields.

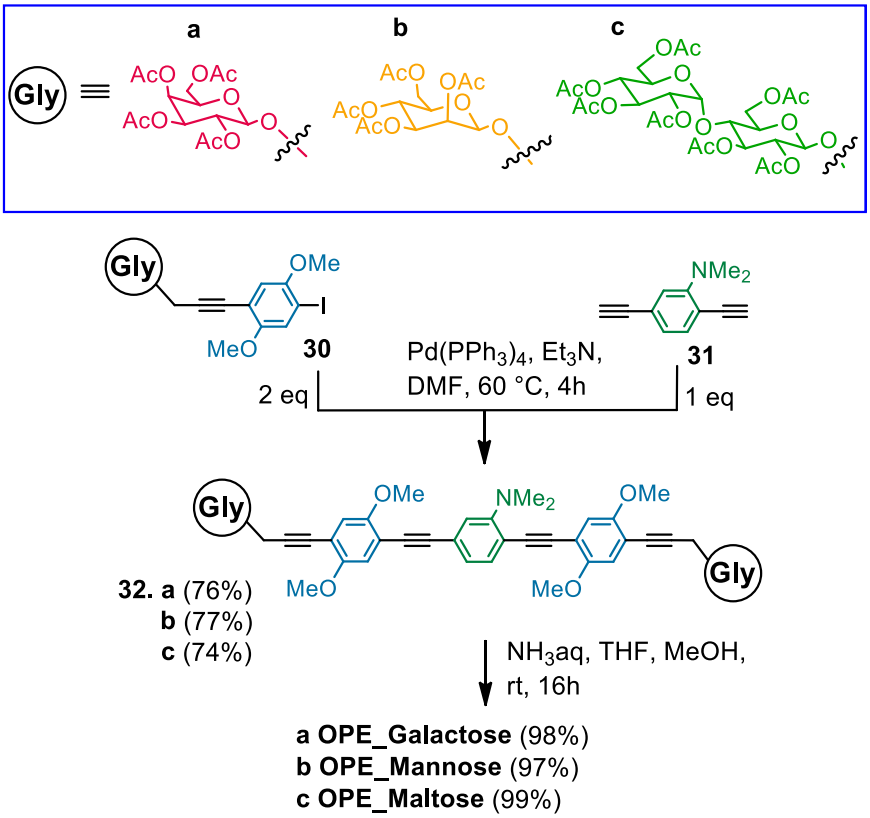

Scheme 2.13

Some relevant details of the ^{1}H_NMR spectra of **9**, **32a** and **32b** are reported in **Figure 2.6**. While the signals of the aromatic, methoxy and dymethylamino protons are completely superimposible, the region between 3.6-5.6 ppm is peculiar for the different carbohydrates. First of all, as reported in the literature,

the chemical shift for an equatorial proton is generally found farther downfield than an axial proton.[140] Moreover, the coupling constants between the vicinal protons of the pyranose rings (8-14 Hz for diaxial protons and 1-7 Hz for axial-equatorial protons), causes multiplicities of the signals typical for each glycosidic moiety.

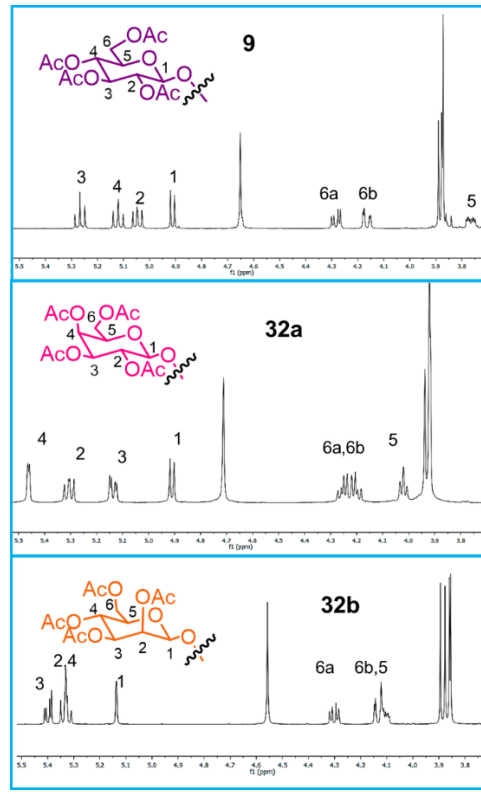

Figure 2.6. ^{1}H-NMR in $CDCl_3$ of **9**, **32a** and **32b**

The presence of the acetyl groups causes a strong downfield shift for the resonances of neighbouring sugar-skeleton protons.[141] Taking as example the maltosidic derivative,[142] in **Figure 2.7**, the effect of the deacetylation of the sugar

[140] Pearson, W. A.; Spessard, G. O. *J. Chem. Educ.* **1975**, *52*, 814
[141] Haverkamp, J.; Van Halbeek, H.; Dorland, L.; Vliegenthart, J. F. G.; Pfeil, R.; Schauer, R. *Eur. J. Biochem.* **1982**, *122*, 305.
[142] Braitsch, M.; Kählig, H.; Kontaxis, G.; Fischer, M.; Kawada, T.; Konrat, R.; Schmid, W. *Beilstein J. Org. Chem.* **2012**, *8*, 448.

moieties is shown. Thus, in ^{1}H_NMR spectrum of the acetyl maltosidic residue **32c**, all the signals related to the sugar-skeleton protons fall between 3.7- 5.4 ppm. On the contrary, in **OPE_Maltose**, the absence of the acetyl groups causes a shift to higher fields; only H-1 and H-1', which are not subject to deacetylation, result less influenced.

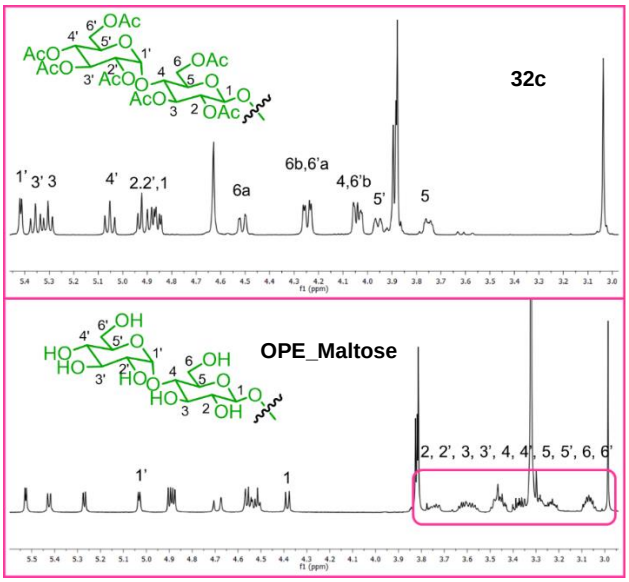

Figure 2.7. ^{1}H-NMR in $CDCl_3$ of **32c** and ^{1}H-NMR in DMSO-*d6* of **OPE_Maltose**

In paragraph **3.2B** the results of the preliminary biological tests made on **OPE_Maltose** will also be discussed.

2.4 DIMETHYLAMINO GROUP QUATERNARIZATION

All the until now here reported OPEs possess one or two dimethylamino groups, bearing the lone pairs at the nitrogen atoms shared with the conjugated phenylenethynylenic system. With the aim to go on modulating their chemical, physical and biological behaviour of our OPE system, it was thought to transform the amino group into tetralkylammonium salt (**Figure 2.8**).

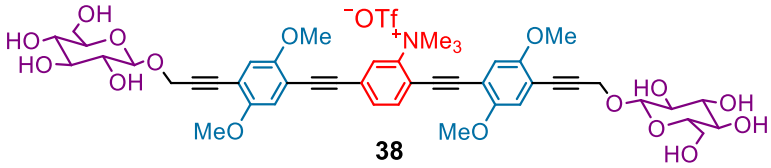

38

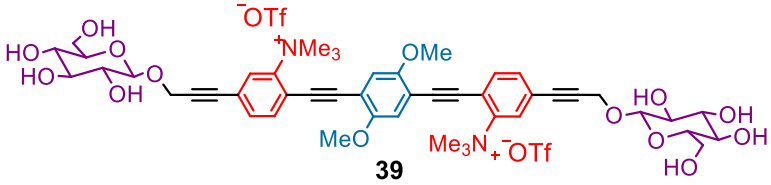

39

Figure 2.8

It was thought that the presence of a charged group could increase the solubility of the synthesized molecules in water and, at the same time, the absence of the lone pair on nitrogen could cause an alteration of the photophysical properties. Moreover, it was considered that the new positive charge at nitrogen, directly linked to the planar phenylene-ethynylene chain, joint with the presence of the hydrogen bonding-sugar groups, could help the new OPEs to interact with the negative charged double helix of DNA (paragraph **1.2** and **3.2A**).[143]

The first test of quaternarization was performed using iodomethane as methylating agent (**Scheme 2.14**). Reaction of the acetylated **9** with a large excess of volatile iodomethane in refluxing acetone (bp=63°C) did not lead to the formation of the expected quaternarized product. The same reaction, conducted with a large excess of CH_3I, in refluxing acetonitrile (bp=82°C) in a sealed tube, did not give any results, leaving **9** unaltered.

[143] Mancuso, A.; Barattucci, A.; Bonaccorsi, P.; Giannetto, A.; La Ganga, G.; Musarra-Pizzo, M.; Salerno, T. M. G.; Santoro, A.; Sciortino, M. T.; Puntoriero, F.; Di Pietro, M. L. *Chem. Eur. J.* **2018**, *24*, 16972.

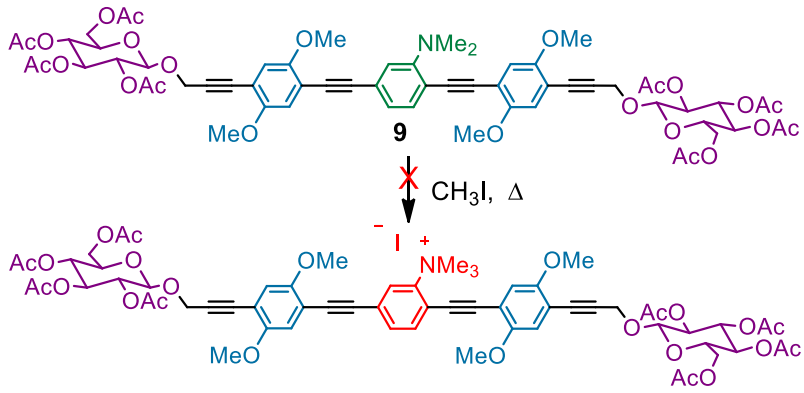

Scheme 2.14

The lack of reactivity of **9** is attributable to the low nucleophilicity of the aromatic nitrogen. Therefore, it was necessary to use a stronger methylating agent like methyl trifluoromethanesulfonate (TfOMe) (**Scheme 2.15**). TfOMe was reacted with **9** in refluxing CH_2Cl_2, in 1:1 molecular ratio, giving after two hours the quantitative formation of the quaternarized product **40**.

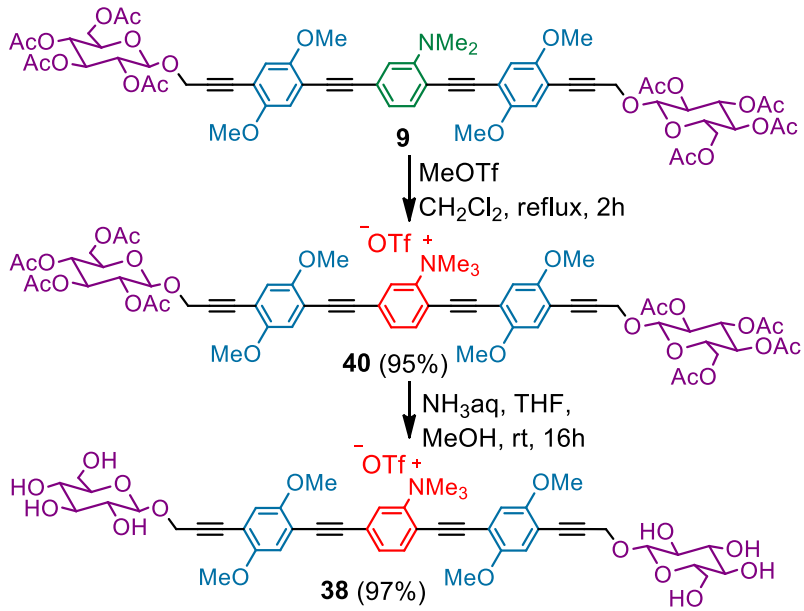

Scheme 2.15

It was observed that a strict molecular ratio between **9** and triflate has to be maintained because a larger amount of TfOMe, which contains a small but critical amount of triflic acid, causes the decomposition of the resulting compound **40**. After evaporation under *vacuo*, the obtained solid was washed with Et_2O to remove eventual residues of unreacted starting materials and the product **40** was obtained pure as an orange crystalline powder. A good success in terms of yields of the above described reaction is to utilize of properly stored methyl trifluoromethanesulfonate (freezed and under nitrogen atmosphere) because it is extremely sensitive to air, humidity and heat, decomposing to triflic acid.

The typical deacetylation procedure (aqueous ammonia in a THF/MeOH solution) was performed on the resulted protected compound **40** to finally obtain the desired glycosylated tetralkylammonium salt **38**.

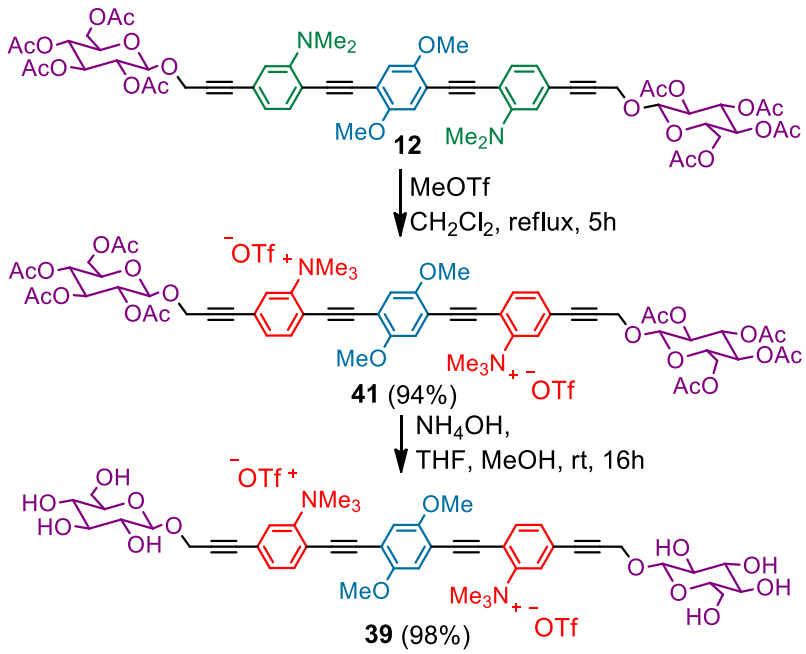

Scheme 2.16

The same reaction was performed on the bis-dimethylamino OPE **12**, with the aim of obtaining the doubly quaternarized salt (**Scheme 2.16**). Thus, reaction

of TfOMe with **12** in 2/1 molecular ratio, in refluxing CH_2Cl_2 solution, afforded the double quaternary ammonium salt **41**, in quantitative yield as a brilliant orange powder, in five hours; also in this case no further purification was needed. Again, the treatment with ammonia solution, followed by washes with Et_2O to remove the resulting acetamide, gave the deacetylated bis-charged compound **39**.

In **Figure 2.9** two details of the ^1H_NMR spectra, in $CDCl_3$, of the dimethylamino glucoside **9** in comparison with its quaternarized analogue **40** are reported.

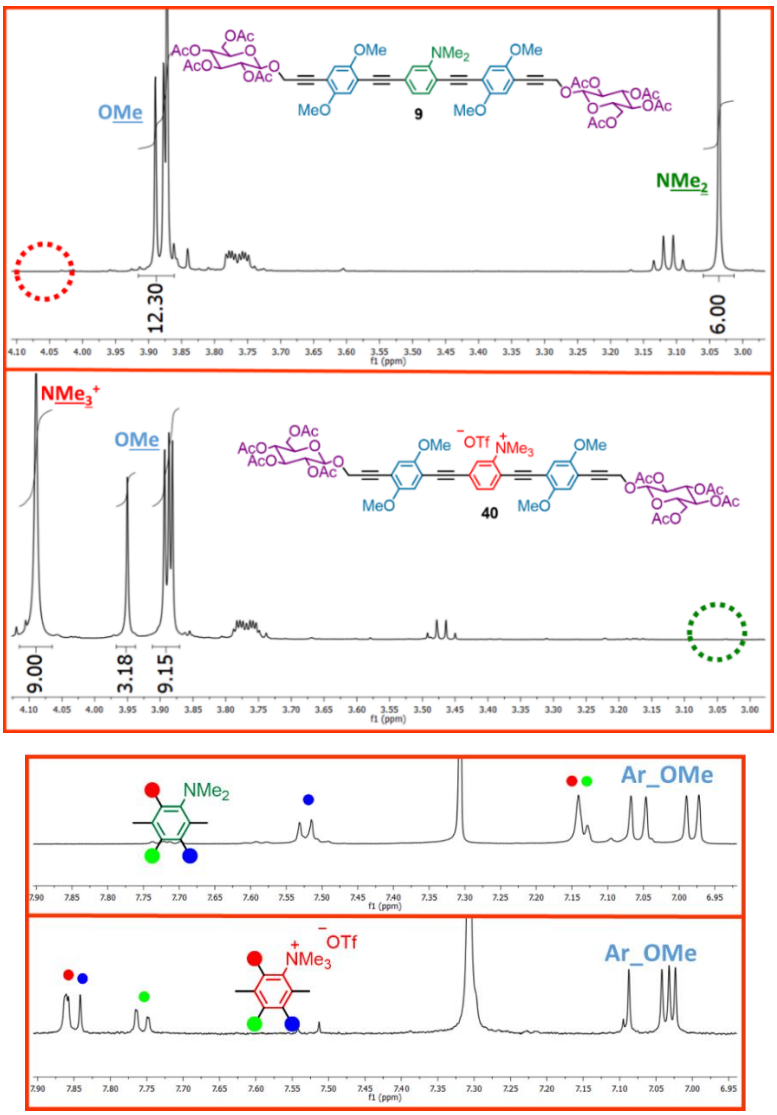

Figure 2.9

The disappearance of the signal at 3.04 ppm related to the six protons of the dimethylamino group in **9**, and the simultaneous appearance of a signal shifted to 4.09 ppm, related to the most deshielded nine protons of the the NMe^{3+} group in **40** can be noticed. On the other hand, only one of the four methoxy groups, probably the nearest to the NMe^{3+} group, is influenced by the introduction of the new function and shifts to lower fields.

Moreover, also the aromatic protons, belonging to the nitrogen substituted ring, result deshielded in **40**: the proton in meta position to the NMe^{3+} group shifts from 7.52 to 7.75 ppm, while the ortho and para protons are even more influenced, shifting from 7.13 to 7.85 ppm. Finally, only one dimethoxy ring proton, probably the one facing the charged group, is influenced by the introduction of the new function, while the sugar terminations, farther from the central aromatic chain, are not influenced at all.

With the same attitude, it was thought to apply the same procedure to the glucosylated pentamers **17** and **25** and to the galactosidic OPE **32a**. This is meant to study the influence of the positive charge on the water solubility of the elongated OPEs, whose extended aromatic and hydrophobic *core* lead to a lower affinity with the polar solvent, but also to investigate any different biological behaviour when the sugar termination is changed. Thus **17**, **25** and **32a** were treated with MeOTf (1:1 for the mono-dimethylamino OPEs **17** and **32a**, 1:2 for the bis-dimethlamino OPE **25**) to obtain respectively: **42**, **44** and **46** (**Scheme 2.17**). Finally, the acetylated sugar terminations of the new quaternarized species were deprotected with an excess of aqueous ammonia. The desired compounds **43**, **45** and **47** were obtained in quantitative yields as brilliant orange solids.

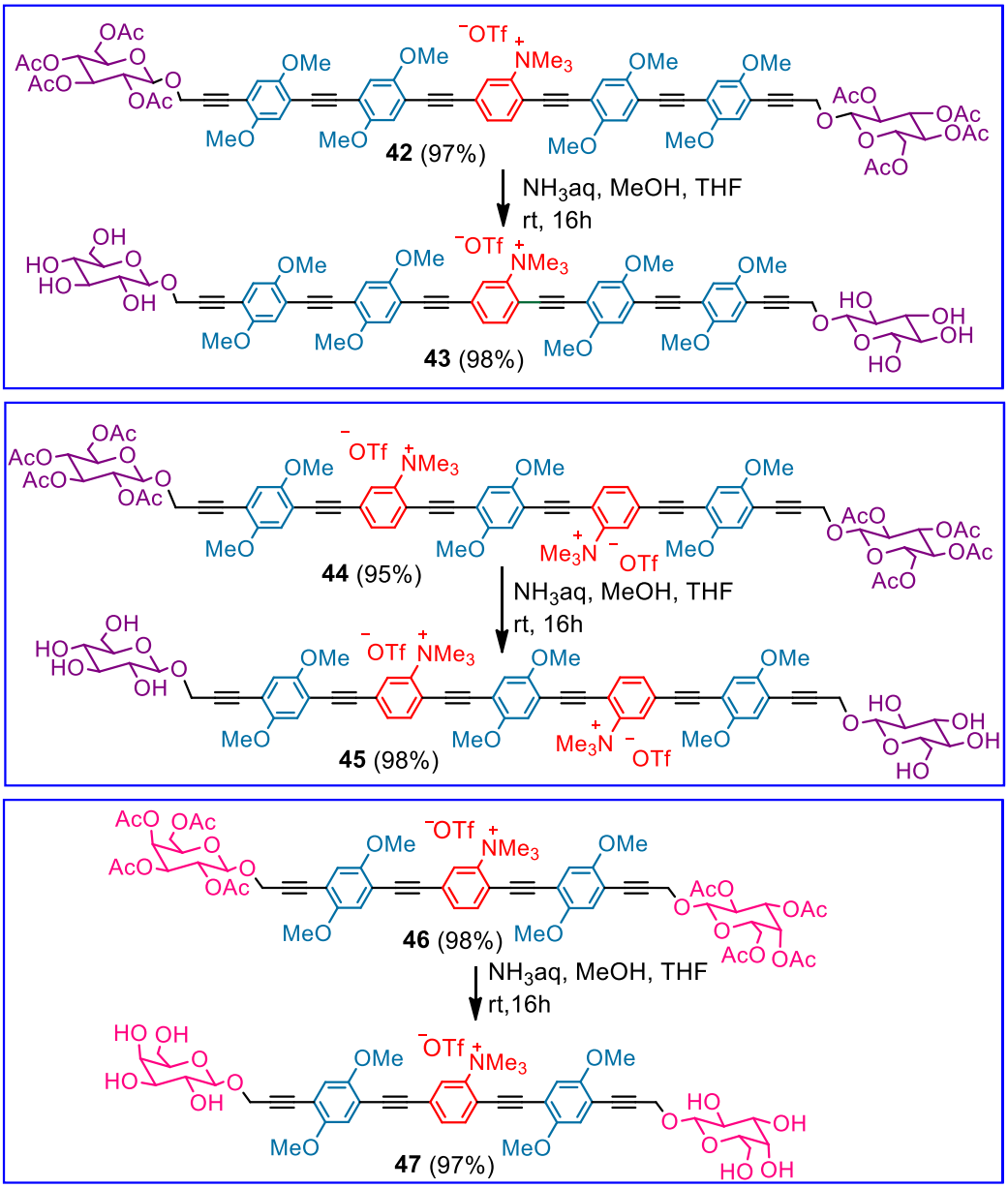

Scheme 2.17

The spectroscopic features (absorption, emission, emission quantum yield and lifetime) of these new compounds, together with the studies of DNA interactions with two of them are reported in Chapter **3**.

2.5 CHAIN DESYMMETRIZATION

The last part of the structural modifications introduced on our glycosydic amino OPEs consisted in finding the best synthetic strategies leading to the desymmetrization of the aromatic chain. This was realized with two different aims:

5A) introducing electron withdrawing groups that, together with the presence of the electron donating –OMe and $–NMe_2$ groups could influence the absorption and emission features of the resulting OPEs;

5B) introducing new terminations that could be used to anchor our systems to a variety of different materials (e.g. upconverting nanoparticles).

2.5A. Introduction of strong electronwithdrawing groups. As regards the first of the two purposes, we thought to modify the symmetric chain of OPEs by the insertion of a 2,3,5,6-tetrafluoro aryl moiety. Due to their unique properties, polyfluorinated aromatic compounds find broad utility. For instance, fluorine substituted organic compounds play prominent role in biological, pharmaceutical and agrochemical products, and more recently were also applied as liquid crystals, organocatalysts and other various materials.[144] Moreover, fluorinated aromatic oligomers are employed as electron-transporting layers in organic light diodes (OLEDs), as thermoplastic materials but also in supramolecular self-assembly.[145]

The presence of one or more fluorine atoms in an organic compound confers properties and reactivity, which are significantly different from those of the non-fluorinated counterpart, without significant modification of sterics, because the

[144] Kulhánek, J.; Bureš, F.; Pytela, O.; Pippig, F.; Danko, M.; Mikysek, T.; Padělková, Z.; Ludwig, M. *J. Fluorine Chem.* **2014**, *161*, 15.
[145] Sapegina, A.; Krasavina, M. *J. Fluorine Chem.* **2018**, *209*, 56.

length of the CF bond is almost the same as the length as the CH bond (1.39 and 1.09 Å respectively). Furthermore, the C-F bond is the strongest single bond in organic chemistry (105.4 kcal mol^{-1}) and this can be explained by the high electronegativity of the fluorine atom (3.98 for F vs 2.55 for C). The high strength of the bond can be understood to be due to an electrostatic attraction between $C^{\delta+}$ and $F^{\delta-}$ rather than an apolar covalent bond with electron sharing.[146] Thanks to these features, fluorinated aromatic systems also represent interesting electron acceptor moieties for organic push–pull systems:[147] an example of the latter systems is given by organic π-systems end-capped with an electron donor (D) and an electron acceptor (A) (**Figure 2.10**). Due to the D–A charge-transfer interaction (ICT), a new low energy molecular orbital (MO) is formed. Facile excitation of the electrons within the new MO can be achieved using visible light, and therefore push–pull molecules are generally coloured and referred to as charge-transfer chromophores. Push-pull systems can be found as active substances in organic electronics and optoelectronics, conductors, photovoltaics and solar photon conversion.

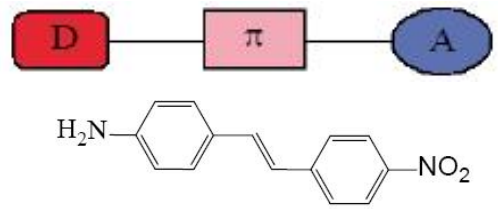

Figure 2.10

Fluorinated chemicals are of growing importance, with applications in medicine.[148] For instance, they are known to influence the activity of various enzymes. Fluorine-containing drugs are used in medicine as anaesthetics, antibiotics, anti-cancer and anti-inflammatory agents, psychopharmaceuticals,

[146] O'Hagan, D. *Chem. Soc. Rev.* **2008**, *37*, 308.
[147] Bureš, F. *RSC Adv.* **2014**, *4*, 58826.
[148] Strunecká, A.; Patočka, J.; Connett, P. *J. Appl. Biomed.* **2004**, *2*, 141.

and in many other applications. As already seen, fluorine substitution has profound effects on the properties of organic compounds. The high electronegativity of fluorine can also here modify electron distribution in the molecule, affecting its absorption, distribution and metabolism.[149] In a metabolic cascade of chemical reactions this effect can be significantly magnified, so even a single fluorine atom can completely change biological properties of a drug.

On the basis of these observations, we planned the synthesis of two new fluorinated OPEs **48** and **49** (**Figure 2.11**) bearing, together with the tetrafluoroaryl moiety at the end of the conjugated chain, our usual electron-rich dimethoxy and dimethylamino aromatic rings. Their synthesis was projected with the aim to study these systems as push-pull system and, in particular, to study the influence of the relative distance of the electron-donating aromatic rings from the electron-accepting fluorinated termination, being substituent in the central ring in the dimethylamino group in **48**, and the dimethoxy one in **49**.

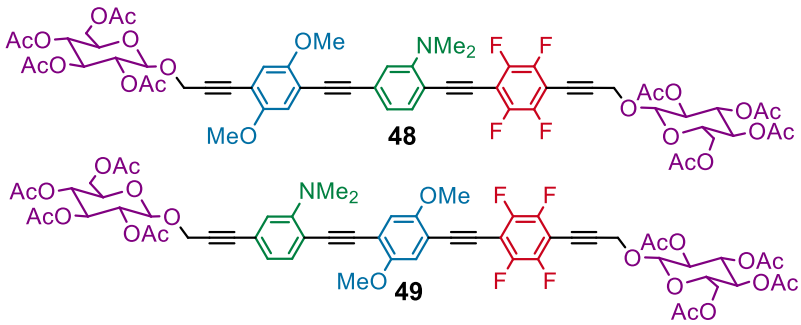

Figure 2.11

One of such ubiquitous synthons for the construction of polyfluorinated compounds is 1,4-diiodo-2,3,5,6-tetrafluorobenzene whose high reactivity, particularly in metal-catalysed reactions, is likely determined by the activation due to the four fluorine atoms present in the structure.[150]

[149] Wang, J.; Sánchez-Roselló, M.; Aceña, J. L.; del Pozo, C.; Sorochinsky, A. E.; Fustero, S.; Soloshonok, V. A.; Liu, H *Chem. Rev.* **2014**, *114*, 2432.
[150] Sapegina, A.; Krasavina, M. *J. Fluorine Chem.* **2018**, *209*, 56.

The convergent approach shown until now is not possible to be used in the synthetic routes leading to asymmetrically substituted OPE **48** and **49**; one alternative way is to create two differently and opportunely derivatized side-arms, whose cross-coupling reaction could take to the desired asymmetric OPE sequence.

Being, in our project, the fluorinated ring at the end of our two chains, the first step was the synthesis of the new fluorinated *side-arm* **51** (**Scheme 2.18**) containing a sugar termination, and a iodoaryl function able to react in a further Pd-mediated coupling. But, as described in paragraph 1.4, iodoarenes functionalized with electron withdrawing groups are highly reactive in Sonogashira couplings[151] and, in our case, compound **51** resulted even more reactive than its precursor **50**. This made the product more susceptible to further couplings, giving great amount of the bis-glycosilated product **51-bis.**

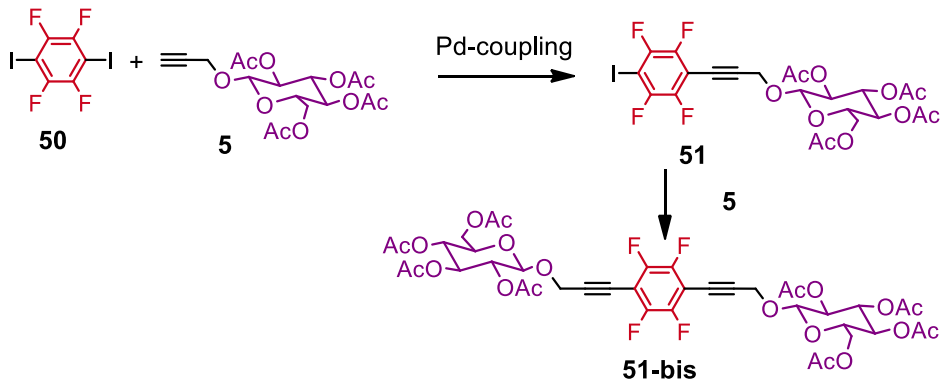

Scheme 2.18

All the attempted reaction conditions to obtain the glucosylated **51** in good yields, starting from 1,4-diiodo-2,3,5,6-tetrafluorobenzene and propargyl glucoside **5** are reported in **Table 2.1**.

After several attempts, with different catalysts, solvents, temperatures and times, we managed in the obtainment of **51** as the major product in highly reactive

[151] Chinchilla R.; Nájera C. *Chem. Rev.* **2007**, *107*, 874.

medium [Pd(II), CuI, PPh_3 as activator and only Et_3N as solvent], at high temperature (80 °C) and short reaction time (1h) (Entry **I** in **Table 2.1**).

Table 2.1. Conditions for the coupling reaction between **50** and **5** to form **51** (**Scheme 2.18**)

Entry	**50** (eq.)	**5** (eq.)	Catalysts	Solvents	Time / Temp	Products
A	2	1	$Pd(PPh_3)_4$ (0.1 eq.)	DMF / Et_3N 1:1	24 h / 60 °C	**5** + **51-bis**
B	3	1	$Pd(PPh_3)_2Cl_2$ (0.025 eq.) / CuI (0.025 eq.) / PPh_3 (0.05 eq.)	DMF / Et_3N 1:2	1 h / 65 °C	**51/51-bis** 1:3
C	3	1	$Pd(PPh_3)_2Cl_2$ (0.025 eq.) / CuI (0.025 eq.)	DMF / Et_3N 1:2	1 h / 65 °C	**51/51-bis** 1:4
D	3	1	$Pd(PPh_3)_2Cl_2$ (0.01 eq.) / CuI (0.01 eq.)	DMF / Et_3N 1:2	1 h / 65 °C	**51/51-bis** 1:5
E	3	1	$Pd(PPh_3)_2Cl_2$ (0.025 eq.)	DMF / Et_3N 1:2	24 h / 80 °C	Almost only **5**
F	3	1	$Pd(PPh_3)_2Cl_2$ (0.025 eq.) / CuI (0.025 eq.)	DMF / Et_3N 1:2	24 h / rt	Almost only **5**
G	3	1	$Pd(PPh_3)_2Cl_2$ (0.025 eq.) / CuI (0.025 eq.) / PPh_3 (0.05 eq.)	DMF / Et_3N 1:2	24 h / rt	**5/51/51-bis** 2:1:4
H	3	1	$Pd(PPh_3)_2Cl_2$ (0.025 eq.) / CuI (0.025 eq.)	$^iPr_2NH$	1 h / 65 °C	**51/51-bis** 1:4
I	4	1	$Pd(PPh_3)_2Cl_2$ (0.025 eq.) / CuI (0.025 eq.) / PPh_3 (0.05 eq.)	Et_3N	1 h / 80 °C	**51/51-bis** 3:1

Moreover, after most of the reaction crude chromatographic separations, we could observe that **51** could not be separated by a small quantity of a by-product, characterized by the same *rf* even in different solvent systems and by a very similar ^{1}H-NMR spectrum. By searching in literature, it was found out that one commonly observed by-product of cross-coupling reactions of the fluorinated aromatic halides is the hydrodehalogenation one (ArF−X → ArF−H; X = halide), then affecting the efficiency and selectivity of the overall catalytic process (**Figure 2.12**).[152] Finally, it was observed that the conditions **I** were the best ones to avoid, or at least minimize, both the formation of **51-bis** and also the hydrodehalogenation product. However, in some cases a small amount of the

[152] Orbach, M.; Choudhury, J.; Lahav, M.; Zenkina, O. V.; Diskin-Posner, Y.; Leitus, G.; Iron, M. A.; van der Boom, M. E. *Organometallics* **2012**, *31*, 1271.

latter is anyway formed. Nevertheless, considering that the two products are extremely difficult to be separated by chromatography and since the hydrodehalogenated compound is not reactive anymore in cross-couplings, the mixture of the two could be used as it was, for further metal-catalysed derivatizations, remaining unreacted and easily separated in this second step.

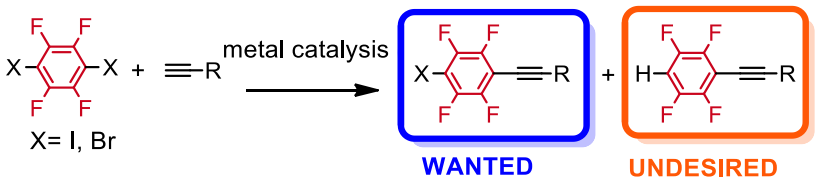

Figure 2.12

Thus, once obtained our desired fluorinated building block **51**, it has been subjected to a Ag_2O-cocatalized Sonogashira coupling with **24** (**Scheme 2.19**), already synthesized for the convergent synthesis of **25** (**Scheme 2.9**), to give rise to the first fluorinated OPE **48**, obtained pure after purification by chromatography column.

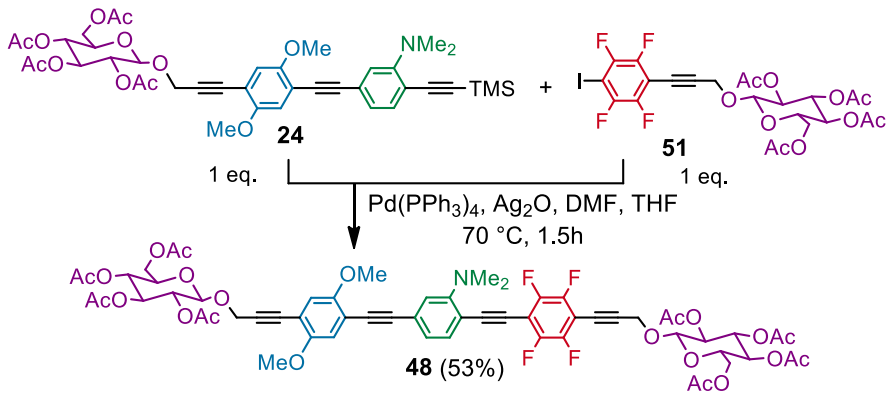

Scheme 2.19

The same approach was planned for the second fluoro-derivative **49**, characterized by the central dimethoxy aromatic ring. In this case, it was needed

a different two-ring *side-arm*, similar to **24**, but with the dimethylamino-substituted aromatic ring adjacent to the sugar moiety. We chose as starting product **11**, already used in the synthesis of **OPE_Glucose 2** (**Scheme 2.4**), that bears a trimethylsylyl acetylenic group, as already shown reactive in a Sonogashira cross-coupling mediated by Pd(0) an co-catalysed by Ag_2O. In this conditions, and in order to minimize the functionalization of both iodo-substituents on **7**, an excess of the latter was reacted with **11** (**Scheme 2.19**). After the removing of **7** through precipitation from methanol (paragraph **2.1**), **52** was obtained pure and in good yields after the purification of the resulting crude by chromatography. Cross-coupling reaction of **52** with ethynyl trimethylsylane, in a Pd(II)/Cu(I) catalysed Sonogashira conditions, gave **53**, which could directly react with the fluoro-derivative **51** to afford **49**, obtained pure as a yellow powder after purification by chromatography column.

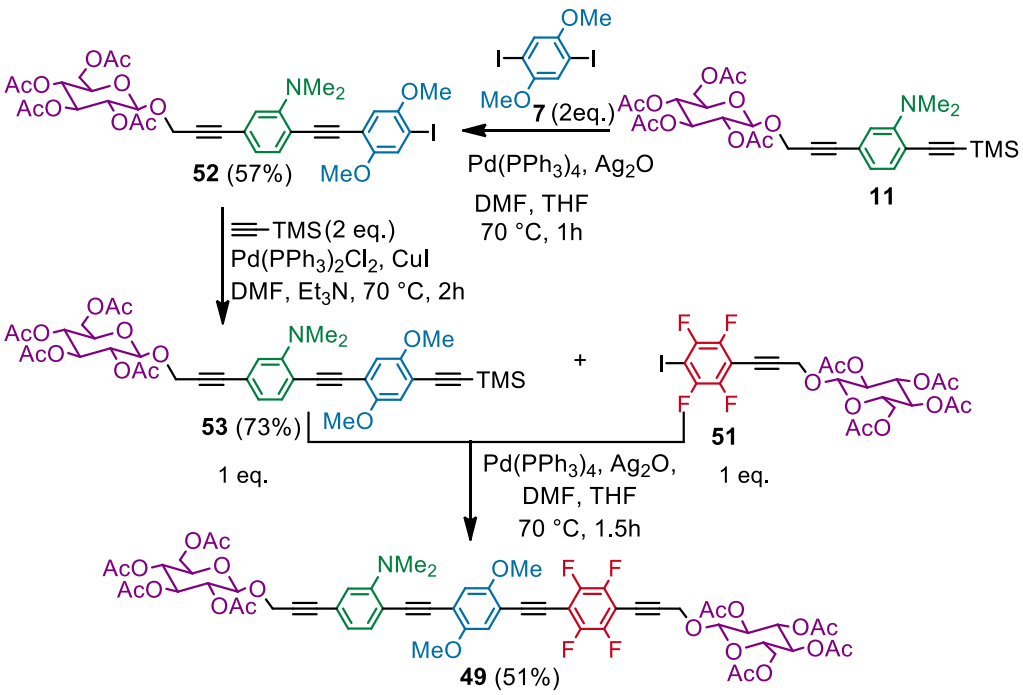

Scheme 2.19

The newly formed structures, containing a tetrafluoroaryl moiety, were also characterized by NMR analysis. In this case, ^{13}C-NMR spectrum of the species resulted more interesting than the ^{1}H_NMR spectrum, because of the lack of protons in the fluorinated aromatic ring. Actually, ^{13}C-NMR spectra of fluorinated compounds are difficult to obtain for several reasons. On the one hand, in the absence of directly bound protons, lack of nuclear Overhauser enhancement and slow relaxation rates can give very weak carbon signals. On the other hand, coupling to fluorine reduces even more the intensity of the peaks and can render spectra very cumbersome to attribute: the complexity results not only from the strong one-bond, but also from the long-range ^{13}C-^{19}F couplings ($^{1}J_{F,C}$ ~245 Hz; $^{2}J_{F,C}$ ~21 Hz; $^{3}J_{F,C}$ ~7.8 Hz; $^{4}J_{F,C}$ ~3.2 Hz).[153]

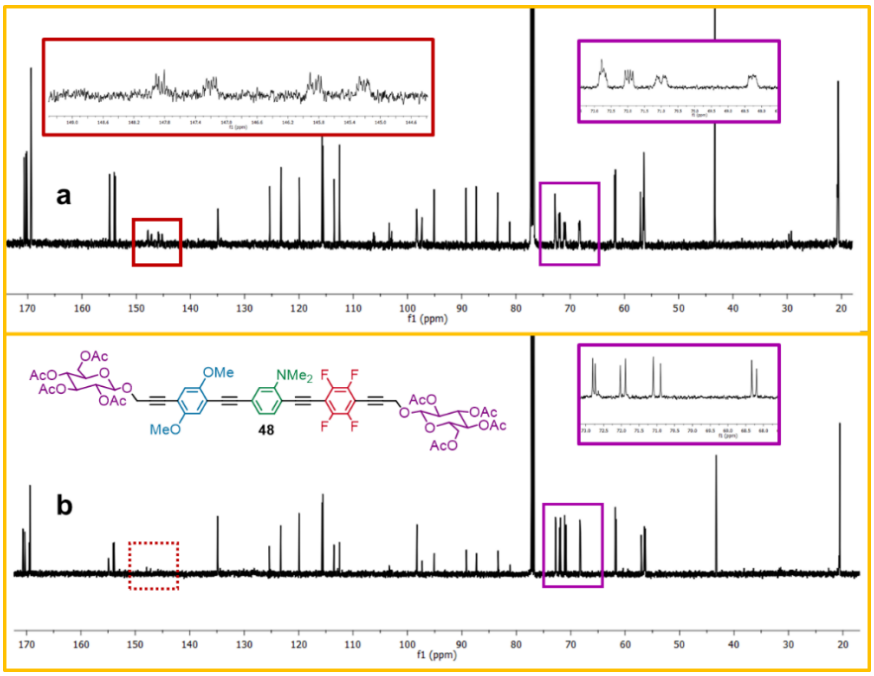

Figure 2.13. ^{13}C-NMR spectra of concentrated (**a**) and dilute (**b**) solutions of **48** in $CDCl_3$

In **Figure 2.13** the ^{13}C-NMR spectrum in $CDCl_3$ of the fluorinated OPE **48**, registered from solution of different concentration [$5\cdot10^{-2}$ M **(a)** and $3\cdot10^{-3}$ M **(b)**]

[153] Pons, M.; Feliz, M.; Giralt, E. *Tetrahedron Lett.* **1985**, *26*, 2817.

solution is reported. According to literature, the appearance of the splitted signals related to the aromatic carbons directly linked to the fluorine atoms ($^1J_{C\text{-}F}$=258Hz), in the region between 140 and 150 ppm is detectable only from the most concentrated solution **(a)**. C-F long-range coupling constants with the other quaternary carbons of the fluorinated ring and the ethynyl quaternary carbons are also detected (Chapter 3). Finally, it is worth a comparison between the pattern related to the pyranose ring carbon in the two different spectra. The sharp signals related to these carbons in **(b)**, resulting splitted in multiplets in **(a)** could be diagnostic of the formation of aggregates. Further studies are ongoing.

2.5B. Anchoring to nanoparticles. The last part of my work consisted in the synthesis of a different type of asymmetrically substituted OPEs able to be anchored to nanomaterials. In particular, one of the intended purposes was to try to shift the absorption of our luminescent biocompatible dyes (**OPE_Glucose 1**: λ_{abs}=388 nm and **OPE_Glucose 2**: λ_{abs}=392 nm) in the so-called *biological window*, the range of wavelengths from 650 to 1350 nm (Near-Infrared NIR) where light has its maximum depth of penetration in tissues. In this way, it could have in principles been possible to extend their use not only in superficial Photodynamic Therapy (paragraph **1.3**), but also for deeper therapeutic treatments.

In order to achieve this result, it was thought to anchor our systems onto up-converting nanoparticles (UCNPs) that, because of a mechanism of two-photon excitation (paragraph **1.2**),[154] are characterised by some emission bands centred at higher-energy wavelengths than the absorption maximum. The linkage of our OPE system, having the absorption maxima matching with those UCNPs emission bands, could give the new system shown in **Figure 2.14**. This one, after irradiation with NIR light, is expected to undergo an initial upconversion followed by energy transfer to the OPE chain (**OPE_Glucose 1**: λ_{em}=472 nm and

[154] Wen, S.; Zhou, J.; Zheng, K.; Bednarkiewicz, A.; Liu, X.; Jin, D. *Nat Commun.* **2018**, *9*, 2415.

OPE_Glucose 2: λ_{em}=474 nm), that, in its deactivation process, is expected to partially produce singlet oxygen (as already explained in paragraph 1.2), useful in PDT. Moreover, the formation of a *glucosidic shell* surrounding the system, could guarantee solubility and biocompatibility to the decorated nanoparticles, but also selectivity for the sugar avid cancer cells.[155]

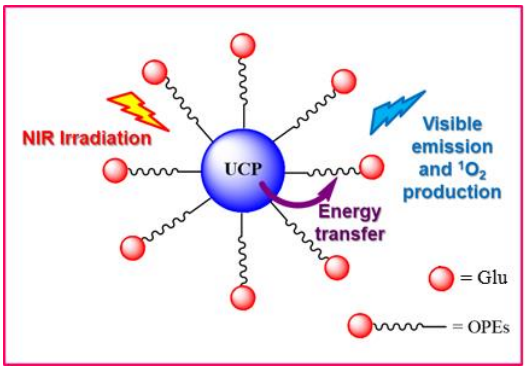

Figure 2.14

In 2015, the research group of Prof. J. Capobianco,[156] from Concordia University (Montreal), published an article reporting a system for the controlled release of doxorubicin from lanthanide doped upconverting nanoparticles (Ln-UCNPs). These nanoparticles ($LiYF_4$:Tm^{3+}/Yb^{3+}-UCNPs), excitable in the NIR region (980 nm), have two strong and wide UV emission bands centred at 353 and 368 nm, which can be used as an internal source for UV light. Doxorubicin (Dox), a famous anticancer drug, was loaded onto the surface of the nanoparticles (approximately 1500 molecules of Dox per nanoparticle) through a photocleavable (360nm) linkage (**Figure 2.15**). After irradiation of the Dox-loaded Ln-UCNPs with NIR light, it was observed a time-dependent release of doxorubicin from the Ln-UNCPs into solution.

[155] Warburg, O.; Wind, F.; Negelein, E. *J. Gen. Physiol*., **1927**, 8, 519–530; Warburg, O. *Science*, **1956**, 123, 309.
[156] Dcona, M. M.; Yu, Q.; Capobianco, J. A.; Hartman, M.C.T. *Chem. Commun.* **2015**, *51*, 8477.

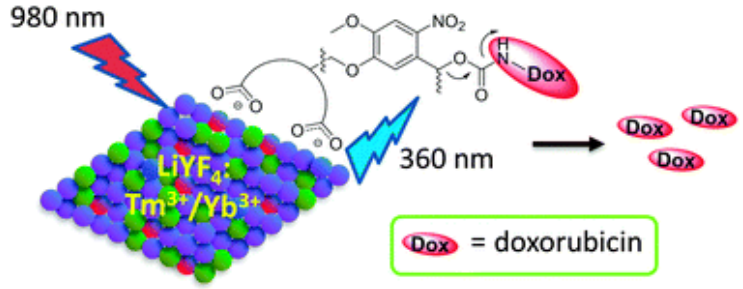

Figure 2.15

On the basis of these studies, we got interested in these specific nanoparticles that show photophysical properties that could be suitable for interactions with our OPEs. Therefore, in collaboration with Prof. Capobianco, and Proff.s M. Ribagorda and D. H. Ortgies from Universidad Autónoma de Madrid, we began a research project directed to the linkage of our gluco OPEs to Prof. Capobianco's nanoparticles.

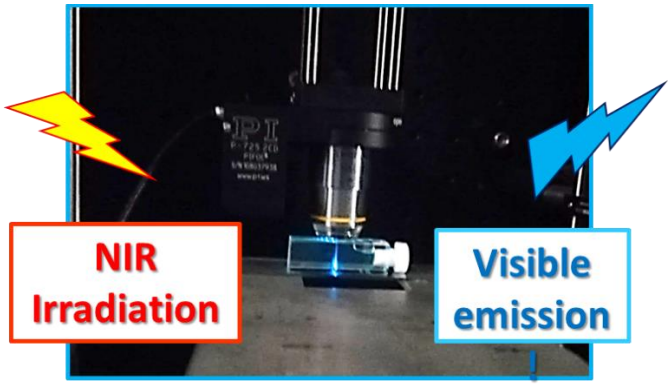

Figure 2.16. NIR irradiation of Ln-UCNPs in dispersion in presence of **OPE_Glucose 1**

First of all, it should have been attempted if the emission of the nanoparticles could match the absorption of our OPE systems and if the two species could properly go through the energy transfer process. Thus, a previous test on a water dispersion of the nanoparticles, in the presence of **OPE_Glucose 1**, was attempted. Thus, after irradiation with 980 nm light, the typical visible emission of **OPE_Glucose 1** (**Figure 2.16**) was detected.

Then, we studied the best way to anchor our systems to the nanoparticles, knowing that, generally, the positive charged $LiYF_4:Tm^{3+}/Yb^{3+}$-UCNPs are capped with oleate as counterion. Thus, asymmetric substituted OPE **54** (**Figure 2.17**) has been projected as best candidate for the UCNPs capping: in fact, besides maintaining the already studied aromatic chain - so maintaining the same spectroscopic features of **OPE_Glucose 1** - and one glucose moiety – in order to create the glucosidic external shell - the insertion of a phosphonate group as second termination could operate the ligand exchange with oleate.

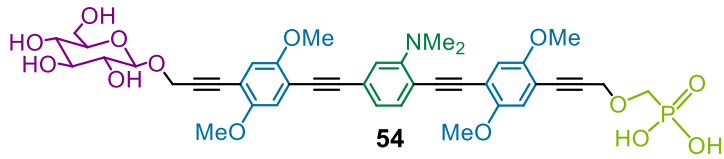

54

Figure 2.17

We began with the synthesis a new *side-arm* (**57**), analogous to **8** (synthesis in **Scheme 2.2**), but containing a diethylphosphonate moiety, that could be deprotected to phosphonic acid at the end of the synthetic route. Thus, commercially available diethyl (hydroxymethyl)phosphonate **55**, treated with sodium hydride and propargyl bromide (**Scheme 2.20**),[157] led to **56** which was then cross-coupled with an excess of 1,4-diiodo-2,5-dimethoxy benzene **7** to form **57** in good yields.

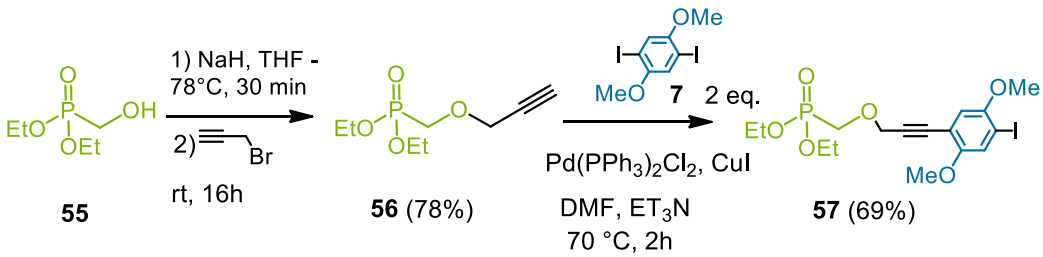

Scheme 2.20

[157] Delain-Bioton, L.; Villemin, D.; Jaffrès, P.-A. *Eur. J. Org. Chem.* **2007**, *8*, 1274.

Before going on with a very tricky synthetic route, we previously tried to think about the best way to hydrolyse the phosphonate and the acetyl groups without affecting our OPE glucose systems. For this reason, we synthesized the model compound **58** (**Scheme 2.21**), characterised by the presence of the two protected terminations (glucosidic and phosphonyl) spaced by only one dimethoxy aromatic ring, through the Pd(0)-mediated cross-coupling between **57** and propargyl glucoside **5**.

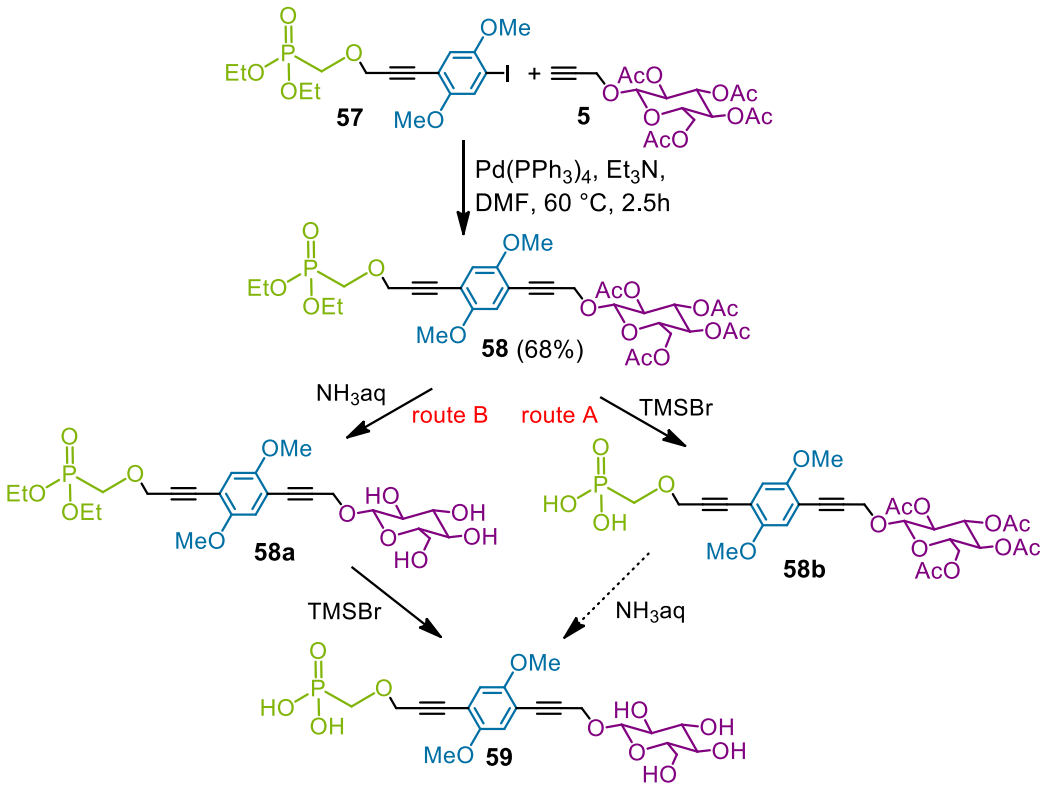

Scheme 2.21

For what concerned the phosphonate ester hydrolysis, having a deep look at the literature, we only found procedures involving bromotrimethylsilane (TMSBr) as reagent in methanol,[158] through to a two-step deprotection, followed

[158] Carbonneau, C.; Frantz, R.; Durand, J.-O.; Granier, M.; Lanneau,G. F., Corriu, R. J. P. *J. Mater. Chem.* **2002**, *12*, 540.

by a final methanolysis step, but we could not find any example of this kind of reaction carried out in presence of acetylated or free sugar moieties.

For this reason, at first we investigated the best strategy for the phosphonate hydrolysis in the presence of the protected sugar, as shown in route A, **Scheme 2.21**. Unfortunately, after many attempts to obtain **58b** in different conditions of time, temperature and TMSBr ratio (**Table 2.2**), we were only once (Entry **4**) able to obtain a very small amount of **58b**, but the complexity of the crude made the purification impossible.

Table 2.2: reaction conditions for **58** phosphonate group hydrolysis in CH_2Cl_2

Entry	TMSBr	Temp.	Time	Products
1	1) 3 eq. 2) 3 eq.	1) rt 2) rt	1) 4h 2) 10h	starting and decomposition products
2	6 eq.	rt	4h	decomposition products
3	8 eq.	0°C	1h	decomposition products
4	8 eq.	rt	1h	**60** (very low yeld and difficult purification)

By analysing all the resulting reaction crudes by NMR, we could notice that actually the linkage between the sugar moiety and the propargylaromatic system was not affected by the treatment with the TMSBr. Therefore in a second attempt, we tried a previous deacetylation of the sugar (**Scheme 2.21**, route B). **58a** was quantitatively obtained from **58** in presence of an excess of ammonia, and then subjected to phosphonate deprotection, under the best conditions we had found (TMSBr 8 eq., rt, 1h). Unfortunately, the reaction led to the sole formation of decomposition products without the obtainment of **59**. The last attempt of deprotection was attempted on *side-arm* **57**. The analysis of the complex reaction crude ^{1}H_NMR, and the detection of two triplets at 6.26 and 6.35 ppm, maybe corresponding to two -CH_2OH groups, made us conclude that these kind of propargyl system undergo the undesired cleavage shown in **Scheme 2.22**.

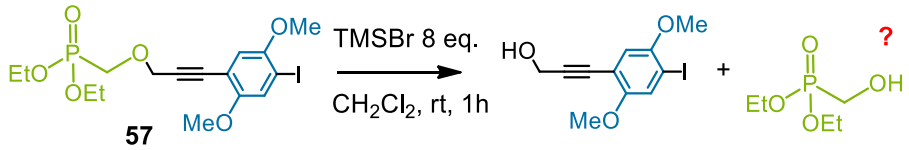

Scheme 2.22

An alternative synthetic strategy, introducing a (3-azidopropyl)phosphonic acid through a Huisgen 1,3-dipolar cycloaddition ("click" reaction,)[159] onto an asymmetrically substituted OPE (**63**), was then projected (**Scheme 2.23**).

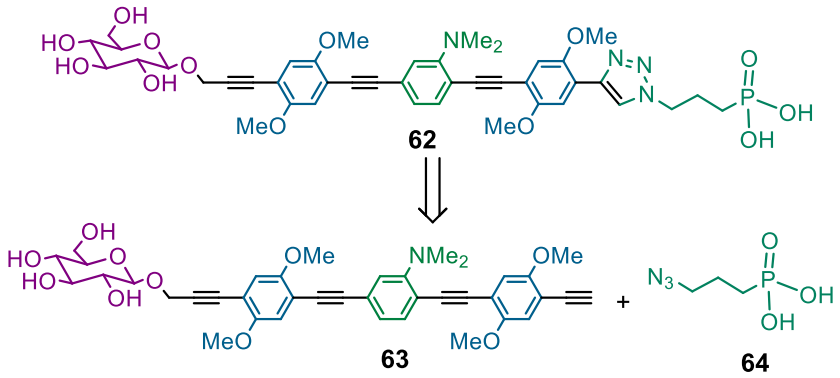

Scheme 2.23

First of all, the synthesis of the azidophosphonic dipole was attempted: commercially available (3-bromopropyl)phosphonic acid diethyl ester **65** was reacted with sodium azide to give the azido derivative **66**, in quantitative yields (**Scheme 2.24**).[160] Unfortunately, reaction with TMSBr/methanol, always led to the formation of the mono-ethyl ester **67**; further attempts for the total deprotection to **64** were unfruitful.

[159] Liang, L.; Astruc, D. *Coord. Chem. Rev.* **2011**, *255*, 2933.
[160] Prabhu, ; Pillarsetty, N.; GaliKattesh, H.; Katti, V. *J. Am. Chem. Soc.* **2000**, *122*, 1554.

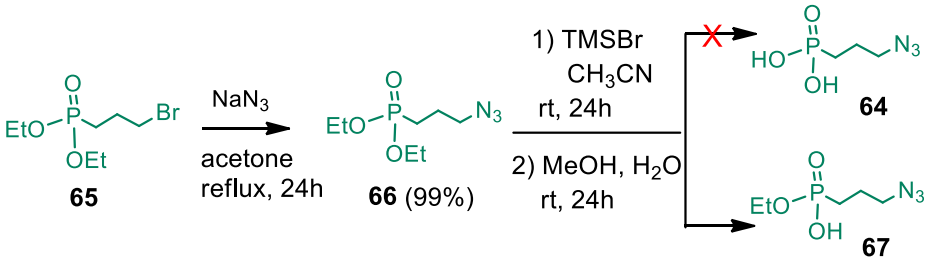

Scheme 2.24

Therefore, we decided to abandon the phosphonate group and to synthesize **68** (**Figure 2.18***)*, that bears the carboxylate group as alternative nanoparticles-capper; in fact, the synthesis of azidocarboxylic acids of modulable chain length, useful for the projected click reaction with **63**, was already reported.[161]

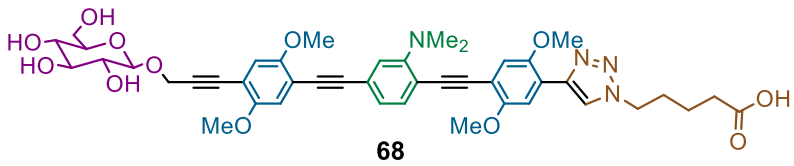

Figure 2.18

Once solved the dipole synthesis, we focused our attention to the synthesis of the asymmetrically substituted OPE **63** (**Scheme 2.25**). The already reported synthesis of **71**,[162] containing one masked and one reactive triple bond, was first of all performed; **70**, coming from a first mono-functionalization with ethynyltrimethylsilane of **7** to **69**, and a second coupling on **69** with 2-methyl-3-butyn-2-ol was synthesized.

[161] Chan-Seng, D.; Lutz, J.-F. *ACS Macro Lett.* **2014**, *3*, 291.
[162] Lu, Q.; Liu, K.; Zhang, H.; Du, Z.; Wang, X.; Wang, F. *ACS Nano* **2009**, *3*, 3861.

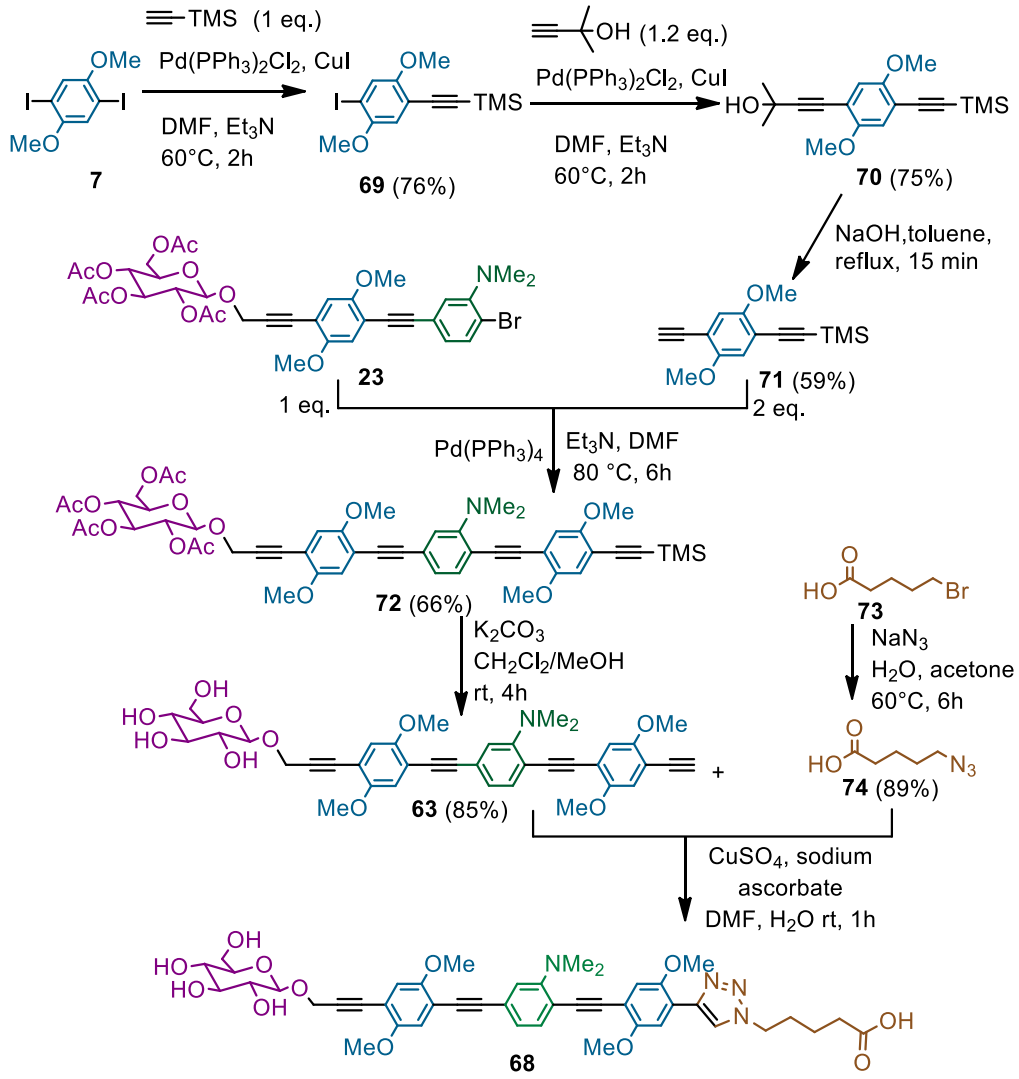

Scheme 2.25

By treatment of **70** with NaOH in refluxing toluene, deprotection to **71** was performed, even if not in high yields, because of the unavoidable ratio of deprotection of both ethynyl residues in the reported harsh conditions.

Thus, in order to promote the substitution of the sterically hindered bromo substituent in **23** (paragraph **2.2**), it was reacted with an excess **71**, in presence of $Pd(PPh_3)_4$ (**Scheme 2.25**). The acetylated compound **72** was obtained in good yield after simple purification by chromatography and the glucose termination

and the trimethylsilyl group were finally simultaneously deprotected with K_2CO_3 to final OPE **63**. A click cycloaddition, catalized by copper (II) sulphate and sodium ascorbate in a mixture 1:1 of DMF and water, between **63** and 5-azido-valeric acid **74** [163] (prepared from the commercially available bromide **73**) was finally performed. The desired cycloadduct **68** was extracted with ethyl acetate from the aqueous solution, obtained as a bright orange powder, and recognized by ^{1}H-NMR. However, the ^{13}C-NMR spectrum of **68**, and the related bidimensional experiments, showed us the product was not pure and not suitable for the complete characterization. In fact, the supposed presence of carboxylic-Cu complexes, did not allow the clear attribution of the methylenic carbon of the aliphatic chain. For this reason **68**, as it was, was sent to the Madrid Labs to be purified through finest separation methods, characterized and then anchored on UCNPs.

The full *dmso-d6* ^{1}H_NMR spectrum of **68** (a), together with its enlarged down-field significative area (b) compared with the same detail of **OPE_Glucose 1** ^{1}H-NMR (c), are reported in **Figure 2.19**. It is worth to notice that, as it happens for similar compounds known from the literature,[164] it is possible to notice the downfield shift (from7.1 to 7.8 ppm) of the aromatic dymethoxyaryl proton near to the triazole ring and the appearance of a singlet at 8.45 ppm, related to the only one proton of the triazolic ring, diagnostic of the success of the click reaction.

[163] Chan-Seng, D.; Lutz, J.-F. *ACS Macro Lett.* **2014**, *3*, 291.
[164] Pertici, F.; Varga, N.; van Duijn, A.; Rey-Carrizo, M.; Bernardi, A.; Pieters, R. J. *Beilstein J. Org. Chem.* **2013**, *9*, 215.

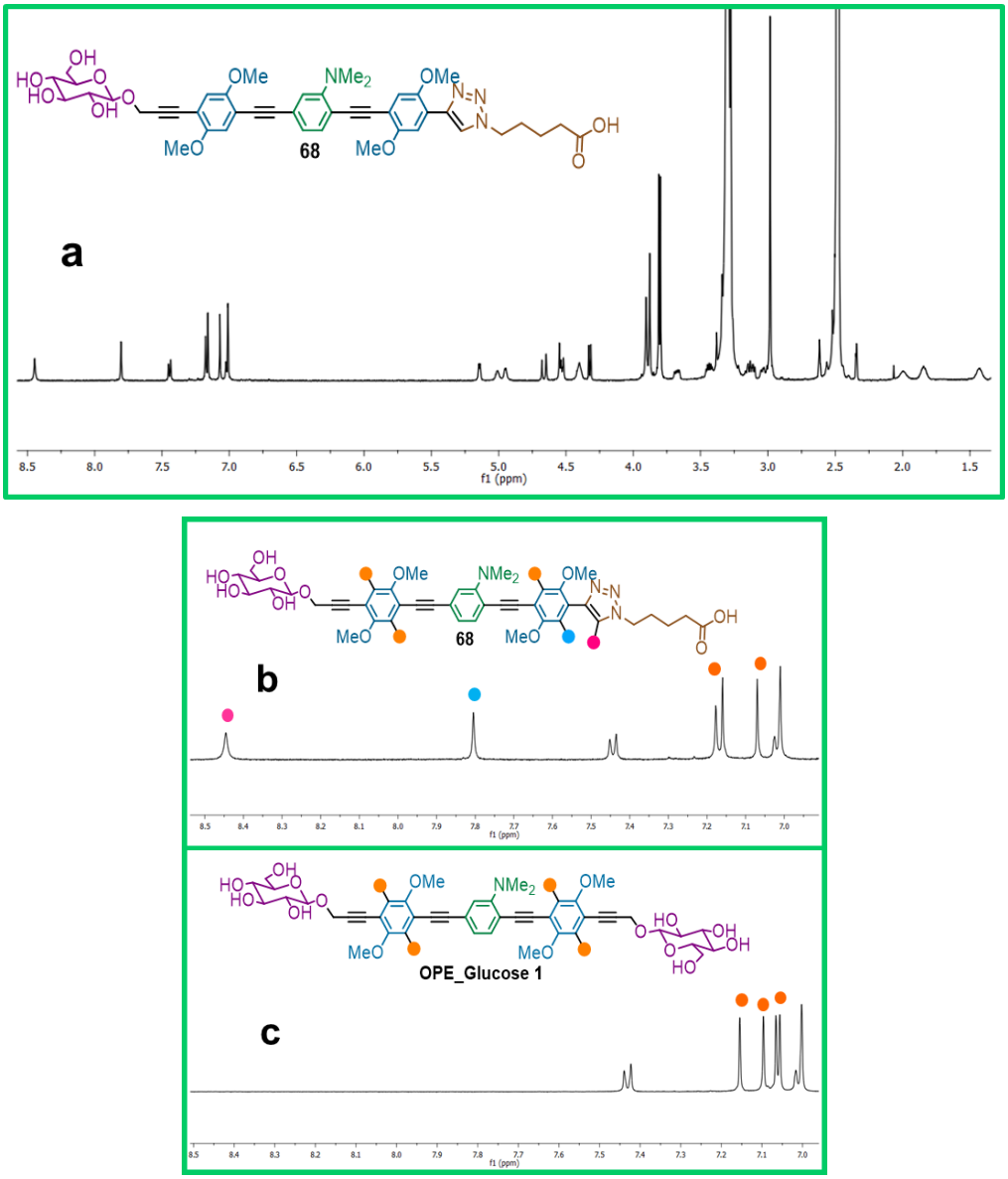

Figure 2.19

Finally, the spectroscopic features of **63** and **68** are reported in **Figure 2.20**. The absorption spectra are characterized by intense broad low-energy bands centred at 375 nm and at 364 nm, for **63** and **68** respectively. Both OPEs are luminescent at room temperature in aqueous solution and are characterized by extremely similar emission spectra (λ_{em}=480 nm). Both the absorption and emission spectra of the two species are comparable with those of **OPE_Glucose**

1 (**Figure 1.22**), demonstrating that the photophysical properties only depend on the central conjugated chain and also that the introduction of the triazole ring does not have any influence on them.

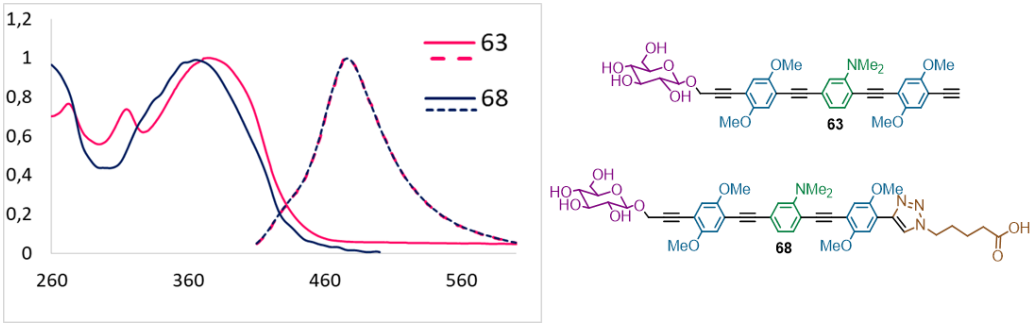

Figure 2.20. Absorption (full lines) and emission (dashed lines) spectra of **63** and **68** in water.

Now the functionalization of the UCP-nanoparticles with the new OPE is going on and the photophysical and biological properties of the new system will be investigated.

CHAPTER 3

Photophysical studies and preliminary biological applications

In order to determine how the modifications of the conjugated phenylene ethynylene system and the presence of different substituents could modulate the properties of the synthesized OPEs, preliminary photophysical studies and biological tests of some selected compounds were performed.

In particular, paragraph **3.1** deals with effect of the chain length and substituents modifications on the spectroscopic features of our OPE chains. On the other hand, the first biological tests on some selected compounds are the subject of paragraph **3.2**.

3.1 PHOTOPHYSICAL STUDIES

3.1A. Photophysical properties of 38 and 39.[165] In paragraph **2.4**, the synthesis of two new tetralkylammonium-OPEs (**38** and **39**, **Figure 2.8**) bearing one or two cationic groups directly linked to the phenynelethynylenic residues and two glucose terminations is been reported.

[165] Mancuso, A.; Barattucci, A.; Bonaccorsi, P.; Giannetto, A.; La Ganga, G.; Musarra-Pizzo, M.; Salerno, T. M. G.; Santoro, A.; Sciortino, M. T.; Puntoriero, F.; Di Pietro M. L. *Chem. Eur. J.* **2018**, *24*, 16972.

The spectroscopic features of the quaternarized species **38** and **39** have been investigated in collaboration with Prof. Fausto Puntoriero, from ChiBioFarAm Department of University of Messina. In **Table 3.1** the spectroscopic features of the already reported **OPE_Glucose 1** and **OPE_Glucose 2** are reported for comparison.

Table 3.1. Spectroscopic features of **OPE_Glucose 1** and **OPE_Glucose 2** in aqueous solution.

OPE	Absorption λ_{max} nm (ε/ M^{-1} cm^{-1})	Luminescence 298 K			
		λ_{max}, nm	Φ	τ/ns	Φ_{1O2}
OPE_Glucose 1	388 (38900)	472	0.57	2.47	0.15
OPE_Glucose 2	392 (40000)	474	0.74	3.54	0.09

The absorption and emission spectra of **38** and **39** are reported in **Figure 3.1**. The spectra are characterized by intense broad low-energy absorption bands centred at 389 nm and at 394 nm, respectively, with ε values in the range 10^4–10^5 M^{-1} cm^{-1}. Both OPEs are luminescent at room temperature in aqueous solution (λ_{em}=508 nm and 463 nm for **38** and **39**, respectively) with relatively high quantum yields (Φ=0.3 and 0.62) and excited-state lifetimes in the order of a few ns (τ=0.8 ns and 1.8 ns). The presence of a symmetrical substitution in **39** is reflected into a small Stokes Shift and higher quantum yield with respect to **38**. By comparison of the absorption and emission spectra of **38** and **39** with their dimethylamino analogues **OPE_Glucose 1** and **OPE_Glucose 2**, the luminescence can be attributed, in both cases, to the deactivation of a pure singlet $\pi \rightarrow \pi^*$ excited state. Moreover, while there is almost no shift of the absorption maxima, a slight shift (to red for **38** and to blue for **39**) is observed in emission, with respect to **OPE_Glucose 1** and OPE_**Glucose 2**.

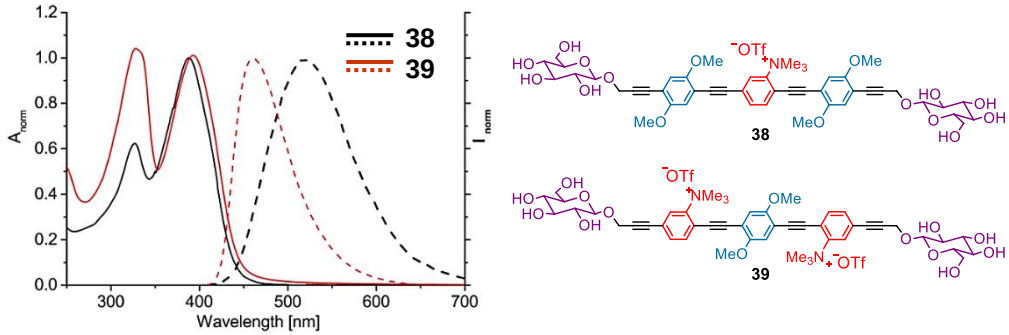

Figure 3.1. Absorption (full lines) and emission (dashed lines) spectra of **38** (black) and **39** (red) in water.

It is worth to point to point out the significant increase of the quantum yield of emission of **38** and **39**, compared to their dimethylamino analogues, as a consequence of the loss of the lone pair. In fact, the lone pair can act as electron donor to the excited state in **OPE_Glucose 1** and **OPE_Glucose 2**, activating a further non-radiative deactivation pathways via partial population of a charge separated state. The absence of this deactivation channel in the quaternarized species brings to higher quantum yields and longer emission lifetimes.

Studies of interaction of the two species with DNA are reported in paragraph **3.2A**.

3.1B. Effects of chain elongation and nitrogen quaternarization. As seen in paragraph **2.2**, two new pentameric OPEs (**13** and **14**, **Figure 2.2**) have been synthesized. With the aim to study the effect of the chain elongation on the spectroscopic features, the absorption and emission spectra of their acetylated analogues **17** (**Scheme 2.5**) and **25** (**Scheme 2.9**), in CH_2Cl_2, have been compared to the already reported trimers **9** (**Scheme 2.3**) and **12** (**Scheme 2.4**). The absorption spectra of the four species are reported in **Figure 3.2**. The two new elongated species are characterized by intense broad low-energy absorption bands, extending up to 450 nm, which can be attribute, as for **9** and **12**, to spin-allowed $\pi \rightarrow \pi^*$ transitions centred on the aromatic skeleton of OPEs. The

introduction of the two phenylene ethynylene units, resulting in an extension of the π-conjugated system, causes a decrease in the HOMO-LUMO energy gap. For what concerns the two mono-dimethylamino species **9** and **17**, the extended conjugation leads to a red-shift of the absorption band, from 389 nm to 400 nm; the same effect is observed for the bis-dimethylamino compounds **12** and **25** (from 402 nm to 413 nm).

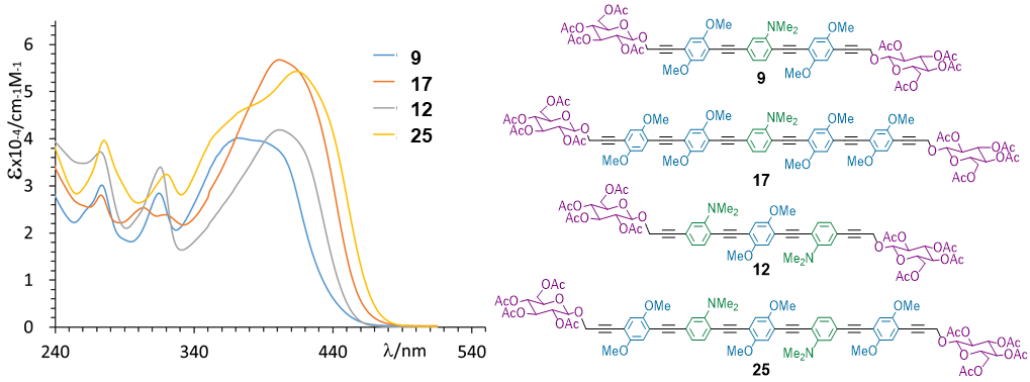

Figure 3.2. Absorption spectra of **17** and **25** in CH_2Cl_2 in comparison with **9** and **12**.

All the analysed species are luminescent at room temperature in CH_2Cl_2. The emission spectra of **17** and **25**, in comparison with their shorter analogues **9** and **12**, are reported in **Figure 3.3**. For both **17** and **25**, red-shifted emission maxima (~15 nm) are observed (λ_{em}=495 nm and λ_{em}=492, respectively) with respect to the model compounds **9** and **12** (λ_{em}=479 nm and λ_{em}=475) (paragraph **1.3**). For all the considered species, the lack of emission structured bands suggests a partial charge transfer character, due to the presence of the lone electron pairs on the nitrogen atoms.

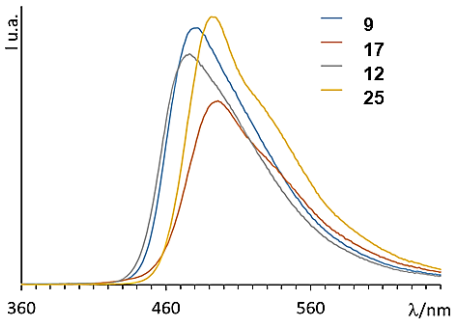

Figure 3.3. Emission spectra of **17** and **25** in CH_2Cl_2 in comparison with **9** and **12**.

It is worth to highlight that the emission quantum yields of both pentamers **17** and **25** are remarkably high (Φ=0.68 and 0.87, τ/ns=1.62 and 1.5) and increase passing from **17** to **25**. This effect can be explained considering that the Stokes shift is higher in **17** than **25**: this is due to a higher polarity of the excited state of **17** (4798 cm^{-1}), with respect to its ground state; this difference is less pronounced in **25** (3888cm^{-1}).

Table 3.2. Emission wavelength and Stokes Shift of some commercial fluorophores.

Compound	**λ^{em}_{max} (nm)**	**Δν (cm^{-1})**
Fluorescein	518	938
5-Carboxyfluorescein	520	1430
Fluorescein isothiocyanate	518	938
Rhodamine 123	528	981
Rhodamine 6G	552	823
Rhodamine Green™	520	1012
Cy2	506	521
Nile red	650	1856
BODIPY 493	504	401
BODIPY 505	512	389
Mito-Tracker Green™	516	1028
Mito-Tracker Red™	599	577

High Stokes shifts values are particularly interesting for bioimaging applications, since they help to increase the sensitivity through reduction of autofluorescence and interferences between excitation and emission.[166]

Moreover, it is worth to notice that the Stokes shift values of **17** and **25** are even higher than the ones of numerous typical commercial fluorescent dyes (**Table 3.2**).[167]

As described in paragraph **2.4**, the two elongated species **17** and **25** were also subjected to nitrogen quaternarization in order to study the influence of the cationic residues on the photophysical properties. In **Figure 3.4**, the absorption and emission spectra of the mono and dicationic pentamers **42** and **44** in CH_2Cl_2 are reported in comparison with their dimethylamino analogues **17** and **25**.

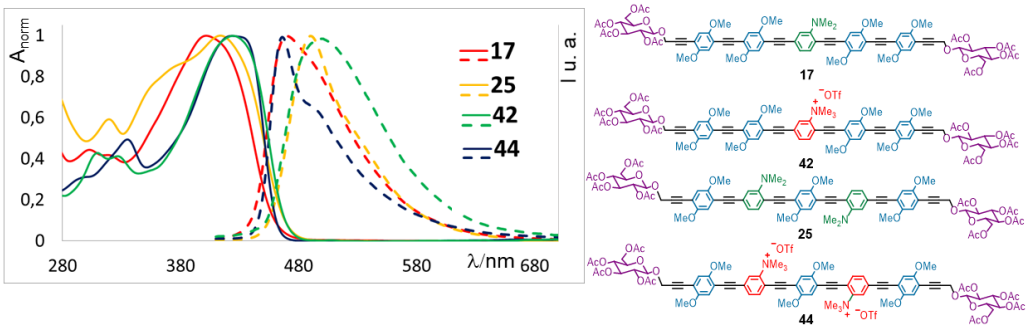

Figure 3.4. Absorption (full lines) and emission (dashed lines) spectra of **42** and **44** in CH_2Cl_2 in comparison with **17** and **25**.

In this case, the absorption spectra of the quaternarized species are characterized by intense broad low-energy absorption bands, centred at 425 nm (**42**) and 430 nm (**44**), which can be attribute, as for **17** and **25**, to spin-allowed $\pi \rightarrow \pi^*$ transitions centred on the aromatic skeleton of OPEs. All the species are luminescent in CH_2Cl_2 at room temperature. **44** exhibits a higher-energy structured emission with respect to its bis-dimethylamino analogue **25**; this effect

[166] Yang, Y.; An, F.; Liu, Z.; Zhang, X.; Zhou, M.; Li, W.; Hao, X.; Lee, C.-s.; Zhang, X. *Biomaterials* **2012**, *33*, 7803.
[167] Gao, Z.; Hao, Y.; Zhenga, M.; Chen, Y. *RSC Adv.* **2017**, *7*, 7604.

can be attributed to the disappearance of the charge-transfer character, present in **25**, which leads to a pure ligand-centred emission in **44**.

On the other hand, the emission of **42** results red-shifted and less structured with respect to **17**. In this case, the charge-transfer character seems to be opposite: in **17**, the free lone pair on the nitrogen atom acts as donor on the OPE skeleton, while in **42**, the lower-energy emission and the absence of structure in the emission band could be tentatively attributed to a donation from the dimethoxy side rings to the central one. The emission quantum yields of both **42** and **44** are very high (Φ=0.95 and 0.85, τ/ns=1.6 and 1.83 respectively). It is worth to highlight that the trend exhibited in the emission spectra of this series of compounds (**17**, **42**, **25** and **44**) is analogue to that of the corresponding three-rings long OPEs, previously discussed and that the emission exhibited by this series of compounds (**17**, **42**, **25** and **44**) is analogue to the one of the corresponding trimeric series (**OPE_Glucose 1**, **38**, **OPE_Glucose 2** and **39**). In fact, both the bis-quaternarized **44** and **39** are characterized by more structured emission and smaller Stokes Shifts, with respect to **42** and **38**, which seem to have an opposite charge-transfer mechanism. Further studies on this behaviour (electrochemistry measures, time-resolved spectroscopy and theoretical calculations) are now going on to with the aim to better investigate the excited states that are actually interested in these transitions.

Moreover, the spectroscopic features of the deacetylated analogues of **42** and **44** (**43** and **45**, **Scheme 2.17**) have been preliminary studied. In particular, while at a first sight **45** seems to be soluble in aqueous medium, the absorption spectrum of the species, at higher concentration than $5 \cdot 10^{-6}$ M (**Figure 3.5**), is characterized not only by the typical broad band, but also by the appearance of a new lower-energy narrow one.

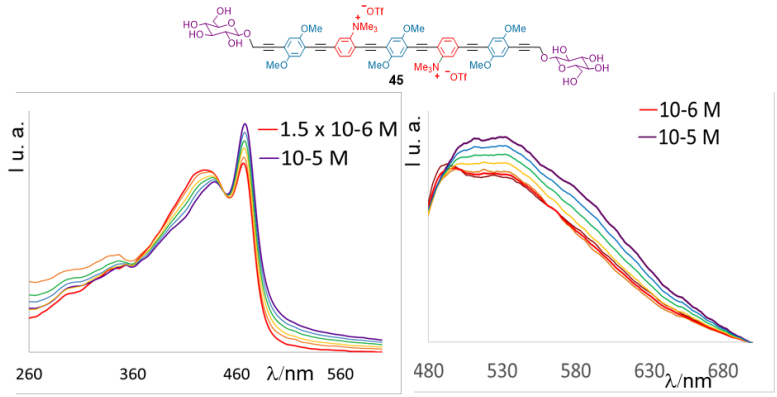

Figure 3.5. Absorption (left) and emission (right) of **45** at different concentrations in water.

The intensity ratio between the two bands depends on the concentration: in fact, at high dilutions, the lower-energy contribution decreases, while tends to increase together with the concentration. The emission spectra (on the right in **Figure 3.5**) show the same trend, appearing less intense and broader with respect to its acetylated analogue **44**. This behaviour suggests rigidity in the OPEs structure in solution, so an aggregation phenomenon of the species in aqueous medium can be taken into account. The presence of more than one species in solution is also confirmed by the excited state life time, which results at least biexponential, with two principal contributions (2 ns at 550 nm and 8 ns at 600 nm). The rate of these two contributions is function of the excitation wavelenght, confirming the presence of different species in solution. The same effect is not evident in **43**. Further studies are also ongoing.

3.1C. Effect of chain desymmetrization and introduction of strong electron withdrawing groups. The synthetic pathaways, leading to the introduction of a fluoroaryl moiety in the OPE chain, has been described in paragraph **2.5A**. The presence of strong electron withdrawing atoms was expected to influence the spectroscopic features of our conjugated dyes. In particular, two different systems have been projected with the aim to study the influence of the relative distance of the electron-donating $–NMe_2$ and -OMe aromatic rings from

the electron-accepting fluorinated termination, through the synthesis of **48**, bearing a central dimethylamino aromatic ring, and **49**, bearing a central dimethoxy aromatic ring (**Figure 2.11**). The absorption spectra, in CH_2Cl_2, of the two fluorinated species **48** and **49** are reported in **Figure 3.6**, in comparison with the already known compound **9**. Both the compounds are characterized, similarly to **9**, by intense broad low-energy absorption bands centred at λ_{abs}=370 nm for **48** and at 388 nm for **49**, due to due to spin-allowed $\pi \rightarrow \pi^*$ transitions centred on the conjugated skeleton of OPEs.

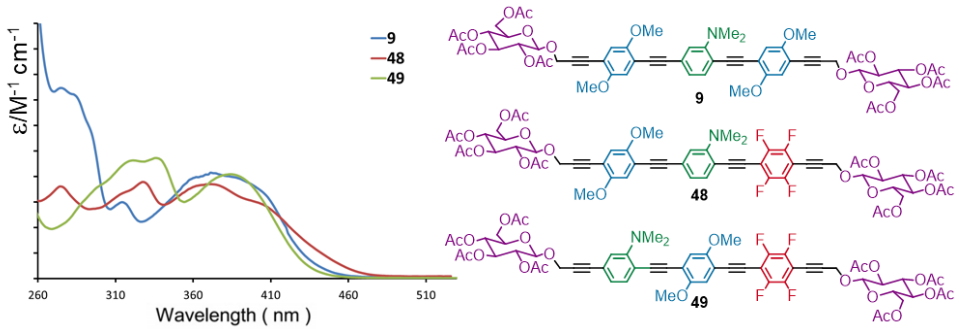

Figure 3.6. Absorption spectra of **9** (blue line), **48** (red line) and **49** (green line) in CH_2Cl_2.

Both **48** and **49** are luminescent at room temperature in CH_2Cl_2. In **Figure 3.7** their emission spectra, in comparison with **9**, are reported. While the absorption spectra resulted quite similar for the three species, red-shifted emission maxima, with respect to the model compound **9** (λ_{em}=472 nm), are observed for both the fluorinated **48** and **49** (λ_{em}=501 nm and λ_{em}=541 nm, respectively). This effect demonstrates that the introduction of the fluoroaryl moiety, in the presence of electron-donating groups, influences the energy gap between HOMO and LUMO in the excited state, creating a push-pull system (paragraph **2.5A**); this effect is more pronounced in **49** (~70 nm shift in emission, in comparison with **9**), where the dimethylamino aromatic unit is farther from the fluorinated one, probably because of the different relative distance between the electron-donating and

electron-acceptor groups and the different localization of the acceptor excited state.

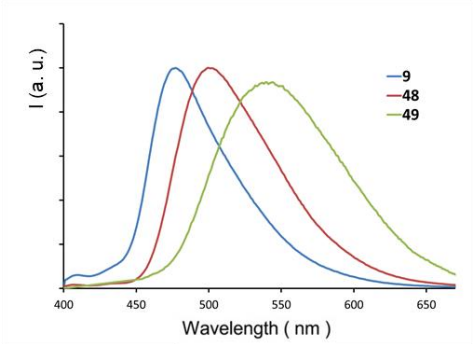

Figure 3.7. Emission spectra of **9** (blue line), **48** (red line) and **49** (green line) in CH_2Cl_2.

To further investigate the influence of the electron-donating groups, it was thought to study the spectroscopic features of **48** and **49** in acidic conditions, leading to the protonation of the $–NMe_2$ substituent. In fact, as described in paragraph **1.2**, many fluorescent probes, characterized by a pH-dependent luminescence, are used for qualitative pH intracellular measurements.

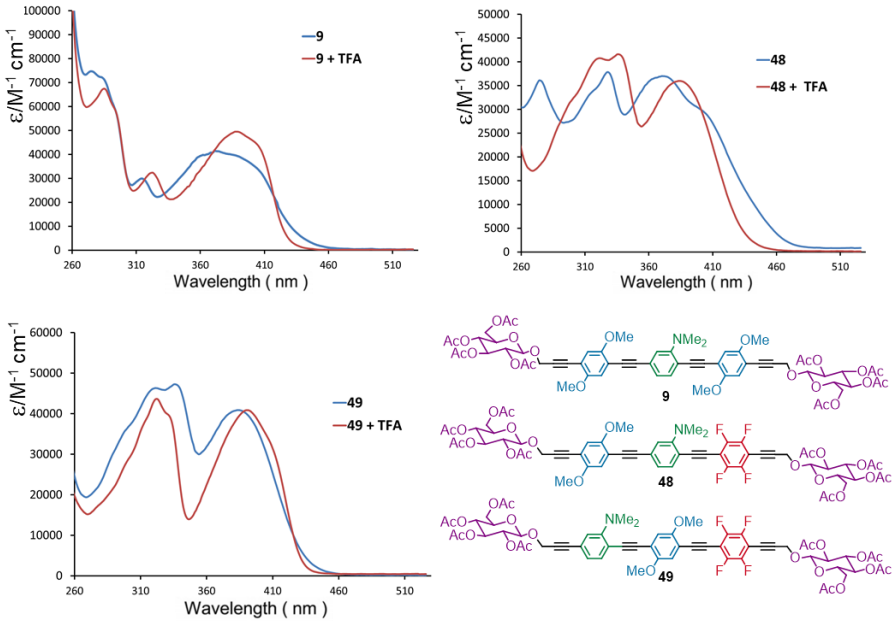

Figure 3.8. Absorption spectra of **9**, **48** and **49** (blue line) in CH_2Cl_2. In red the absorption spectra after the addiction of an aqueous solution of TFA.

The possible modulation of the push-pull effect in **48** and **49**, by the protonation of the electron-donating dimethylamino group, was only preliminary studied in organic medium without the deprotection of the sugar moiety. The absorption spectra, in CH_2Cl_2, of **48**, **49** and the model compound **9** are reported in **Figure 3.8** (blue lines); the red lines show the spectra of the three species after adding and mixing an excess of an aqueous solution of trifluoroacetic acid (TFA). By comparison of the absorption spectra of the three species, with the ones obtained in acidic medium, no considerable shift of the absorption maxima is observed.

On the other hand, in the emission spectra of **48**, **49** and **9** different behaviors are observed (**Figure 3.9**). In fact, **9** and **48** emission spectra in acidic medium (red lines) show almost no changes in the spectral region, with respect to the spectra in dichloromethane (blue lines): a slight shift (to the red for **48**, from λ_{em}=500 nm to 515 nm, and to the blue for **9**, from λ_{em}=479 nm to 465 nm) and a broadening of the emission bands is observed for the two protonated species, with respect to their dimethylamino analogues.

Surprisingly, the emission of compound **49** showed a greater shift, if compared with **9** and **48**, resulting highly blue-shifted to 446 nm in acidic medium (more than 100nm shift). These results demonstrate that the protonation of the dimethylamino group, which causes substantial changes in its electron-donating properties, together with its relative position with respect to the electron-accepting fluorinated moiety, highly influence the spectroscopic features of our OPE systems (the emission energy increases up to 0.5 eV in **49**, with respect to **9** which shows a shift of 0.07 eV).

Once demonstrated the sensitivity of the emission of **49**, in relation with its protonation, further studies are now ongoing with the aim to investigate possible applications as pH sensor. First of all, the deacetylation of the glucose terminations will be essential to study the photophysical properties in aqueous solution; moreover, theoretical calculations will be carried on to get insight the

importance of the relative positions of the –NMe_2 and -OMe groups, with respect to the fluorinated aromatic unit, on our OPEs features.

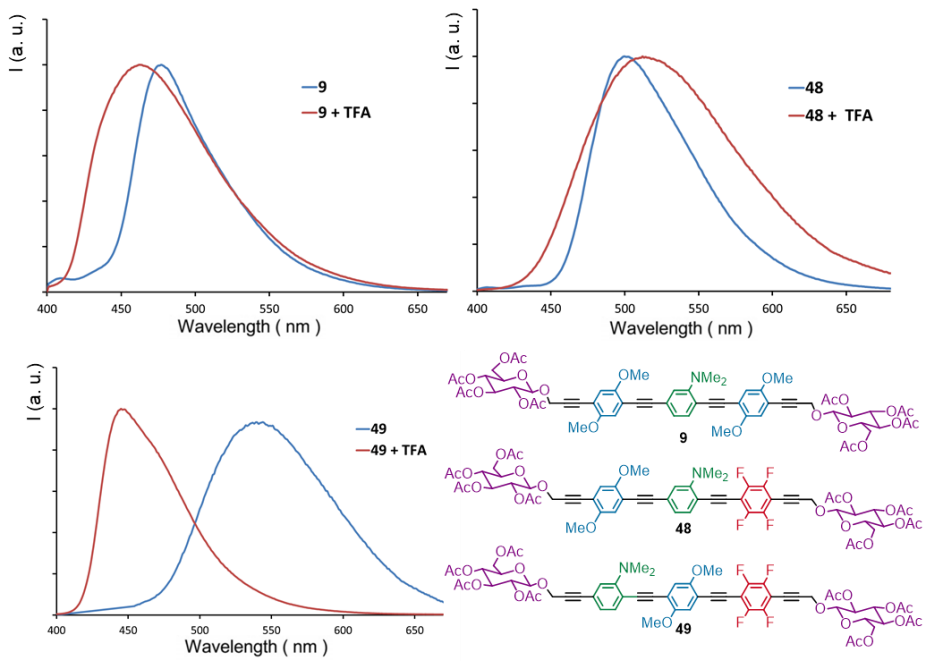

Figure 3.9. Emission spectra of **9**, **48** and **49** (blue line) in CH_2Cl_2. In red the emission spectra after the addiction of an aqueous solution of TFA.

3.2 PRELIMINARY BIOLOGICAL STUDIES ON SELECTED COMPOUNDS

3.2A. Studies of DNA binding of 38 and 39.[168] The peculiar structural features of the mono- and bis-tetralkylammonium OPEs **38** and **39** (**Figure 3.1**), joint with the biologically relevant sugar moieties, flat aromatic cores and positive charges were expected to help the solubility of these luminescent dyes in aqueous medium and make them interact with the negative charged double helix of DNA

[168] Mancuso, A.; Barattucci, A.; Bonaccorsi, P.; Giannetto, A.; La Ganga, G.; Musarra-Pizzo, M.; Salerno, T. M. G.; Santoro, A.; Sciortino, M. T.; Puntoriero, F.; Di Pietro, M. L. *Chem. Eur. J.* **2018**, *24*, 16972.

(paragraph **1.2**). First of all, the solubility in aqueous medium, useful for our DNA interaction studies, was investigated: a better solubility of the double positive charged **39**, with respect to **38**, was observed (up to $1 \cdot 10^{-3}$ M versus $6 \cdot 10^{-4}$ M).

In order to get insight into the binding modes of **38** and **39** with DNA (paragraph **1.2C**), several studies have been realized.

First of all, spectrophotometric titrations of the two species with DNA solution were performed. **Figure 3.11** shows the absorption changes of **38** and **39** with increasing amounts of DNA. In both cases, they are characterized by hypochromism of the absorption maxima, accompanied by a red-shift for **39** and by a slight hypsochromic effect for **38**. Moreover, the spectral changes are completely reversible by addition of sodium chloride, propending a non-covalent interaction with the biopolymer.

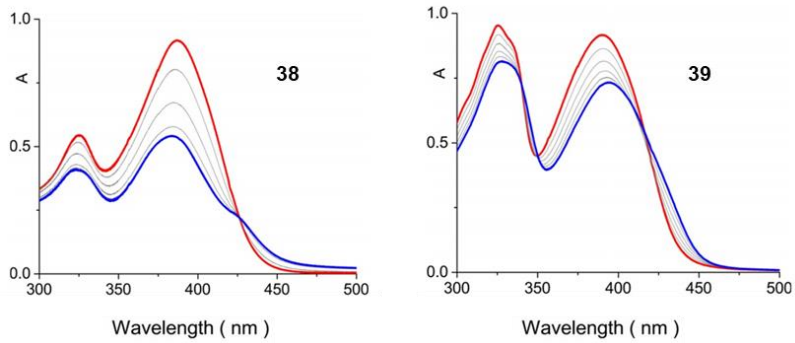

Figure 3.11. Absorption spectra of **38** (left) ($2.1 \cdot 10^{-5}$ M) and (right) **39** ($2.9 \cdot 10^{-5}$ M) at 25°C and pH 7 ($1 \cdot 10^{-3}$ M phosphate buffer and $2.1 \cdot 10^{-2}$ M NaCl) upon successive addition of calf-thymus DNA. The initial spectrum is the red one, whereas the blue one is the end of titration.

The shift to longer or shorter wavelengths could suggest a different kind of non-covalent interaction. In fact, intercalation of aromatic rings within the nucleobases is usually characterized by hypochromism and shift to the red of the absorption maxima, whereas a blue shift suggests an external binding. For the monocationic species, these observations could suggest an electrostatic interaction at high [**38**]/[DNA] ratio, that slightly moves to a different binding

mode increasing the DNA concentration, as highlighted by the red-shift at around 430 nm.

Moreover, a detailed investigation on the optical effect of this interaction was performed, studying the effect of the DNA on the luminescence of **38** and **39**. In both cases (**Figure 3.12**), increasing amounts of DNA induce a strong decrease of the emission intensity. The quenching is partial for **38**, whereas in the case of **39** the interaction with the polynucleotide induces a quasi-complete emission switch-off.

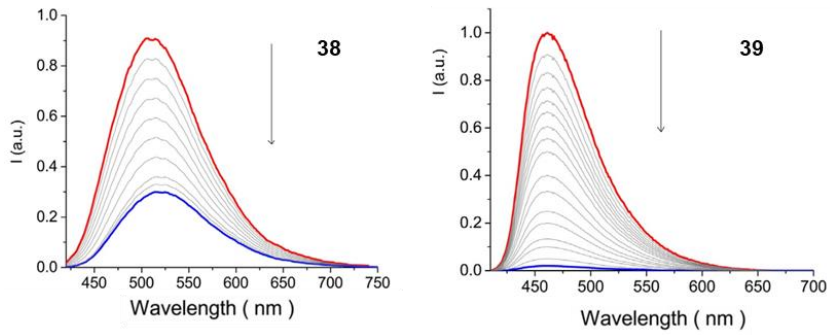

Figure 3.12. Emission of **38** (left) ($2 \cdot 10^{-6}$ M) and (right) **39** ($3 \cdot 10^{-6}$ M) at 25°C and pH 7 ($1 \cdot 10^{-3}$ M phosphate buffer and $2.1 \cdot 10^{-2}$ M NaCl) upon successive addition of calf-thymus DNA. Excitations have been performed at an isosbestic point.

Due to the presence of the well-known electron-donating effect of guanine residues, the emission quenching of both species in presence of DNA is attributed to an electron-transfer process involving this nucleobase moieties, according to general findings.[169] In this case, the driving force for the reductive electron-transfer quenching of **38** emission by guanine bases is thermodynamically allowed by about 0.33 eV, whereas for **39** it is at least 0.18 eV easier. Although some interaction between the new chromophores and DNA was expected, due to

[169] Augustyn, K .E.; Pierre, V. C.; Bartonin, J. K. *Metallointercalators as Probes of DNA Recognition and Reactions* **2008**, Wiley, New York.

the positive charges, such substantial effects on luminescence can hardly be attributed to a simple electrostatic interaction.

To further investigate the reversible interactions of **38** and **39** with DNA, the increase in the melting temperature (ΔT_m) of the biopolymer in the presence of the two species was determined and compared with the rise produced by the well-known intercalator ethidium bromide (EB).[170] Large increments are usually observed for the intercalation, but also groove-binders can increase DNA melting temperature by stacking parallel with the helix and rigidifying the DNA:[171] at $3 \cdot 10^{-3}$ M ionic strength value T_m is affected by **38** and **39** (ΔT_m=12.9 ± 0.5 and 11.0 ± 0.5 °C, respectively), similar to what happens in the presence of EB (ΔT_m =11.9 ± 0.5 °C). Moreover, the intercalation of a molecule among its nucleobases, as well as stabilizing the DNA double helix, causes an elongation and a simultaneous stiffening of the structure of the biopolymer, which is reflected in a significant increase in viscosity of its solutions.[172]

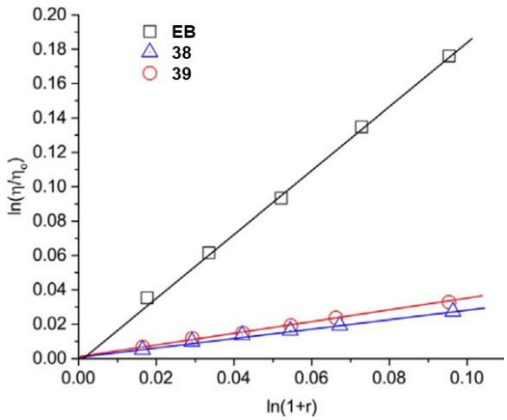

Figure 3.13. Viscometric titrations of calf-thymus DNA solutions ($6.0 \cdot 10^{-4}$ M) with **38** (blue triangles), **39** (red circles), and EB (black squares) at 25 °C and pH 7 ($1 \cdot 10^{-3}$ M phosphate buffer, and $1.0 \cdot 10^{-3}$ M NaCl). η_0=reduced viscosity of the DNA solution; η =reduced viscosity of the DNA solution in the presence of compounds; r=$[compound]_{bound}/[DNA]_{tot}$.

[170] LePecq, J. B.; Paoletti, C. *J. Mol. Biol.* **196**7, *27*, 87.
[171] Siters, K. E.; Sander, S. A.; Morrow, J. R. *Progress in Inorganic Chemistry* **2014**, 59, 245, Wiley, Hoboken.
[172] Satyanarayana, S.; Dabrowiak, J. C.; Chaires, J. B. *Biochemistry* **1992**, *31*, 9319.

On the other hand, compounds that bind in the DNA grooves by partial and/or non-classical intercalation, may cause less positive changes in DNA solution viscosity.[173] The viscometric titrations were performed on a rodlike (about 600 base pairs long) DNA solution with increasing amounts of **38** and **39**, comparing the trend with that determined, under the same experimental conditions in the presence of EB (**Figure 3.13**). Surprisingly, both the titrations with **38** and **39** are characterized by a small increase in the viscosity of the DNA solution if compared to that observed for EB.

Small DNA ligands often do not exhibit any CD response in solution; however, when bound to the chiral DNA, an induced CD signal appears in the range where the dye absorbs. The interaction of **38** with DNA (**Figure 3.14**) produces two induced negative bands at around 325 and 380 nm and a positive one at 445 nm, whereas the addition of DNA to the solution of **39** causes the appearance of a negative signal around 320 nm and two positive ones at 350 and 430 nm, respectively.

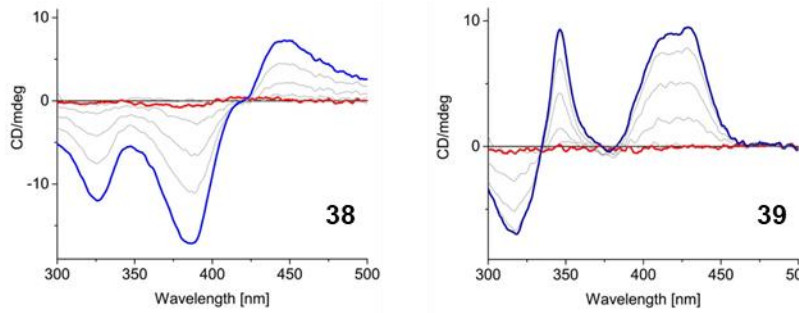

Figure 3.14. CD spectra of (left) **38** ($2.1 \cdot 10^{-5}$ M) and (right) **39** ($2.9 \cdot 10^{-5}$ M) in buffered solution at 25 °C and pH 7 ($1 \cdot 10^{-3}$ M phosphate buffer, and $1.0 \cdot 10^{-2}$ M NaCl) upon successive addition of calf-thymus DNA. The red lines correspond to **38** and **39** spectra.

This behaviour is not surprising because the sign and magnitude of a CD band depends not only on the binding mode, but also on the DNA sequence, and

[173] Bera, R.; Sahoo, B. K.; Ghosh, K. S.; Dasgupta, S. *Int. J. Biol. Macromol.* **2008**, *42*, 14.

the orientation of the transition dipole of the interacting species. However, intercalators often exhibit lower intensity CD spectra compared with groove binders, most likely due to the fact that they only contact two base pairs and exhibit little or no twist of the helix, unlike groove binders. The experimental results suggest that not only **38** and **39** interact with DNA in a similar way, but that, at low [compound]/[DNA] ratios, they prefer to engage in DNA groove binding or surface binding, rather than in classical intercalation, as shown by the small increase in DNA viscosity.

On the basis of the aforementioned overall behaviour, in particular absorption titrations and melting point measurements – that suggest intercalation – and CD and viscosity results - that propend instead for an external interaction – a mixed binding mode is proposed. The cationic species, initially attracted by the negatively charged DNA, seem to interact with the biopolymer partially inserting their central aromatic core into the bases with their long axis almost perpendicular to the long axis of adjacent base pairs, while the sugar moieties stabilize the OPEs/DNA interaction by establishing H-bonds with the groups accessible from the grooves.[174] Due to this mixed binding mode, just a rough evaluation of the binding constant values (K_B) of the two OPEs with DNA is possible. By analysing the absorption titration data, the K_B values were higher than $2.0 \cdot 10^{-6}$ M^{-1} for both species at 25 °C and pH 7.

Finally, in order to verify the biocompatibility of the investigated species, cytotoxicity tests have been performed (**Figure 3.15**). In particular, healthy (Vero) and human larynx epidermoid carcinoma cells (HEp-2) were incubated for 24h, with 100 μM and 10 μM buffered solutions of **38** and **39**.

The results show that in both cases **38** and **39** induce no cytotoxicity effect in Vero cells. In HEp-2 cell lines exposed to **39** solution, instead, a reduction of cellular proliferation as a function of the concentration was detected. Various

[174] Arigon, J.; Prata, C. A. H.; Grinstaff, M. W.; Barthélémy, P. *Bioconjugate Chem.* **2005**, *16*, 864.

factors, such as differences in **38** and **39** chemo-physical properties and variations in cell-membrane characteristics, may have influenced the uptake processes.

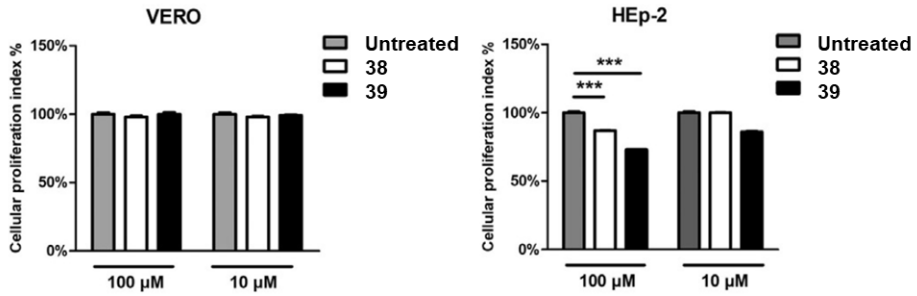

Figure 3.15. Viability assay in Vero and HEp-2 cell lines after **38** and **39** exposition. The untreated sample represents an internal control to monitor the two cell lines cellular viability.

The characteristics of the two used cell lines determine the different behaviours of the two OPEs as well as the different results in cellular proliferation. The continued occurrence of mitosis in cancer cells, giving access to the genetic material,[175] justify the higher susceptibility of HEp-2 compared to the Vero cells. Further studies of cellular localization and on the interactions of the pentameric homologues **43** and **45** with the double helix of DNA are now ongoing.

3.2B. Effect of sugar change: preliminary internalization and PDT studies on OPE_Maltose. As written in Chapter 2, three new OPEs, bearing the same conjugated internal OPE chain of **OPE_Glucose 1** but having different sugar terminations (galactose, mannose and maltose), were synthesized. In fact,[176] the responsible of the photophysical behavior of this kind of dyes is the OPE chain, independently from their terminations and the spectra of the four species are totally superimposable. The change of the carbohydrate termination was

[175] Denais, C. M.; Gilbert, R. M.; Isermann, P.; McGregor, A. L.; teLindert, M.; Weigelin, B.; Davidson, P. M.; Friedl, P.; Wolf, K.; Lammerding, J. *Science* **2016**, *352*, 353.
[176] Barattucci, A.; Deni, E.; Bonaccorsi, P.; Ceraolo, M. G.; Papalia, T.; Santoro, A.; Sciortino, M. T.; Puntoriero F. *J. Org. Chem.* **2014**, *79*, 5113; Deni, E.; Zamarrón, A.; Bonaccorsi, P.; Carreño, M. C.; Juarranz, A.; Puntoriero, F.; Sciortino, M. T.; Ribagorda, M.; Barattucci A. *Eur. J. Med. Chem.* **2016**, *111*, 58.

realized in order to understand which was the role of the single sugar on the biological behavior, in particular water solubility, internalization in cancer cells and use as photosensitizer (PS) in photodynamic therapy (PDT).

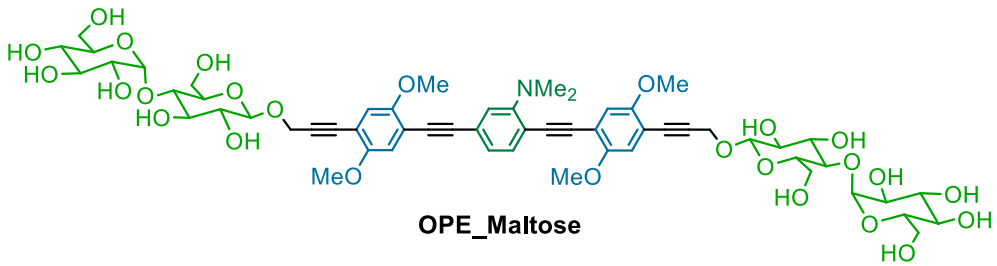

Figure 3.16

A preliminary biological study on **OPE_Maltose** (**Figure 3.16**) was previously carried on by Prof. Francisco Sanz-Rodriguez at the Universidad Autónoma de Madrid, who, as a first attempt, developed the same procedure reported for **OPE_Glucose 1** and **OPE_Glucose 2**. In fact, even if **OPE_Maltose** resulted, for the presence of two disaccharidic terminations, more soluble in water ($1.6 \cdot 10^{-3}$ M,), than the already reported glucosidic OPEs (~10^{-5} M) a 4.2 mM mother solution in DMSO was firstly prepared and then diluted in RPMI medium until the concentration $5 \cdot 10^{-6}$ M, to compare the results with those of the old experiments.

Being the efficiency of a photosensitizer for PDT related to its cellular internalization and localization,[177] preliminary cellular uptake experiments of **OPE_Maltose** were performed. Internalization of **OPE_Maltose** in healthy HaCaT cells (human keratinocyte cells) and HeLa cells (human cervical cancer cells) cells was analyzed by fluorescence microscopy under UV excitation light (360-370nm) and blue excitation light (460-490 nm) (**Figure 3.16**). The intracellular luminescent signals of **OPE_Maltose** was observed after 6h and 24h of incubation with two solutions at different concentration (10^{-5} and $5 \cdot 10^{-6}$ M) of

[177] Kessel, D. *J. Natl. Compr. Canc. Netw.* **2012**, *10*, 56.

the species. Corresponding controls (without PSs incubation) of each cell type were also performed. Even if after 6h incubation of the HeLa cells, the internalization of **OPE_Maltose** was very poor, a massive uptake was observed after 24h. This suggested an alternative mechanism of internalization, maybe also caused by the longer maltose chain, in comparison with the corresponding **OPE_Glucose 1**, massively internalized only after 6h incubation. **OPE_Maltose** is up-taken in both the cell lines at the two studied concentrations, localizing, at first sight, into different cell comportments: in fact, while it seems to organize in a vesicular shape in HeLa cells (**Figure 3.17a**), localization in the Golgi apparatus is noticed in the HaCat ones (**Figure 3.17b**).

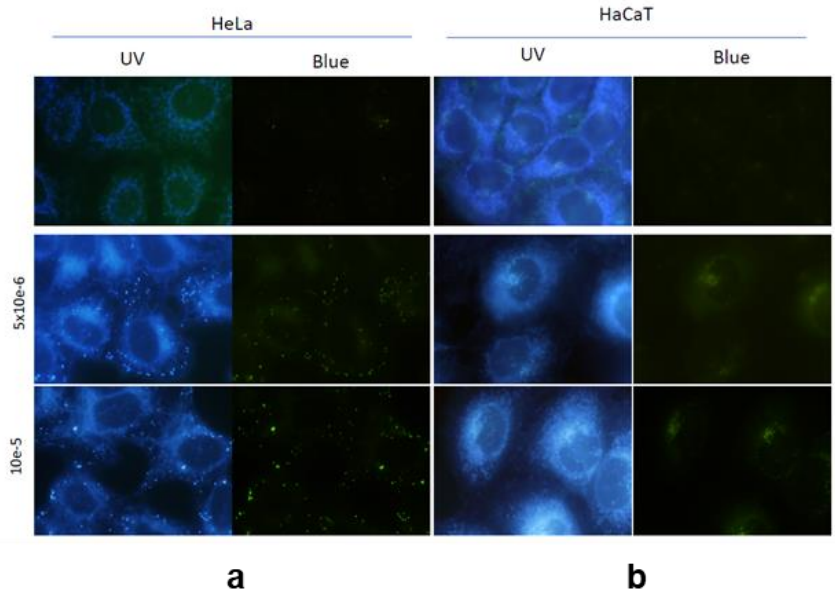

Figure 3.17. Fluorescence microscopy images of HeLa and HaCat cells incubated with **OPE_Maltose**. The images on the top show the untreated cells.

The action of a PS on cells is related to the production of $^1O_2$ and/or other ROS generated after light irradiation. Therefore, we next evaluated the toxicity of **OPE_Maltose** firstly in the absence of light. The toxicity experiments (MTT assay) were performed by incubation of HeLa and HaCaT cells with different

concentration of **OPE_Maltose**, ranging from $3 \cdot 10^{-6}$ to $2.5 \cdot 10^{-5}$ M, in the dark. The results (**Figure 3.18**) show that the drug causes no cytotoxicity at any concentration.

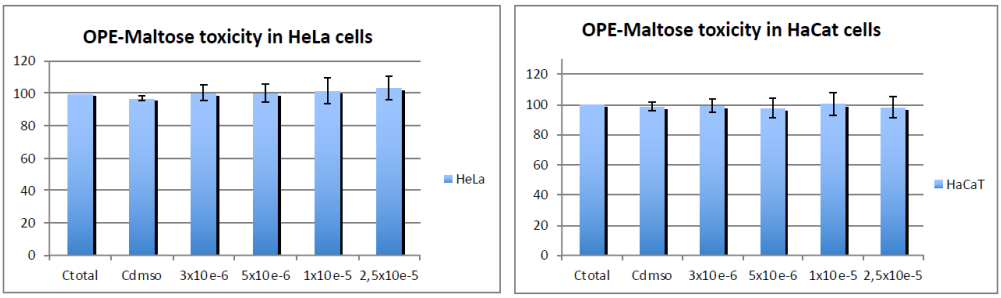

Figure 3.18. Viability assay in HeLa and HaCat cell lines after **OPE_Maltose** exposition.

The absorption spectrum of **OPE_Glucose 1**, totally superimposable with that of **OPE_Maltose**, suggests that these dyes can be excited also in the blue region (this observation is also deducible from **Figure 3.16**). For this reason, even if in our previous work the effect of the gluco_PS was evaluated through UVA irradiation on the cell cultures, the new PDT tests on **OPE_Maltose** incubated cells were carried on through non-toxic blue-light irradiation (450 nm). The photodynamic treatments, carried out by incubation with a $5 \cdot 10^{-6}$ M solution of the drug for 24h followed by blue light exposure, induced a time-dependent cytotoxic effect in HaCaT and HeLa (**Figure 3.19a**). In fact, the PDT treatment resulted in the massive death for both the cell lines (more than the 80% after three minutes irradiation). Unfortunately, for what concerns the healthy HaCat cells, this result is strongly evident also after only 1 minute irradiation (almost 60%). A lower drug concentration (10^{-8} M) did not induce any PDT effect on both the cell lines, while a shorter incubation time (18h) did not induced any change in the PDT results at 10^{-6} M concentration (**Figure 3.19b**).

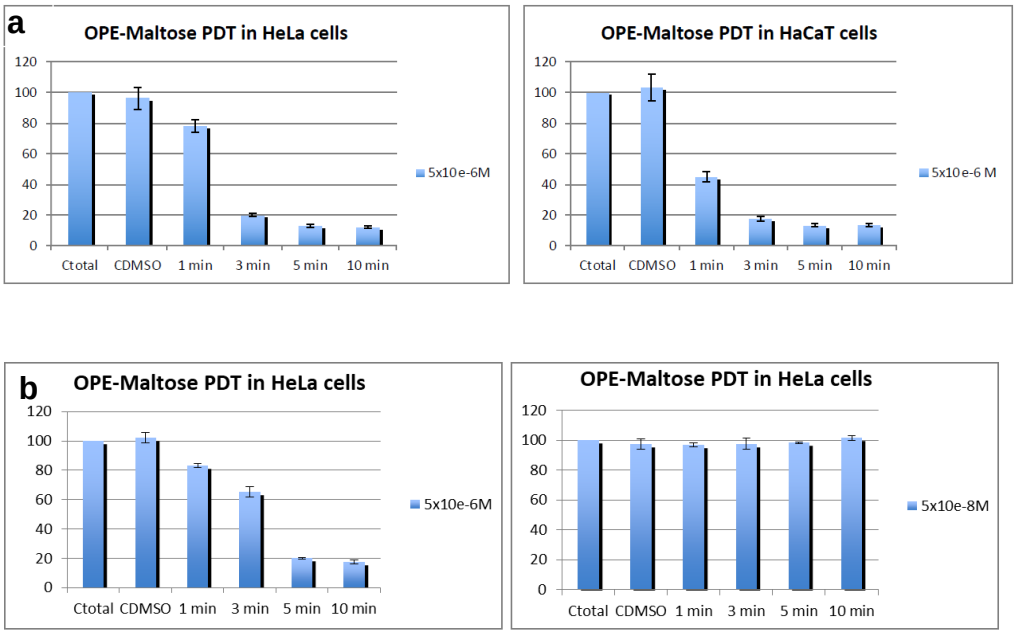

Figure 3.19. Cell survival rates after **OPE_Maltose** based PDT. The effects have been observed 24h (a) and 18h (b) after PDT.

From these results, we concluded that, even if the drug can act as powerful PS in visible-light induced PDT, strongly producing ROS only after few minutes irradiation, no selectivity for cancer cells is observed. The observed different localization of the drug in the cancer and healthy cells can be the cause of the stronger effect on healthy cells (localization in Golgi apparatus). Further studies on **OPE_Galactose** and **OPE_Mannose** (**Figure 2.7**) are now ongoing to investigate any different biological behavior.

Conclusions

The work reported in this thesis led to:

1) The optimization of yields and methods for the obtainment of the already reported **OPE_Glucose 1** and **OPE_Glucose 2**.

2) The synthesis of two new elongated five-rings OPEs, characterized by red-shifted absorption and emission spectra and by higher emission quantum yields, with respect to **OPE_Glucose 1** and **OPE_Glucose 2**.

3) The synthesis of three new derivatives, analogue to **OPE_Glucose 1**, containing different sugar terminations (galactose, mannose and maltose). In particular the first biological tests, performed on the maltosidic OPE (which also resulted more soluble in water, with respect to its monosaccharidic analogues) showed the massive cellular uptake of the compound, both in healthy (HaCat) and cancer (HeLa) cells after 24h incubation and no dark-toxicity at any concentration. Moreover, preliminary PDT studies, on cell cultures treated with the maltose derivative, carried out with blue light, instead of UV light used for **OPE_Glucose 1** and **OPE_Glucose 2**, resulted in a huge cell death only after 3 minutes from the treatment. Unfortunately, no selectivity for cancer cells is observed.

4) The nitrogen quaternarization and the obtainment of cationic tetralkylammonium OPEs. In particular, it has been demonstrated that **38** and **39**, quaternarized analogues of **OPE_Glucose 1** and **OPE_Glucose 2**, thanks to the joint presence of the new positive charge and the hydrogen bonding-sugar groups, strongly interact with the negative charged double helix of DNA, inducing a switch-off effect of their absorption and emission and causing a reduction in cancer Hep2 cells proliferation.

5) The synthesis of two new OPEs, bearing an electron withdrawing fluorinated aromatic group as chain termination. Both the obtained species show red-shifted emissions because of a push-pull effect, due to the interaction of the

fluorinated moiety with the methoxy and dimethylamino electron donating groups. Moreover, preliminary photophysical studies, performed in acidic medium, show that one of the two species has a pH-dependent emission, opening the way to its deacetylated derivative to be used as intracellular pH sensor.

6) The optimization of the synthetic pathways that led to the obtainment of new asymmetrically substituted OPEs. In particular, the synthetic modifications led to the introduction of a suitable termination for the functionalization of upconverting nanoparticles (UCNPs), which emit UV light, matching the absorption of our OPE systems (~380 nm), upon NIR excitation (980 nm). The introduction of an azido carboxylic acid, through a "click" cycloaddiction, on a conjugated chain of OPE, bearing a free ethynylenic residue, could be useful to operate a ligand exchange with the oleate capped UCNPs: the obtained system, thanks to an energy transfer process from the NPs to our conjugated dye, could be used to extend OPEs applications as photosensitizers in NIR-PDT.

CHAPTER 4

Experimental methods

4.1 GENERAL SYNTHETIC METHODS

Chemicals. Solvents were purified according to standard procedures. All of the reactions were monitored by TLC on commercially available precoated plates (silica gel 60 F254), and the products were visualized with vanillin [1 g dissolved in MeOH (60 mL) and conc. H_2SO_4 (0.6 mL)] and UV lamp. Silica gel 60 was used for column chromatography. Calf thymus DNA was purchased from Sigma Chemical Co. and purified as previously described.[178] The concentration, expressed in base pairs, was determined spectrophotometrically using the molar absorptivity:[179] 1.3 x 10^4 M^{-1} cm^{-1} (260 nm). All the experiments with DNA were carried out at 25°C and pH 7, in a phosphate buffer 1x10^{-3} M and enough NaCl to give the desired ionic strength value.

Instrumentation. Proton (^1H) and carbon (^{13}C) NMR spectra were recorded on a Varian 500 spectrometer (at 500 MHz for ^1H; and 125 MHz for ^{13}C) using $CDCl_3$ as solvent, unless differently stated. Chemical shifts are given in parts per million (ppm) (δ relative to residual solvent peak for ^1H and ^{13}C: δ 7.26 and 77.0 ppm respectively), coupling constants (*J*) are given in hertz; the attributions are supported by heteronuclear single-quantum coherence (HSQC), Heteronuclear Multiple Bond Correlation (HMBC) and correlation spectroscopy

[178] Cusumano, M.; Giannetto, A. *J. Inorg. Biochem.* **1997**, *65*, 137.
[179] Wells, R. D.; Larson, J. E.; Grant, R. C.; Shortle, B. E.; Cantor, C. R. *J. Mol. Biol.* **1970**, *54*, 465.

(COSY) experiments, and given in accordance with the numeration indicated in the designed structures.

Mass spectra (m/z) and HRMS were recorded under the conditions of electron impact (EI) and electrospray (ES) in a Waters VG Autospect spectrometer. Melting points were obtained in open capillary tubes and are uncorrected.

Absorption spectra were recorded with a Cintra 3030 GBC spectrophotometers. Circular dichroism experiments were performed by a Jasco J-810 spectropolarimeter. The thermal denaturation temperature of compound–DNA mixtures (1:10) was determined in $1x10^{-3}$ M phosphate buffer (pH 7) solutions containing the compound ($7.8x10^{-6}$ M) and $2x10^{-3}$ M NaCl. Melting curves were recorded at 260 nm. The temperature has been increased at a rate of 0.5 °C/min by using a GBC Peltier system. Viscosity titrations were performed by means of a Cannon-Ubbelhode semi-micro-dilution viscometer (Series No. 75, Cannon Instrument Co.), thermostatically maintained at 25 °C in a water bath. The viscometer contained 2 mL of sonicated DNA solution, in $1x10^{-3}$ M phosphate buffer (pH = 7) and $1x10^{-2}$ M NaCl. The compound solution ($(0.85\div2.5)x10^{-4}$ M), containing also DNA ($6.0x10^{-4}$ M) at the same concentration as that in the viscometer, was delivered in increments of 90÷570 µL from a micropipette. Solutions were freed of particulate material by passing them through nylon Acrodisc syringe filters before use. Flow times were measured by hand with a digital stopwatch. Reduced viscosities were calculated by established methods and plotted as ln $\eta/\eta 0$ against ln (1+r) for rodlike DNA (600 base pairs) (η= reduced viscosity of the biopolymer solution in the presence of compound; $\eta 0$= reduced viscosity of the biopolymer solution in the absence of compound; r= $[compound]_{bound}/[biopolymer]_{tot}$). Spectrophotometric titrations were performed by adding to a complex solution ($(2.1\div2.9)x10^{-5}$ M) successive aliquots of DNA, containing also the complex, in a 10 mm stoppered quartz cell and recording the spectrum after each addition. The data were analysed by a nonlinear least-squares

fitting program, applied to McGhee and von Hippel equation.[180] The binding constant, K_B, was determined by the program, using the extinction coefficient of the compounds, the free complex concentration and the ratio of bound complex per mole of DNA. Extinction coefficient for bound compound was determined by Beer's law plots in the presence of a large excess of DNA. For steady-state luminescence measurements, a Jobin Yvon-Spex Fluoromax P spectrofluorimeter was used, equipped with a Hamamatsu R3896 photomultiplier. The spectra were corrected for photomultiplier response using a program purchased with the fluorimeter. For the luminescence lifetimes, an Edinburgh OB 900 time-correlated single-photon-counting spectrometer was used. As excitation sources, a Hamamatsu PLP 2 laser diode (59 ps pulse width at 408 nm) and/or the nitrogen discharge (pulse width 2 ns at 337 nm) were employed. Luminescence quantum yields have been determined using the optically diluted method,[181] using 9,10-diphenyl-anthracene in cyclohexane as quantum yield standard (Φ = 0.90).[182]

Biological assay. Cell proliferation assay was performed on Vero (African green monkey kidney cells) and HEp-2 (human larynx epidermoid carcinoma cells), or HaCat (human keratinocyte cells) and HeLa (human cervical cancer cells) cell lines grown in minimal essential medium (EMEM) supplemented with 6% fetal bovine serum (FBS) (Lonza) and RPMI 1640 supplemented with 10% of FBS, respectively. All cell lines were incubated with different concentrations of the selected compounds for 24 h at 37 °C under 5% CO_2. The cell viability was determined evaluating the ATP levels by ViaLight™ plus cell proliferation and cytotoxicity bioassay kit (Lonza Group Ltd., Basel, Switzerland) according to the manufacturer's instructions. The emitted light intensity related to ATP degradation is directly proportional to the number of metabolically active cells. Measured luminescence value was converted in cell proliferation index (%) according to the following equation: Cell viability $\% = \frac{A-B}{C-B} \times 100$ where A

[180] McGhee, J. D.; von Hippel, P. H. *J. Mol. Biol.* **1974**, *86*, 469.
[181] Crosby, G. A.; Demas, J. N. *J. Phys. Chem.* **1971**, *75*, 991.
[182] Hamai, S.; Hirayama, F. *J. Phys. Chem.* **1983**, *87*, 83.

denotes the average of treated samples, C the average of untreated samples and B represents background luminescence.

Photodynamic treatment. A stock solution of **OPE_Maltose** was prepared in DMSO (Pan-reac) at a concentration of 4.2 mM. The work solutions were obtained by dissolving the compound in DMEM/RPMI with 1% FBS. Thefinal concentration of DMSO was always lower than 0.5% (v/v), and the lack of toxicity of this solvent for the cells was also tested and confirmed. All the treatments were performed when cultures reached around 60-70% of confluence. Cells seeded on 24 well plates were incubated for 24h with variable concentrations of **OPE_Maltose** (from $5 \cdot 10^{-8}$ M to $5 \cdot 10^{-6}$ M). Afterwards, the media were removing, replaced by fresh media and cells were irradiated with blue light. After irradiation, cells were washed three times with PBS, complete DMEM or RPMI was added, and were maintained in the incubator for 18 or 24h until evaluation. To assess the possible dark cytotoxic effect of **OPE_Maltose**, cells were incubated in the dark for 24h with different concentrations of the compound.

4.2 SYNTHETIC METHODOLOGIES AND CHARACTERIZATIONS

The compound citation order in this paragraph follows the one used in the text and schemes reported in Chapter 2. The synthesis of the compounds, already reported by my research group,[183] which were re-synthesized by me at the beginning of my PhD, are here reported, together with their characterizations, for an easier reading. In the mass spectra of brominated compounds **10**, **20**, **21** and **23** only the peaks related to the ^{79}Br isotope are reported.

[183] Barattucci, A.; Deni, E.; Bonaccorsi, P.; Ceraolo, M. G.; Papalia, T.; Santoro, A.; Sciortino, M. T.; Puntoriero F. *J. Org. Chem.* **2014**, *79*, 5113; Deni, E.; Zamarrón, A.; Bonaccorsi, P.; Carreño, M. C.; Juarranz, A.; Puntoriero, F.; Sciortino, M. T.; Ribagorda, M.; Barattucci A. *Eur. J. Med. Chem.* **2016**, *111*, 58.

General Procedure for quantitative deacetylation (Procedure A). The starting product (0.2 mmol) was dissolved in THF/MeOH (1:1, 40 mL). To this mixture a large excess of aqueous ammonia (12 mL) was added and the reaction was then maintained under continuous stirring at room temperature overnight, until the disappearance of the starting product by TLC. Solvents were removed under reduced pressure and the undesired acetamide was eliminated by a series of Et_2O washings of the obtained solid.

General Procedure for Nitrogen quaternarization (Procedure B). The starting product (0.25 mmol, 1 eq.) was dissolved in dry dichloromethane (5 mL). To this solution MeOTf was added (1 eq. each amino group) under Ar atmosphere. The mixture was heated at reflux temperature (40 °C) and maintained under continuous stirring until the disappearance of the starting product by TLC. The solvent was removed under reduced pressure.

Compound 2. A DMF solution (12 mL) of 2,5-dibromoaniline **1** (1.00 g, 3.98 mmol, 1 eq.) was added at RT under Ar atmosphere to anhydrous K_2CO_3 (5.00 g, 36.18 mmol). To the obtained suspension, 1.2 mL of iodomethane (20 mmol, 5 eq.) were added, the mixture was heated at 100 °C, and maintained in these conditions under continuous stirring until completion by TLC (hexane/EtOAc 9.5:0.5). After 24 h, the reaction was quenched by adding water (7 mL) and extracted with dichloromethane (3 x 10 mL). The organic phases were dried over anhydrous Na_2SO_4, the solvent evaporated under reduced pressure to give pure **2** as a transparent oil (1.10 g, 3.94 mmol, 99%).

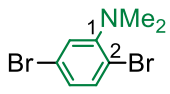

2

TLC: *Rf*= 0.85 (hexane/EtOAc 95:5). ^{1}H NMR: δ 7.35 (d, 1H, $J_{3,4}$ = 8.8, H-3), 7.14 (d, 1H, $J_{4,6}$ = 2.4, H-6), 6.96 (dd, 1H, $J_{3,4}$ = 8.8, $J_{4,6}$ = 2.4, H-4), 2.76 [s, 6H,

$N(CH_3)_2$]. ^{13}C NMR: δ 152.8 (C-1), 134.7 (C-3), 126.2 (C-4), 123.5 (C-6), 119.9 and 117.2 (C-2,5), 43.7 [$N(CH_3)_2$]. Anal. Calcd for $C_8H_9Br_2N$ (278.97): C, 34.44; H, 3.25; N, 5.02. Found: C, 34.50; H, 3.26; N, 5.03.

Compound 3. To a solution in dry DMF (15 mL) of **2** (1.00 g, 3.58 mmol, 1 eq.), commercial ethynyltrimethylsilane (3.05 mL, 21.60 mmol, 6 eq.) and $Pd(PPh_3)_4$ (0.41 g, 0.35 mmol, 0.1 eq.) Et_3N (15 mL) was slowly added. The mixture was heated at 80 °C and maintained under Ar atmosphere and continuous stirring until the disappearance of starting products (after 24 hours) by TLC (hexane/EtOAc 9:1). Column chromatography was performed with hexane as eluent, and compound **3** was obtained as a transparent oil (0.67 g, 2.15 mmol, 60%).

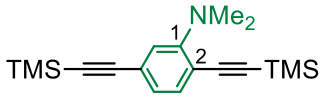

3

TLC: *Rf* =0.67 (hexane/EtOAc 90:10). ^1H NMR: δ 7.33 (d, 1H, $J_{3,4}$ = 7.9, H-3), 6.94 (m, 2H, H-4,6), 2.93 [s, 6H, $N(CH_3)_2$], 0.25 [s, 18H, 2 x $Si(CH_3)_3$]. ^{13}C NMR: δ 154.7 (C-1), 134.6 (C-3), 123.8 and 120.1 (C-4,6), 115.0 and 105.1 (C-2,5), 104.3, 104.2, 101.4, and 95.3 (2 x C≡C), 43.1 [$N(CH_3)_2$], - 0.02 and - 0.17 [2 x $Si(CH_3)_3$]. Anal. Calcd for $C_{18}H_{27}NSi_2$ (313.58): C, 68.94; H, 8.68; N, 4.47. Found: C, 68.88; H, 8.70; N, 4.48.

Compound 5.[184] To a solution of 1,2,3,4,6-penta-*O*-acetyl-β-D-glucopyranose **4** (5.0 g, 12.55 mmol) in 36 mL of dry CH_2Cl_2, at 0°C and under Argon, 1.48 mL of propargyl alchol (25.10 mmol, 2eq. d = 0.958 g/mL), 4.59 mL di trimethylsilyltriflate (25.10 mmol, 2 eq. d=1.228 g/mL) and molecular sieves

[184] Giovenzana, G. B.; Lay, L.; Monti, D.; Palmisano, G.; Panza, L. *Tetrahedron* **1999**, *55*, 14123.

4 Å were added. The mixture was heated to RT and maintained under continuous stirring until the disappearance of **4** by TLC (1 hour). The reaction was quenched by adding $NaHCO_3$ (40 mL) and the organic phase washed with water (2 x 30 mL). The organic phases were dried over anhydrous Na_2SO_4, the solvent evaporated under reduced pressure. Column chromatography was performed with hexane/EtOAc 70:30 as eluent, and compound **5** was obtained as a white solid (3.0 g, 7.53 mmol, 60%). TLC: *Rf* = 0.50 (hexane/EtOAc 70:30).

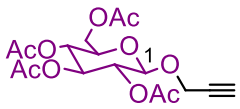

5

Compound 7.[185] To a solution of H_5IO_6 (0.73 g, 3.44 mmol, 1.2 eq.) in 5 mL of CH_3OH, I_2 (1.60 g, 15.10 mmol) was added; after ten minutes under vigorous stirring at RT commercial 1,4-dimethoxybenzene **6** (0.675 g, 2.78 mmol, 1 eq.) was added. The mixture was refluxed and maintained under continuous stirring for 4h. The reaction was quenched by adding a solution of $Na_2S_2O_5$ 10% wt (5 mL) and extracted with dichloromethane (3 x 10 mL). The organic phases were washed with brine and then dried over anhydrous Na_2SO_4. The solvent evaporated under reduced pressure to give **7** as a white solid (1.80 g, 4.63mmol, 95%). TLC: *Rf*= 0.90 (hexane/EtOAc 95:5).

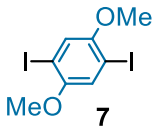

7

Compound 8. 2-propyn-1-yl β-D-glucopyranoside 2,3,4,6-tetraacetate **5** (1.42 g, 3.67 mmol, 1 eq.), 1,4-diiodo-2,5-dimethoxybenzene **7** (3.00 g, 7.69

[185] Yi, C.; Blum, C.; Lehamann, M.; Keller, S.; Liu, S. X.; Frei, G.; Neels, A.; Hauser, J.; Schürch, S.; Decurtins, S. *J. Org. Chem.* **2010**, *75*, 3350

mmol, 2 eq.) and $Pd(PPh_3)_4$ (0.50 g, 0.43 mmol, 0.12 eq.) were dissolved in dry DMF (30 mL). To the mixture Et_3N (30 mL) was slowly added. The mixture was heated at 60 °C and maintained under continuous stirring and under Ar atmosphere for 3h, until the disappearance of **5** by TLC. After evaporation of the solvents, the excess of unreacted **7** was separated through precipitation from methanol. Column chromatography of the crude obtained from evaporation of the mother liquors was performed with hexane/EtOAc 70:30 as eluent, and compound **8** was obtained as a white solid (1.90 g, 2.93 mmol, 80%).

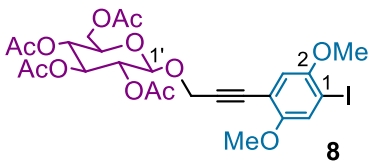

8

TLC: *Rf* =0.64 (hexane/EtOAc 60:40). Mp 65-67 °C. ^{1}H NMR: δ 7.29 (s, 1H, H-6), 6.84 (s, 1H, H-3), 5.25 (t, $J_{2',3'} = J_{3',4'} = 9.3$, 1H, H-3'), 5.11 (t, $J_{3',4'} = J_{4',5'} = 9.3$, 1H, H-4'), 5.03 (dd, $J_{1',2'} = 7.7$, $J_{2',3'} = 9.3$, 1H, H-2'), 4.88 (d, $J_{1',2'} = 7.7$, 1H, H-1'), 4.61 (s, 2H, $CH_2C\equiv$), 4.27 and 4.15 (split AB system, $J_{5',6'A} = 4.4$, $J_{5',6'B} = 2.5$, $J_{6'A,6'B} = 12.2$, 2H, H_2-6'), 3.84 and 3.83 (two s, 6H, 2 x OCH_3), 3.75 (ddd, $J_{4',5'} = 9.3$, $J_{5',6'A} = 4.4$, $J_{5',6'B} = 2.5$, 1H, H-5'), 2.07, 2.03, 2.02, and 2.00 (four s, 12H, 4 x CH_3CO). ^{13}C NMR: δ 170.7, 170.3, and 169.4 (4 x CO), 154.8 (C-5), 152.3 (C-2), 122.3 (C-6), 115.1 (C-3), 111.9 (C-4), 98.3 (C-1'), 88.4 (C-1), 87.3 and 85.4 (C≡C), 72.8 (C-3'), 71.9 (C-5'), 71.1 (C-2'), 68.4 (C-4'), 61.8 (C-6'), 57.2, 57.0, and 56.5 (2 x OCH_3 and $CH_2C\equiv$), 20.7 and 20.6 (4 x CH_3CO). Anal. Calcd for $C_{25}H_{29}IO_{12}$ (648.40): C, 46.31; H, 4.51. Found: C, 46.44; H, 4.50.

Compound 9. Compounds **3** (0.18 g, 0.57 mmol, 1 eq.) and **8** (0.75 g, 1.16 mmol, 2 eq.), Ag_2O (0.27 g, 1.16 mmol, 2 eq.) and $Pd(PPh_3)_4$ (0.10 g, 0.09 mmol, 0.16 eq.) were suspended in dry DMF (4 mL) and THF (2 mL). The obtained mixture was heated at 70 °C and maintained under Ar atmosphere and continuous

stirring for 4 h, until the disappearance of starting products by TLC (hexane/EtOAc 3:7) After filtration over Celite, the solvents were removed under reduced pressure, and the obtained reaction crude was subjected to silica gel column chromatography. Column chromatography was performed with hexane/EtOAc 50:50 as eluent, and compound **9** was obtained as a brilliant yellow solid (0.38 g, 0.31 mmol, 54%).

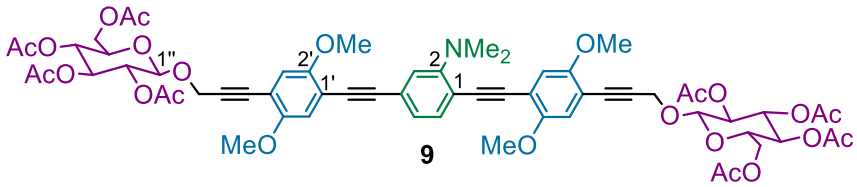

9

TLC: *Rf* =0.38 (hexane/EtOAc 40:60). Mp 91-93 °C. ^{1}H NMR: δ 7.46 (d, $J_{5,6}$ = 8.4, 1H, H-6), 7.08 (m, 2H, H-3,5), 7.00, 6.99, 6.93 and 6.91 (four s, 4H, 2 x H-3',6'), 5.25 (t, $J_{2'',3''} = J_{3'',4''}$ = 9.5, 2H, 2 x H-3''), 5.10 (t, $J_{3'',4''} = J_{4'',5''}$ = 9.5, 2H, 2 x H-4''), 5.03 (dd, $J_{1'',2''}$ = 8.0, $J_{2'',3''}$ = 9.5, 2H, 2 x H-2''), 4.90 (d, $J_{1'',2''}$ = 8.0, 2H, 2 x H-1''), 4.64 (s, 4H, 2 x $CH_2C{\equiv}$), 4.27 and 4.16 (split AB system, $J_{5'',6''A}$ =4.9, $J_{5'',6''B}$ = 2.4, $J_{6''A,6''B}$ = 12.7, 4H, 2 x H_2-6''), 3.87, 3.86, and 3.85 (three s, 12H, 4 x OCH_3), 3.76 (ddd, $J_{4'',5''}$ = 9.5, $J_{5'',6''A}$ =4.9, $J_{5'',6''B}$ = 2.4, 2H, 2 x H-5''), 3.02 [br s, 6H, $N(CH_3)_2$], 2.06, 2.03, 2.02, and 2.01 (four s, 24H, 8 x CH_3CO). ^{13}C NMR: δ 170.7, 170.3, 169.5, and 169.4 (8 x CO), 154.5, 154.1, 153.9, and 153.8 (C-2, 2 x C-2',5'), 134.3 (C-6), 128.2 (C-4), 123.7 and 120.0 (C-3,5), 115.7, 115.6, 115.5, and 115.1 (2 x C-3',6'), 115.0, 114.4, 113.8, 112.3, and 111.9 (C-1, 2 x C-1',4'), 98.3 (2 x C-1''), 95.5, 94.6, 92.6, 89.1, 88.9, 86.6, 83.5, and 83.4 (4 x C≡C), 72.8 (2 x C-3''), 71.9 (2 x C-5''), 71.1 (2 x C-2''), 68.3 (2 x C-4''), 61.8 (2 x C-6''), 57.1 (2 x $CH_2C{\equiv}$), 56.5, 56.4 and 56.3 (4 x OCH_3), 43.5 [$N(CH_3)_2$], 20.7 and 20.6 (8 x CH_3CO). Anal. Calcd for $C_{62}H_{67}NO_{24}$ (1210.19): C, 61.53; H, 5.58; N, 1.16. Found: C, 61.66; H, 5.57; N, 1.16.

Compound OPE_Glucose 1. It was obtained following **procedure A** starting from 17 (0.24 g), as a yellow solid (0.17g, 0.19 mmol, 97%).

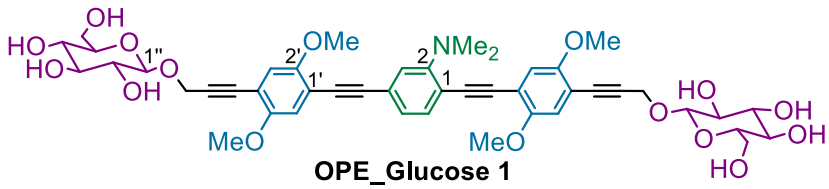

OPE_Glucose 1

TLC: *Rf* =0.05 ($CHCl_3$/MeOH 80:20). Mp 202-203 °C. ^{1}H NMR (dmso-*d6*): δ 7.44 (d, $J_{5,6}$ = 8.3, 1H, H-6), 7.16, 7.10, 7.07 and 7.06 (four s, 4H, 2 x H-3',6'), 7.01 (m, 2H, H-3,5), 5.14 (d, J_{vic} = 4.9, 2H, 2 x OH), 4.97 (d, J_{vic} = 4.8, 2H, 2 x OH), 4.92 (d, J_{vic} = 5.4, 2H, 2 x OH), 4.67 and 4.54 (AB system, J_{gem} = 16.1, 4H, 2 x CH_2C≡), 4.56 (t, $J_{OH,6"}$ = 5.9, 2H, 2 x 6"-OH), 4.33 (d, $J_{1",2"}$ = 7.8, 2H, 2 x H-1"), 3.81 and 3.80 (two s, 12H, 4 x OCH_3), 3.66 and 3.44 (split AB m, 4H, 2 x H_2-6"), 3.18 - 2.97 (m, 8H, 2 x H-2"-5"), 2.97 [s, 6H, $N(CH_3)_2$]. ^{13}C NMR (dmso-*d6*): δ 154.1, 153.8, 153.7, and 153.5 (C-2, 2 x C-2',5'), 134.5 (C-6), 123.3 (C-4), 122.7 and 119.2 (C-3,5), 115.8, 115.6, and 115.0 (2 x C-3',6'), 113.7, 113.2, 112.5, 112.4, and 112.0 (C-1, 2 x C-1',4'), 101.1 (2 x C-1"), 94.8, 94.3, 92.8, 91.3, 91.2, 87.3, 82.1, and 82.0 (4 x C≡C), 77.1 and 76.7 (2 x C-3",5"), 73.3 (2 x C-2"), 70.1 (2 x C-4"), 61.2 (2 x C-6"), 56.3 and 56.2 (4 x OCH_3), 55.9 (2 x CH2C≡), 42.7 [$N(CH_3)_2$]. Anal. Calcd for $C_{46}H_{51}NO_{16}$ (873.89): C, 63.22; H, 5.88; N, 1.60. Found: C, 63.25; H, 5.87; N, 1.60.

Compound 10. To a flask were added $Pd(PPh_3)_4$ (0.45 g, 0.39 mmol, 0.15 eq.), **5** (1.00 g, 2.59 mmol, 1 eq.) and **2** (1.45 g, 5.18 mmol, 2 eq.); the flask was capped with a rubber septum and evacuated. After backfilling with N_2, this process was repeated three times. To the flask were added dry DMF (20 mL) and Et_3N (20 mL) at room temperature. The reaction mixture was heated at 60°C, and maintained under continuous stirring for 4 h, until the disappearance of compound **5** by TLC (hexane/EtOAc 70:30). Solvents were removed under reduced pressure

and the solid residue was dissolved in CH_2Cl_2 ad filtered on celite. The volatiles were removed in vacuo and the reaction crude was purified by flash chromatography on silica gel, using hexane/EtOAc (90:10) as eluent, giving compound **10** as a pale yellow oil (0.91g, 1.55mmol, 66%).

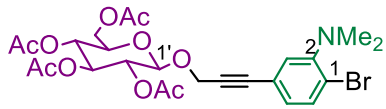

10

TLC: *Rf* =0.60 (hexane/EtOAc 70:30). ^{1}H NMR: δ (d, $J_{5,6}$ = 8.1, 1H, H-5), 7.11 (d, $J_{2,6}$ = 1.0, 1H, H-2), 6.93 (dd, $J_{5,6}$ = 8.1, $J_{2,6}$ = 1.0, 1H, H-6), 5.25 (t, $J_{2',3'} = J_{3',4'}$ = 9.3, 1H, H-3'), 5.10 (t, $J_{3',4'} = J_{4',5'}$ = = 9.3, 1H, H-4'), 5.02 (bdd, $J_{1',2'}$ = 8.3, $J_{2',3'}$ = 9.3, 1H, H-2'), 4.80 (d, $J_{1',2'}$ = 8.3, 1H, H-1'), 4.56 (s, 2H, $CH_2C\equiv$), 4.27 and 4.14 (split AB system, $J_{5',6'A}$ = 4.2, $J_{5',6'B}$ = 1.8, $J_{6'A,6'B}$ = 12.6, 2H, H_2-6'), 3.79 (m, 1H, H-5'),2.78 (s, 6H, [$N(CH_3)_2$]), 2.06, 2.03, 2.01 and 1.99 (four s, 12H, 4 x CH_3CO). ^{13}C NMR: δ 170.2 and 169.4 (4 x CO), 151.9 (C-3), 134.0 (C-5), 126.8 and 123.6 (C-2 and C-6), 121.9 and 119.9 (C-1 and C-4), 98.4 (C-1'), 86.3 and 83.9 (C≡C), 72.7 (C-3'), 71.8 (C-5'), 71.1 (C-2'), 68.2 (C-4'), 61.8 (C-6'), 56.8 ($CH_2C\equiv$), 44.0 ([$N(CH_3)_2$]), 20.6 and 20.5 (4 x CH_3CO). Calcd for $C_{25}H_{30}BrNO_{10}$ 583.11; found positive ESI-MS: [$M-H^+$] = 584.1114.

Compound 11. To a flask were added $Pd(PPh_3)_4$ (0.27 g, 0.23 mmol, 0.15 eq.), **10** (0.91 g, 1.55 mmol, 1 eq.) and ethynyltrimethylsilane (1.31 mL, 9.3 mmol, 6 eq.); the flask was capped with a rubber septum and evacuated. After backfilling with N_2, this process was repeated three times. To the flask were added dry DMF (11 mL) and Et_3N (11 mL) at room temperature. The mixture was heated at 80°C, and maintained under continuous stirring for 24 h, until the disappearance of compound **10** by TLC (hexane/EtOAc 7:3). Solvents were removed in vacuo and the solid residue was dissolved in CH_2Cl_2 ad filtered on celite. The volatiles were removed under reduced pression and the crude purified

by flash chromatography on silica gel using hexane/EtOAc (70:30) as eluent to give compound **11** as a yellow oil (0.54 g, 0.90 mmol, 58%).

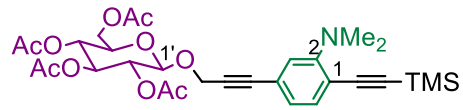

11

TLC: *Rf* =0.55 (hexane/EtOAc 70:30). ^{1}H NMR: δ (d, $J_{5,6}$ = 7.8, 1H, H-5), 6.86 (d, $J_{2,6}$ = 1.2, 1H, H-2), 6.87 (dd, $J_{5,6}$ = 7.8, $J_{2,6}$ = 1.2, 1H, H-6), 5.24 (t, $J_{2',3'} = J_{3',4'}$ = 9.3, 1H, H-3'), 5.09 (t, $J_{3',4'} = J_{4',5'}$ = 9.3, 1H, H-4'), 5.01 (bdd, $J_{1',2'}$ = 8.1 $J_{2',3'}$ = 9.3, 1H, H-2'), 4.82 (d, $J_{1',2'}$ = 8.1, 1H, H-1'), 4.57 (s, 2H, $CH_2C\equiv$), 4.27 and 4.15 (split AB system, $J_{5',6'A}$ = 4.5, $J_{5',6'B}$ = 2.1, $J_{6'A,6'B}$ = 12.3, 2H, H_2-6'), 3.74 (m, 1H, H-5'), 2.94 (s, 6H, [$N(CH_3)_2$]), 2.06, 2.03, 2.01 and 1.99 (four s, 12H, 4 x CH_3CO), 0.24 (s, 9H, [$Si(CH_3)_3$]). ^{13}C NMR: δ 170.2, 169.4 and 169.3 (4 x CO), 154.8 (C-3), 134.8 (C-5), 123.2 and 119.8 (C-2 and C-6), 122.8 and 116.2 (C-1 and C-4), 104.0, 101.7, 87.2 and 84.4 (C≡C), 98.4 (C-1'), 72.8 (C-3'), 71.9 (C-5'), 71.1 (C-2'),68.3 (C-4'), 61.8 (C-6'), 56.9 ($CH_2C\equiv$), 43.1[$N(CH_3)_2$], 21.0, 20.7 and 20.5 (4 x CH_3CO), 0.2 ([$Si(CH_3)_3$]). Calcd for $C_{30}H_{39}NO_{10}Si$ 601.23; found positive ESI-MS: [M-H^+] = 602.2422.

Compound 12. To a flask were added $Pd(PPh_3)_4$ (0.11 g, 0.09 mmol, 0.15 eq.), Ag_2O (0.30 g, 1.28 mmol, 2 eq.), **11** (0.77 g, 1.28 mmol, 2 eq.) and 1,4-iodo-2,5-dimethoxybenzene **7** (0.25 g, 0.64 mmol, 1 eq.); the flask was capped with a rubber septum and evacuated. After backfilling with N_2, this process was repeated three times. To the flask were added dry DMF (10mL) and dry THF (5mL). The reaction mixture was heated at 65°C for 5 h, until the disappearance of the starting compounds by TLC (hexane/EtOAc 1:1). Solvents were removed in vacuo and the solid residue was dissolved in CH_2Cl_2 and filtered on celite. The volatiles were removed under reduced pression and the crude purified by column

chromatography on silica gel using hexane/EtOAc (60:40) as eluent to give compound **12** as a brilliant yellow solid (0.43 g, 0.36 mmol, 57%).

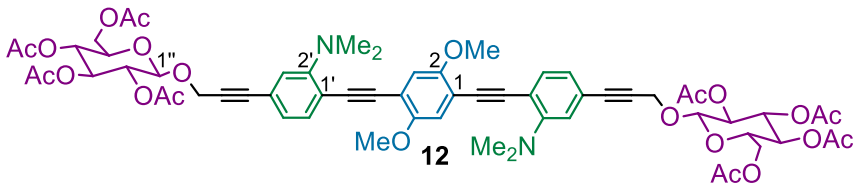

TLC: *Rf* =0.35 (hexane/EtOAc 40:60).). Mp 94-96 °C. ^{1}H NMR: δ 7.40 (d, $J_{5',6'}$ = 7.8, 2H, 2 x H-6'), 6.99 (s, 2H, H-3 and H-6), 6.97 (d, $J_{3',6'}$ = 1.2, 2H, 2 x H-3'), 6.96 (dd, $J_{5',6'}$ = 7.8, $J_{3',6'}$ = 1.2, 2H, 2 x H-5'), 5.28 (t, $J_{2'',3''}$ = $J_{3'',4''}$ = 9.3, 2H, 2 x H-3''), 5.12 (t, $J_{3'',4''}$ = $J_{4'',5''}$ = 9.3, 2H, 2 x H-4''), 5.04 (bdd, $J_{1'',2''}$ = 8.0, $J_{2'',3''}$ = 9.3, 2H, 2 x H-2''), 4.85 (d, $J_{1'',2''}$ = 8.2, 2H, 2 x H-1''), 4.60 (s, 4H, 2 x $CH_2C\equiv$), 4.29 and 4.17 (split AB system, $J_{5'',6''A}$ = 4.4, $J_{5'',6''B}$ = 2.5, $J_{6''A,6''B}$ = 12.2, 4H, 2 x H_2-6''), 3.89 (s, 6H, 2 x OCH_3), 3.77 (m, 2H, 2 x H-5''), 3.03 (s, 12H, 2 x [$N(CH_3)_2$]), 2.08, 2.05, 2.03 and 2.02 (four s, 24H, 8 x CH_3CO). ^{13}C NMR: δ 170.2, 169.4 and 169.3 (8 x CO), 154.3 and 153.9 (C-2, C-5, C-2'), 134.3 (C-6'), 123.5 (C-5'), 122.6 (C-4'), 119.9 (C-3'), 115.5, 114.9 and 114.8 (C-1, C-3, C-4 and C-6), 113.6 (C-1'), 98.4(C-1''), 98.1, 93.0, 87.2 and 84.4 (C≡C), 72.7 (C-3''), 71.8 (C-5''), 71.1 (C-2''),68.3 (C-4''), 61.7 (C-6''), 56.9 ($CH_2C\equiv$), 56.3 (OCH_3), 43.3 [$N(CH_3)_2$], 20.7 and 20.5 (8 x CH_3CO). Calcd for $C_{62}H_{68}N2O_{22}$ 1192.43: found positive MALDI [M^+] = 1192.4.

Compound OPE_Glucose 2. It was obtained following **procedure A** starting from **12** (0.43g, 0.36mmol) with the final obtaining of compound **OPE_Glucose 2** as a brilliant yellow solid (0.30 g, 0.35 mmol, 97%).

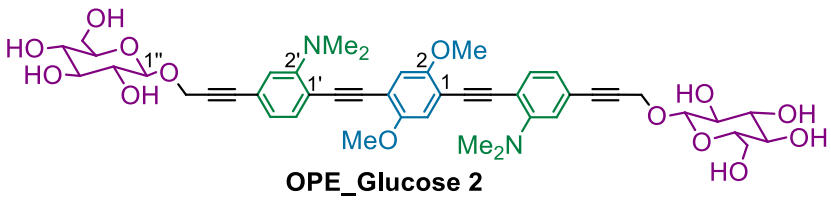

OPE_Glucose 2

TLC: *Rf* =0.05 ($CHCl_3$/MeOH 80:20). Mp 123-125°C. ^{1}H NMR (dmso-*d6*): δ 7.40 (d, $J_{5',6'}$ = 8.7, 2H, 2 x H-6'), 7.12 (s, 2H, H-3 and H-6), 6.95 (m, 4H, 2xH-3' and 2xH-3'), 5.14 (d, $J_{OH,2''}$ = 4.4, 2H, 2 x OH-2), 4.97 and 4.92 (two d, $J_{OH,3''}$ = $J_{OH,4''}$ =4.4, 4H, 2 x OH-3'' and 2 x OH-4''), 4.64 and 4.51 (AB system and m, J_{gem} =15.7, 6H, 2 x $CH_2C\equiv$ and 2 x OH-6''), 4.31 (d, 2H, $J_{1'',2''}$ = 7.8, 2 x H-1''), 3.83 (s, 6H, 2 x OCH_3), 3.70 and 3.46 (split AB m, 4H, 2 x H_2-6''), 3.16-2.98 (m, 8H, 2 x H-2''-5''), 2.96 (s, 12H, 2 x [$N(CH_3)_2$]). ^{13}C NMR (dmso-*d6*): δ 153.9 and 153.5 (C-2, C-5 and C-2'), 134.4 (C-6'), 131.5 (C-4'), 122.8, 122.6, 119.5 and 119.4 (C-3', 5'), 114.9 and 114.8 (C-3 and C-6), 113.7 and 112.9 (C-1, C-4 and C-1'), 101.2 (C-1''), 94.2, 92.8, 87.1 and 85.6 (C≡C), 77.0 and 76.5 (C-3'', 5''), 73.3 (C-2''), 70.0 (C-4''), 61.3 (C-6''), 56.2 ($CH_2C\equiv$), 55.7 (OCH_3), 42.6 [$N(CH_3)_2$]. Calc. for $C_{46}H_{52}N_2O_{14}$ 856.34; found positive ESI-MS: [M-H^+] = 857.3515.

Compound 15. To a solution of compound **8** (1.00 g, 1.54 mmol, 1 eq.) and $Pd(PPh_3)_4$ (0.18 g, 0.16 mmol) in dry DMF (7 mL), commercial ethynyltrimethylsilane (0.65 mL, 4.62 mmol) and dry Et_3N (7 mL) were slowly added. The mixture, under Ar atmosphere, was heated at 65 °C and maintained under continuous stirring for 2 h, until the disappearance of **8** by TLC (hexane/EtOAc 60:40). Column chromatography was performed with hexane/EtOAc 80:20 as eluent, and compound **15** was obtained as a white solid (0.67 g, 1.08 mmol, 70%).

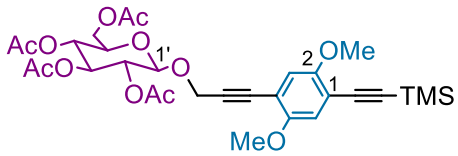

15

TLC: *Rf* =0.68 (hexane/EtOAc 60:40). Mp 59-61 °C. ^{1}H NMR: δ 6.95 and 6.89 (two s, 2H, H-3, 6), 5.25 (t, $J_{2',3'} = J_{3',4'} = 9.4$, 1H, H-3'), 5.10 (t, $J_{3',4'} = J_{4',5'} = 9.4$, 1H, H-4'), 5.03 (dd, $J_{1',2'} = 7.7$, $J_{2',3'} = 9.4$, 1H, H-2'), 4.88 (d, $J_{1',2'} = 7.7$, 1H, H-1'), 4.62 (s, 2H, $CH_2C\equiv$), 4.28 and 4.15 (split AB system, $J_{5',6'A} = 4.7$, $J_{5',6'B} = 2.4$, $J_{6'A,6'B} = 12.2$, 2H, H_2-6'), 3.85 and 3.84 (two s, 6H, 2 x OCH_3), 3.74 (ddd, $J_{4',5'} =$ = 10.0, $J_{5',6'A} = 4.7$, $J_{5',6'B} = 2.5$, 1H, H-5'), 2.07, 2.04, 2.03, and 2.01 (four s, 12H, 4 x CH_3CO), 0.27 [s, 9H, $Si(CH_3)_3$]. ^{13}C NMR: δ 170.7, 170.3, 169.4, and 169.3 (4 x CO), 154.2 and 153.9 (C-2, 5), 116.1 and 115.8 (C-3, 6), 113.7 and 112.4 (C-1, 4), 100.7 and 100.6 (C≡CSi), 98.2 (C-1'), 89.0 and 83.4 ($CH_2C\equiv C$), 72.8 (C-3'), 71.9 (C-5'), 71.1 (C-2'), 68.3 (C-4'), 61.8 (C-6'), 57.0 ($CH_2C\equiv$), 56.5 and 56.3 (2 x OCH_3), 20.7, 20.6, and 20.5 (4 x CH_3CO), - 0.05 [$Si(CH_3)_3$]. Anal. Calcd for $C_{30}H_{38}O_{12}Si$ (618.70): C, 58.24; H, 6.19. Found: C, 58.30; H, 6.20.

Compound 16. To a flask were added $Pd(PPh_3)_4$ (0.53 g, 0.46 mmol, 0.16 eq.), Ag_2O (1.33 g, 5.80 mmol, 2 eq.), **3** (0.90 g, 2.90 mmol, 1 eq.), and 1,4-iodo-2,5-dimethoxybenzene **7** (6.78 g, 17.4 mmol, 6 eq.); the flask was capped with a rubber septum and evacuated. After backfilling with N_2, this process was repeated three times. To the flask were added dry DMF (20 mL) and dry THF (10 mL). The reaction mixture was heated at 70°C for 2 h, until the disappearance of compound **3** by TLC (hexane/EtOAc 80:20). Solvents were removed in vacuo and the solid residue was dissolved in CH_2Cl_2 and filtered on celite. The volatiles were removed under reduced pression and the excess of unreacted **7** was precipitated from methanol. The crude obtained from evaporation of the mother liquors was purified by column chromatography on silica gel using hexane/EtOAc (97.5:2.5) as eluent to give compound **16** as a pale yellow solid (0.76 g, 1.10 mmol, 38%).

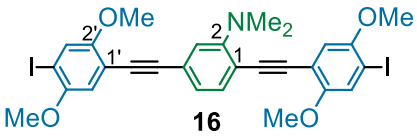

16

TLC: *Rf* =0.73 (hexane/EtOAc 80:20). Mp 117-119 °C. ^{1}H NMR: δ 7.47 (d, 1H, $J_{5,6}$ = 8.2, H-6), 7.31, 7.29, 6.95 e 6.93 (quattro s, 4H, H-3'-6'), 7.10 (broad s, 2H, H-3-5), 3.88, 3.86 e 3.85 (tre s, 12H, 4 x CH_3O), 3.03 [s, 6H, $N(CH_3)_2$]. ^{13}C NMR: δ 154.6, 154.5, 154.4 and 152.2(C-2, 2 x C-2',5'), 134.2 (C-6), 123.7 (C-4), 123.6 (C-5), 122.3, 122.1, 115.1 and 114.6 (2 x C-3',6'), 120.0 (C-3), 115.2, 113.6 and 113.0 (C-1, 2 x C-1'), 94.7, 93.8, 92.4, 86.85 and 86.4 (2 x C≡C, 2 x C-4') 57.0, 56.9, 56.7 and 56.5 (4 x OCH_3), 43.4 [$N(CH_3)_2$]. Calcd for $C_{28}H_{25}I_2NO_4$ 692,99; found positive APCI-MS: [M-H$^+$] = 693.9951;

Compound 17. To a flask were added $Pd(PPh_3)_4$ (0.25 g, 0.22 mmol, 0.16 eq.), Ag_2O (0.64 g, 2.80 mmol), 2 eq.), **16** (0.95 g, 1.4mmol, 1 eq.), and **15** (1.69 g, 2.80 mmol, 2 eq.); the flask was capped with a rubber septum and evacuated. After backfilling with N_2, this process was repeated three times. To the flask were added dry DMF (18 mL) and dry THF (9 mL). The reaction mixture was heated at 70°C for 3 h, until the disappearance of the starting compounds by TLC (hexane/EtOAc 40:60). Solvents were removed in vacuo and the solid residue was dissolved in CH_2Cl_2 and filtered on celite. The volatiles were removed under reduced pression and the crude was purified by column chromatography on silica gel using hexane/EtOAc (50:50) as eluent to give compound **17** as a yellow solid (1.13 g, 0.74 mmol, 53%).

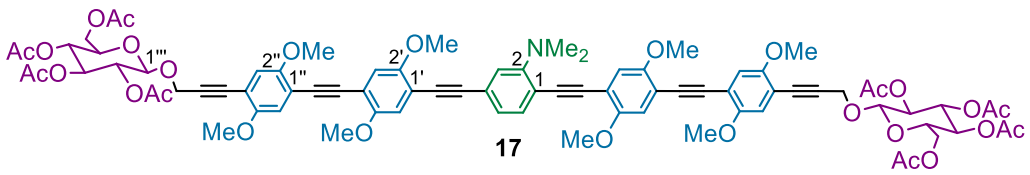

17

TLC: *Rf* =0.20 (hexane/EtOAc 40:60). Mp 115-117 °C. ^{1}H NMR: δ 7.48 (d, $J_{5,6}$ = 8.0, 1H, H-6), 7.10 (m, 2H, H-3, 5), 7.06, 7.05, 7.04, 7.02 and 6.94 (five s, 8H, 2 x H-3', 6', 3", 6"), 5.27 (t, $J_{2''',3'''} = J_{3''',4'''}$ = 9.4, 2H, 2 x H-3'''), 5.13 (t, $J_{3''',4'''} = J_{4''',5'''}$ = 9.4, 2H, 2 x H-4'''), 5.05 (dd, $J_{1''',2'''}$ = 8.0, $J_{2''',3'''}$ = 9.4, 2H, 2 x H-2'''), 4.92 (d, $J_{1''',2'''}$ = 8.0, 2H, 2 x H-1'''), 4.66 (s, 4H, 2 x $CH_2C{\equiv}$), 4.29 and 4.17 (split AB system, $J_{5''',6'''B}$ = 4.7, $J_{6'''A,6'''B}$ = 12.4, 4H, 2 x H_2-6'''), 3.93, 3.92, 3.91, 3.90 and 3.88 (five s, 24H, 8 x OCH_3), 3.77 (m, 2H, 2 x H-5'''), 3.05 [s, 6H, $N(CH_3)_2$], 2.08, 2.05, 2.03 and 2.02 (four s, 24H, 8 x CH_3CO). ^{13}C NMR: δ 170.7, 170.3, 169.5 and 169.4 (8 x CO), 154.1, 154.0 and 153.9 (C-2, 2 x C-2', 5', 2", 5"), 134.3 (C-6), 123.8 (C-4), 123.7 (C-5), 120.0 (C-3), 115.7 115.6, 115.4, 115.2, 115.1, 114.2, 114.0, 113.5, 113.3, 113.0, 112.3 (C-1, 2 x C-1', 4', 1", 4", 3', 6', 3", 6"), 98.3 (2 x C-1'''), 95.6, 94.7, 92.9, 91.7, 91.6, 91.2, 91.1, 89.1, 86.9, 83.5 (6 x C≡C), 72.9 (2 x C-3'''), 71.9 (2 x C-5'''), 71.1 (2 x C-2'''), 68.4 (2 x C-4'''), 61.8 (2 x C-6'''), 57.1 (2 x $CH_2C{\equiv}$), 56.6, 56.5, 56.4, 56.3 (8 x OCH_3), 43.5 [$N(CH_3)_2$], 20.7 and 20.6 (8 x CH_3CO). Anal. calcd for $C_{82}H_{83}NO_{28}$ (1530,53): C, 64.35; H, 5.47; N, 0.92. Found: C, 64.27; H, 5.48; N, 0.92.

Compound 13. It was obtained following **procedure A** starting from **17** (0.55 g, 0.35 mmol) with the final obtaining of compound **13** as a brilliant yellow solid (0.41 g, 0.34 mmol, 98%).

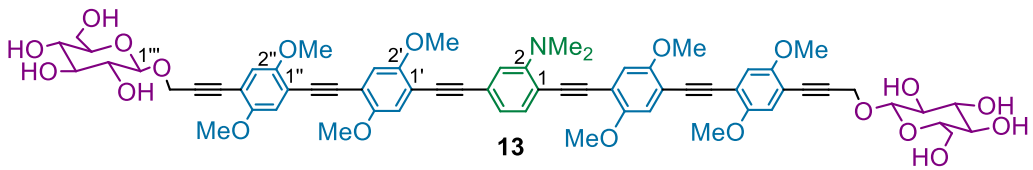

13

TLC: *Rf* =0.05 ($CHCl_3$/MeOH 80:20). Mp 250-252 °C. ^{1}H NMR (dmso-*d6*): δ 7.46 (d, $J_{5,6}$ = 6.8, 1H, H-6), 7.20, 7.14, 7.13, 7.12. 7.11, 7.10 and 7.08 (six s, 8H, 2 x H-3',6' and 3",6"), 7.04 (m, 2H, H-3, 5), 5.14 (d, J_{vic} = 4.9, 2H, 2 x OH), 4.97

(d, J_{vic} = 4.4, 2H, 2 x OH), 4.92 (d, J_{vic} = 4.9, 2H, 2 x OH), 4.67 and 4.55 (m AB system, J_{gem} = 16.2, 6H, 2 x $CH_2C\equiv$ and 2 x 6'''-OH), 4.33 (d, $J_{1''',2'''}$ = 7.8, 2H, 2 x H-1'''), 3.84, 3.82 and 3.81 (three s, 24H, 8 x OCH_3), 3.68 and 3.44 (split AB m, 4H, 2 x H_2- 6'''), 3.18 – 3,01 (m, 8H, 2 x H-2'''-5'''), 2.99 [s, 6H, $N(CH_3)_2$]. ^{13}C NMR (dmso-*d6*): δ 154.0, 153.7, 153.5, 153.4 and 153.3 (C-2, 2 x C-2', 5', 2'', 5''), 134.4 (C-6), 122.7 (C-4), 122.6 and 119.2 (C-3, 5), 115.9, 115.7, 115.4, 115.1, 112.7, 112, 5 and 112,3 (C-1, 2 x C-1', 4', 1'', 4'', 3',6', 3'',6''), 101.1 (2 x C-1'''), 96.0, 95.2, 94.9, 92.8, 91.3, 90.7, 87.3, 85.1, 83.5 and 80.0 (6 x C≡C), 77.0, 76.7, 73.3 and 70.1 (2 x C-2''', 3''', 4''', 5'''), 61.2 (2 x C-6'''), 56.3, 56.1 and 55.8 (8 x OCH_3, 2 x $CH_2C\equiv$), 42.7 [$N(CH_3)_2$]. Anal. calcd for $C_{82}H_{83}NO_{28}$ (1530,53): C, 64.35; H, 5.47; N, 0.92. Found: C, 64.23; H, 5.45; N, 0.92.

Compound 20. To a solution of compound **2** (1.00 g, 3.60 mmol, 1 eq.), $Pd(PPh_3)_2Cl_2$ (60 mg, 0.09 mmol, 0.025 eq.) and CuI (20 mg, 0.09 mmol, 0.025 eq.) in dry DMF (4 mL), commercial ethynyltrimethylsilane (1 mL, 7.2 mmol) and dry Et_3N (8 mL) were slowly added. The mixture, under Ar atmosphere, was heated at 40 °C and maintained under continuous stirring for 1 h, until the disappearance of **2** by TLC (hexane/DCM 80:20). Solvents were removed in vacuo and the solid residue was dissolved in CH_2Cl_2 and filtered on celite. The volatiles were removed under reduced pression and the crude was purified by column chromatography on silica gel using hexane (100%) as eluent to give first compound **20** as a pale yellow oil (0.83 g, 2.80 mmol, 78%) and immediately after a small amount of **3**.

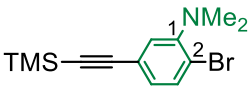

20

TLC: *Rf* =0.60 (hexane/DCM 80:20). ^1H NMR: δ 7.46 (d, 1H, $J_{3,4}$ = 8.3, H-3), 7.14 (d, 1H, $J_{4,6}$ =2.0, H-6), 6.97 (m, 1H, $J_{3,4}$ = 8.3, $J_{4,6}$ =2.0, H-4), 2.78 [s, 6H,

$N(CH_3)_2$], 0.25 [s, 9H, $Si(CH_3)_3$]. ^{13}C NMR: δ 151.7 (C-1), 133.8 (C-3), 127.2 (C-4), 123.9 (C-6), 122.9 and 119.8 (C-2,5), 104.3 and 94.8 (C≡C), 44.0 [$N(CH_3)_2$], - 0.1 [$Si(CH_3)_3$]. Calcd for $C_{13}H_{18}BrNSi$: 296,04; found positive GC-EI: [$M\text{-}1^+$] = 297.0377.

Compound 21. Compound **20** (1.0 g, 3.38 mmol) was dissolved in a mixture of MeOH (7 mL) and CH_2Cl_2 (7 mL), and K_2CO_3 (3.68 g, 26.68 mmol) was added. The reaction mixture stirred at room temperature for 1 h. The reaction was quenched by adding H_2O and the mixture was extracted with CH_2Cl_2 (3 x 15 mL), and then the combined organic extracts were washed with brine (3 x 15 mL). The combined organic extracts were then dried (Na_2SO_4) and filtered, and the solvent was evaporated in vacuo to give **21** as a pale yellow oil (0.74 g, 3.31 mmol., 98%)

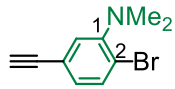

21

TLC: *Rf* =0.65 (hexane/DCM 80:20). ^1H NMR: δ 7.48 (d, 1H, $J_{3,4}$ = 8.0, H-3), 7.17 (d, 1H, $J_{4,6}$ =2.0, H-6), 6.99 (dd, 1H, $J_{3,4}$ = 8.0, $J_{4,6}$ =2.0, H-4), 3.10 (s, 1H, ≡CH), 2.79 [s, 6H, $N(CH_3)_2$]. ^{13}C NMR: δ 151.8 (C-1), 133.9 (C-3), 127.2 (C-4), 124.0 (C-6), 121.9 and 120.0 (C-2,5), 82.9 (-C≡CH), 77.7 (-C≡CH), 43.9 [$N(CH_3)_2$]. Calcd for $C_{10}H_{10}BrN$: 223,00; found positive GC-EI: [$M\text{-}1^+$] = 221.9929.

Compound 23. To a flask were added $Pd(PPh_3)_2Cl_2$ (39 mg, 0.06 mmol, 0.025 eq.), CuI (11 mg, 0.06 mmol, 0.025 eq.), **8** (1.45 g, 2.20 mmol, 1 eq.) and **21** (0.50 g, 2.20 mmol, 1 eq.); the flask was capped with a rubber septum and evacuated. After backfilling with N_2, this process was repeated three times. To

the flask were added dry DMF (2.6 mL) and Et_3N (5.2 mL) at room temperature. The reaction mixture was heated at 60°C, and maintained under continuous stirring for 1.5 h, until the disappearance of the starting compounds by TLC (hexane/EtOAc 60:40). Solvents were removed under reduced pressure and the solid residue was dissolved in CH_2Cl_2 ad filtered on celite. The volatiles were removed in vacuo and the reaction crude was purified by chromatography on silica gel, using hexane/EtOAc (70:30) as eluent, giving compound **23** as a yellow solid (1.28 g, 0.17 mmol, 77%).

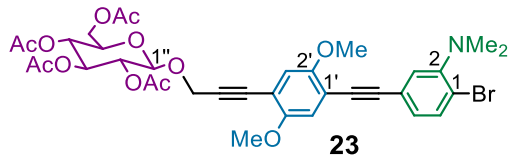

23

TLC: *Rf* =0.52 (hexane/EtOAc 60:40). Mp 102-104 °C ^{1}H NMR: δ 7.52 (d, $J_{5,6}$ = 8.1, 1H, H-6), 7.24 (d, $J_{3,5}$ = 1.9, 1H, H-3), 7.07 (dd, $J_{5,6}$ = 8.1, $J_{3,5}$ = 1.9, 1H, H-5), 7.01 and 6.94 (two s, 2H, H-3',6'), 5.27 (t, $J_{2'',3''}$ = $J_{3'',4''}$ = 9.5, 1H, H-3''), 5.12 (t, $J_{3'',4''}$ = $J_{4'',5''}$ = 9.5, 1H, H-4''), 5.05 (dd, $J_{1'',2''}$ = 8.0, $J_{2'',3''}$ = 9.5, 1H, H-2''), 4.91 (d, $J_{1'',2''}$ = 8.0, 1H, H-1''), 4.65 (s, 2H, $CH_2C\equiv$), 4.28 and 4.17 (split AB system, $J_{5'',6''A}$ = 2.4, $J_{5'',6''B}$ =4.6, $J_{6''A,6''B}$ = 12.3, 2H, H_2-6''), 3.89 and 3.88 (two s, 6H, 2 x OCH_3), 3.76 (ddd, 1H, H-5''), 2.81 [s, 3H, $N(CH_3)_2$], 2.08, 2.04, 2.03 and 2.01 (four s, 12H, 4 x CH_3CO). ^{13}C NMR: δ 170.7, 170.3, 169.4 and 169.3 (4 x CO), 154.1, 153.8 e 151.9 (C-2 and C-2',5'), 133.9 (C-6), 127.0 (C-5), 123.6 (C-3), 122.9, 119.8, 113.6 and 112.3 (C-1,4,1',4'), 115.7 and 115.6 (C3',6'), 98.3 (C-1''), 94.5, 89.1, 85.9 and 83.4 (2 x C≡C), 72.8 (C-3''), 71.9 (C-5''), 71.1 (C-2''), 68.4 (C-4''), 61.8 (C-6''), 57.1 ($CH_2C\equiv$), 56.5 and 56.3 (2 x OCH_3), 44.1 [$N(CH_3)_2$], 20.7 and 20.6 (4 x CH_3CO). Calcd for $C_{35}H_{38}BrNO_{12}$: 743.16; found positive ESI-MAXIS: [$(M-H)^+$] = 744.1643.

Compound 24. To a flask were added $Pd(PPh_3)_2Cl_2$ (19 mg, 0.03 mmol, 0.025 eq.), CuI (5 mg, 0.03 mmol, 0.025 eq.) and PPh_3 (14 mg, 0.06 mmol, 0.05 eq); the flask was capped with a rubber septum and evacuated. After backfilling with N_2, this process was repeated three times. To the flask was added dry Et_3N (5.2 mL) at room temperature and the suspension was heated at 80°C, and maintained under continuous stirring. After 1 h, a solution of compound **23** (0.8 g, 1.08 mmol, 1eq.) in dry DMF (2.6 mL) was added at room temperature and the mixture was stirred to uniform; then commercial ethynyltrimethylsilane (0.92 mL, 6.48 mmol, 6 eq.) was slowly added. The reaction mixture was heated at 80°C and maintained under continuous stirring for 5.5 h, until the disappearance of **23** by TLC (hexane/EtOAc 60:40). Column chromatography was performed with hexane/EtOAc 70:30 as eluent, and compound **24** was obtained as a yellow solid (0.58 g, 0.76 mmol, 70%).

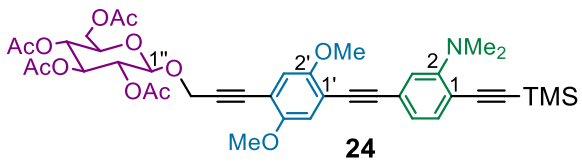

24

TLC: R_f 0.52 (hexane/EtOAc 50:50). Mp 107-109 °C ^{1}H NMR: δ 7.52 (d, $J_{5,6}$ = 8.1, 1H, H-6), 7.03 and 6.94 (two s, 2H, H-3'-6'), 7.01 (m, 2H, H-3,5), 5.27 (t, $J_{2",3"} = J_{3",4"}$ = 9.5, 1H, H-3"), 5.12 (t, $J_{3",4"} = J_{4",5"}$ = 9.5, 1H, H-4"), 5.05 (dd, $J_{1",2"}$ = 8.0, $J_{2",3"}$ = 9.5, 1H, H-2"), 4.91 (d, $J_{1",2"}$ = 8.0, 1H, H-1"), 4.65 (s, 2H, $CH_2C\equiv$), 4.28 e 4.16 (split AB system, $J_{5",6"A}$ = 2.3, $J_{5",6"B}$ =4.7, $J_{6"A,6"B}$ = 12.4, 2H, H_2-6"), 3.88 e 3.87 (two s, 6H, 2 x OCH_3), 3.77 (ddd, 1H, H-5"), 2.97 [s, 3H, $N(CH_3)_2$], 2.13, 2.09, 2.08 and 2.06 (four s, 12H, 4 x CH_3CO), 0.26 [$Si(CH_3)_3$]. ^{13}C NMR: δ 170.7, 170.3, 169.5 e 169.4 (4 x CO), 154.9, 154.1 e 153.8 (C-2 e C-2',5'), 134.8 (C-6), 123.4 (C-5), 119.9 (C-3), 123.7, 115.0, 113.8 and 112.3 (C-1,4,1',4'), 115.7 and 115.6 (C3',6'), 104.3, 101.6, 95.4, 89.0, 86.4 and 83.5 (3 x C≡C), 98.3 (C-1"), 72.9 (C-3"), 71.9 (C-5"), 71.1 (C-2"), 68.4 (C-4"), 61.8 (C-6"), 57.1 ($CH_2C\equiv$),

56.5 and 56.3 (2 x OCH_3), 43.2 [$N(CH_3)_2$], 20.7 and 20.6 (4 x CH_3CO), - 0.09 [$Si(CH_3)_3$]. Calcd for $C_{40}H_{47}NO_{12}Si$: 761,29; found positive ESI-MAXIS: [(M-H)$^+$] = 762.2973.

Compound 26. Compound **24** (0.46 g, 0.60 mmol) was dissolved in a mixture of MeOH (25 mL) and CH_2Cl_2 (25 mL), and K_2CO_3 (3.34 g, 24.16 mmol) was added. The reaction mixture stirred at room temperature for 4 h. The reaction was quenched by adding H_2O and the mixture was extracted with CH_2Cl_2 (3 x 20 mL), and then the combined organic extracts were washed with brine (3 x 20 mL). The combined organic extracts were then dried (Na_2SO_4) and filtered, and the solvent was evaporated in vacuo to give **26** as a yellow solid (0.17 g, 0.32 mmol., 53%) without any further purification.

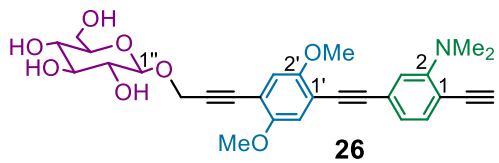

26

TLC: R_f 0.40 (acetonitrile/DCM 60:40). Mp 183-185 °C. ^{1}H NMR (dmso-*d6*): δ 7.38 (d, $J_{5,6}$ = 10.0, 1H, H-6), 7.16 and 7.07 (two s, 2H, H-3',6'), 6.99 (m, 2H, H-3,5), 5.13 (bs, 1H, OH), 4.98 (bs, 1H, OH), 4.94 (bs, 1H, OH), 4.67 and 4.54 (m AB system, J_{gem} = 15.0, 3H, $CH_2C\equiv$ and 6"-OH), 4.53 (s, 1H, ≡CH), 4.33 (d, $J_{1",2"}$ = 10.0, 1H, H-1"), 3.81 and 3.80 (two s, 6H, 2 x OCH_3), 3.68 and 3.44 (split AB m, 2H, H_2- 6''), 3.15 – 2.97 (m, 4H, H-2"-5"), 2.87 [s, 6H, $N(CH_3)_2$]. ^{13}C NMR (dmso-*d6*): δ 154.8, 153.6, 153.6 and 153.4 (C-2, C-2' and C-5'), 134.8 (C-6), 123,0 (C-5), 123.4, 113.8, 112.4 and 112.3 (C-1, C-4, C-1', C-4'), 119.5 (C-3), 115.8 and 115.6 (C-3', C-6'), 101.1 (C-1"), 94.5, 91.3, 87.4, 87.1, 82.6 and 82.0 (C≡C and C≡CH), 77.0, 76.7, 73.3, 70.1 (C-2",C-3", C-4", C-5"), 61.2 (C-6'"), 56.2 and 56.1 (2 x OCH_3), 55.8 ($CH_2C\equiv$), 42.7 [$N(CH_3)_2$]. Anal. Calcd for

$C_{29}H_{31}NO_8$ (521.56): C, 66.78; H, 5.99; N, 2.69. Found: C, 66.59; H, 6.00; N, 2.70.

Compound 25. To a flask were added $Pd(PPh_3)_4$ (0.21 g, 0.18 mmol, 0.15 eq.), Ag_2O (0.53 g, 2.30 mmol, 2 eq.), **24** (1.75 g, 2.30 mmol, 2 eq.) and 1,4-iodo-2,5-dimethoxybenzene **7** (0.47 g, 1.15 mmol, 1 eq.); the flask was capped with a rubber septum and evacuated. After backfilling with N_2, this process was repeated three times. To the flask were added dry DMF (23 mL) and dry THF (12.5 mL). The reaction mixture was heated at 70°C for 2.5 h, until the disappearance of the starting compounds by TLC (hexane/EtOAc 40:60). Solvents were removed in vacuo and the solid residue was dissolved in CH_2Cl_2 and filtered on celite. The volatiles were removed under reduced pression and the crude purified by column chromatography on silica gel using hexane/EtOAc (60:40) as eluent to give compound **25** as a brilliant yellow solid (0.87 g, 0.58 mmol, 50%).

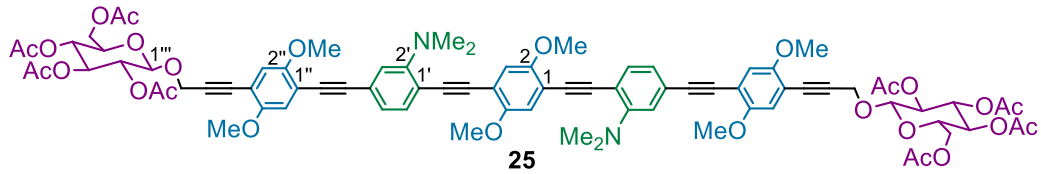

25

TLC: R_f 0.22 (hexane/EtOAc 40:60). Mp 120-122 °C. ^{1}H NMR: δ 7.48 (d, $J_{5,6}$ = 8.2, 2H, 2 x H-6'), 7.09 (m, 4H, 2 x H-3',5'), 7.02, 7.00 and 6.94 (three s, 6H, H-3,6 and 2 x H3''-6''), 5.27 (t, $J_{2''',3'''} = J_{3''',4'''}$ = 9.5, 2H, 2 x H-3'''), 5.12 (t, $J_{3''',4'''} = J_{4''',5'''}$ = 9.5, 2H, 2 x H-4'''), 5.04 (dd, $J_{1''',2'''}$ = 8.0, $J_{2''',3'''}$ = 9.5, 2H, 2 x H-2'''), 4.91 (d, $J_{1''',2'''}$ = 8.0, 2H, 2 x H-1'''), 4.65 (s, 4H, 2 x $CH_2C{\equiv}$), 4.28 and 4.16 (split AB system, $J_{5'''',6''''B}$ = 4.6, $J_{5''',6''',A}$ = 2.0, $J_{6''',A,6''',B}$ = 12.3, 4H, 2 x H_2-6'''), 3.89 and 3.88 (two s, 18H, 6 x OCH_3), 3.77 (m, 2H, 2 x H-5'''), 3.04 (s, 12H, 2 x $[N(CH_3)_2]$).

2.08, 2.05, 2.03 and 2.01 (four s, 24H, 8 x CH_3CO). ^{13}C NMR: δ 170.7, 170.3, 169.4 and 169.3 (8 x CO), 154.4, 154.1, 154.0 and 153.8 (C-2, 5, 2 x C-2', 2", 5"), 134.3 (2 x C-6'), 123.7 (2 x C-5'), 123.5 115.4, 113.8 113.5, 112.2 (C-1, 4, 2 x C-1', 4', 1", 4"), 120.0 (2 x C-3'), 115.7, 115.6 and 114.9 (C-3, 6, 2 x C-3", 6"), 98.2 (2 x C-1'"), 95.6, 94.7, 93.1, 89.0, 86.5 and 83.6 (6 x C≡C), 72.8 (2 x C-3'"), 71.9 (2 x C-5'"), 71.1 (2 x C-2'"), 68.4 (2 x C-4'"), 61.8 (2 x C-6'"), 57.1 (2 x CH_2C≡), 56.5 and 56.3 (6 x OCH_3), 43.4 [2 x $N(CH_3)_2$], 20.7 and 20.6 (8 x CH_3CO). Anal. calcd for $C_{82}H_{84}N_2O_{26}$ (1513,54): C, 65.07; H, 5.59; N, 1.85. Found: C, 64.99; H, 5.60; N, 1.85.

Compound 14. It was obtained following **procedure A** starting from **25** (0.14 g, 0.09 mmol) with the final obtaining of compound **14** as a brilliant yellow solid (0.09 g, 0.09 mmol, 98%).

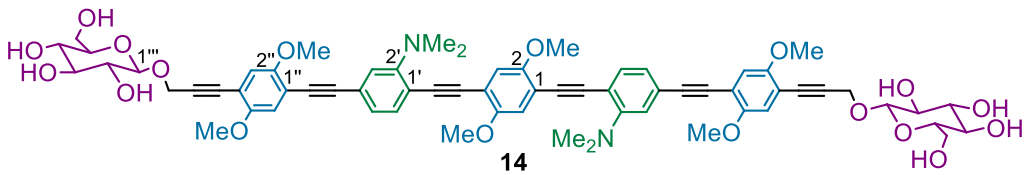

14

TLC: R_f 0.05 ($CHCl_3$/MeOH 80:20). Mp 258-260 °C. ^1H NMR (dmso-*d6*): δ 7.45 (d, $J_{5',6'}$ = 8.0, 2H, 2 x H-6'), 7.17, 7.14, and 7.08 (three s, 6H, H-3,6 and 2 x H3",6"), 7.02 (m, 4H, 2 x H-3',5'), 5.14 (bd, J_{vic} = 4.8, 2H, 2 x OH), 4.97 (bd, J_{vic} = 4.8, 2H, 2 x OH), 4.93 (bd, J_{vic} = 4.8, 2H, 2 x OH), 4.68 and 4.55 (m AB system, J_{gem} = 15.8, 6H, 2 x CH_2C≡ and 2 x 6'"-OH), 4.33 (d, $J_{1''',2'''}$ = 7.7, 2H, 2 x H-1'"), 3.85, 3.82 and 3.81 (three s, 18H, 6 x OCH_3), 3.68 and 3.45 (split AB m, 4H, 2 x H_2- 6'"), 3.18 – 2.97 (m, 8H, 2 x H-2'"-5'"), 2.99 (s, 12H, 2 x [$N(CH_3)_2$]). ^{13}C

NMR (dmso-*d6*): δ 154.0, 153.7, 153.6 and 153.4 (C-2, 5, 2 x C-2', 2", 5"), 134.4 (2 x C-6'), 123.3 (2 x C-4'), 122.7 (2 x C-5'), 119.2 (2 x C-3'), 115.8 115.6 and 114.9 (C-3, 6, 2 x C-3", 6"), 113.8, 112.9, 112.4 and 112.3 (C-1, 4, 2 x C-1', 1", 4"), 101.1 (2 x C-1'"), 94.8, 94.4, 93.0, 91.3, 87.3 and 82.1 (6 x C≡C), 77.0, 76.7, 73.3 and 70.1 (2 x C-2'",3'", 4'", 5'"), 61.2 (2 x C-6'"), 56.2, 56.1, 55.8 (2 x CH_2C≡, 6 x OCH_3), 42.7 [2 x $N(CH_3)_2$]. Anal. calcd for $C_{66}H_{68}N_2O_{18}$ (1177,25): C, 67.34; H, 5.82; N, 2.38. Found: C, 67.43; H, 5.83; N, 2.38.

Compound 27c.[186] Commercial D-(+)-Maltose monohydrate (2.1 g, 5.8 mmol, 1 eq.) was suspended in dry pyridine (7.5 mL) and acetic anhydride (6.6 mL), and a catalytic amount of 4-dimethylaminopyridine was added. The solution was stirred at ambient temperature for 16 h. The reaction mixture was diluted with ethyl acetate and washed successively with HCl 1 N (20 mL) and saturated $NaHCO_3$ (20mL). The resulting organic phase was dried (anhydrous Na_2SO_4) and filtered; the filtrate was concentrated under reduced pressure to afford **27c** (3.9 g, 5.7mmol, 98%) as a white solid. TLC: *Rf*= 0.56 (hexane/EtOAc 40:60).

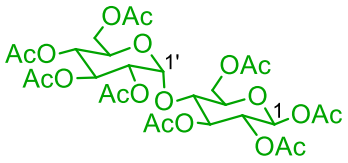

27c

Compound 29a.[187] To a solution of 1,2,3,4,6-Penta-O-acetyl-β-D-galactopyranose **27a** (7.5 g, 18.83 mmol) in 54 mL of dry CH_2Cl_2, at 0°C and

[186] Braitsch, M.; Kählig, H.; Kontaxis, G.; Fischer, M.; Kawada, T.; Konrat, R.; Schmid, W. *Beilstein J. Org. Chem.* **2012**, *8*, 448.
[187] Junqueira, G. G.; Carvalho, M. R.; de Andrade, P.; Lopes, C. D.; Carneiro, Z. A.; Sesti-Costa, R.; Silva, J. S.; Carvalho, I. *J. Braz. Chem. Soc.* **2014**, *25*, 1872.

under Argon, 2.22 mL of propargyl alchol (37.65 mmol, 2eq. d = 0.958 g/mL), 6.89 mL di trimethylsilyltriflate (37.65 mmol, 2 eq. d=1.228 g/mL) and molecular sieves 4 Å were added. The mixture was heated to RT and maintained under continuous stirring until the disappearance of **27a** by TLC (1 hour). The reaction was quenched by adding $NaHCO_3$ (60 mL) and the organic phase washed with water (2 x 40 mL). The organic phases were dried over anhydrous Na_2SO_4, the solvent evaporated under reduced pressure. Column chromatography was performed with hexane/EtOAc 70:30 as eluent, and compound **29a** was obtained as a white solid (4.4 g, 11.49 mmol, 61%). TLC: *Rf* = 0.50 (hexane/EtOAc 70:30).

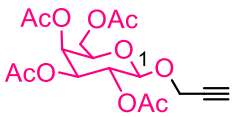

29a

Compound 29b.[188] To a solution of 1,2,3,4,6-Penta-O-acetyl-α-D-mannopyranose **27b** (7.5 g, 18.83 mmol) in 54 mL of dry CH_2Cl_2, at 0°C and under Argon, 2.22 mL of propargyl alchol (37.65 mmol, 2eq. d = 0.958 g/mL), 6.89 mL di trimethylsilyltriflate (37.65 mmol, 2 eq. d=1.228 g/mL) and molecular sieves 4 Å were added. The mixture was heated to RT and maintained under continuous stirring until the disappearance of **27b** by TLC (1 hour). The reaction was quenched by adding $NaHCO_3$ (60 mL) and the organic phase washed with water (2 x 40 mL). The organic phases were dried over anhydrous Na_2SO_4, the solvent evaporated under reduced pressure. Column chromatography was performed with hexane/EtOAc 70:30 as eluent, and compound **29b** was obtained as a white solid (4.1 g, 10.73 mmol, 57%). TLC: *Rf* = 0.50 (hexane/EtOAc 70:30).

[188] Bergeron-Brlek, M.;Chieh Shiao, T.; Trono, M. C.; Roy, R. *Carbohydr. Res.* **2011**, *346*, 1479.

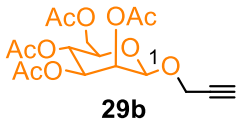

29b

Compound 29c.[189] To a solution of 1,2,3,6,2′,3′,4′,6′-Octa-O-acetyl-D-maltose **27c** (16.2 g, 18.83 mmol) in 54 mL of dry CH_2Cl_2, at 0°C and under Argon, 2.22 mL of propargyl alchol (37.65 mmol, 2eq. d = 0.958 g/mL), 6.89 mL di trimethylsilyltriflate (37.65 mmol, 2 eq. d=1.228 g/mL) and molecular sieves 4 Å were added. The mixture was heated to RT and maintained under continuous stirring until the disappearance of **27c** by TLC (1 hour). The reaction was quenched by adding $NaHCO_3$ (60 mL) and the organic phase washed with water (2 x 40 mL). The organic phases were dried over anhydrous Na_2SO_4, the solvent evaporated under reduced pressure. Column chromatography was performed with hexane/EtOAc 70:30 as eluent, and compound **29c** was obtained as a white solid (8.0 g, 11.86 mmol, 63%). TLC: *Rf* = 0.50 (hexane/EtOAc 70:30).

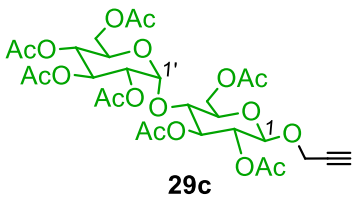

29c

Compound 30a. Compound **29a** (2.00 g, 4.97 mmol, 1 eq.), 1,4-diiodo-2,5-dimethoxybenzene **7** (3.88 g, 9.94 mmol, 2 eq.) and $Pd(PPh_3)_4$ (0.68 g, 0.60 mmol, 0.12 eq.) were dissolved in dry DMF (42 mL). To the mixture Et_3N (42 mL) was slowly added. The mixture was heated at 60 °C and maintained under continuous stirring and under Ar atmosphere for 3h, until the disappearance of **29a** by TLC. After evaporation of the solvents, the excess of unreacted **7** was separated through

[189] Fu, Q.; Guo, Z.; Liang, T.; Zhang, X.; Xua, Q.; Liang, X. *Anal. Method.*, **2010**, *2*, 217.

precipitation from methanol. Column chromatography of the crude obtained from evaporation of the mother liquors was performed with hexane/EtOAc 70:30 as eluent, and compound **30a** was obtained as a transparent oil (2.13 g, 3.28 mmol, 66%).

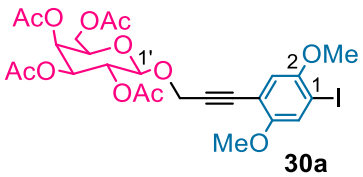

30a

TLC: *Rf* =0.64 (hexane/EtOAc 60:40). ^{1}H NMR: δ 7.29 (s, 1H, H-6), 6.85 (s, 1H, H-3), 5.40 (dd, $J_{3',4'}$ = 2.0, $J_{4',5'}$= 0.5, 1H, H-4'), 5.24 (dd, $J_{2',3'}$ = 10.3, $J_{1',2'}$ = 7.8, 1H, H-2'), 5.07 (dd, $J_{2',3'}$ = 10.3, $J_{3',4'}$ = 2.0, 1H, H-3'), 4.84 (d, $J_{1',2'}$ = 7.8, 1H, H-1'), 4.63 (s, 2H, $CH_2C\equiv$), 4.19 e 4.12 (m AB system, $J_{5',6'A}$ = $J_{5',6'B}$ = 6.4, $J_{6'A,6'B}$ = 9.3, 2H, H_2-6'), 3.96 (t, 1H, H-5'), 3.84 and 3.83 (two s, 6H, 2 x OCH_3), 2.15, 2.05, 2.04 and 1.99 (4 s, 12H, 4 x CH_3CO). ^{13}C NMR: δ 170.3, 170.2, 170.1 and 169.5 (4 x CO), 154.7 (C-5), 152.2 (C-2), 122.3 (C-6), 115.1 (C-3), 111.9 (C-4), 98.8 (C-1'), 88.5 (C-1), 87.3 and 82.9 (C≡C), 70.9 and 70.7 (C-3', 5'), 68.6 (C-2'), 66.9 (C-4'), 61.4 (C-6'), 57.1, 57.0 and 56.5 (2 x OCH_3, $CH_2C\equiv$), 20.7 and 20.6 (4 x $\underline{C}H_3CO$). Anal. Calcd for $C_{25}H_{29}IO_{12}$ (648.40): C, 46.31; H, 4.51. Found: C, 46.22; H, 4.52.

Compound 30b. Compound **29b** (2.00 g, 4.97 mmol, 1 eq.), 1,4-diiodo-2,5-dimethoxybenzene **7** (3.88 g, 9.94 mmol, 2 eq.) and $Pd(PPh_3)_4$ (0.68 g, 0.60 mmol, 0.12 eq.) were dissolved in dry DMF (42 mL). To the mixture Et_3N (42 mL) was slowly added. The mixture was heated at 60 °C and maintained under continuous stirring and under Ar atmosphere for 3h, until the disappearance of **29b** by TLC. After evaporation of the solvents, the excess of unreacted **7** was separated through precipitation from methanol. Column chromatography of the

obtained crude was performed with hexane/EtOAc 70:30 as eluent, and compound **30b** was obtained as a transparent oil (2.09 g, 3.23 mmol, 65%).

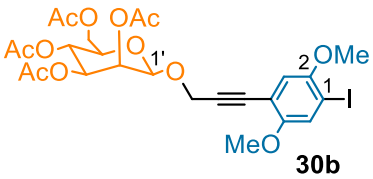

30b

TLC: *Rf* =0.64 (hexane/EtOAc 60:40). ^{1}H NMR: δ 7.27 (s, 1H, H-6), 6.85 (s, 1H, H-3), 5.38 (dd, $J_{2',3'}$ = 3.4, $J_{3',4'}$ = 10.3, 1H, H-3'), 5.31 (m, 2H, H-2',4'), 5.11 (d, $J_{1',2'}$ =1.5, 1H, H-1'), 4.52 (s, 2H, $CH_2C\equiv$), 4.28 and 4.11 (m AB system, $J_{5',6'A}$=4.9, $J_{5',6'B}$ = 2.4, $J_{6'A,6'B}$ = 12.3, 2H, H_2-6'), 4.08 (m, 1H, H-5'), 3.83 and 3.82 (two s, 6H, 2 x OCH_3), 2.15, 2.09, 2.03 and 1.99 (4 s, 12H, 4 x CH_3CO). ^{13}C NMR: δ 170.6, 169.9, 169.8 and 169.6 (4 x CO), 154.7 (C-5), 152.2 (C-2), 122.2 (C-6), 115.3 (C-3), 111.7 (C-4), 96.4 (C-1'), 88.2 (C-1), 87.3 and 83.0 (C≡C), 69.5, 69.0, 68.9 and 66.0 (C-2'-5'), 62.3 (C-6'), 57.0, 56.5 and 56.0 (2 x OCH_3, $CH_2C\equiv$), 20.9, 20.7 and 20.6 (4 x $\underline{C}H_3CO$). Anal. Calcd for $C_{25}H_{29}IO_{12}$ (648.40): C, 46.31; H, 4.51. Found: C, 46.43; H, 4.51.

Compound 30c. Compound **29c** (3.35 g, 4.97 mmol, 1 eq.), 1,4-diiodo-2,5-dimethoxybenzene **7** (3.88 g, 9.94 mmol, 2 eq.) and $Pd(PPh_3)_4$ (0.68 g, 0.60 mmol, 0.12 eq.) were dissolved in dry DMF (42 mL). To the mixture Et_3N (42 mL) was slowly added. The mixture was heated at 60 °C and maintained under continuous stirring and under Ar atmosphere for 3h, until the disappearance of **29c** by TLC. After evaporation of the solvents, the excess of unreacted **7** was separated through precipitation from methanol. Column chromatography of the crude obtained from evaporation of the mother liquors was performed with hexane/EtOAc 60:40 as eluent, and compound **30c** was obtained as a with solid (2.88 g, 3.08 mmol, 62%).

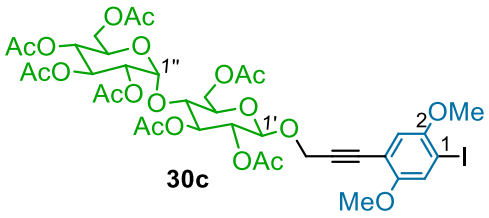

30c

TLC: *Rf* =0.58 (hexane/EtOAc 40:60). Mp 121-123 °C. ^{1}H NMR: δ 7.28 (s, 1H, H-6), 6.84 (s, 1H, H-3), 5.39 (d, $J_{1'',2''}$ =4.0, 1H, H-1''), 5.33 (t, $J_{2'',3''}$ = $J_{3'',4''}$ = 10.0, 1H, H-3''), 5.27 (t, $J_{2',3'}$ = $J_{3',4'}$ = 8.8, 1H, H-3'), 5.03 (t, $J_{3'',4''}$ =$J_{4'',5''}$ =10.0, 1H, H-4''), 4.88 (t, $J_{1',2'}$ = $J_{2',3'}$ = 8.8, 1H, H-2'), 4.86 - 4.82 (m, 2H, H-1'',2''), 4.58 (s, 2H, $CH_2C\equiv$), 4.23, 4.11 and 4.02 (m, 5H, H_2-6', H_2-6'', H-4'), 3.94 (m, 1H, H-5''), 3.83 and 3.82 (two s, 6H, 2 x OCH_3), 3.72 (m, 1H, H-5'), 2.11, 2.08, 2.02, 2.00, 1.99, 1.98 and 1.97 (7 s, 21H, 7 x CH_3CO). ^{13}C NMR: δ 170.5, 170.4, 170.2, 169.9, 169.7 and 169.3 (7 x CO), 154.9 (C-5), 152.3 (C-2), 122.2 (C-6), 115.1 (C-3), 111.8 (C-4), 97.6 (C-1'), 95.5 (C-1''), 88.3 and 83.1 (C≡C), 87.3 (C-1), 69.5, 69.0, 68.9 and 66.0 (C-2'-5'), 62.3 (C-6'), 57.0, 56.5 and 56.0 (2 x OCH_3, $CH_2C\equiv$), 20.9, 20.7 and 20.6 (4 x $\underline{C}H_3CO$). Anal. Calcd for $C_{37}H_{45}IO_{20}$ (936,65): C, 47.45; H, 4.84. Found: C, 47.32; H, 4.83.

Compound 31.[190] Compound **3** (2.0 g, 6.38 mmol) was dissolved in a mixture of MeOH (13 mL) and CH_2Cl_2 (13 mL), and K_2CO_3 (6.96 g, 50.36 mmol) was added. The reaction mixture stirred at room temperature for 1 h. The reaction was quenched by adding H_2O and the mixture was extracted with CH_2Cl_2 (3 x 20 mL), and then the combined organic extracts were washed with brine (3 x 20 mL). The combined organic extracts were then dried (Na_2SO_4) and filtered, and the solvent was evaporated in vacuo to give **31** as a pale yellow oil (1.07 g, 6.31 mmol., 99%). TLC: *Rf* =0.65 (hexane/DCM 80:20).

[190] Thomas, S. W.; Swager, T. M. *Macromolecules* **2005**, *38*, 2716.

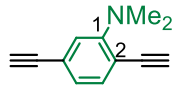

31

Compound 32a. To a flask were added $Pd(PPh_3)_4$ (0.40 g, 0.35 mmol, 0.15 eq.), **30a** (1.50 g, 2.31 mmol, 2 eq.) and **31** (0.20 g, 1.16 mmol, 1 eq.); the flask was capped with a rubber septum and evacuated. After backfilling with N_2, this process was repeated three times. To the flask were added dry DMF (18 mL) and Et_3N (18 mL) at room temperature. The reaction mixture was heated at 60°C, and maintained under continuous stirring for 4 h, until the disappearance of the starting compounds by TLC (hexane/EtOAc 60:40). Solvents were removed under reduced pressure and the reaction crude was purified by chromatography on silica gel, using hexane/EtOAc (50:50) as eluent, giving compound **32a** as a yellow solid (1.06 g, 0.88 mmol, 76%).

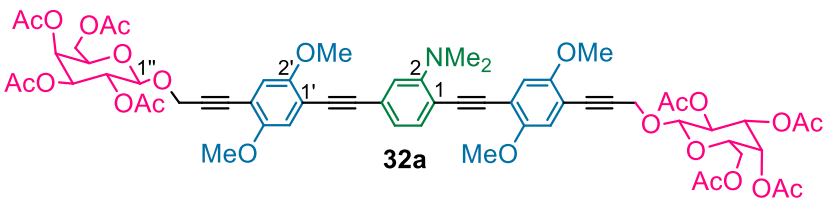

32a

TLC: *Rf* =0.36 (hexane/EtOAc 40:60). Mp 86-90 °C.^{1}H NMR: δ 7.47 (d, $J_{5,6}$ = 8.2, 1H, H-6), 7.09 (m, 2H, H-3, 5), 7.00, 6.99, 6.93 and 6.91 (four s, 4H, 2 x H-3',6'), 5.42 (d, 2H, $J_{3'',4''}$ = 2.4, 2H, 2 x H-4''), 5.25 (dd, 2H, $J_{2'',3''}$ = 10.4, $J_{1'',2''}$ =8.0, 2 x H-2''), 5.08 (dd, 2H, $J_{2'',3''}$ = 10.4, $J_{3'',4''}$ = 2.4, 2H, 2 x H-3''), 4.85 (d, 2H, $J_{1'',2''}$ = 8.0, 2H, 2 x H-1''), 4.66 (s, 4H, 2 x $CH_2C\equiv$), 4.17 (split AB system, $J_{5'',6''A}$ = $J_{5'',6''B}$ = 6.5, $J_{6''A,6''B}$ = 121.0, 4H, 2 x H_2-6''), 3.96 (t, $J_{5'',6''A}$ = $J_{5'',6''B}$ = 6.5, 2H, 2 x H-5''), 3.88, 3.87 and 3.86 (three s, 12H, 4 x OCH_3), 3.03 [s, 6H, $N(CH_3)_2$], 2.16, 2.05, 2.04 and 1.99 (four s, 24H, 8 x CH_3CO). ^{13}C NMR: δ 170.4, 170.2, 170.1 and 169.6 (8 x CO), 154.4, 154.1, 153.9 and 153.8 (C-2, 2 x C-2',5'), 134.4 (C-6), 123.7(C-4), 123.6 and 120.0 (C-3,5), 115.8, 115.7, 115.6 and 115.0 (2 x C-

3',6'), 115.1, 114.5, 113.9, 112.3 and 111.9 (C-1, 2 x C-1',4'), 98.8 (2 x C-1"), 95.5, 94.7, 92.6, 89.2, 86.6, 83.4 and 83.3 (4 x C≡C), 70.9 and 70.8 (2 x C-3", 5"), 68.7 (2 x C-2"), 67.0 (2 x C-4"), 61.2(2 x C-6"), 57.1 (2 x CH_2C≡), 56.5, 56.4 and 56.3(4 x OCH_3), 43.5[$N(CH_3)_2$], 20.8, 20.7 and 20.6 (8 x CH_3CO). Calcd for $C_{62}H_{67}NO_{24}$: 1209.41; found positive ESI-MAXIS: [$(M+Na)^+$] = 1232.3929.

Compound 32b. To a flask were added $Pd(PPh_3)_4$ (0.40 g, 0.35 mmol, 0.15 eq.), **30b** (1.50 g, 2.31 mmol, 2 eq.) and **31** (0.20 g, 1.16 mmol, 1 eq.); the flask was capped with a rubber septum and evacuated. After backfilling with N_2, this process was repeated three times. To the flask were added dry DMF (18 mL) and Et_3N (18 mL) at room temperature. The reaction mixture was heated at 60°C, and maintained under continuous stirring for 4 h, until the disappearance of the starting compounds by TLC (hexane/EtOAc 60:40). Solvents were removed under reduced pressure and the reaction crude was purified by chromatography on silica gel, using hexane/EtOAc (50:50) as eluent, giving compound **32b** as a yellow solid (1.08 g, 0.89 mmol, 77%).

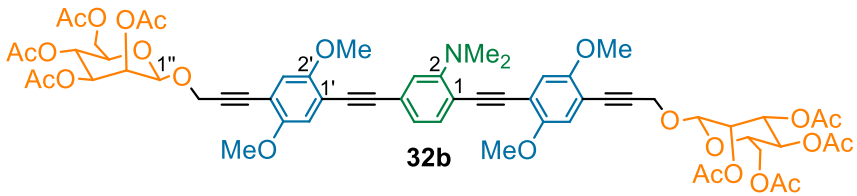

32b

TLC: *Rf* =0.36 (hexane/EtOAc 40:60). Mp 109-111 °C.^{1}H NMR: δ 7.47 (d, $J_{5,6}$ = 8.5, 1H, H-6), 7.08 (m, 2H, H-3, 5), 7.00, 6.98, 6.97 and 6.95 (four s, 4H, 2 x H-3',6'), 5.39 (dd, $J_{2",3"}$ = 3.5, $J_{3",4"}$ = 10.0, 2H, 2 x H-3"), 5.33 (m, 4H, 2 x H-2",4"), 5.14 (d, 2H, $J_{1",2"}$ = 1.5, 2H, 2 x H-1"), 4.56 (s, 4H, 2 x CH_2C≡), 4.30 and 4.13 (m AB system, $J_{5",6"A}$=5, $J_{5",6"B}$ = 2.5, $J_{6"A,6"B}$ = 12.5, 2H, H_2-6"), 4.10 (m, 2H, 2 x H-5"), 3.89, 3.88, 3.86 and 3.85 (four s, 12H, 4 x OCH_3), 3.03 [s, 6H, $N(CH_3)_2$], 2.17, 2.10, 2.05 and 2.00 (four s, 24H, 8 x CH_3CO). ^{13}C NMR: δ 170.6, 169.9,

169.8 and 169.7 (8 x CO), 154.4, 154.0, 153.9 and 153.8 (C-2, 2 x C-2',5'), 134.3 (C-6), 123.7(C-4), 123.6 and 120.0 (C-3,5), 115.9, 115.7, 115.5 and 115.0 (2 x C-3',6'), 115.1, 114.4, 113.7, 112.1 and 111.8 (C-1, 2 x C-1',4'), 96.4 (2 x C-1''), 95.4, 94.6, 92.7, 88.9, 88.8, 86.6, 83.5 and 83.4 (4 x C≡C), 69.5, 69.2, 69.0 and 66.1 (2 x C-2''- 5''), 62.3 (2 x C-6''), 56.5, 56.3 and 56.0 (2 x $CH_2C\equiv$ and 4 x OCH_3), 43.4 [$N(CH_3)_2$], 20.9, 20.7 and 20.6 (8 x CH_3CO). Anal. Calcd for $C_{62}H_{67}NO_{24}$ (1210.19): C, 61.53; H, 5.58; N, 1.16. Found: C, 61.37; H, 5.56; N, 1.16.

Compound 32c. To a flask were added $Pd(PPh_3)_4$ (0.40 g, 0.35 mmol, 0.15 eq.), **30c** (2.16 g, 2.31 mmol, 2 eq.) and **31** (0.20 g, 1.16 mmol, 1 eq.); the flask was capped with a rubber septum and evacuated. After backfilling with N_2, this process was repeated three times. To the flask were added dry DMF (18 mL) and Et_3N (18 mL) at room temperature. The reaction mixture was heated at 60°C, and maintained under continuous stirring for 4 h, until the disappearance of the starting compounds by TLC (hexane/EtOAc 60:40). Solvents were removed under reduced pressure and the reaction crude was purified by chromatography on silica gel, using hexane/EtOAc (40:60) as eluent, giving compound **32b** as a yellow solid (1.53 g, 0.85 mmol, 74%).

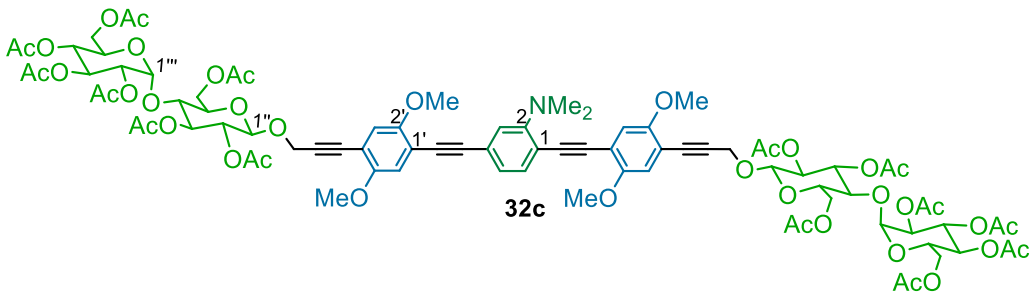

32c

TLC: *Rf* =0.42 (hexane/EtOAc 30:70). Mp 140-142 °C.^{1}H NMR: δ 7.47 (d, $J_{5,6}$ = 8.5, 1H, H-6), 7.09 (m, 2H, H-3, 5), 7.02, 7.00, 6.95 and 6.94 (four s, 4H, 2 x H-3',6'), 5.42 (d, $J_{1''',2'''}$ =3.5, 2H, 2 x H-1'''), 5.36 (t, $J_{2''',3'''} = J_{3''',4'''}$ = 10.0, 2H, 2 x H-

3'''), 5.30 (t, $J_{2'',3''}$ = $J_{3'',4''}$ = 9.0, 2H, 2 x H-3''), 5.04 (t, $J_{3''',4'''}$ =$J_{4''',5'''}$ = 10.0, 2H, 2 x H-4'''), 4.92 (t, $J_{1'',2''}$ = $J_{2'',3''}$ = 8.0, 2H, 2 x H-2''), 4.90 - 4.84 (m, 4H, 2 x H-1''',2'''), 4.63 (s, 4H, 2 x $CH_2C\equiv$), 4.51, 4.24 and 4.04 (m, 10H, 2 x H_2-6'', 6''', H-4''), 3.95 (m, 2H, 2 x H-5'''), 3.90, 3.88, and 3.87 (three s, 12H, 4 x OCH_3), 3.75 (m, 2H, 2 x H-5''), 3.04 [s, 6H, $N(CH_3)_2$], 2.13, 2.10, 2.04, 2.02, 2.01 and 2.00 (six s, 42H, 14 x CH_3CO). ^{13}C NMR: δ 170.5, 170.4, 170.2,, 169.9, 169.7 and 169.4 (14 x CO), 154.4, 154.1, 153.9 and 153.8 (C-2, 2 x C-2',5'), 134.3 (C-6), 123.7 (C-4), 123.6 and 120.0 (C-3,5), 115.8, 115.5, and 115.0 (2 x C-3',6'), 115.2, 114.4, 113.8, 112.2 and 111.9 (C-1, 2 x C-1',4'), 97.8 (2 x C-1''), 95.5 (2 x C-1'''), 95.5, 94.6, 92.6, 89.0, 88.9, 86.6, 83.5 and 83.4 (4 x C≡C), 75.4, 72.6, 72.2, 71.9, 70.0, 69.3, 68.5 and 68.0 (2 x C-2''- 5'',2 x C-2'''- 5'''), 62.7 and 61.5 (2 x C-6'', 6'''), 57.0, 56.5 and 56.3 (2 x $CH_2C\equiv$ and 4 x OCH_3), 43.4 [$N(CH_3)_2$], 20.9, 20.8, 20.7 and 20.5 (14 x CH_3CO). Anal. Calcd for $C_{86}H_{99}NO_{40}$ (1786.69): C, 57.81; H, 5.58; N, 0.78. Found: C, 57.90; H, 5.60; N, 0.78.

Compound OPE_Galactose. It was obtained following **procedure A** starting from **32a** (0.50 g, 0.41 mmol), as a yellow solid (0.35 g, 0.40 mmol, 98%).

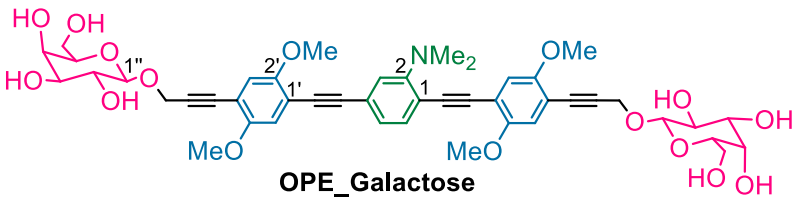

OPE_Galactose

TLC: *Rf* =0.05 ($CHCl_3$/MeOH 80:20). Mp 225-228 °C. ^{1}H NMR (dmso-*d6*): δ 7.43 (d, $J_{5,6}$ = 8.2, 1H, H-6), 7.16, 7.10, 7.06 and 7.05 (four s, 4H, 2 x H-3',6'), 7.01 (m, 2H, H-3,5), 5.00 (bs, 2H, 2 x OH), 4.77 (bs, 2H, 2 x OH), 4.67 and 4.54 (AB system, J_{gem} = 16.1, 4H, 2 x $CH_2C\equiv$), 4.55 (bs, 2H, 2 x OH), 4.40 (bs, 2H, 2 x OH), 4.33 (d, $J_{1'',2''}$ = 7.8, 2H, 2 x H-1''), 3.83, 3.82 and 3.81 (three s, 12H, 4 x OCH_3), 3.65 - 3.30 (m, 12H, 2 x H2''-6''), 2.97 [s, 6H, $N(CH_3)_2$]. ^{13}C NMR (dmso-*d6*): δ 154.1, 153.7, 153.6, and 153.4 (C-2, 2 x C-2',5'), 134.4 (C-6), 123.3 (C-4),

122.7 and 119.2 (C-3,5), 115.8, 115.6, and 115.0 (2 x C-3',6'), 113.7, 113.1, 112.4 and 112.0 (C-1, 2 x C-1',4'), 101.8 (2 x C-1''), 94.8, 94.2, 92.7, 91.4, 91.3, 87.3, 82.0, and 81.9 (4 x C≡C), 75.4, 73.4, 70.4 and 68.1 (2 x C-2''-5''), 60.5 (2 x C-6''), 56.3. 56.2 and 56.1 (4 x OCH_3), 55.7 (2 x CH2C≡), 42.7 [$N(CH_3)_2$]. Calcd for $C_{46}H_{51}NO_{16}$: 873.32; found positive ESI-MAXIS: [$(M-H)^+$] = 874.3275.

Compound OPE_Mannose. It was obtained following **procedure A** starting from **32b** (0.50 g, 0.41 mmol), as a yellow solid (0.34 g, 0.39 mmol, 97%).

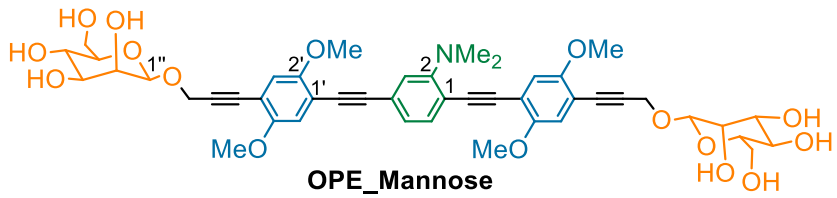

OPE_Mannose

TLC: *Rf* =0.05 ($CHCl_3$/MeOH 80:20). Mp 224-226 °C. ^{1}H NMR (dmso-*d6*): δ 7.44 (d, $J_{5,6}$ = 8.0, 1H, H-6), 7.16, 7.10, 7.09 and 7.08 (four s, 4H, 2 x H-3',6'), 7.01 (m, 2H, H-3,5), 4.87 (bs, 2H, 2 x H-1''), 4.83 (d, J_{vic}=4.5, 2H, 2 x OH), 4.75 (d, J_{vic}=5.0, 2H, 2 x OH), 4.62 (d, J_{vic}=6.0, 2H, 2 x OH), 4.53 - 4.43 (m AB system, J_{gem} = 16.5, 6H, 2 x CH_2C≡, 2 x OH-6''), 3.82, 3.81 and 3.80 (three s, 12H, 4 x OCH_3), 3.71 - 3.34 (m, 12H, 2 x H2''-6''), 2.98 [s, 6H, $N(CH_3)_2$]. ^{13}C NMR (dmso-*d6*): δ 154.0, 153.7, 153.6, 153.4 and 153.3 (C-2, 2 x C-2',5'), 134.4 (C-6), 123.3 (C-4), 122.7 and 119.2 (C-3,5), 115.8, 115.7, 115.5 and 114.9 (2 x C-3',6'), 113.7, 113.1, 112.4, 112.0 and 11.8 (C-1, 2 x C-1',4'), 98.3 (2 x C-1''), 94.8, 94.3, 92.7, 91.1, 91.0, 87.2, 82.1, and 82.0 (4 x C≡C), 74.4, 70.9, 70.1 and 66.9 (2 x C-2''-5''), 61.1 (2 x C-6''), 56.3, 56.2 and 56.1 (4 x OCH_3), 53.8 (2 x CH2C≡), 42.7 [$N(CH_3)_2$]. Anal. Calcd for $C_{46}H_{51}NO_{16}$ (873.89): C, 63.22; H, 5.88; N, 1.60. Found: C, 63.29; H, 5.89; N. 1.60.

Compound OPE_Maltose. It was obtained following **procedure A** starting from **32c** (0.73 g, 0.41 mmol), as a yellow solid (0.49 g, 0.40 mmol, 99%).

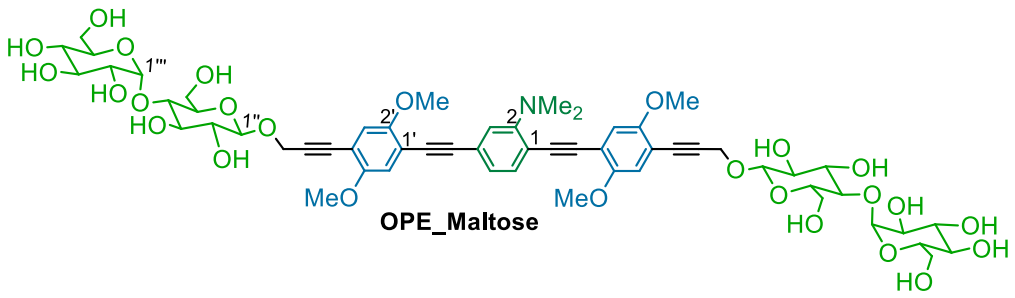

TLC: *Rf* =0.42 (hexane/EtOAc 30:70). Mp 224-226 °C.^{1}H NMR: δ 7.45 (d, $J_{5,6}$ = 8.5, 1H, H-6), 7.18, 7.12, 7.09 and 7.08 (four s, 4H, 2 x H-3',6'), 7.03 (m, 2H, H-3, 5), 5.53 (d, J_{vic}=3.5, 2H, 2 x OH), 5.42 (d, J_{vic}=6.5, 2H, 2 x OH), 5.27 (d, J_{vic}=5.0, 2H, 2 x OH), 5.03 (d, $J_{1''',2'''}$=4.0, 2H, 2 x H-1'''), 4.90 (d, J_{vic}=5.5, 2H, 2 x OH), 4.88 (d, J_{vic}=5.0, 2H, 2 x OH), 4.70 - 4.50 (m AB system, J_{gem} = 15.5, 6H, 2 x $CH_2C\equiv$, 2 x OH-6''), 4.38 (d, $J_{1'',2''}$=8.0, 2H, 2 x H-1''), 3.83, 3.82, and 3.81 (three s, 12H, 4 x OCH_3), 3.78 – 3.04 (m, 12H, 2 x H-2''-6'', 2 x H-2'''-6'''), 2.99 [s, 6H, $N(CH_3)_2$]. ^{13}C NMR: δ 154.0, 153.7 and 153.4 (C-2, 2 x C-2',5'), 134.4 (C-6), 123.3 (C-4), 122.7 and 119.2 (C-3,5), 115.8, 115.6 and 114.9 (2 x C-3',6'), 113.7, 113.1, 112.4, 112.3 and 111.9 (C-1, 2 x C-1',4'), 101.0 and 100.7 (2 x C-1'', 1'''), 94.8, 94.2, 92.7, 91.2, 91.1, 87.2, 82.2 and 82.1 (4 x C≡C), 759.5, 76.4, 75.3, 73.4, 73.2, 72.8, 72.4 and 69.9 (2 x C-2''- 5'', 2 x C-2'''- 5'''), 60.8 and 60.7 (2 x C-6'', 6'''), 56.3, 56.2, 56.1 and 56.0 (2 x $CH_2C\equiv$ and 4 x OCH_3), 42.7 [$N(CH_3)_2$]. Anal. Calcd for $C_{58}H_{71}NO_{26}$ (1198.18): C, 58.14; H, 5.97; N, 1.17. Found: C, 58.07; H, 5.98; N, 1.17.

Compound 40. It was obtained following **procedure B**, starting from compound **9** (0.50 g, 0.41 mmol, 1 eq.) and an equimolar amount of MeOTf, as a yellow-orange solid (0.53 g, 0.39 mmol, 95%). The reaction, monitored by TLC (hexane/AcOEt 30:70) was complete in 2 h.

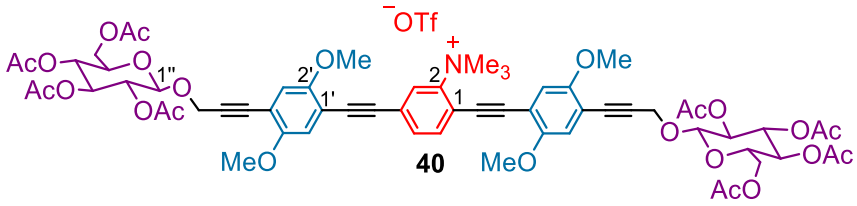

TLC: *Rf* =0.10 (hexane/EtOAc 30:70). Mp 162-164 °C.^{1}H NMR: δ (d, $J_{3,5}$ = 1.0, 1H, H-3), 7.78 (d, $J_{5,6}$ = 7.8, 1H, H-6), 7.70 (dd, $J_{3,5}$ = 1.0, $J_{5,6}$ = 7.8, 1H, H-5), 7.07, 6.98 and 6.96 (three s, 4H, 2 x H-3',6'), 5.27 (t, $J_{2'',3''}$ = $J_{3'',4''}$ = 9.3, 2H, 2 x H-3''), 5.12 (t, $J_{3'',4''}$ = $J_{4'',5''}$ = 9.3, 2H, 2 x H-4''), 5.04 (*broad* dd, $J_{1'',2''}$ = 7.9, $J_{2'',3''}$ = 9.3, 2H, 2 x H-2''), 4.90 (d, $J_{1'',2''}$ = 7.8, 2H, 2 x H-1''), 4.66 and 4.65 (two s, 4H, 2 x $CH_2C{\equiv}$), 4.28 and 4.17 (split AB m, 4H, 2 x H_2-6''), 4.09 [(s, 9H, $N(CH_3)_3$], 3.95, 3.90, 3.89, and 3.88 (four s, 12H, 4 x OCH_3), 3.77 (m, 2H, 2 x H-5''), 2.08, 2.05, 2.03, and 2.01 (four s, 24H, 8 x CH_3CO). ^{13}C NMR: δ 170.3, 169.5 and 169.4 (8 x CO), 155.2 and 154.1 (2 x C-2',5'), 145.1 (C-2), 137.1 (C-6), 133.1 (C-5), 125.9 (C-4), 122.9 (C-3), 115.7, 115.5, 114.8, 114.5, 113.6, 112.2, and 110.8 (C-1, 2 x C-1',3',4',6'), 100.2, 92.2, 91.3, 90.5, 89.8, 88.7, 83.2, and 82.9 (4 x C≡C), 98.3 (2 x C-1''), 72.8 (2 x C-3''), 71.9 (2 x C-5''), 71.1 (2 x C-2''), 68.3 (2 x C-4''), 61.8 (2 x C-6''), 57.1 and 57.0 (2 x $CH_2C{\equiv}$), 56.5, 56.4 and 56.3 (4 x OCH_3), 56.0 [$N(CH_3)_3$], 20.7 and 20.6 (8 x CH_3CO). Anal. Calcd for $C_{64}H_{70}F_3NO_{27}S$ (1374.29): C, 55.93; H, 5.13; N, 1.02. Found: C, 56.03; H, 5.12; N, 1.02.

Compound 38. Following **procedure A**, starting from **40** (0.55 g, 0.40 mmol) compound **38** was obtained as a brilliant yellow solid (0.4 g, 0.39 mmol, 97%).

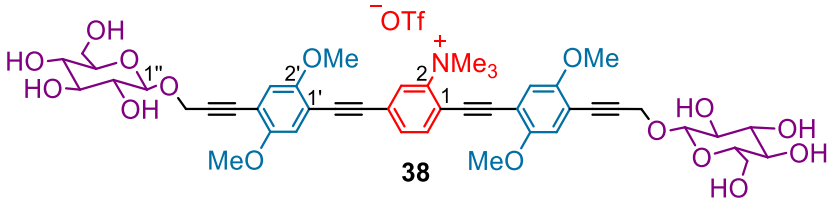

TLC: *Rf* =0.10 (EtOAc). Mp 165-167 °C. ^{1}H NMR (dmso-*d6*): δ 8.04 (broad s, 1H, H-3), 7.92 (broad d, $J_{5,6}$ = 7.9, 1H, H-6), 7.82 (broad d, $J_{5,6}$ = 7.9, 1H, H-5), 7.31, 7.19, 7.16 and 7.15 (four s, 4H, 2 x H-3', 6'), 5.14 (m, 2H, 2 x OH), 4.98 (broad d, 2H, 2 x OH), 4.95 (broad d, 2H, 2 x OH), 4.61-4.53 (m, 6H, 2 x $CH_2C\equiv$ and 2 x 6"-OH), 4.34 (d, $J_{1",2"}$ = 8.1, 2H, 2 x H-1"), 3.92 [(s, 9H, $N(CH_3)_3$], 3.90, 3.84, and 3.82 (three s, 12H, 4 x OCH_3), 3.70 and 3.46 (split AB m, 4H, 2 x H_2-6"), 3.18 - 2.98 (m, 8H, 2 x H-2"-5"). ^{13}C NMR: δ 154.5, 153.8, 153.7 and 153.6 (2 x C-2',5'), 145.1 (C-2), 136.9 (C-6), 132.9 (C-5), 124.6 (C-3), 124.1 (C-4), 116.0, 115.8, 115.6, and 115.4 (2 x C-3',6'), 115.0, 113.9, 113.3, 111.4, and 110.8 (C-1, 2 x C-1',3',4',6'), 101.1 and 101.0 (2 x C-1"), 98.8, 92.8, 92.2, 91.8, 90.3, and 81.9 (4 x C≡C), 77.1 and 76.7 (2 x C-3",-5"), 73.3 (2 x C-2"), 70.1 (2 x C-4"), 61.2 (2 x C-6"), 56.4, 56.3 and 56.2 (4 x OCH_3), 55.8 (2 x $CH_2C\equiv$), 55.3 [$N(CH_3)_3$]. Anal. Calcd for $C_{48}H_{54}F_3NO_{19}S$ (1038.00): C, 55.54; H, 5.24; N, 1.35. Found: C, 55.48; H, 5.23; N, 1.35.

Compound 40. It was obtained following **procedure B**, starting from compound **12** (0.40 g, 0.33 mmol, 1 eq.) and a twofold amount of MeOTf, as a yellow-orange solid (0.47 g, 0.31 mmol, 94%). The reaction, monitored by TLC (hexane/AcOEt 20:80) was complete in 6 h.

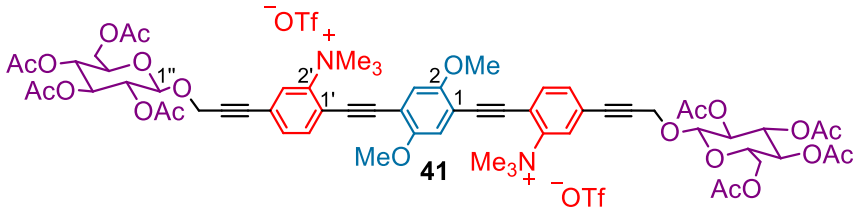

TLC: *Rf* =0.10 (hexane/EtOAc 20:80). Mp 210-213 °C. ^{1}H NMR: δ 7.90 (s, 2H, 2 x H-3'), 7.80 (d, $J_{5',6'}$ = 7.8, 2H, 2 x H-6'), 7.59 (d, $J_{5',6'}$ = 7.8, 2H, 2 x H-5'), 7.07 (s, 2H, H-3, 6), 5.26 (t, $J_{2'',3''}$ = $J_{3'',4''}$ = 9.3, 2H, 2 x H- 3''), 5.12 (t, $J_{3'',4''}$ = $J_{4'',5''}$ = 9.3, 2H, 2 x H-4''), 5.00 (bdd, $J_{1'',2''}$ = 8.2, $J_{2'',3''}$ = 9.3, 2H, 2 x H- 2''), 4.84 (d, $J_{1'',2''}$ = 8.2, 2H, 2 x H-1''), 4.62 (s, 4H, 2 x $CH_2C{\equiv}$), 4.27 and 4.17 (split AB system, $J_{5'',6A''}$ = 4.4, $J_{5'',6B''}$ = 2.5, $J_{6A'',6B''}$ = 12.2, 4H, 2 x H_2-6''), 4.06 (s, 18H, 2 x [$N(CH_3)_3$]), 3.97 (s, 6H, 2 x OCH_3), 3.83 (m, 2H, 2 x H5''), 2.06, 2.04, 2.01 and 2.00 (four s, 24H, 8 x CH_3CO). ^{13}C NMR: δ 170.2 and 169.4 (8 x CO), 155.1 and 145.1 (C-2, C-5, 2 x C-2'), 137.3 (2 x C-6'), 133.3 (2 x C-5'), 133.1 (2 x C-4'), 128.4 (2 x C-3'), 119.4, 116.1, 114.4 and 112.7 (C-1, 3, 4, 6), 113.6 (2 x C-1'), 99.7 (2 x C-1''), 98.8, 90.9, 89.4 and 84.3 (4 x C≡C), 72.7 (2 x C-3''), 71.8 (2 x C-5''), 71.3 (2 x C-2''),68.2 (2 x C-4''), 61.8 (2 x C-6''), 56.7 (2 x $CH_2C{\equiv}$), 56.4 (OCH_3), 56.0 [$N(CH_3)_3$], 20.7 and 20.5 (8 x CH_3CO). Anal. Calc. for $C_{66}H_{74}F_6N_2O_{28}S_2$ (1521.41): C, 52.10; H, 4.90; N, 1.84. Found: C, 52.21; H, 4.91; N, 1.84.

Compound 39. Following **procedure A**, starting from **41** (0.40 g, 0.26 mmol), compound **39** was obtained as a yellow solid (0.30 g, 0.25 mmol, 98%).

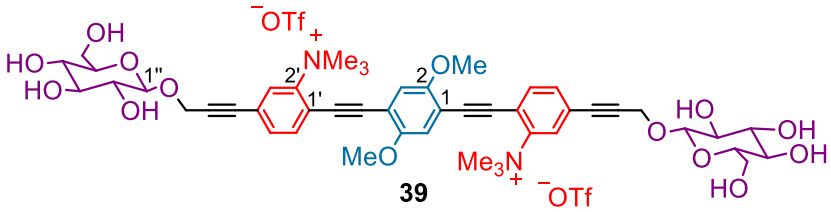

39

TLC: *Rf* =0.05 (EtOAc). Mp 165-169 °C. ^{1}H NMR (dmso-*d6*): δ 8.01 (broad s, 2H, 2 x H-3'), 7.90 (broad d, $J_{5',6'}$ = 7.9, 2H, 2 x H-6'), 7.77 (broad d, $J_{5',6'}$ = 7.9, 2H, 2 x H-5'), 7.40 (s, 2H, H-3,6), 5.14 (broad d, 2H, 2 x OH), 5.01 (broad d, 2H, 2 x OH), 4.96 (broad d, 2H, 2 x OH), 4.72-4.55 (m, 6H, 2 x $CH_2C\equiv$ and 2 x 6"-OH), 4.33 (d, 2H, 2 x H-1") 3.93 [(s, 18H, 2 x $N(CH_3)_3$], 3.90 (s, 6H, 2 x OCH_3), 3.70 and 3.46 (split AB m, 4H, 2 x H_2-6"), 3.18 - 2.98 (m, 8H, 2 x H-2"-5"). ^{13}C NMR: δ 155.7 and 154.8 (C-2,5), 145.2 (2 x C-2'), 137.0 (2 x C-6'), 133.2 (2 x C-5'), 125.2 (2 x C-3'), 124.0 (2 x C-4'), 116.3, 115.6, 115.3 and 115.1 (C-3,6), 114.0, 112.5, and 110.8 (C-1,3,4,6 and 2 x C-1'), 101.6 and 101.5 (2 x C-1"), 98.9, 98.6, 91.0, 90.7 (4 x C≡C), 77.3, 77.0 and 76.9 (2 x C-3",-5"), 73.9 and 74.4 (2 x C-2"), 70.2 (2 x C-4"), 68.9 (2 x C-6"), 61.3 (4 x OCH_3), 58.6 (2 x $CH_2C\equiv$), 55.6 [$N(CH_3)_3$]. Anal. Calc. for $C_{50}H_{58}F_6N_2O_{20}S_2$ (1185.12): C, 50.67; H, 4.93; N, 2.36. Found: C, 50.59; H, 4.94; N, 2.36.

Compound 40. It was obtained following **procedure B**, starting from compound **17** (0.46 g, 0.30 mmol, 1 eq.) and an equimolar amount of MeOTf, as an orange solid (0.49 g, 0.29 mmol, 97%). The reaction, monitored by TLC (hexane/AcOEt 20:80) was complete in 2h.

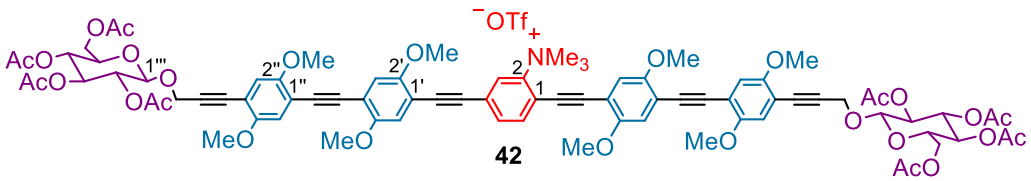

42

TLC: *Rf* =0.10 ($CHCl_3$/MeOH 95:5). Mp 172-174 °C. ^{1}H NMR (dmso-*d6*): δ 8.06 (s, 1H, H-3), 7.95 (d, $J_{5,6}$ = 8.0, 1H, H-6), 7.84 (d, $J_{5,6}$ = 8.0, 1H, H-5), 7.34, 7.24, 7.22, 7.20, 7.13, 7.12, 7.11 and 7.10 (eight s, 8H, 2 x H-3', 6', 3", 6"), 5.33 (t, $J_{2''',3'''} = J_{3''',4'''}$ = 7.5, 2H, 2 x H-3'''), 5.00 (d, $J_{1''',2'''}$ = 7.5, 2H, 2 x H-1'''), 4.95 (t, $J_{3''',4'''} = J_{4''',5'''}$ = 7.5, 2H, 2 x H-4'''), 4.82 (t, $J_{1''',2'''} = J_{2''',3'''}$ = 7.5, 2H, 2 x H-2'''), 4.66 and 4.56 (AB system, J_{gem}=15.5, 4H, 2 x $CH_2C\equiv$), 4.21 and 4.05 (m, $J_{6'''A,6'''B}$ = 11.0, 6H, 2 x H-5''', 2 x H_2-6'''), 3.94 [s, 9H, $N(CH_3)_3^+$], 3.88, 3.87, 3.86, 3.83,

3.82 and 3.81 (six s, 24H, 8 x OCH_3), 2.02, 2.00, 1.99 and 1.95 (four s, 24H, 8 x CH_3CO). ^{13}C NMR: δ 170.0, 169.5, 169.2 and 169.0 (8 x CO), 154.6, 153.8, 153.7, 153.6 and 153.4 (2 x C-2', 5', 2", 5"), 145.0 (C-2), 136.9 (C-6), 132.8 (C-5), 124.6 (C-3), 124.1 (C-4), 116.0, 115.7, 115.6, 115.4, 115.1, 114.4, 113.8, 112.8, 112.7, 112.2, 112.1, 111.5, 110.8 (C-1, 2 x C-1', 4', 1", 4", 3', 6', 3", 6"), 98.0 (2 x C-1'"), 98.9, 93.0, 92.1, 91.7, 91.6, 91.1, 90.5, 90.4 and 82.5 (6 x C≡C), 72.0, 70.8, 70.6 and 68.0 (2 x C-2'",3'", 4'", 5'"), 61.6 (2 x C-6'"), 56.7, 56.4, 56.3, 56.2 and 56.1 [2 x CH_2C≡, 8 x OCH_3 and $N(CH_3)_3^+$], 20.4, 20.3 and 20.2 (8 x CH_3CO). Anal. calcd for $C_{84}H_{86}F_3NO_{31}S$ (1694.63): C, 59.54; H, 5.12; N, 0.83. Found: C, 59.46; H, 5.11; N, 0.83.

Compound 43. Following **procedure A**, starting from **42** (0.30 g, 0.18 mmol) compound **43** was obtained as a brilliant yellow solid (0.24 g, 0.17 mmol, 98%).

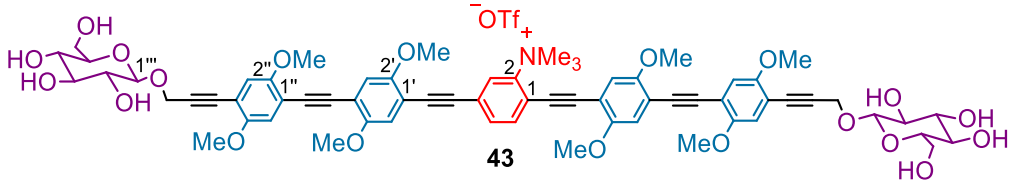

43

TLC: *Rf* =0.10 ($CHCl_3$/MeOH 70:30). Mp 247-249 °C. ^1H NMR (dmso-*d6*): 8.06 (s, 1H, H-3), 7.95 (d, $J_{5,6}$ = 8.0, 1H, H-6), 7.84 (d, $J_{5,6}$ = 8.0, 1H, H-5), 7.34, 7.24, 7.22, 7.20, 7.12, 7.11, 7.10 and 7.109 (eight s, 8H, 2 x H-3', 6', 3", 6"), 5.15 (d, J_{vic} = 4.9, 2H, 2 x OH), 4.98 (d, J_{vic} = 4.9, 2H, 2 x OH), 4.94 (d, J_{vic} = 5.5, 2H, 2 x OH), 4.68 and 4.56 (m AB system, J_{gem} = 15.5, 6H, 2 x CH_2C≡ and 2 x 6'"-OH), 4.35 (d, $J_{1''',2'''}$ = 8.0, 2H, 2 x H-1'"), 3.94 [s, 9H, $N(CH_3)_3^+$], 3.88, 3.86, 3.83, 3.82 and 3.81 (five s, 24H, 8 x OCH_3), 3.71 – 3.00 (m, 8H, 2 x H-2"-6"). ^{13}C NMR (dmso-*d6*): δ 154.6, 153.8, 153.7, 153.6 and 153.4 (2 x C-2', 5', 2", 5"), 145.0 (C-2), 136.9 (C-6), 132. 8 (C-5), 124.6 (C-3), 124.1 (C-4), 116.0, 115.9, 115.8, 115.6, 115.4, 115.3, 115.1, 114.5, 113.9, 112.6, 112.5, 112, 4, 111.5 and 110.8 (C-1, 2 x

C-1', 4', 1", 4", 3', 6', 3",6"), 101.1 (2 x C-1'"), 104.8, 99.0, 93.0, 92.2, 91.8, 91.4, 91.3, 91.0, 90.5, 90.4 and 82.0 (6 x C≡C), 77.1, 76.7, 73.3 and 70.1 (2 x C-2'", 3'", 4'", 5'"), 61.2 (2 x C-6'"), 56.5, 56.4, 56.3, 56.1, 55.8 and 55.3 [8 x OCH_3, 2 x CH_2C≡, $N(CH_3)_3^+$]. Anal. calcd for $C_{68}H_{70}F_3NO_{23}S$ (1358.34): C, 60.13; H, 5.19; N, 1.03. Found: C, 60.22; H, 5.20; N, 1.03.

Compound 42. It was obtained following **procedure B**, starting from compound **25** (0.45 g, 0.30 mmol, 1 eq.) and a twofold amount of MeOTf, as an orange solid (0.51 g, 0.28 mmol, 95%). The reaction, monitored by TLC (hexane/AcOEt 20:80) was complete in 5h.

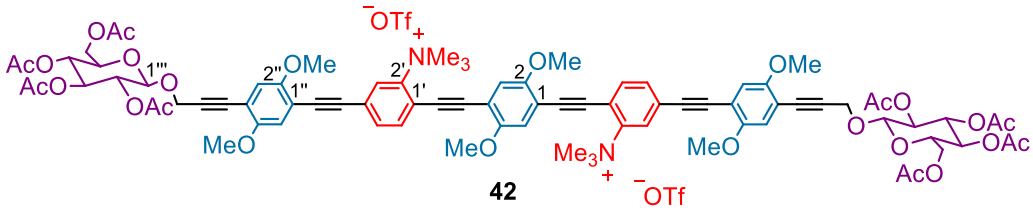

42

TLC: *Rf* =0.05 ($CHCl_3$/MeOH 95:5). Mp 223-225 °C. ^{1}H NMR (dmso-*d6*): δ 8.07 (s, 2H, 2 x H-3'), 7.95 (d, $J_{5',6'}$ = 8.0, 2H, 2 x H-6'), 7.85 (d, $J_{5',6'}$ = 8.0, 2H, 2 x H-5'), 7.43, 7.20 and 7.16 (three s, 6H, H-3, 6 and 2 x H-3", 6"), 5.32 (t, $J_{2''',3'''}$ = $J_{3''',4'''}$ = 9.5, 2H, 2 x H-3'"), 4.99 (d, $J_{1''',2'''}$ = 8.0, 2H, 2 x H-1'"), 4.95 (t, $J_{3''',4'''}$ = $J_{4''',5'''}$ = 9.5, 2H, 2 x H-4'"), 4.83 (dd, $J_{1''',2'''}$ =8.0, $J_{2''',3'''}$ = 9.5, 2H, 2 x H-2'"), 4.67 and 4.57 (AB system, J_{gem}=16.0, 4H, 2 x CH_2C≡), 4.21 and 4.06 (m, $J_{6'''A,6'''B}$ = 10.5, 6H, 2 x H-5'", 2 x H_2-6'"), 3.94 [s, 18H, 2 x $N(CH_3)_3^+$], 3.96, 3.85 and 3.83 (three s, 18H, 6 x OCH_3), 2.02, 1.99 and 1.95 (three s, 24H, 8 x CH_3CO). ^{13}C NMR: δ 170.1, 169.6, 169.3 and 169.1 (8 x CO), 154.7, 153.7 and 153.6 (C-2, 5 and 2 x 2", 5"), 145.1 (2 x C-2'), 137.0 (2 x C-6'), 132.9 (2 x C-5'), 124.7 (2 x C-3'), 124.3 (2 x C-4'), 116.1, 115.6, 115.2, 115.0, 113.0, 112.4 and 111.6 (C-1, 3, 4, 6, and 2 x C-1', 1", 3", 4", 6"), 98.1 (2 x C-1'"), 98.6, 92.9, 91.1, 90.9, 90.3 and 82.4 (6 x C≡C), 72.0, 70.8, 70.7 and 68.1 (2 x C-2'",3'", 4'", 5'"), 61.7 (2 x C-6'"),

56.8, 56.6, 56.3, 56.2 and 55.3 [2 x $CH_2C\equiv$, 8 x OCH_3 and $N(CH_3)_3^+$], 20.5, 20.4 and 20.3 (8 x CH_3CO). Anal. calcd for $C_{86}H_{89}F_6N_2O_{32}S_2$ (1840.74): C, 56.11; H, 4.87; N, 1.52. Found: C, 56.27; H, 4.85; N, 1.52.

Compound 43. Following **procedure A**, starting from **42** (0.32 g, 0.18 mmol) compound **43** was obtained as a brilliant yellow solid (0.26 g, 0.17 mmol, 98%).

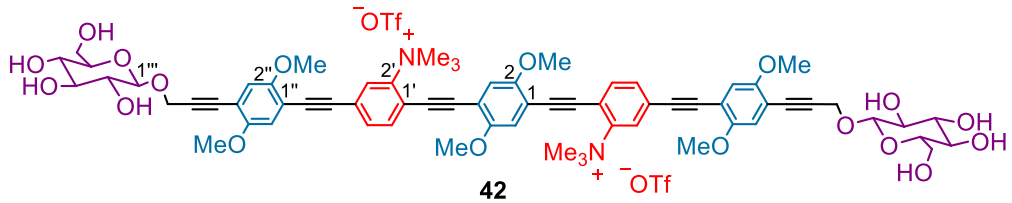

42

TLC: *Rf* =0.05 ($CHCl_3$/MeOH 70:30). Mp 294-296 °C. ^{1}H NMR (dmso-*d6*): 8.07 (s, 2H, 2 x H-3'), 7.95 (d, $J_{5',6'}$ = 7.5, 2H, 2 x H-6'), 7.85 (d, $J_{5',6'}$ = 7.5, 2H, 2 x H-5'), 7.43, 7.19 and 7.15 (three s, 6H, H-3, 6 and 2 x H-3'', 6''), 5.15 (d, J_{vic} = 4.5, 2H, 2 x OH), 4.99 (d, J_{vic} = 4.5, 2H, 2 x OH), 4.95 (d, J_{vic} = 5.0, 2H, 2 x OH), 4.69 and 4.56 (m AB system, J_{gem} = 15.5, 6H, 2 x $CH_2C\equiv$ and 2 x 6'''-OH), 4.35 (d, $J_{1''',2'''}$ = 7.5, 2H, 2 x H-1'''), 3.94 [s, 18H, 2 x $N(CH_3)_3^+$], 3.96, 3.85 and 3.83 (three s, 18H, 6 x OCH_3), 3.72 – 3.00 (m, 8H, 2 x H-2''-6''). ^{13}C NMR (dmso-*d6*): δ 154.7, 153.7 and 153.6 (C-2, 5 and 2 x 2'', 5''), 145.1 (2 x C-2'), 137.0 (2 x C-6'), 132.9 (2 x C-5'), 124.7 (2 x C-3'), 124.3 (2 x C-4'), 116.0, 115.9, 115.6, 115.2, 115.0, 113.3, 112.4 and 111.4 (C-1, 3, 4, 6 and 2 x C-1', 1'', 3'', 4'', 6''), 101.1 (2 x C-1'''), 104.9, 98.6, 92.8, 91.8, 91.1, 90.4 and 81.9 (6 x C≡C), 77.1, 76.7, 73.3 and 70.1 (2 x C-2''', 3''', 4''', 5'''), 61.2 (2 x C-6'''), 56.5, 56.3, 56.2, 55.8 and 55.3 [8 x OCH_3, 2 x $CH_2C\equiv$, $N(CH_3)_3^+$]. Anal. calcd for $C_{70}H_{73}F_6N_2O_{24}S_2$ (1504.45): C, 55.88; H, 4.89; N, 1.86. Found: C, 55.95; H, 4.88; N, 1.86.

Compound 46. It was obtained following **procedure B**, starting from compound **32a** (0.45 g, 0.36 mmol) and an equimolar amount of MeOTf, as an

orange solid (0.48 g, 0.35 mmol, 98%). The reaction, monitored by TLC (hexane/AcOEt 20:80) was complete in 2h.

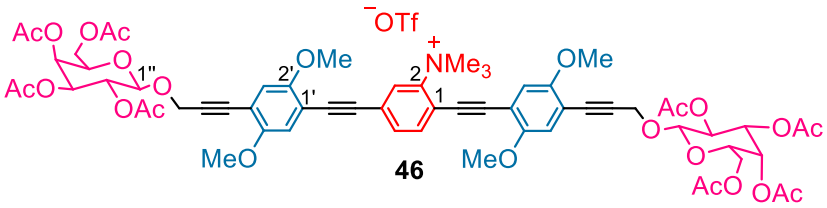

46

TLC: *Rf* =0.10 (hexane/EtOAc 30:70). Mp 145-148°C. ^{1}H NMR: δ 7.92 (s, 1H, H-3), 7.77 (d, $J_{5,6}$ = 8.2, 1H, H-6), 7.69 (d, $J_{5,6}$ = 8.2, 1H, H-5), 7.08, 6.98, 6.97 and 6,94 (four s, 4H, 2 x H-3', 6'), 5.41 (d, 2H, $J_{3'',4''}$=3.0, 2H, 2 x H-4''), 5.25 (bdd, 2H, $J_{1'',2''}$= $J_{2'',3''}$= 10.0, 2H, 2 x H-2''), 5.08 (dd, 2H, $J_{2'',3''}$= 10.0, $J_{3'',4''}$=3.0, 2 x H-3''), 4.84 (d, 2H, $J_{1'',2''}$= 10.0, 2H, 2 x H-1''), 4.66 (s, 4H, 2 x $CH_2C\equiv$), 4.24.- 3.90 (m, 6H,2 x H-5'' and 2 x H_2-6''), 4.09 [s, 9H, $N(CH_3)_3^+$], 3.88, 3.87 and 3.80 (three s, 12H, 4 x OCH_3), 2.16, 2.06, 2.04, 1.99 (four s, 24H, 8 x CH_3CO). ^{13}C NMR: δ 170.4, 170.2, 170.1 and 169.6(8 x CO), 155.1, 154.1, 154.0 and 153.9 (2 x C-2', 5'), 145.1 (C-2), 137.0 (C-6), 133.1 (C-5), 125.8 (C-4), 125.2 (C-3), 115.7, 115.6, 115.4, 114.6, 114.3, 113.4, 112.1 and 110.8 (C-1, 2 x 1', 3', 4', 6'), 98.8 (2 x C-1''), 100.0, 92.3, 91.1, 90.5, 89.9, 89.7, 83.0 and 82.8 (4 x C≡C), 70.8 and 70.7 (2 x C-3'', 5''), 68.5 (2 x C-2''), 67.0 (2 x C-4''), 61.1 (2 x C-6''), 56.4, 56.3, 56.2, and 56.0 [2 x $CH_2C\equiv$, 4 x (OCH_3), $N(CH_3)_3^+$], 20.8 and 20.6 (8 x CH_3CO). Calcd for $C_{64}H_{70}F_3NO_{27}S$: 1373.38; found positive ESI-MAXIS: [$(M\text{-}OTf)^+$] = 1224.4272.

Compound 43. Following **procedure A**, starting from **46** (0.49 g, 0.40 mmol) compound **47** was obtained as a brilliant yellow solid (0.34 g, 0.39 mmol, 97%).

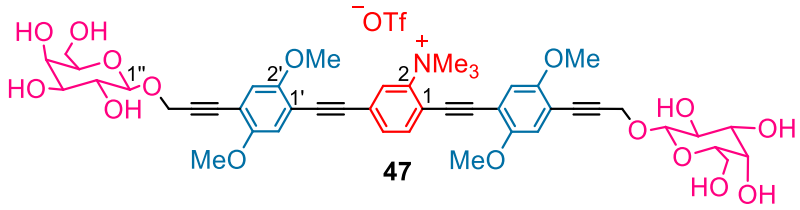

TLC: *Rf* 0.05 ($CHCl_3$/MeOH 80:20). Mp 198-200 °C. ^{1}H NMR: δ 8.0 (bs, 1H, H-3), 7.93 (d, $J_{5,6}$ = 8.0, 1H, H-6), 7.82 (d, $J_{5,6}$ = 8.0, 1H, H-5), 7.30, 7.18, 7.17 and 7.14 (four s, 4H, 2 x H-3',6'), 5.00 (bs, 2H, 2 x OH), 4.73 (bs, 2H, 2 x OH), 4.68-4.52 (m, 6H, 2x $CH_2C\equiv$, 2 x OH), 4.40 (bs, 2H, 2 x OH), 4.28 (d, 2H, $J_{1'',2''}$= 7.1, 2H, H-1''), 3.92 [s, 9H, $N(CH_3)_3^+$], 3.89, 3.84, 3.83 and 3.82 (four s, 12H, 4 x OCH_3), 3.65 – 3.30 (m, 12H, 2 x H2''-6''). ^{13}C NMR (dmso-*d6*): δ 154.6, 153.8 and 153.7 (2 x C-2', 5'), 145.1 (C-2), 137.0 (C-6), 132.9 (C-5), 124.6(C-3), 124.1 (C-4), 116.0, 115.8, 115.6, 115.4, 115.0, 114.0, 113.3 and 110.8 (C-1, 2 x 1', 3', 4', 6'), 101.8 (2 x C-1''), 101.9, 98.9, 92.7, 92.4, 92.0, 90.3 and 81.8 (4 x C≡C), 75.5, 73.5, 70.4 and 68.2 (2 x C-2'', 3'', 4'', 5''), 60.6 (2 x C-6''), 56.4, 56.3, 56.2, 55.8 and 55.3 [2 x $CH_2C\equiv$, 4 x (OCH_3), $N(CH_3)_3^+$]. Calcd for $C_{48}H_{54}F_3NO_{19}S$: 1037.30; found positive ESI+: $[(M\text{-}OTf)^+]$ = 888.3455.

Compound 51. To a flask were added $Pd(PPh_3)_2Cl_2$ (45 mg, 0.06 mmol, 0.025 eq.), CuI (12 mg, 0.06 mmol, 0.025 eq.) and PPh_3 (34 mg, 0.13 mmol, 0.05 eq); the flask was capped with a rubber septum and evacuated. After backfilling with N_2, this process was repeated three times. To the flask was added dry Et_3N (5 mL) at room temperature and the suspension was heated at 80°C, and maintained under continuous stirring. After 1 h, a solution of 2-propyn-1-yl β-D-glucopyranoside,2,3,4,6-tetraacetate **5** (1.00 g, 2.59 mmol, 1 eq.) and 1,4-diiodo-2,3,5,6-tetrafluorobenzene **50** (4.16 g, 10.36 mmol, 4 eq.) in dry Et_3N (10 mL) was added at room temperature and the mixture was stirred to uniform. The reaction mixture was heated at 80°C and maintained under continuous stirring for 1h, until the disappearance of **5** by TLC (hexane/EtOAc 60:40). Column

chromatography was performed with hexane/EtOAc 70:30 as eluent, and compound **51** was obtained as a yellow solid (0.80 g, 1.21 mmol, 47%) and followed by **51-bis** (0.36 g, 0.39 mmol, 15%).

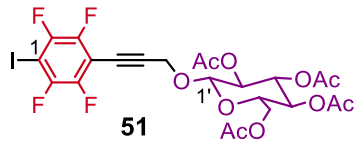

51

TLC: *Rf* =0.58 (hexane/EtOAc 60:40). Mp 124-126 °C. ^{1}H NMR: δ 5.22 (t, $J_{2',3'}$ = $J_{3',4'}$ = 9.5, 1H, H-3'), 5.09 (t, $J_{3',4'}$ = $J_{4',5'}$ = 9.5, 2H, 2 x H-4'), 5.02 (dd, $J_{1',2'}$ = 8.0, $J_{2',3'}$ = 9.5, 2H, 2 x H-2'), 4.79 (d, $J_{1',2'}$ = 8.0, 2H, 2 x H-1'), 4.63 (AB system, J_{vic}=4, 2H, $CH_2C\equiv$), 4.25 and 4.14 (split AB system, $J_{5',6'A}$ = 5.0, $J_{5',6'B}$ = 2.0, $J_{6'A,6'B}$ = 12.5, 2H, H_2-6'), 3.73 (ddd, $J_{4',5'}$ = 9.5, $J_{5',6'A}$ = 5.0, $J_{5',6'B}$ = 2.0, 1H, H-5'), 2.14, 2.06, 2.04 and 2.03 (four s, 12H, 4 x CH_3CO). ^{13}C NMR: δ 170.5, 170.1, 169.4 and 169.3 (4 x CO), 148.0, 147.2, 146.0 and 145.1 (m, J_{F-C}=245, C-2, 3, 5, 6), 104.0 (t, J_{F-C}=27.7, C-4), 98.3 (C-1'), 97.0 and 72.3 (two t, J_{F-C}=3.8, C≡C), 74.1 (t, J_{F-C}=27.7, C-1), 72.6 (C-3'), 72.0 (C-5'), 70.8 (C-2'), 68.1 (C-4'), 61.6 (C-6'), 56.3 (t, J_{F-C}=5.7, $CH_2C\equiv$), 20.6 and 20.5 (4 x CH_3CO). Anal. Calcd for $C_{23}H_{21}F_4IO_{10}$ (660.30): C, 41.84; H, 3.21. Found: C, 41.97; H, 3.20.

Compound 48. Compounds **24** (1.07 g, 1.4 mmol, 1 eq.) and **51** (0.92 g, 1.4 mmol, 1 eq.), Ag_2O (0.32 g, 1.4 mmol, 1 eq.) and $Pd(PPh_3)_4$ (0.16 g, 0.14 mmol, 0.1 eq.) were suspended in dry DMF (6.4 mL) and THF (3.2 mL). The obtained mixture was heated at 70 °C and maintained under Ar atmosphere and continuous stirring for 1.5h, until the disappearance of starting products by TLC (hexane/EtOAc 50:50) After filtration over Celite, the solvents were removed under reduced pressure, and the obtained reaction crude was subjected to silica gel column chromatography. Column chromatography was performed with hexane/EtOAc 60:40 as eluent, and compound **48** was obtained as a brilliant yellow solid (0.91 g, 0.74 mmol, 53%).

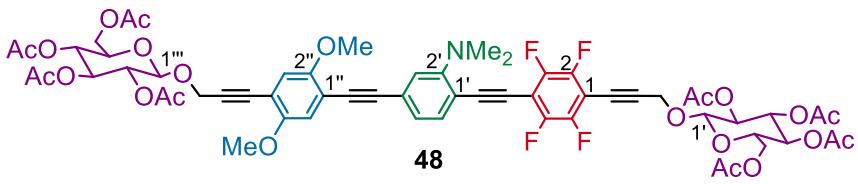

48

TLC: *Rf* =0.45 (hexane/EtOAc 50:50). Mp 128-130 °C. ^{1}H NMR: δ 7.49 (d, $J_{5,6}$ = 7.8, 1H, H-6'), 7.08 (m, 2H, H-3', 5'), 7.02 and 6.95 (two s, 2H, H-3",6"), 5.25 (m, 2H, 2 x H-3'''), 5.14 (m, 2H, 2 x H-4'''), 5.05 (m, $J_{1''',2'''}$ = 7.8, 2H, 2 x H-2'''), 4.91 and 4.83 (two d, $J_{1''',2'''}$ = 7.8, 2H, 2 x H-1'''), 4.68 and 4.65 (AB system and s, J_{vic}=4.9, 4H, 2 x $CH_2C\equiv$), 4.28 and 4.17 (m AB system, 4H, 2 x H_2-6'''), 3.89 and 3.88 (two s, 6H, 2 x OCH_3), 3.76 (m, 2H, 2 x H-5'''), 3.04 [s, 6H, $N(CH_3)_2$], 2.09, 2.08, 2.06, 2.05, 2.04, 2.03, 2.02, and 2.01 (eight s, 24H, 8 x CH_3CO). ^{13}C NMR: δ 170.9, 170.8, 170.6, 170.5, 169.8, 169.7, and 169.6 (8 x CO), 155.2, 154.3 and 154.2 (C-2', 2", 5"), 148.2, 147.5, 146.1 and 145.5 (m, $J_{F\text{-}C}$=252, C-2, 3, 5, 6), 135.2 (C-6'), 125.6 (C-4'), 123.6 and 120.2 (C-3',5'), 116.0 and 115.8 (C-3",6"), 113.8 and 112.8 (C-1', 1",4"), 106.5 and 103.2 (two t, $J_{F\text{-}C}$=18.1, C-1,4), 103.6 and 97.6 (two t, $J_{F\text{-}C}$=4.2, C≡C-Ar_F), 98.3 (2 x C-1'''), 95.1, 89.2, 87.3 and 83.4 (2 x C≡C), 81.1 and 72.7 (two t, $J_{F\text{-}C}$=3.2, C≡C-Ar_F), 72.8 and 72.7 (2 x C-3'''), 72.0 and 71.9 (2 x C-5'''), 71.1 and 70.9 (2 x C-2'''), 68.3 and 68.2 (2 x C-4'''), 61.8 and 61.7 (2 x C-6'''), 57.3, 57.0, 56.7 and 56.6 (2 x $CH_2C\equiv$ and 2 x OCH_3), 43.6 [$N(CH_3)_2$], 21.0, 20.9, 20.8 and 20.7 (8 x CH_3CO). Anal. Calcd for $C_{60}H_{59}F_4NO_{22}$ (1222.10): C, 58.97; H, 4.87; N, 1.15. Found: C, 58.85; H, 4.87; N, 1.15.

Compound 52. To a flask were added $Pd(PPh_3)_4$ (0.15 g, 0.13 mmol, 0.1 eq.), Ag_2O (0.30 g, 1.28 mmol, 1 eq.), **11** (0.77 g, 1.28 mmol, 1 eq.) and 1,4-iodo-2,5-dimethoxybenzene **7** (1.00 g, 2.56 mmol, 2 eq.); the flask was capped with a rubber septum and evacuated. After backfilling with N_2, this process was repeated three times. To the flask were added dry DMF (13.6 mL) and dry THF (6.8 mL).

The reaction mixture was heated at 70°C for 1 h, until the disappearance of the starting compound **11** by TLC (hexane/EtOAc 60:40). Solvents were removed in vacuo and the solid residue was dissolved in CH_2Cl_2 and filtered on celite. After evaporation of the solvents, the excess of unreacted **7** was separated through precipitation from methanol. The crude obtained from the evaporation of mother liquors was purified by column chromatography on silica gel using hexane/EtOAc (70:30) as eluent to give compound **52** as a yellow solid (0.58 g, 0.73 mmol, 57%).

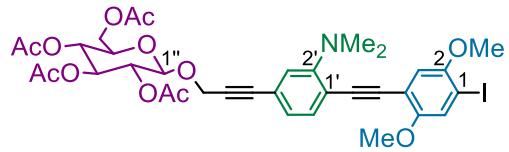

52

TLC: *Rf* =0.52 (hexane/EtOAc 60:40). Mp 105-107 °C. ^{1}H NMR: δ 7.44 (d, $J_{5',6'}$ = 7.8, 1H, H-6'), 7.29 (s, 1 H, H-6), 6.95 (m, H-3', 5'), 6.92 (s, 1H, H-3), 5.27 (dd, $J_{2'',3''}$ = 9.8, $J_{3'',4''}$ = 10.3, 1H, H-3''), 5.11 (t, $J_{3'',4''}$ = $J_{4'',5''}$ = 10.3, 1H, H-4''), 5.04 (dd, $J_{1'',2''}$ = 8.4, $J_{2'',3''}$ = 9.8, 1H, H-2''), 4.84 (d, $J_{1'',2''}$ = 8.4, 1H, H-1''), 4.60 (AB system, J_{vic}=1.0, 2H, $CH_2C\equiv$), 4.28 and 4.16 (split AB system, $J_{5'',6''A}$ = 4.9, $J_{5'',6''B}$ = 2.5, $J_{6''A,6''B}$ = 12.7, 1H, H_2-6''), 3.85 and 3.84 (two s, 6H, 2 x OCH_3), 3.76 (ddd, $J_{4'',5''}$ = 10.3, $J_{5'',6''A}$ = 4.9, $J_{5'',6''B}$ = 2.5, 1H, H-5''), 3.02 (s, 6H, [$N(CH_3)_2$]), 2.08, 2.05, 2.02 and 2.01 (four s, 12H, 4 x CH_3CO). ^{13}C NMR: δ 170.5,170.1, 169.3 and 169.2 (4 x CO), 154.6, 154.2 and 152.2 (C-2, C-5, C-2'), 134.2 (C-6'), 123.4 (C-4'), 122.6 (C-5'), 122.0 (C-6), 119.9 (C-3'), 115.3 (C-1'), 114.4 (C-3), 113.3 (C-4), 98.3 (C-1''), 93.3, 92.4, 86.5 and 84.4 (2 x C≡C), 87.2 (C-1), 72.7 (C-3''), 71.8 (C-5''), 71.0 (C-2''), 68.2 (C-4''), 61.7 (C-6''), 56.9, 56.8 and 56.4 ($CH_2C\equiv$ and 2 x OCH_3), 43.2 [$N(CH_3)_2$], 20.6, 20.5 and 20.4 (4 x CH_3CO). Anal. Calcd for $C_{35}H_{38}INO_{12}$ (791.58): C, 53.11; H, 4.84; N, 1.77. Found: C, 52.98; H, 4.85; N, 1.76.

Compound 53. To a flask were added $Pd(PPh_3)_2Cl_2$ (11 mg, 0.03 mmol, 0.025 eq.), CuI (3 mg, 0.03 mmol, 0.025 eq.) and **52** (0.50 g, 0.63 mmol, 1 eq); the flask was capped with a rubber septum and evacuated. After backfilling with N_2, this process was repeated three times. To the flask was added dry Et_3N (3 mL) and dry DMF (1.5 mL) at room temperature; then commercial ethynyltrimethylsilane (0.18 mL, 1.26 mmol, 2 eq.) was slowly added. The reaction mixture was heated at 70°C and maintained under continuous stirring for 2 h, until the disappearance of **52** by TLC (hexane/EtOAc 60:40). The resulting crude was filtered on Celite and column chromatography was performed with hexane/EtOAc 70:30 as eluent, and compound **53** was obtained as a yellow solid (0.35 g, 0.46 mmol, 73%).

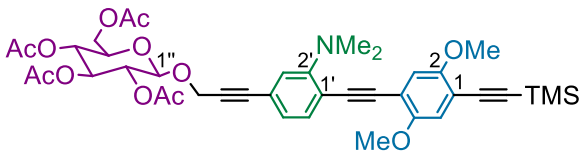

53

TLC: *Rf* =0.48 (hexane/EtOAc 60:40). Mp 110-112 °C. ^{1}H NMR: δ 7.43 (d, $J_{5',6'}$ = 7.8, 1H, H-6'), 6.94 (m, 4H, H-3, 6, 3', 5'), 5.27 (dd, $J_{2'',3''}$ = 9.3, $J_{3'',4''}$ = 9.8, 1H, H-3''), 5.11 (t, $J_{3'',4''}$ = $J_{4'',5''}$ = 9.8, 1H, H-4''), 5.03 (dd, $J_{1'',2''}$ = 7.8, $J_{2'',3''}$ = 9.3, 1H, H-2''), 4.83 (d, $J_{1'',2''}$ = 7.8, 1H, H-1''), 4.59 (AB system, J_{vic}=1.0, 2H, $CH_2C\equiv$), 4.28 and 4.15 (split AB system, $J_{5'',6''A}$ = 4.4, $J_{5'',6''B}$ = 3.0, $J_{6''A,6''B}$ = 12.2, 1H, H_2-6''), 3.85 and 3.84 (two s, 6H, 2 x OCH_3), 3.75 (ddd, $J_{4'',5''}$ = 9.8, $J_{5'',6''A}$ = 4.4, $J_{5'',6''B}$ = 3.0, 1H, H-5''), 3.01 (s, 6H, $[N(CH_3)_2]$), 2.07, 2.04, 2.01 and 2.00 (four s, 12H, 4 x CH_3CO), 0.26 [s, 9H, $Si(CH_3)_3$]. ^{13}C NMR: δ 170.6, 170.2, 169.4 and 169.3 (4 x CO), 154.6, 154.2 and 153.8 (C-2, C-5, C-2'), 134.3 (C-6'), 123.4 and 119.9 (C-3', 5'), 122.7 (C-4'), 115.8 and 115.2 (C-3, 6), 115.4, 113.9 and 113.0 (C-1, 4, 1'), 98.4 (C-1''), 100.9, 100.4, 94.1, 92.8, 87.3 and 84.4 (3 x C≡C), 72.8 (C-3''), 71.9 (C-5''), 71.1 (C-2''), 68.3 (C-4''), 61.8 (C-6''), 56.9, 56.5 and 56.4 ($CH_2C\equiv$ and 2 x OCH_3), 43.3 $[N(CH_3)_2]$, 20.7 and 20.5 (4 x CH_3CO), -0.04 $[Si(CH_3)_3]$.

Anal. Calcd for $C_{40}H_{47}NO_{12}Si$ (761.89): C, 63.06; H, 6.22; N, 1.84. Found: C, 63.21; H, 6.21; N, 1.84.

Compound 49. Compounds **53** (0.33 g, 0.43 mmol, 1 eq.) and **51** (0.29 g, 0.43 mmol, 1 eq.), Ag_2O (0.10 g, 0.43 mmol, 1 eq.) and $Pd(PPh_3)_4$ (0.05 g, 0.04 mmol, 0.1 eq.) were suspended in dry DMF (2 mL) and THF (1 mL). The obtained mixture was heated at 70 °C and maintained under Ar atmosphere and continuous stirring for 1.5h, until the disappearance of starting products by TLC (hexane/EtOAc 50:50) After filtration over Celite, the solvents were removed under reduced pressure, and the obtained reaction crude was subjected to silica gel column chromatography. Column chromatography was performed with hexane/EtOAc 60:40 as eluent, and compound **49** was obtained as a brilliant yellow solid (0.27 g, 0.22 mmol, 51%).

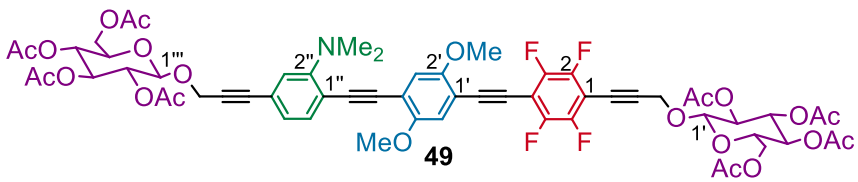

49

TLC: *Rf* =0.45 (hexane/EtOAc 50:50). Mp 126-128 °C. ^{1}H NMR: δ 7.46 (d, $J_{5,6}$ = 7.9, 1H, H-6'), 7.03 and 7.01 (two s, 2H, H-3",6"), 6.96 (m, 2H, H-3', 5'), 5.25 (m, 2H, 2 x H-3'"), 5.12 (m, 2H, 2 x H-4'"), 5.05 (m, 2H, 2 x H-2'"), 4.84 (m, 2H, 2 x H-1'"), 4.68 and 4.60 (AB system and s, J_{vic}=4.9, 4H, 2 x $CH_2C\equiv$), 4.28 and 4.17 (m AB system, 4H, 2 x H_2-6'"), 3.91 and 3.90 (two s, 6H, 2 x OCH_3), 3.76 (m, 2H, 2 x H-5'"), 3.03 [s, 6H, $N(CH_3)_2$], 2.09, 2.08, 2.06, 2.05, 2.04, 2.03 and 2.01 (seven s, 24H, 8 x CH_3CO). ^{13}C NMR: δ 170.7, 170.6, 170.3, 170.2, 169.5, 169.4 and 169.3 (8 x CO), 154.5, 154.4 and 153.9 (C-2', 5', 2"), 147.8, 147.4, 145.8 and 145.3 (m, $J_{F\text{-}C}$=252.7, C-2, 3, 5, 6), 134,5 (C-6"), 123.5 and 120.0 (C-3",5"), 123.0 (C-4"), 115.4 and 115.2 (C-3',6'), 115.8, 115.1 and 111.2 (C-1', 4', 1"), 105.9 and 103.8 (two t, $J_{F\text{-}C}$=17.5, C-1,4), 100.1 and 97.4 (two t, $J_{F\text{-}C}$=4.4,

C≡C-Ar_F), 98.4 (2 x C-1'''), 95.1, 92.6, 87.2 and 84.6 (2 x C≡C), 79.6 and 72.7 (two t, J_{F-C}=3.2, C≡C-Ar_F), 72.8 (2 x C-3'''), 71.9 (2 x C-5'''), 71.0 (2 x C-2'''), 68.2 (2 x C-4'''), 61.7 (2 x C-6'''), 56.9, 56.6 and 56.3 (2 x CH_2C≡ and 2 x OCH_3), 43.3 [$N(CH_3)_2$], 20.8, 20.7, 20.6 and 20.4 (8 x CH_3CO). Anal. Calcd for $C_{60}H_{59}F_4NO_{22}$ (1222.10): C, 58.97; H, 4.87; N, 1.15. Found: C, 59.07; H, 4.86; N, 1.15.

Compound 69.[191] To a flask were added $Pd(PPh_3)_2Cl_2$ (68 mg, 0.1 mmol, 0.025 eq.), CuI (18 mg, 0.1 mmol, 0.025 eq.) and 1,4-diiodo-2,5-dimethoxybenzene **7** (1.50 g, 3.85 mmol, 1 eq); the flask was capped with a rubber septum and evacuated. After backfilling with N_2, this process was repeated three times. To the flask was added dry Et_3N (20 mL) and dry DMF (10 mL) at room temperature; then commercial ethynyltrimethylsilane (0.54 mL, 3.85 mmol, 1 eq.) was slowly added. The reaction mixture was heated at 60°C and maintained under continuous stirring for 2 h, until the disappearance of **7** by TLC (hexane/DCM 80:20). The resulting crude was filtered on Celite and column chromatography was performed with hexane/DCM 90:10 as eluent, and compound **69** was obtained as a white solid (0.98 g, 2.91 mmol, 76%). TLC: *Rf* =0.75 (hexane/DCM 80:20).

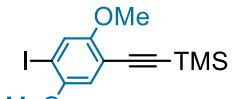

69

Compound 70.[192] To a flask were added $Pd(PPh_3)_2Cl_2$ (24 mg, 0.03 mmol, 0.025 eq.), CuI (6 mg, 0.03 mmol, 0.025 eq.) and **69** (0.50 g, 1.39 mmol, 1 eq.); the flask was capped with a rubber septum and evacuated. After backfilling with

[191] Schneider, R. V.; Waibel, K. A.; Arndt, A. P.; Lang, M.; Seim, R.; Busko, D.; Bräse, S.; Lemmer, U.; Meiera, M. A. R. Sci. Rep. **2018**, *8*, 17483.
[192] Whitten, D. G.; Tang, Y.; Zhou, Z.; Yang, J.; Wang, Y.; Hill, E. H.; Pappas, H. C.; Donabedian, P. L.; Chi, E. Y. *Langmuir* **2019**, *35*, 307.

N_2, this process was repeated three times. To the flask was added dry Et_3N (7 mL) and dry DMF (3.5 mL) at room temperature; then commercial 2-methyl-3-butyn-2-ol (0.16 mL, 1.69 mmol, 1.2 eq.) was slowly added. The reaction mixture was heated at 60°C and maintained under continuous stirring for 2 h, until the disappearance of **69** by TLC (hexane/DCM 50:50). The resulting crude was filtered on Celite and column chromatography was performed with hexane/DCM 50:50 as eluent, and compound **70** was obtained as a white solid (0.33 g, 1.04 mmol, 75%). TLC: *Rf* =0.75 (hexane/DCM 80:20).

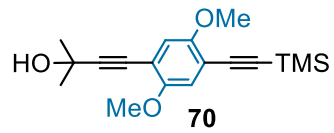

70

Compound 71.[193] Compound **70** (0.34 g 1.07 mmol) was dissolved into dry toluene (11 mL); NaOH was added (0.04 mg, 1.07 mmol) and the mixture was then refluxed for 15 minutes. The mixture was stirred at room temperature before being poured into water. The solution was extracted with ethyl acetate (3 x 10) and washed with brine (3 x 10). After drying over Na_2SO_4, the solvent was evaporated *in vacuo* and column chromatography of the obtained crude was performed with hexane/DCM 50:50 as eluent. Compound **71** was obtained as a white solid (0.16 g, 0.63 mmol, 59%). TLC: *Rf* =0.75 (hexane/DCM 80:20).

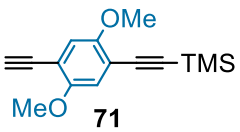

71

Compound 72. To a flask were added $Pd(PPh_3)_4$ (0.03 g, 0.03 mmol, 0.1 eq.), **23** (0.21 g, 0.29 mmol, 1 eq.) and **71** (0.15 g, 0.58 mmol, 2 eq.); the flask

[193] Q. Lu, K. Liu, H. Zhang, Z. Du, X. Wang e F. Wang, *ACS Nano*, **2009**, *3*, 3861.

was capped with a rubber septum and evacuated. After backfilling with N_2, this process was repeated three times. To the flask were added dry DMF (1.5 mL) and Et_3N (1.5 mL) at room temperature. The reaction mixture was heated at 80°C, and maintained under continuous stirring for 6 h, until the disappearance of the starting compound **23** by TLC (hexane/EtOAc 60:40). Solvents were removed under reduced pressure and the reaction crude was purified by chromatography on silica gel, using hexane/EtOAc (70:30) as eluent, giving compound **72** as a brilliant yellow solid (0.18 g, 0.19 mmol, 66%).

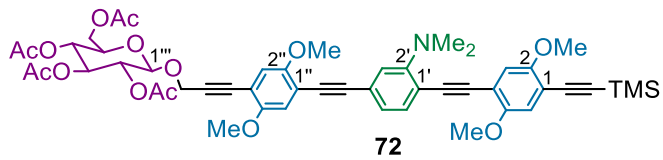

72

TLC: R_f 0.22 (hexane/EtOAc 40:60). Mp 130-132 °C. ^{1}H NMR: δ 7.46 (d, $J_{5,6}$ = 7.8, 1H, H-6'), 7.08 (m, 2H, H-3',5'), 7.01, 7.00 and 6.93 (three s, 4H, H-3, 6, 3", 6"), 5.26 (t, $J_{2''',3'''} = J_{3''',4'''}$ = 9.2, 1H, H-3'''), 5.11 (t, $J_{3''',4'''} = J_{4''',5'''}$ = 9.2, 1H, H-4'''), 5.03 (t, $J_{1''',2'''} = J_{2''',3'''}$ = 9.2, 1H, H-2'''), 4.90 (d, $J_{1''',2'''}$ = 9.2, 1H, H-1'''), 4.64 (s, 2H, $CH_2C\equiv$), 4.27 and 4.15 (m AB system, 2H, H_2-6'''), 3.87, 3.86 and 3.84 (three s, 12H, 4 x OCH_3), 3.75 (m, 1H, H-5'''), 3.03 (s, 6H, [$N(CH_3)_2$]), 2.07, 2.03, 2.02 and 2.00 (four s, 24H, 8 x CH_3CO), 0.26 [s, 9H, $Si(CH_3)_3$]. ^{13}C NMR: δ 170.5, 170.2, 169.3 and 169.2 (4 x CO), 154.2, 154.0 and 153.7 (C-2, 5, 2', 2", 5"), 134.2 (C-6'), 123.7, 123.6 and 120.0 (C-3', 4', 5'), 115.8, 115.6, 115.5 and 115.1 (C-3, 6, 3", 6"), 115.2, 113.9, 113.7, 112.9 and 112.1 (C-1, 4, 1', 1", 4"), 98.1 (2 x C-1'''), 100.9, 100.3, 95.4, 94.2, 92.9, 89.0, 86.6 and 83.4 (4 x C≡C), 72.7 (C-3'''), 71.8 (C-5'''), 71.0 (C-2'''), 68.2 (C-4'''), 61.7 (C-6'''), 57.0 ($CH_2C\equiv$), 56.4, 56.3, 56.2 and 56.1 (4 x OCH_3), 43.3 [$N(CH_3)_2$], 20.6 and 20.5 (4 x CH_3CO),

-0.1 [$Si(CH_3)_3$]. Anal. calcd for $C_{50}H_{55}NO_{14}Si$ (922.06): C, 65.13; H, 6.01; N, 1.52. Found: C, 65.05; H, 5.99; N, 1.52.

Compound 63. Compound **72** (0.15 g, 0.16 mmol) was dissolved in a mixture of MeOH (1.5 mL) and CH_2Cl_2 (1.5 mL), and K_2CO_3 (0.88 g, 6.40 mmol) was added. The reaction mixture stirred at room temperature for 4 h. The reaction was quenched by adding H_2O and the mixture was extracted with CH_2Cl_2 (3 x 7 mL), and then the combined organic extracts were washed with brine (3 x 7 mL). The combined organic extracts were then dried (Na_2SO_4) and filtered, and the solvent was evaporated *in vacuo* to give **63** as a yellow solid (0.09 g, 0.14 mmol, 85%) without any further purification.

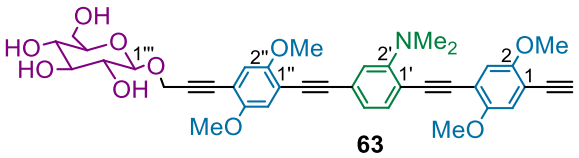

63

TLC: *Rf* =0.35 (acetonitrile/DCM 90:10). Mp 182-185 °C. ^{1}H NMR (dmso-*d6*): δ 7.44 (d, $J_{5',6'}$= 13.5, 1H, H-6'), 7.17- 7.02 (m, 6H, H-3, 6, 3', 5', 3", 6"), 5.12 (d, J_{vic}= 8.5 ,1H, OH), 4.95 (d, J_{vic}= 8.0, 1H, OH), 4.91 (d, J_{vic}=8.5, 1H, OH), 4.67 and 4.54 (m AB system, J_{gem} = 15.0, 3H, $CH_2C\equiv$ and 6'''-OH), 4.40 (s, 1H, ≡CH), 4.33 (d, $J_{1''',2'''}$ =13.0, 1H, H-1'''), 3.82 and 3.81 (two s, 12H, 4 x OCH_3), 3.68 and 3.46 (split AB m, 2H, H_2- 6'''), 3.20-3.00 (m, 4H, H-2''',5'''), 2.98 [s, 6H, $N(CH_3)_2$]. ^{13}C NMR (dmso-*d6*): δ 154.1, 154.0, 153.6 and 153.4 (C-2, 5, C-2', 2", 5"), 134.4 (C-6'), 123.3 (C-4'), 122.6 (C-5'), 119.1 (C-3'), 115.9, 115.8, 115.6 and 114.9 (C-3, 6, 3", 6"), 113.6, 113.2, 112.4, 112.3 and 111.8 (C-1, 4, 1', 1", 4"), 101.1 (C-1'''), 94.8, 92.7, 91.3, 87.2, 82.0 and 80.0 (4 x C≡C), 77.0, 76.7, 73.3 and 70.1 (C-2''',3''', 4''', 5'''), 61.2 (C-6'''), 56.2, 56.1 and 55.8 ($CH_2C\equiv$, 4 x OCH_3), 42.6

[$N(CH_3)_2$]. Anal. calcd for $C_{39}H_{39}NO_{10}$ (681.73): C, 68.71; H, 5.77; N, 2.05. Found: C, 68.81; H, 5.79; N, 2.05.

Compound 74.[194] Commercially available 5-bromovaleric acid **73** (1.00 g, 5.52 mmol, 1 eq.), NaN_3 (0.90 g, 13.81 mmol, 2.5 eq.), water (10 mL) and acetone (2 mL) were added to a round bottom flask, which was then placed in an oil bath thermostated at 60 °C. The reaction mixture was stirred at this temperature for 6 h. The reaction mixture was then acidified by addition of concentrated HCl until pH 2 was reached and extracted with ethyl acetate (3 x 20 mL). The organic phase was washed with brine (3 x 20), dried over Na_2SO_4 and concentrated under vacuum to obtain **74** (0.70 g, 4.91 mmol, 89%) as a white oil without any further purification. TLC: *Rf* =0.45 (AcOEt).

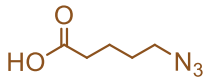

74

Compound 68. 5-azidopentanoic acid **74** (0.04 g, 0.26 mmol, 1.2 eq.) was added to a solution of **63** (0.15 g, 0.22 mmol, 1 eq.), sodium ascorbate (5 mg, 0.02 mmol, 0.1 eq.), and copper sulphate (0.08 g, 0.52 mmol, 2 eq.) in a mixture of DMF (9 mL) and water (1 mL) at room temperature. The reaction mixture was maintained under continuous stirring at room temperature for 1 h, until the disappearance of the starting compound **63** by TLC (acetonitrile/DCM 70:30). The reaction was extracted with ethyl acetate (3 x 15 mL) and the combined organic layers were washed with brine (3 x 15 mL), dried over anhydrous Na_2SO_4, filtered, and concentrated *in vacuum*. Compound **68** was obtained as a yellow solid.

[194] Chan-Seng, D.; Lutz, J.-F. *ACS Macro Lett.* **2014**, *3*, 291.

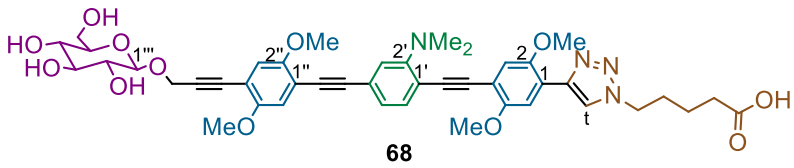

68

TLC: *Rf* =0.25 (acetonitrile/DCM 70:30). Mp=147-149 °C. ^{1}H NMR (dmso-*d6*): δ 8.46 (s,1H, H-t), 7.82 (s, 1H, H-6), 7.46 (d, $J_{5',6'}$= 8.3, 1H, H-6'), 7.20, 7.18 and 7.09 (three s, 3H, H-3, 3'', 6''), 7.03 (m, 2H, H-3', 5'), 5.16 (bd, 1H, OH), 5.03 (bs, 1H, OH), 4.97 (bd, 1H, OH), 4.68 and 4.55 (m AB system, J_{gem} = 15.7, 3H, $CH_2C\equiv$ and 6'''-OH), 4.42 (bt, 2H, CH_2N), 4.34 (d, $J_{1''',2'''}$ =7.9, 1H, H-1'''), 3.92, 3.90, 3.83 and 3.82 (four s, 12H, 4 x OCH_3), 3.71-3.03 (m, 5H, H-2''', 6'''), 3.32 (2H, CH_2CO), 3.00 [s, 6H, $N(CH_3)_2$], 1.87 (bt, 2H, $C\underline{H_2}CH_2N$), 1.45 (bs, 2H, $C\underline{H_2}CH_2CO$).

PUBLICATIONS

1) De Luca, G.; Bonaccorsi, P.; Trovato, V.; Mancuso, A.; Papalia, T.; Pistone, A.; Casaletto, M. P.; Mezzi, A.; Brunetti, B.; Minuti, L.; Temperini, A.; Barattucci, A.; Plutino, M. R. Plutino *New J. Chem.* **2018**, *42*, 16436. Tripodal tris-disulfides as capping agents for a controlled mixed functionalization of gold nanoparticles.

2) Barattucci, A.; Aversa, M. C.; Mancuso, A.; Salerno, T. M. G.; Bonaccorsi, P. *Molecules*, **2018**, 23, 1030. Transient sulfenic acids in the synthesis of biologically relevant products.

3) Mancuso, A.; Barattucci, A.; Bonaccorsi, P.; Giannetto, A.; La Ganga, G.; Musarra-Pizzo, M.; Salerno, T. M. G.; Santoro, A.; Sciortino, M. T.; Puntoriero, F.; Di Pietro, M. L. *Chem. Eur. J.* **2018**, *24*, 16972. Carbohydrates and charges on oligo(phenylenethynylenes): towards the design of cancer bullets.

COMUNICATIONS

1) **Workshop delle sezioni Sicilia e Calabria**, Messina, 9-10 February 2017.
Oral communication "Sintesi di sistemi *star-shaped* a separazione di carica fotoindotta". Mancuso, A.; Bonaccorsi, P.; Puntoriero, F.; Salerno, T. M. G.; Barattucci, A.

2) **4th International Workshop on Pericyclic Reactions and Synthesis of Hetero- and Carbocyclic Systems**, Milan, 28-30 June 2017.
Oral communication "Tuning Sugar Functionalized OPEs with biological interest". Mancuso, A.; Bonaccorsi, P.; Salerno, T. M. G.; Barattucci, A.
Oral communication "Curcumin: how much more is there to explore?". Salerno, T.M.G.; Barattucci, A.; Mancuso, A.; Bonaccorsi, P.

3) **Congresso Congiunto delle Sezioni Sicilia e Calabria SCI 2018**, Catania, 9-10 February 2018.
Oral communication "Nuove frontiere nella progettazione di fluorofori biocompatibili" Mancuso, A.; Bonaccorsi, P.; Salerno, T. M. G.; Barattucci, A.

4) **XLIII "A. Corbella" International Summer School on Organic Synthesis - ISOS 2018**, Gargnano (Bs), 10-14 June 2018.

Oral communication "The use of Curcumin in the synthesis of luminescent probes". Salerno, T.M.G.; Barattucci, A.; Mancuso, A.; Bonaccorsi, P.

5) **XVI Convegno-Scuola Chimica dei Carboidrati- XVI CSCC 2018**, Pontignano (Si), 17-20 June 2018.

Oral communication "Design and synthesis of modified glycoamino opes for the finding of new potential photosensitizers" Mancuso, A.; Bonaccorsi, P.; Salerno, T. M. G.; Barattucci, A.

6) **I DOCTOCHEM-UNIME,** Messina, 22 June 2018.

Oral communication "Modified Glycoamino OPEs as New Potential Photosensitizers" Mancuso, A.; Bonaccorsi, P.; Carreño, M. C.; Ribagorda, M.; Salerno, T. M. G.; Barattucci, A.

Oral communication "Curcumin: a natural dye. Synthesis of new derivatives and their applications" Salerno, T.M.G.; Barattucci, A.; Mancuso, A.; Bonaccorsi, P.

7) **XXXVIII Convegno Nazionale della Divisione di Chimica Organica della Società Chimica Italiana- CDCO 2018**, Milan, 9-13 September 2018.

Poster communication "Glycoamino OPEs: from bioimaging to nanotechnology" Mancuso, A.; Bonaccorsi, P.; Salerno, T. M. G.; Barattucci, A.

Oral communication "Curcumin from nature to laboratory: new ways to improve its properties" Salerno, T.M.G.; Barattucci, A.; Mancuso, A.; Puntoriero, F.; Campagna, S.; Bonaccorsi, P.

8) **Congresso Congiunto delle Sezioni Sicilia e Calabria SCI 2019**, Palermo, 1-2 March 2019.

Poster communication "Nuove applicazioni di glucoammino oligo-fenilenetinileni" Mancuso, A.; Bonaccorsi, P.; Salerno, T. M. G.; Barattucci, A.

9) **XLIV "A. Corbella" International Summer School on Organic Synthesis - ISOS 2018**, Gargnano (Bs), 9-13 June 2018.

Oral communication "Push-Pull fluorinated OPEs: synthesis and properties" Mancuso, A.; Bonaccorsi, P.; Barattucci, A.

10) **II DOCTOCHEM-UNIME,** Messina, 5 July 2019.

Oral communication "Structural modifications and properties of glycoamino OPEs" Mancuso, A.; Bonaccorsi, P.; Barattucci, A.

11) **XXXIX Convegno Nazionale della Divisione di Chimica Organica della Società Chimica Italiana- CDCO 2019**, Turin, 8-12 September 2019.

Oral communication "Structural modifications of glycoamino OPEs: synthesis and properties" Mancuso, A.; Bonaccorsi, P.; Barattucci, A.

MEMBER OF COMMITTEES

1) **II DOCTOCHEM-UNIME,** Messina, 5 July 2019. **Member of the organizing committee**.